

DEVELOPMENT OF NOVEL CATALYTIC METHODOLOGIES FOR
CARBON-CARBON BOND CONSTRUCTION

A THESIS SUBMITTED TO
THE GRADUATE SCHOOL OF NATURAL AND APPLIED SCIENCES
OF
MIDDLE EAST TECHNICAL UNIVERSITY

BY

SERKAN EYMUR

IN PARTIAL FULFILLMENT OF THE REQUIREMENTS
FOR
THE DEGREE OF DOCTOR OF PHILOSOPHY
IN
CHEMISTRY

DECEMBER 2012

Approval of the thesis:

**DEVELOPMENT OF NOVEL CATALYTIC METHODOLOGIES FOR
CARBON-CARBON BOND CONSTRUCTION**

submitted by **SERKAN EYMUR** in partial fulfillment of the requirements for
the degree of **Doctor of Philosophy in Chemistry Department, Middle East
Technical University** by,

Prof. Dr. Canan Özgen _____
Dean, Graduate School of **Natural and Applied Sciences**

Prof. Dr. İlker Özkan _____
Head of Department, **Chemistry**

Prof. Dr. Ayhan S. Demir _____
Supervisor, **Chemistry Dept., METU**

Examining Committee Members:

Prof. Dr. Metin Balcı _____
Chemistry Dept., METU

Prof. Dr. Metin Zora _____
Chemistry Dept., METU

Prof. Dr. Özdemir Doğan _____
Chemistry Dept., METU

Prof. Dr. Mustafa Yılmaz _____
Chemistry Dept., Selçuk University

Assist. Prof. Dr. Akın Akdağ _____
Chemistry Dept., METU

Date: 06.12.2012

I hereby declare that all information in this document has been obtained and presented in accordance with academic rules and ethical conduct. I also declare that, as required by these rules and conduct, I have fully cited and referenced all material and results that are not original to this work.

Name, Last name: Serkan Eymur

Signature:

ABSTRACT

DEVELOPMENT OF NOVEL CATALYTIC METHODOLOGIES FOR CARBON-CARBON BOND CONSTRUCTION

Eymur, Serkan

Ph.D., Department of Chemistry

Supervisor: Prof. Dr. Ayhan S. Demir

December 2012, 195 pages

Addition reactions of nucleophilic trifluoromethyltrimethylsilane (CF_3TMS) to acyl phosphonates were investigated. Various acyl phosphonates reacted readily with CF_3TMS in the presence of K_2CO_3 to give 1-alkyl-2,2,2-trifluoro-1-trimethylsilyloxyethylphosphonate in 70-90% yields. When benzoyl phosphonates were used as starting material, after addition of CF_3 , the formed alcoholate undergoes phosphonate-phosphate rearrangement to form the acyl anion, followed by elimination of F⁻ to give 1-aryldifluoroethenyl phosphates in 87-97% yields.

The proline-thiourea host-guest complex catalyzed intermolecular aldol reaction of aromatic aldehydes with cyclohexanone is developed. The anti-configured products were obtained in high yields and exclusively excellent enantioselectivities. The reaction is proposed to proceed according to a modified Houk-List model, in which the carboxylate moiety of the proline forms an assembly with the thiourea. These results clearly demonstrate the enormous effect of the thiourea on the reactivity and selectivity, even in an unconventional non-polar reaction medium, without the need to use low temperatures.

A proline–thiourea host–guest complex is described as a good catalyst for the enantioselective nitro-Michael addition of aldehydes to nitroalkenes. The reaction is efficient with 5% of the thiourea, to give moderate to good enantioselectivity (up to 76% *ee*). High syn-selectivity was obtained with both branched and unbranched aliphatic aldehydes. This is the first example of self-assembly of organo- catalysts with an achiral additive in a Michael addition wherein aldehydes are utilized as donors.

An aldol reaction catalyzed by a proline–thiourea host–guest complex in a nonpolar solvent shows excellent nonlinear effects. This proline–thiourea system has the ability to form a hydrogen-bonding network. The enantiomeric excess of proline in a solution can be significantly enhanced by its incorporation with a urea molecule into its solid racemate. This suggests a general and facile route to homochirality, which may be involved in the origin of chirality on earth.

Keywords: Acyl anion, Umpolung, Acylphosphonate, Asymmetric Catalysis, Organocatalysis.

ÖZ

KARBON-KARBON BAĞI OLUŞUMU İÇİN YENİ KATALİTİK METOTLARIN GELİŞTİRİLMESİ

Eymur, Serkan

Doktora, Kimya Bölümü

Tez Yöneticisi: Prof. Dr. Ayhan S. Demir

Aralık 2012, 195 sayfa

Nükleofilik triflorotrimetilsilan'ın (CF_3TMS) açıl fosfonatlara eklenme reaksiyonları incelenmiştir. Çeşitli açıl fosfonatlar potasyum karbonat varlığında CF_3TMS ile kolayca reaksiyona girerek 70-90% verim ile 1-alkil-2,2,2-trifloro-1-trimetilsililoksietil fosfonatları oluşturmuştur. Başlangıç maddesi olarak benzoil fosfonatlar kullanıldığında, CF_3 eklenmesinden sonra oluşan alkolat anyonu açıl anyonu oluşturmak üzere fosfonat-fosfat düzenlenmesine uğmuş ve flor ayrılması ile 87-97% verimle 1-arildifloroetenil fosfonatları oluşturmuştur.

Pirolin-tiyöüre konuk-konak kompleksi katalizörlüğünde sikloheksanon ve aromatik aldehytlerin moleküller arası aldol reaksiyonu geliştirilmiştir. *Anti*-konfigürasyona sahip ürünler yüksek verim ve özellikle yüksek enansiyoseçicilikle elde edilmiştir. Reaksiyonun prolin'in karboksilat kısmı ile tiyöürenin bir birliktelik oluşturduğu değiştirilmiş Houk-List modeline göre ilerlediği önerilmiştir. Bu sonuçlar tiyöürenin düşük sıcaklık kullanılmasına ihtiyaç duyulmadan ve geleneksel olmayan apolar reaksiyon ortamlarında dahi reaktivite ve seçicilik üzerine muazzam etkisini açıkça göstermektedir.

Prolin-tiyöüre konuk-konak kompleksinin aldehitlerin nitro alkenlere enansiyoseçici nitro-Michael eklenmesi için iyi bir katalizör olduđu tanımlanmıştır. Reaksiyon, 5% tiyöüre ile orta ve iyi enansiyoseçicilik (76% *ee*) vermede etkilidir. Dallanmış ve dallanmamış zincirli aldehitlerde yüksek *syn*-seçicilik elde edilmiştir. Bu, aldehitlerin verici olarak kullanıldığı Michael katılma reaksiyonlarında, kiral olmayan katkı maddeleri ile organokatalizörlerin kendiliğinden organize olmalarına ilk örnektir.

Prolin-tiyöüre konuk-konak yapılarının katalizörlüğündeki aldol reaksiyonları polar olmayan çözücülerde çok iyi doğrusal olmayan etki göstermiştir. Bu prolin-tiyöüre sistemleri hidrojen bağı ağı oluşturma becerisine sahiptir. Katı haldeki rasemik prolinin üre molekülü ile birleştirilmesi ile prolinin çözücüdeki enansiyomerik aşırılığı önemli miktarda arttırılabilir. Bu, belki de yer yüzündeki kiralitenin kaynağı olan homokiralite için genel ve basit bir yol önermektedir.

Anahtar Kelimeler: Açıl anyon, Umpolung, Açılfosfonat, Asimetrik Kataliz, Organokataliz.

I dedicate this dissertation to Prof. Dr. Ayhan Sıtkı Demir, who will be remembered long after the content of this thesis is forgotten

ACKNOWLEDGEMENTS

First and foremost, I am deeply indebted to my mentor Prof. Dr. Ayhan S. Demir whose valuable guidance, criticism, suggestions and encouragement lead to the creation of thesis. In addition to helpful discussions, advice and project guidance, he played an important role in allowing me to develop scientific ideas and concepts into concrete experiments and results, and to mature as a scientist. It really is my fortune to have the opportunity to learn and explore chemistry under his intellectual direction and what I learned from him is and will be the treasure of my whole life.

I am really grateful to past and present members of the Demir research group for their helpful advice and discussion about chemistry and making our research group an enjoyable place.

I would like to express thanks to Prof. Dr. Metin Balcı, Prof. Dr. Metin Zora, Prof. Dr. Özdemir Doğan, Prof. Dr. Mustafa Yılmaz, and Assist. Prof. Dr. Akın Akdağ for being committee member for my dissertation.

I wish to convey my sincere appreciations to Assist. Prof. Dr. Akın Akdağ for his precious time, patience, and intellectual conversation in reading all parts of this work and evaluating this dissertation. He even pointed out a single grammar mistake in my dissertation, and that improved my English a lot. I would also like to thank Prof. Dr. Özdemir Doğan for proofreading this document.

I would also like to thank Prof. Dr. Metin Balcı for his support and words of encouragement after the sudden death of my mentor Prof. Dr. Ayhan Sıtkı Demir.

I would like to my endless thanks Dr. Ömer Reis, and Barbaros Reis, for their kind helps, contributions and efforts concerning the chemistry of organocatalysis.

I wish to express also my thanks to dear friend Mehmet Göllü for helping and supporting me whenever I need.

I also wish to thank Ezgi Demircan for her help to write this thesis in its final shape.

I would also like to thank Selçuk University for the financial support during my thesis via Faculty Development Program (ÖYP) and TUBITAK 2214 Scholarship Program.

In the words of Jonas Edward Salk: “Good parents give their children Roots and Wings. Roots to know where home is, wings to fly away and exercise what’s been taught them.” I would like to thank my parents Fatma & Rüstem and my dear sisters’ Şerife & Betül for not only giving me my Roots and Wings, but for inspiring me with their dedication and hard work. I have move so far away, but it does not seem like you are too far from here. Thank you for all of your support.

I love you, Gülüzar. You have been a guiding light and rock throughout my life and I am sure my life would have followed a very different path without your love. None of this would have been possible without you. You have made this whole journey possible. I could not have made it through without your love, prayers, encouragement, and support. It is my greatest honor to be married to

such an amazing woman. This acknowledgement can be hundreds of pages long, but there is a limit so I will keep it short, Love you doodlebug.

TABLE OF CONTENTS

ABSTRACT	iv
ÖZ	vi
TABLE OF CONTENTS	xii
LIST OF FIGURES	xv
LIST OF TABLES	xxii
ABBREVIATIONS	xxiii
CHAPTERS	
1. INTRODUCTION	1
1.1 Catalytic C-C bond forming reactions	1
1.1.1 Nonchiral catalytic C-C bond forming reactions via acyl anion chemistry	2
1.1.1.1 Positional Polar Reactivity	2
1.1.1.2 Benzoin condensation Reactions	7
1.1.1.3 Catalytic Methods for generation of acyl anion equivalents	13
1.2 Organocatalytic Asymmetric C-C Bond Formation Reactions	30
1.2.1 Classification of Organocatalysis	34
1.2.2 Enamine Catalysis	40
1.2.2.1 Enantioselective Organocatalytic Aldol Reactions by Enamine Catalysis	42
1.2.2.2 Enantioselective Organocatalytic Michael Reactions by Enamine Catalysis	53
1.2.3 Asymmetric amplifications in Enantioselective Catalysis	57
1.3 The aim of the work	69
1.3.1 Addition of Trifluoromethyltrimethylsilane to Acyl Phosphonates	69
1.3.2 Development of new supramolecular organocatalytic strategies for the enantioselective asymmetric C-C bond forming reactions	70

1.3.3 Nonlinear effects in proline–thiourea host–guest complex catalyzed aldol reactions in nonpolar solvents	70
2. RESULTS AND DISCUSSION	72
2.1 Addition of Trifluoromethyltrimethylsilane to Acyl Phosphonates	72
2.2 Development of new supramolecular organocatalytic strategies for the enantioselective asymmetric C-C bond forming reactions	89
2.2.1 Direct enantioselective aldol reactions catalyzed by a proline–thiourea host–guest complex	92
2.2.2 Self-assembly of organocatalysts for the enantioselective Michael addition of aldehydes to nitroalkenes	101
2.2.3 Nonlinear effects in proline–thiourea host–guest complex catalyzed aldol reactions in nonpolar solvents	109
3. EXPERIMENTAL	120
3.1 Synthesis of TMS Protected 1-Alkyl-1-trifluoromethyl-1-hydroxyphosphonates and 1-Aryl-difluoroethenyl Phosphates	120
3.1.1 General Procedure for the Addition of TMSCF ₃ to Acyl Phosphonates:	121
3.2 Direct Enantioselective Aldol Reactions catalyzed by a Proline-Thiourea Host-Guest Complex	130
3.2.1 General Procedure for the Enantioselective Direct Aldol Reaction	130
3.3 Self-assembly of organocatalysts for the enantioselective Michael addition of aldehydes to nitroalkenes	135
3.4 Nonlinear effects in proline–thiourea host–guest complex catalyzed aldol reactions in nonpolar solvents	143
4. CONCLUSIONS	145
4.1 Addition of Trifluoromethyltrimethylsilane to Acyl Phosphonates	145
4.2 Development of new supramolecular organocatalytic strategies for the enantioselective asymmetric C-C bond forming reactions	145

4.3 Nonlinear effects in proline–thiourea host–guest complex catalyzed aldol reactions in nonpolar solvents	146
REFERENCES	147
APPENDICES	
A. NMR	160
B. HPLC	173
CURRICULUM VITAE	192

LIST OF FIGURES

FIGURES

Figure 1.1 General rule for the polarity of bond formation.....	3
Figure 1.2 Charge affinity pattern and Seebach notation of β -hydroxy ketone 1	3
Figure 1.3 Seebach notation of a ketone 2	4
Figure 1.4 Polar disconnections for α -hydroxy ketone 6	5
Figure 1.5 Dithiane Umpolung reactivity of carbonyl compound	6
Figure 1.6 Popular examples of acyl anion equivalents.....	7
Figure 1.7 Benzoin condensation mechanism	8
Figure 1.8 Product distribution for dimerization of two different aldehydes.....	10
Figure 1.9 Thiamine Pyrophosphate structure	11
Figure 1.10 Catalytic cycle of TPP dependent enzymes catalyzed benzoin condensation.....	12
Figure 1.11 [1,2] and [1,n]-silyl migrations	14
Figure 1.12 Brook rearrangement mechanism	14
Figure 1.13 Formation of α -silyl alkoxides	15
Figure 1.14 Methods for the synthesis of acylsilanes	16
Figure 1.15 Nucleophilic catalytic additions to acylsilanes	17
Figure 1.16 [1,2]-Brook rearrangement initiated by nucleophilic catalysts.....	18
Figure 1.17 Synthesis of unsymmetrical protected benzoin compound regioselectively.....	19
Figure 1.18 Access to cyanophosphate anions.....	21
Figure 1.19 Generation of acyl anion equivalents from acylphosphonates via.....	22
Figure 1.20 Mechanism of cross-benzoin reaction via cyanide ion promoted generation of acyl anions from acylphosphonates	23
Figure 1.21 Synthesis of acylphosphonate via arbusov reaction	24

Figure 1.22 Catalytic intermolecular aldehyde–ketone coupling via acylphosphonates.....	25
Figure 1.23 Protonation of acyl anion equivalents generated from acylphosphonates.....	25
Figure 1.24 Methods for the synthesis of cyanohydrins	26
Figure 1.25 Cyanide ion promoted addition of acyl phosphonates to ethyl cyanoformate	27
Figure 1.26 Proposed catalytic cycle for synthesis of tertiary carbinols via tandem carbon-carbon bond formations.....	28
Figure 1.27 Uncatalyzed addition of TMSCN to acylphosphonates.....	29
Figure 1.28 Examples of enantiomers	30
Figure 1.29 Compound 102 catalyzed the methanolysis of ketene 100.....	33
Figure 1.30 Hajos-Parrish-Eder-Sauer-Wiechert reaction	34
Figure 1.31 Classification of simplified organocatalytic cycles by List	35
Figure 1.32 Organization of the organocatalysis regarding generic mode of activation of catalytic systems.....	37
Figure 1.33 Enamine catalysis concepts.....	38
Figure 1.34 Iminium catalysis concepts	39
Figure 1.35 General mechanism of the enamine catalysis	41
Figure 1.36 Mechanism of the Hajos-Parrish-Eder-Sauer-Wiechert reaction.....	43
Figure 1.37 Proposed transition states for the Hajos-Parrish-Eder-Sauer-Wiechert reaction	44
Figure 1.38 Direct asymmetric intermolecular aldol reactions	45
Figure 1.39 Screening of catalysts for direct asymmetric intermolecular aldol reactions.....	46
Figure 1.40 Modes of action in proline-catalysis	47
Figure 1.41 Proposed mechanism of the proline-catalyzed intermolecular aldol reaction	49
Figure 1.42 Parasitic off-cycle equilibrium.....	50

Figure 1.43 Typical Substituted ketone donors in asymmetric enamine catalysis.	51
Figure 1.44 A literature selection of proline based organocatalysts used in enamine catalyzed direct aldol reactions	52
Figure 1.45 The Michael reaction of carbon-centered nucleophiles with nitroalkenes	53
Figure 1.46 Organocatalysis of the Michael reactions	54
Figure 1.47 The first organocatalytic asymmetric Michael addition of unmodified aldehydes to nitroolefins	55
Figure 1.48 A literature selection of organocatalytic Michael addition reactions .	56
Figure 1.49 A literature selection of proline based organocatalysts used in enamine catalyzed asymmetric Michael addition reactions.....	57
Figure 1.50 Relationships between enantioselectivity of the reaction product and enantiomeric excess of the chiral catalyst	59
Figure 1.51 (a) Sharpless asymmetric epoxidation (b) oxidation of sulfide 222 ...	60
Figure 1.52 Schematic respresentation of ML_2 system	61
Figure 1.53 Schematic respresentation of reservoir effect model system	62
Figure 1.54 Isopropylation of pyridine-3-carboxyaldehyde (232) in the presence of catalytic amount of the reaction product 230	63
Figure 1.55 Blackmond's mechanistic model for the Soai reaction.....	64
Figure 1.56 Ternary phase diagram for Proline in DMSO	67
Figure 1.57 (a) The asymmetric unit of <i>DL</i> -Proline/chloroform (b) Structure of racemic proline crystallized from a $CHCl_3/CH_3OH$ mixture, with one $CHCl_3$ molecule (black) incorporated per pair of proline molecules.....	68
Figure 2.1 Instability of the naked trifluoromethyl anion	73
Figure 2.2 Facile syntheses of TMS-protected trifluoromethylated alcohols	74
Figure 2.3 Formation of difluoroenol silyl ethers from acylsilanes	74
Figure 2.4 CF_3 additions to acylphosphonates	75
Figure 2.5 CF_3TMS addition to isobutyryl phosphonate 243	76
Figure 2.6 ^{13}C NMR spectra of 244	77

Figure 2.7 ^1H NMR spectra of 244.....	77
Figure 2.8 General reaction scheme of CF_3TMS addition reaction to alkylphosphonates	78
Figure 2.9 General reaction scheme of CF_3TMS addition reaction to aryl phosphonates	80
Figure 2.10 ^1H NMR spectra of 254.....	81
Figure 2.11 ^{13}C NMR spectra of 254	81
Figure 2.12 Addition of CF_3TMS to furoyl phosphonate 265	85
Figure 2.13 A possible mechanism for the formation of intermediates 268-270 from TMSCF_3 and potassium carbonate	86
Figure 2.14 A possible mechanism for the addition of TMSCF_3 to acyl phosphonates	88
Figure 2.15 A literature example of self-assembly of organocatalysts	91
Figure 2.16 Houk model for the proline catalyzed intermolecular aldol reaction..	92
Figure 2.17 Supramolecular self assembly organocatalysts.....	93
Figure 2.18 General reaction schemes for the direct enantioselective aldol reactions catalyzed by a proline–thiourea host–guest complex	94
Figure 2.19 The direct enantioselective aldol reactions	97
Figure 2.20 The ^1H NMR spectra of proline-thiourea complex.....	98
Figure 2.21 Proposed catalytic reaction mechanism for the direct enantioselective aldol reactions catalyzed by a proline–thiourea host–guest complex	100
Figure 2.22 Michael addition reactions of isovaleraldehyde (282) to trans- β - nitrostyrene (283)	102
Figure 2.23 General reaction schemes for the direct asymmetric Michael reaction catalyzed by a proline–thiourea host–guest complex.....	103
Figure 2.24 The direct asymmetric Michael reaction.....	105
Figure 2.25 Stereochemical outcome of the the direct asymmetric Michael reaction catalyzed by a proline–thiourea host–guest complex.....	107

Figure 2.26 Proposed catalytic reaction mechanism for the direct asymmetric Michael reaction catalyzed by a proline–thiourea host–guest complex	108
Figure 2.27 General reaction schemes for the direct enantioselective aldol reactions catalyzed by a proline–thiourea host–guest complex	111
Figure 2.28 Relationship between the enantioselectivity of the reaction product and the enantiomeric excess of proline.	114
Figure 2.29 (A) and (B): The proposed interaction of the thiourea moiety with proline in solution and in the transition state, respectively.	116
Figure 2.30 The <i>ee</i> value of the aldol reaction versus the <i>ee</i> of proline shows a constant <i>ee</i> value when increasing the <i>ee</i> value of proline.....	119
Figure A1. ¹ H NMR spectrum of 244	160
Figure A2. ¹³ C NMR spectrum of 244	160
Figure A3. ¹ H NMR spectrum of 247	161
Figure A4. ¹³ C NMR spectrum of 247	161
Figure A5. ¹ H NMR spectrum of 249	162
Figure A6. ¹³ C NMR spectrum of 249	162
Figure A7. HBMC spectrum of 249.....	163
Figure A8. ¹ H NMR spectrum of 251	164
Figure A9. ¹³ C NMR spectrum of 251	164
Figure A10. HBMC spectrum of 251	165
Figure A11. ¹ H NMR spectrum of 258	166
Figure A12. ¹³ C NMR spectrum of 258	166
Figure A13. ¹ H NMR spectrum of 256	167
Figure A14. ¹³ C NMR spectrum of 256	167
Figure A15. ¹ H NMR spectrum of 253	168
Figure A16. ¹³ C NMR spectrum of 253	168
Figure A17. ¹ H NMR spectrum of 260	169
Figure A18. ¹³ C NMR spectrum of 260	169
Figure A19. ¹ H NMR spectrum of 262	170

Figure A20. ^{13}C NMR spectrum of 262	170
Figure A21. ^1H NMR spectrum of 264	171
Figure A22. ^{13}C NMR spectrum of 264	171
Figure A23. ^1H NMR spectrum of 267 and 268.....	172
Figure B1. HPLC chromatogram of <i>rac</i> -281	173
Figure B2. HPLC chromatogram of enantioenriched 281	173
Figure B3. HPLC chromatogram of <i>rac</i> -283	174
Figure B4. HPLC chromatogram of enantioenriched 283	174
Figure B5. HPLC chromatogram of <i>rac</i> -287	175
Figure B6. HPLC chromatogram of enantioenriched 287	175
Figure B7. HPLC chromatogram of <i>rac</i> -289	176
Figure B8. HPLC chromatogram of enantioenriched 289	176
Figure B9. HPLC chromatogram of <i>rac</i> -291	177
Figure B10. HPLC chromatogram of enantioenriched 291	177
Figure B11. HPLC chromatogram of <i>rac</i> -293	178
Figure B12. HPLC chromatogram of enantioenriched 293	178
Figure B13. HPLC chromatogram of <i>rac</i> -295	179
Figure B14. HPLC chromatogram of enantioenriched 295	179
Figure B15. HPLC chromatogram of <i>rac</i> -190	180
Figure B16. HPLC chromatogram of enantioenriched 190	180
Figure B17. HPLC chromatogram of <i>rac</i> -298	181
Figure B18. HPLC chromatogram of enantioenriched 298	181
Figure B19. HPLC chromatogram of <i>rac</i> -304	182
Figure B20. HPLC chromatogram of enantioenriched 304	182
Figure B21. HPLC chromatogram of <i>rac</i> -312	183
Figure B22. HPLC chromatogram of enantioenriched 312	183
Figure B23. HPLC chromatogram of <i>rac</i> -316	184
Figure B24. HPLC chromatogram of enantioenriched 316	184
Figure B25. HPLC chromatogram of <i>rac</i> -317	185

Figure B26. HPLC chromatogram of enantioenriched 317	185
Figure B27. HPLC chromatogram of <i>rac</i> -319	186
Figure B28. HPLC chromatogram of enantioenriched 319	186
Figure B29. HPLC chromatogram of <i>rac</i> -320	187
Figure B30. HPLC chromatogram of enantioenriched 320	187
Figure B31. HPLC chromatogram of <i>rac</i> -321	188
Figure B32. HPLC chromatogram of enantioenriched 321	188
Figure B33. HPLC chromatogram of <i>rac</i> -304	189
Figure B34. HPLC chromatogram of enantioenriched 304	189
Figure B35. HPLC chromatogram of <i>rac</i> -322	190
Figure B36. HPLC chromatogram of enantioenriched 322	190
Figure B37. HPLC chromatogram of <i>rac</i> -324	191
Figure B38. HPLC chromatogram of enantioenriched 324	191

LIST OF TABLES

TABLES

Table 1. The results of the addition of CF ₃ TMS to different alkyl phosphonates .	79
Table 2. The results of addition of CF ₃ TMS to aryl phosphonate 252 using different catalysts	82
Table 3. CF ₃ TMS Addition to benzoyl phosphonate 252 in different solvents	83
Table 4. The results of the addition of CF ₃ TMS to different aryl phosphonates ...	84
Table 5. Initial Screening of Conditions for the Formation of Aldol 278	95
Table 6. Enantioselective direct aldol reaction of aldehydes and cyclohexanone .	97
Table 7. The enantioselective Michael reaction of 302 and 303 under various conditions	104
Table 8. The enantioselective Michael Addition of aldehydes to nitroalkenes....	106
Table 9. Screening of the solvent for an proline (20% <i>ee</i>)-thiourea 279 complex-(20:20%)-catalyzed enantioselective direct aldol reaction of aldehydes 2 and cyclohexanone	112
Table 10. Relationship between the enantioselectivity of the reaction* and the enantiomeric excess of proline	113
Table 11. Determination of the soluble proline <i>ee</i> value during the experiment after 16h	116
Table 12. The <i>ee</i> value of the aldol reaction catalyzed by proline along with various <i>ee</i> values.	118

ABBREVIATIONS

C-C	Carbon-Carbon
a	Acceptor
d	Donor
FG	Functional Group
E	Electrophile
Nu	Nucleophile
TPP	Thiamine Pyrophosphate
NHC	N-heterocyclic carbene
M	Metal
L	Ligand
A	Acid
B	Base
P	Product
Cat	Catalyst
DBU	1,8-Diazabicyclo[5.4.0]undec-7-ene
TBACN	Tetrabutylammonium Cyanide
DMF	N,N-dimethylformamide
TMS	Trimethylsilyl
TMSCN	Trimethylsilyl cyanide
FDA	Food & Drug Administration
ee	Enantiomeric Excess
dr	Diastereomeric Ratio
HOMO	Highest Occupied Molecular Orbital
LUMO	Lowest Unoccupied Molecular Orbital
SOMO	Singly Occupied Molecular Orbital

LA	Lewis Acid
DMSO	Dimethyl Sulfoxide
TS	Transition state
THF	Tetrahydrofuran
r.t	Room Temperature
NLE	Non-Linear Effect
DET	Diethyl Tartarate
CF ₃ TMS	Trifluoromethyltrimethylsilane
TBAF	Tetra-n-Butylammonium Fluoride
TLC	Thin Layer Chromatography
IR	Infra-Red
MeCN	acetonitrile
°C	degrees Celsius
cm ⁻¹	wavenumber
Conv	conversion
δ	parts per million
Equiv	equivalents
HPLC	high-pressure liquid chromatography
J	coupling constant in Hertz
mg	milligram
min	minutes
mL	millilitre
NMR	nuclear magnetic resonance
S-	sinister (from latin)
R-	rectus (from latin)
Calcd	calculated
Rac-	racemic
Hz	Hertz
HMBC	Heteronuclear Multiple Bond Correlation

CHAPTER 1

INTRODUCTION

1.1 Catalytic C-C bond forming reactions

The synthesis of urea from ammonium cyanate by Friedrich Wöhler in 1828 has been accepted as the turning point for the modern organic chemistry.¹ Thenceforth, with this development, the numerous synthetic organic methods to construct new organic molecules have been established. Carbon-carbon (C-C) bond formation reactions have been the key point for all of organic reactions in the history of organic synthesis.² However, the investigations of catalytic methods for carbon-carbon bond formation, while creating functionality, remain a formidable challenge in the continuing development of efficient and reliable chemical processes. Due to the advantages of catalytic methods such as high atom economy,³ less polluting and workable simplicity, catalytic C-C bond forming reactions have garnered extensive attention in recent years. On the other hand, the developments of catalytic C-C bond construction methods still remain a challenge in organic synthesis. Therefore, it is foreseeable that the development of chemically useful catalytic methods of C-C bond construction has not yet been attained, and extra effort is needed to accomplish desirable transformations in organic chemistry.

Forming or breaking bonds in organic synthesis have been frequently practiced by the combination of a Lewis acid-base pairs. The most sensitive spot of developing a new synthetic plan to get a desired molecule is classifying parts of molecule as

nucleophilic and electrophilic. Furthermore, an applicable retrosynthetic analysis, converting a synthetic target molecule into simple structures, requires identification of an appropriate synthon (“structural units within in a molecule which is related to possible synthetic operations”).³ While synthons do not appear as they are drawn, they help for the correct selection of the reagents. Once the synthons were defined, it is next necessary to figure out the synthetically equivalent reagents that are the real compounds fulfilling the role of synthon to perform the synthetic operation. For this, classification of functional groups for polar bond construction, namely “organizational format” (charge affinity pattern), was introduced by Evans.⁴ In this concept, the latent electrophilic or nucleophilic character of atoms in a carbon skeleton can be easily identified by using the descriptors as (+) and (-).

1.1.1 Nonchiral catalytic C-C bond forming reactions via acyl anion chemistry

1.1.1.1 Positional Polar Reactivity

Seebach established a useful and powerful antithetic tool for identifying the electronic character of each atom in heteroatom containing carbon skeleton.⁵ As seen in **Figure 1**, the electronegativity differences between the carbon atoms and heteroatoms (O, N, and halides) produces inductive polarization which makes atoms in chain partially charged. That is, heteroatoms enforce an alternating donor (d) /acceptor (a) reactivity pattern on the carbon chain. The polarization renders acceptor properties at 1, 3, 5 positions and donor properties at 2, 4, 6 positions while the heteroatom with higher electronegativity is a donor (**Figure 1.1**).

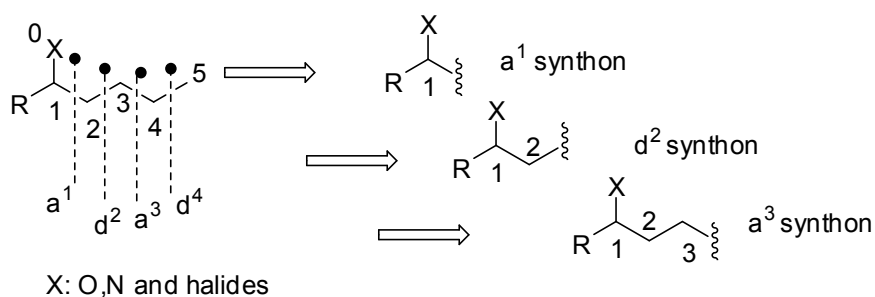


Figure 1.1 General rule for the polarity of bond formation

In Seebach's notation, it is possible that polar disconnections can be applied to various target molecules. In a simple and ideal disconnections, a combination of electrophilic center (a, (+)) and nucleophilic center (d, (-)) is required. Because, many organic reactions, generating C-C bonds, are polar. For instance, charge affinity pattern and Seebach notation of β -hydroxy ketone **1** is outlined together with logical bond disconnections in **Figure 1.2**. It is clear that the heteroatom in functional groups, like =O and -OH, powerfully bias the polar (bond pair) disconnections.

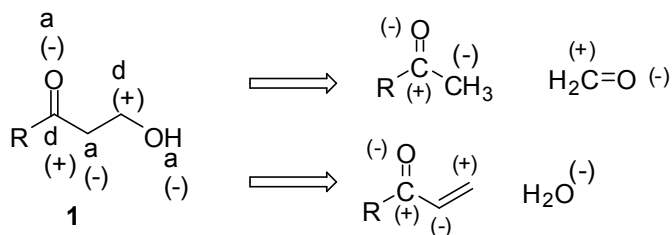


Figure 1.2 Charge affinity pattern and Seebach notation of β -hydroxy ketone **1**

Seebach notation of a simple ketone **2** is depicted in **Figure 1.3**. General charge affinity of carbonyl (C=O) group enables us to make possible polar disconnections as shown in **Figure 1.3**. Therefore, classical organic chemistry can make carbon skeleton with 1, 3 and 1, 5 functional group (FG) substitution patterns. With disconnections done, chemical reagents to achieve the desired polar transformation are necessary. However, some types of substitution pattern need a revised synthetic approach to carry out the desired transformation.

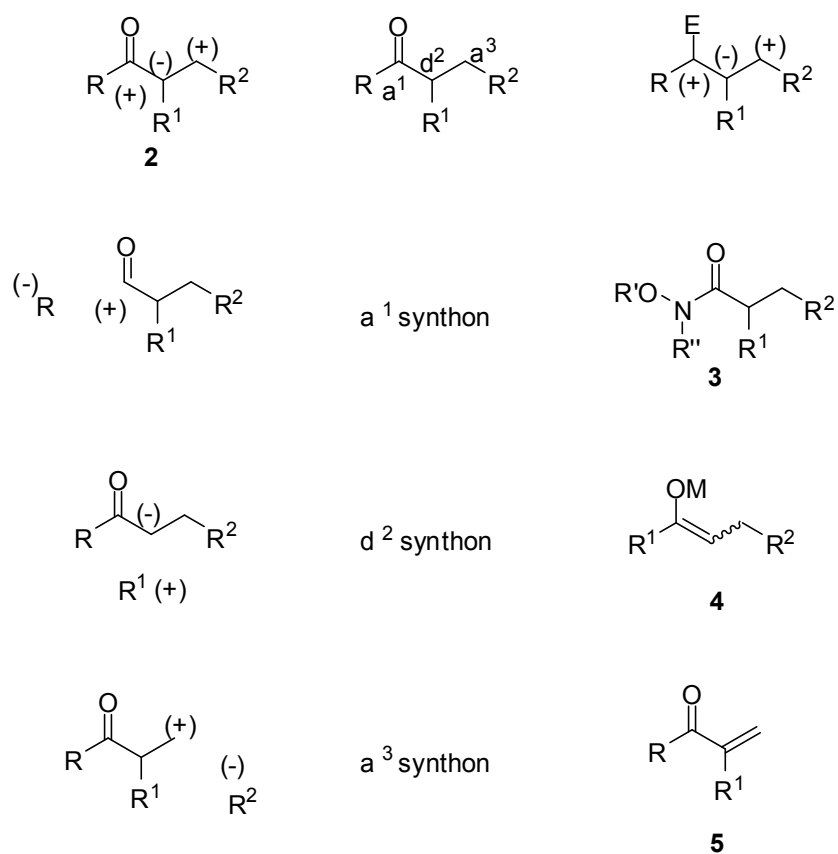


Figure 1.3 Seebach notation of a ketone **2**

The analysis of the polar disconnections for α -hydroxy ketone **6** shows necessity of the combination of the two identical centers with different electronic nature (**Figure 1.4, C**). In reality, an acyl anion is impractical to produce in experimental set up due to the electronic nature of carbonyl group. However, acyl anions can be generated by mainly functional group manipulations that, in practice, convert electrophilic carbonyl to nucleophilic one. This is called “Umpolung”, which is defined by the International Union of Pure and Applied chemists as: “*Any process by which the normal alternating donor and acceptor reactivity pattern of a chain, which is due to the presence of O or N heteroatoms, is interchanged.*”⁶ The original meaning of the term has since been extended to the reversal of any commonly accepted reactivity pattern. Umpolung (polarity reversal) of carbonyl group (acyl anion equivalents) gives a powerful alternative to classical carbon-carbon bond construction methods and adds new dimensions of flexibility to the design of synthetic targets.

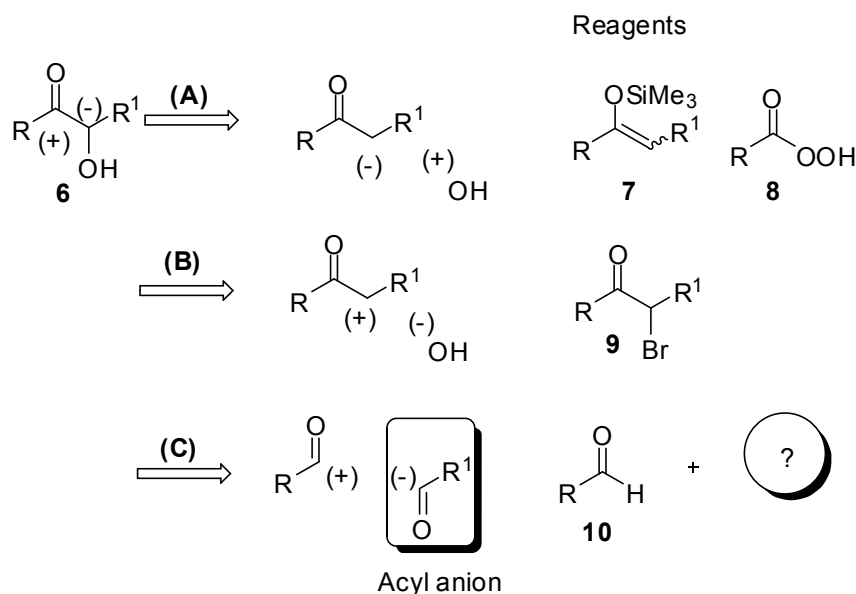


Figure 1.4 Polar disconnections for α -hydroxy ketone **6**

Although acyl anions (d^1 synthons) are not stable, they are traditionally synthesized by functional group manipulation and stoichiometric strong base deprotonation of the corresponding carbonyl compounds. As shown in **Figure 1.5**, Corey-Seebach reaction, in which lithiated dithiane **12** stabilized by the two sulfur atoms employs as an acyl anion nucleophile.⁷ Nucleophilic entities at the carbonyl center are generally called as masked “acyl anion” or “acyl anion equivalents”.

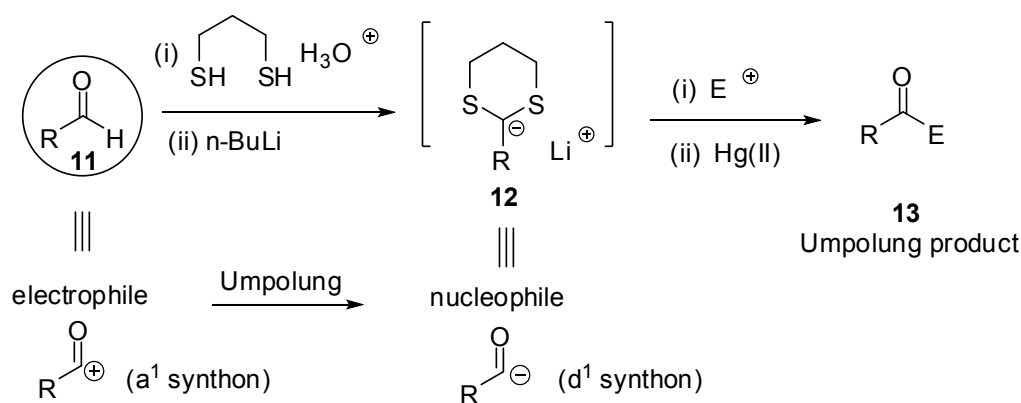


Figure 1.5 Dithiane Umpolung reactivity of carbonyl compound

Well-known examples of acyl anion equivalents are shown in **Figure 1.6**. These equivalents rely on the carbanion stabilizing ability of certain functional groups. With these in hand, new disconnections, different from natural reactivity of the carbonyl group, are possible. Although “acyl anion chemistry” is a promising area in organic chemistry, syntheses of these precursors are not economical in terms of atom and labor due to the multiple protections and deprotection steps. Therefore, recently impressive progress has been made in the catalytic methods for the generation of these useful umpolung entities.⁸

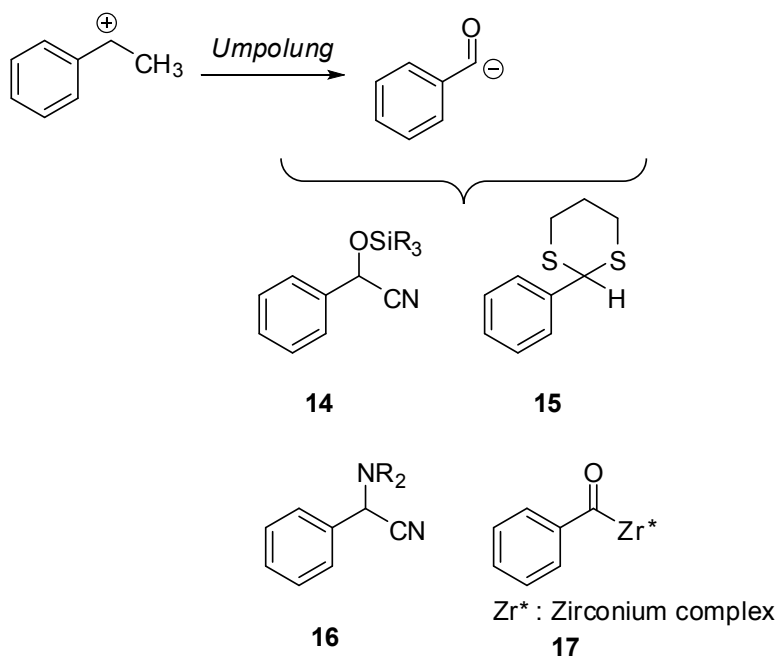


Figure 1.6 Popular examples of acyl anion equivalents

This dissertation is mainly about the development of catalytic methods for C-C bond formation. Therefore, the stoichiometric methods of acyl anion generation are not covered. With this in mind, the catalytically generated acyl anion equivalents will be the main topic for the following remaining part of this chapter.

1.1.1.2 Benzoin condensation Reactions

1.1.1.2.1 Cyanide ion catalyzed benzoin condensation

Benzoin condensation, cyanide ion catalyzed dimerization of two aldehydes, was fortuitously discovered by Liebig and Wöhler in 1832.⁹ The benzoin condensation

is an important strategy to create new C-C bonds leading the formation of α -functionalized carbonyl compounds. This unique process and its mechanism have been intensively studied. In 1903, Lapworth was the first to establish the mechanism of cyanide ion catalyzed benzoin condensation and to determine the formation of crucial carbanion intermediate **20**.¹⁰

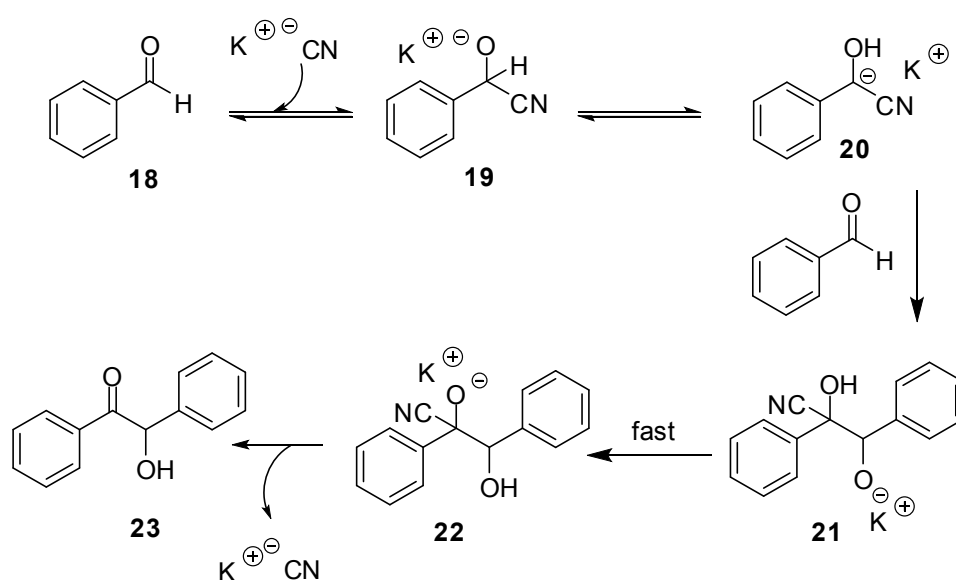


Figure 1.7 Benzoin condensation mechanism

According to putative mechanism in the literature (**Figure 1.7**), this reaction occurs through the cyanide addition to the benzaldehyde (**18**) to yield **19**. A proton transfer follows this from the α -position, producing a carbanion **20** (acyl anion equivalent), which is stabilized via resonance structures. Addition of carbanion **20** to second molecule of an aldehyde occurs to form an unstable cyanohydrin of benzoin **21**, which collapses to generate benzoin **23** and potassium cyanide (catalyst). Cyanide ion owes its ability to act as an effective catalyst in this

reaction to three properties: (1) it is a reactive nucleophile, (2) the cyanide group assists the formation of carbanion species through delocalization of the negative charge on the adjacent carbon, and (3) it acts as a good leaving group.

Although one of the easiest and efficient ways to synthesize α -hydroxy ketones is benzoin condensation, it often suffers from inherent drawbacks. Benzoin condensation has a very limited substrate scope because the aromatic aldehydes with strong electron donating or electron withdrawing groups do not give the corresponding product with consistent yields. Moreover, cyanide ion does not catalyze the benzoin condensation between aliphatic aldehydes, since they tend to undergo an aldol condensation. Another drawback for benzoin condensation is incomplete conversion of reaction caused by reversible steps in the mechanism. Benzoin condensations under classical reaction conditions are also limited to the synthesis of symmetrical homobenzoin.

As we counted several drawbacks for cyanide catalyzed benzoin condensation, it can be concluded that it is not possible to control regioselectivity when two different aldehydes are used. The benzoin condensation is reversible; therefore, the product distribution for dimerization of two different aldehydes is often determined by the relative thermodynamic stabilities of the four possible isomeric products. To exemplify the above discussion, it is better to examine cyanide ion catalyzed benzoin reaction of the two different aldehyde mixtures as shown in **Figure 1.8**. One can infer from the reaction mechanism, attacking of the acyl anion equivalent to another aldehyde in the reaction medium is responsible for the synthesis of the particular benzoin. When two different aldehydes are used, there will be two acceptor aldehydes for each generated acyl anion equivalents. If two different aldehydes were reacting in a kinetically equivalent way, then a statistical mixture of four products would be observed. Consequently, this design fails to give the desired compound as sole product.

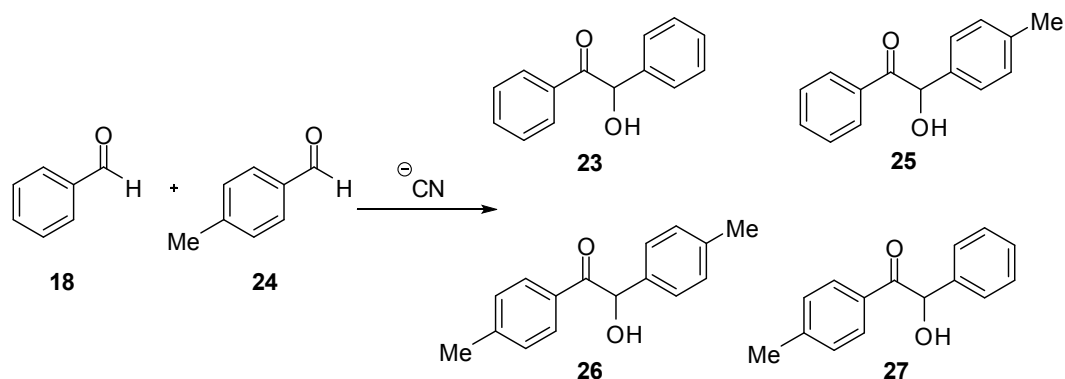


Figure 1.8 Product distribution for dimerization of two different aldehydes

Even though the benzoin reaction has been known in the toolbox of organic chemistry for a long time, employment of this reaction in complex organic synthesis has been restricted due to its inherent drawbacks mentioned *vide supra*. Nevertheless, the nature of benzoin reaction inspires organic chemist to produce practical and easily accessible acyl anion precursors engaging in catalytic C-C bond-forming reactions.^{8,11}

1.1.1.2.2 Thiamine catalyzed benzoin condensation

Numerous enzymes catalyze both nucleophilic acylation and benzoin condensation under mild conditions. Umpolung seems to be basis of these catalytic reactions. To catalyze reactions, enzymes facilitate a cofactor, thiamine pyrophosphate (TPP) (**28**).¹² TPP is a thiazolium salt with three distinctive units: a pyrophosphate part, a thiazolium core, and a pyrimidine unit.

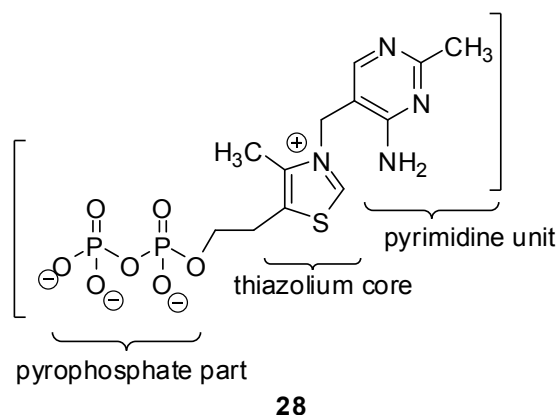


Figure 1.9 Thiamine Pyrophosphate structure

Even though the TPP is mainly involved in a variety of carbon-carbon bond forming reactions, each unit has a special role in enzymatic catalysis. It was reported by Ukai in 1943 that thiazolium salts have ability to catalyze benzoin reaction.¹³ Mizuhara, later showed that thiazolium unit of thiamine is responsible for the catalytic activity of TPP.¹⁴ The function of thiamin diphosphate is similar with the cyanide ion in the benzoin condensation. Based on this, Breslow presented in 1958 a mechanistic model for the thiazolium salt catalyzed benzoin condensation (**Figure 1.10**).¹⁵

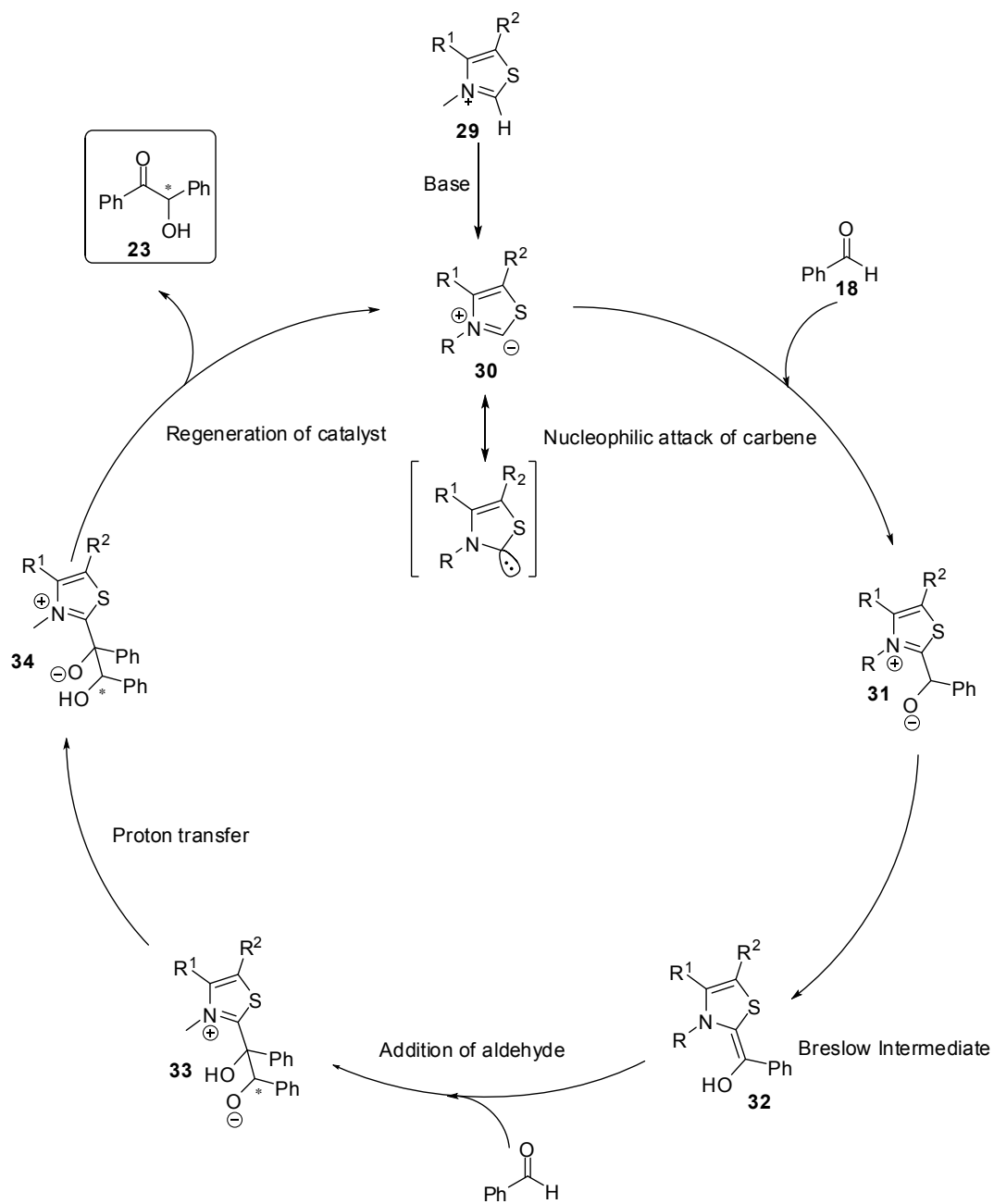


Figure 1.10 Catalytic cycle of TPP dependent enzymes catalyzed benzoin condensation

According to the proposed mechanism, deprotonation of thiazolium salt **29** gives the resulting ylide **30** (in equilibrium with the singlet carbene) that attacks to the carbonyl group of the benzaldehyde (**18**). Rearrangement of the intermediate **31** to **32** creates an umpolung of the carbonyl group. This umpolung enables the formation of the new C–C bond. The carbanion (d^1 -synthon) **32** attacks a new aldehyde to form **33** in stereoselective fashion (Stereoselectivity arises from the active site of an enzyme). A proton shift triggers a detachment of the acyloin **23**. After **23** is released from enzyme active site, the catalyst **30** is now ready for another catalytic cycle.

Explanation of mechanism of thiazolium salt catalyzed acyloin condensation has opened an avenue for a series of investigations for the new nucleophilic carbene based catalysts (NHC).¹⁶ It still remains challenge to achieve intermolecular cross-benzoin condensation because of the competitive self-condensation of aldehydes.

1.1.1.3 Catalytic Methods for generation of acyl anion equivalents

1.1.1.3.1 Brook Rearrangement

The high migratory aptitude of silicon compared to carbon and hydrogen has enabled the study of a large number of silyl migrations to date.¹⁷ In 1952, Speier observed anionic [1,2]-silyl migration from oxygen to carbon.¹⁸ The reverse reaction, the intramolecular anionic [1,2]-silyl migration from carbon to oxygen was found and studied by Brook in the 1950s and 1960s.¹⁹ The migratory aptitude of silyl groups has since been observed to be more general, including whole family of [1,n]-carbon to oxygen silyl migration commonly referred to as Brook rearrangements (**Figure 1.11**).

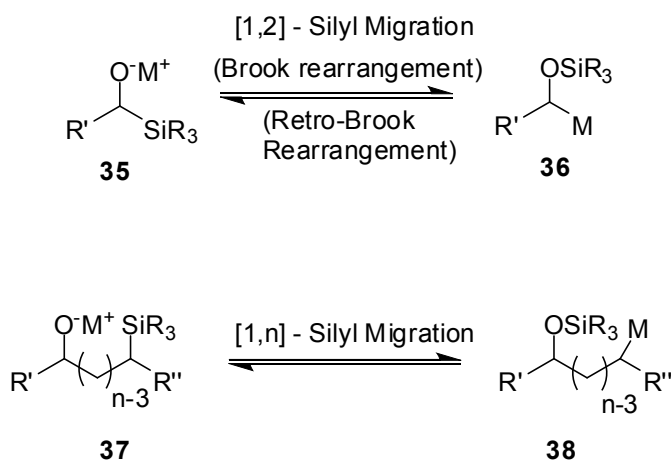


Figure 1.11 [1,2] and [1,n]-silyl migrations

Brook also studied the mechanism of this rearrangement. As seen in **Figure 1.12**, the proposed mechanism goes through formation of an acyl anion equivalent **42** via deprotonation of a carbinol **39** followed by anionic [1,2]-Brook rearrangement. A carbanion-like species **42** quickly are protonated to afford alkoxy silane **43**.

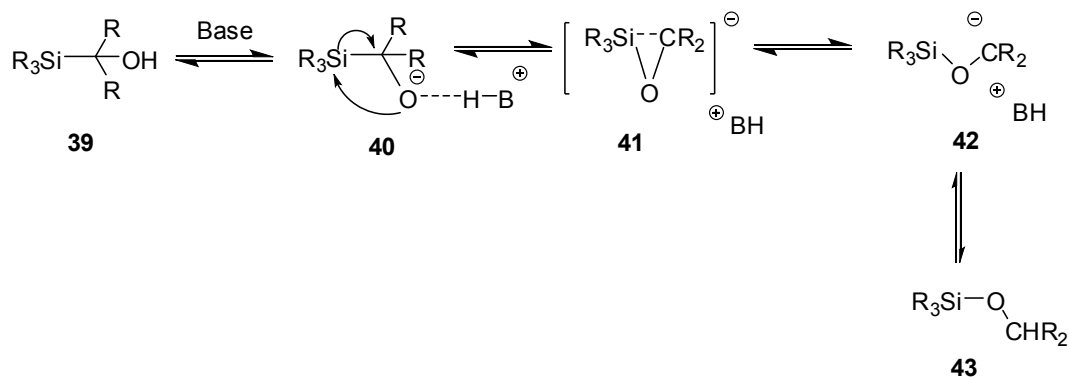


Figure 1.12 Brook rearrangement mechanism

According to thermodynamics, the strength of the oxygen-silicon bond (120-130 kcal mol⁻¹) compared to carbon-silicon bond (70-85 kcal mol⁻¹) provide a driving force for [1,2]-Brook rearrangement from silylalkoxide **40** to silyloxy carbanion **42**.²⁰

It was found sixty years ago, [1,2]-Brook rearrangement has received great attention and been employed in various synthetic methodologies. In general, there are two important methods for the initiation of intramolecular silyl migration (**Figure 1.13**): [1,2]-Brook rearrangement is initiated by the deprotonation of α -silyl alcohol **47** in the presence of base such as alkyl alkali metals (*e.g.* BuLi) or amines. Due to the limitation in the structural diversity of silyl alcohols like **47**, only few applications of base-promoted [1,2]-Brook rearrangement have been found in complex organic syntheses. Second, alternatively, any nucleophilic addition of alkyl metals **45** to acyl silanes **44** also initiates the [1,2]-Brook rearrangement.

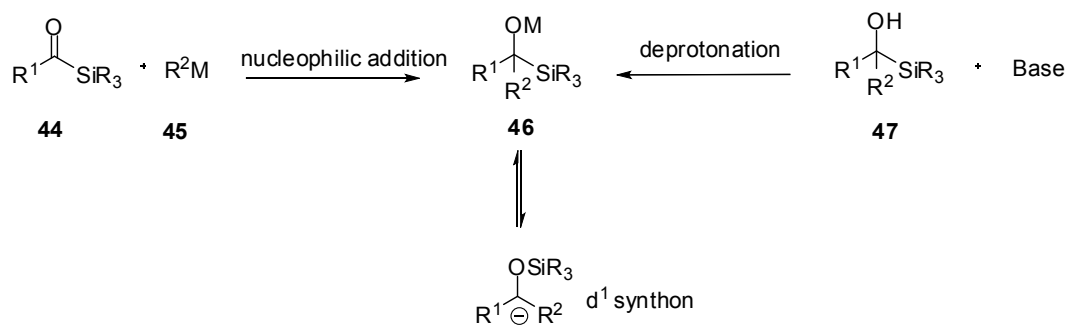


Figure 1.13 Formation of α -silyl alkoxides

1.1.1.3.2 [1,2]-Brook Rearrangement of Acylsilanes

1.1.1.3.2.1 Synthesis of Acylsilanes

As far as the cross-benzoin reaction is concerned, the use of acylsilanes as acyl anion precursors based on the nucleophile promoted [1,2]-Brook rearrangement is one of the most practical and selective method available (**Figure 1.13**).²¹ Therefore, acylsilanes are very useful compounds as unusual acyl anion precursors. However, synthetic protocols for the acylsilanes suffer from tedious steps and low yields. On the top of it, most of the time they are synthesized from the corresponding acyl anions which we eventually seek for.²²

There are many methods to construct the carbonyl carbon-silicon bonds, some of who is shown in **Figure 1.14**. As can be inferred from the **Figure 1.14**, availability of such starting materials has been a long-standing limitation of these methods by which we get acylsilanes.

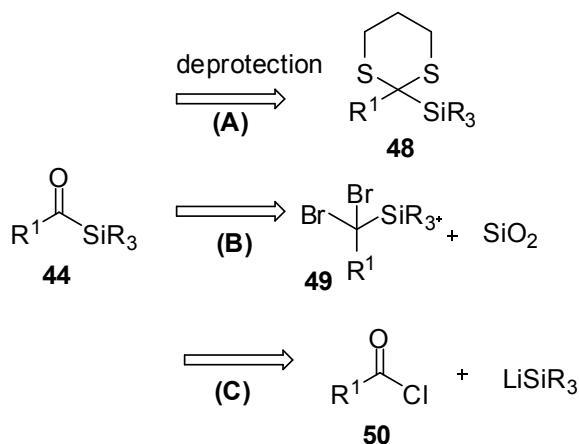


Figure 1.14 Methods for the synthesis of acylsilanes

For instance, dithiane methodology (**Figure 1.14-A**), investigated by Brook^{23a} and Corey^{23b}, is the most utilized method for acylsilane synthesis. The main drawback of this method is the deprotection step from dithiane **48** to **44**. Although the deprotonation of silyl 1,3-dithiane **48** to **44** is relatively easy, compounds like **44** are highly sensitive to the reaction conditions due to the susceptibility of acylsilanes to hydrolysis. Therefore, extensive and practical method for the synthesis of acylsilanes is still in demand.

1.1.1.3.2.2 Catalytic Reactions of Acylsilanes as Acyl Anion Precursors

Nucleophilic catalysts for [1,2]-Brook rearrangement of acylsilanes have been actively studied in the last decade. Thiazolium carbenes, metallophosphites and cyanide anions, are most known examples of nucleophilic catalysts that are used to initiate the Brook rearrangement (general example are shown in **Figure 1.15**).²⁴ Their nucleophilic functions and anion stabilization properties are same as cyanide anion in benzoin condensation.

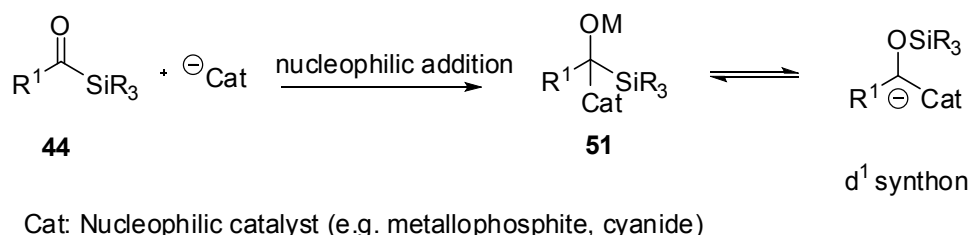
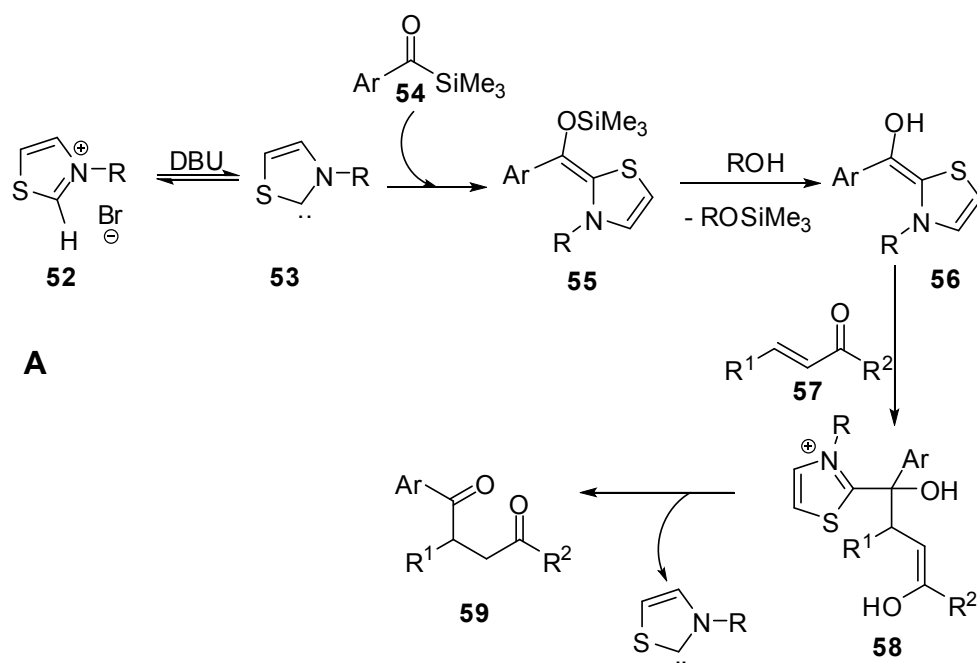


Figure 1.15 Nucleophilic catalytic additions to acylsilanes

Scheidt demonstrated that Brook rearrangement can be induced by carbenes (neutral Lewis base) as shown in **Figure 1.16-A**.²⁵ According to proposed mechanism; carbene catalyst **53**, generated in situ via deprotonation, attacks to the acylsilane **54** and initiates the Brook rearrangement. Desilylation of intermediate **55** produces Breslow intermediate **56** that does the nucleophilic additions to Michael acceptor **57** to yield aryl ketones **59**.



B

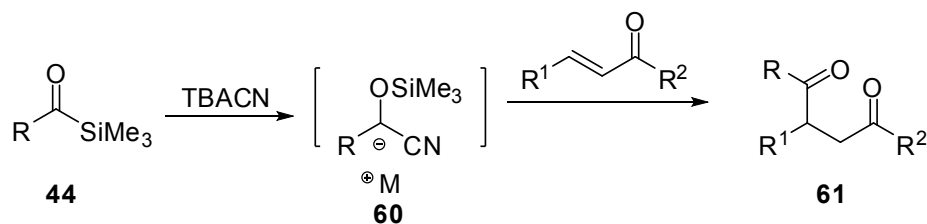


Figure 1.16 [1,2]-Brook rearrangement initiated by nucleophilic catalysts

Cyanide ion initiated the Brook rearrangement of acylsilanes was firstly reported by Degl'Innocenti.²⁶ They showed that acylsilane **44** reacts with α,β -unsaturated carbonyl derivatives **57** to give 1,4-dicarbonyl compounds **61** in the presence of catalytic amount of cyanide ion (**Figure 1.16-B**). Proposed mechanism for this transformation involves generation of silyloxy nitrile intermediate **60** via successively a cyanation and a Brook rearrangement. This reaction was one of the first examples of a catalyzed reaction of acylsilanes.

The silyloxy nitrile anions like **60** generated by cyanide ion added to acylsilanes are interesting intermediates for the numerous organic reactions. Compared to the acylation and alkylation reactions of these intermediates like **60**, the analogous carbonyl addition reactions have been limited to few applications under catalytic conditions. Johnson researched cyanide ion promoted silyl benzoin reactions to synthesize unsymmetrical protected benzoin compounds like **67** with good regioselectivity (**Figure 1.17**).²⁷

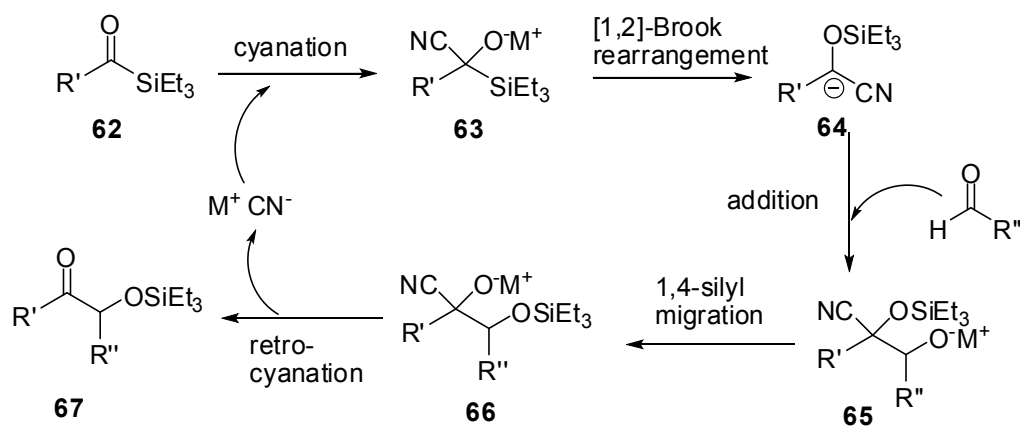


Figure 1.17 Synthesis of unsymmetrical protected benzoin compound regioselectively

As shown in **Figure 1.17**, the proposed mechanism of the reaction is basically same as the classical benzoin condensation catalyzed by the cyanide (**Figure 1.7**) or the thiamine (**Figure 1.10**). The cross silyl benzoin reaction relies on the generation of an acyl anion equivalent **64** by addition of cyanide to an acylsilane **62** followed by [1,2]-Brook rearrangement. Upon attack of **64** to the desired aldehyde, secondary oxyanion **65** is obtained. [1,4]-silyl transfer and a subsequent retro-cyanation yield the desired silyl-benzoin product **67**. On the other hand, Johnson later demonstrated that counterion (M^+) in MCN catalysis is highly critical, and that one lanthanum tricyanide ($La(CN)_3$) was identified as the optimal catalysts after screening of various metal cyanides.²⁸

In summary, acyl silanes are not only useful acyl anion precursors but also good catalysts to achieve regioselective benzoin type products in one step. Nowadays, cyanide catalyzed silyl benzoin reaction have played a prominent and practical role in cross-benzoin condensation reactions.²⁹ It is a well-established method utilizing catalytic generation of acyl anion equivalents. Nevertheless, the major limitation of the acylsilane chemistry is its complexity and difficult availability of the starting acylsilanes as mentioned before. The starting material synthesis is a multi-step process and the deprotection of the dithiane requires superstoichiometric amounts of Hg(II) salts. Recently published alternative method for acylsilane synthesis also stem for the use of stoichiometric amount of a strong base in anhydrous solvents under strict temperature control.³⁰ With all these in mind, there is always a need for a practical and easily accessible acyl anion precursor that can engage in catalytic C-C bond forming reactions.

1.1.1.3.3 Generation of Acyl Anion Equivalents from Acylphosphonates

Phosphorus, like silicon in the Brook rearrangement, has the ability to migrate from carbon to oxygen and oxygen to carbon.³¹ It has been already established that base-catalyzed addition of dialkyl phosphites to acylphosphonates followed by a deprotonation of α -hydroxyphosphonates led to such phosphonate-phosphate rearrangements. This is similar to the [1,2]-Brook rearrangement of acylsilanes.³² Kurihara and co-workers showed that deprotonated cyanophosphates **70** can be effective nucleophilic partners to aldehyde electrophiles as shown in **Figure 1.18**, **route A**.³³ However, same study reported that with R^1 being electron-rich aromatic and aliphatic groups cyano-phosphate anions like **70** are not useful as acyl anion analogous. In route B, surprisingly, cyano-phosphate anions **70** could be catalytically generated from acylphosphonates **69** (**Figure 1.18**).

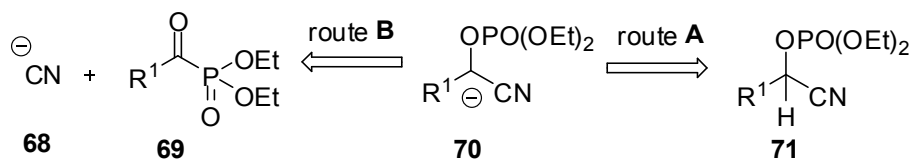


Figure 1.18 Access to cyanophosphate anions

Demir *et al.* have found that acylphosphonates are new generation of potent acyl anion precursors. These precursors undergo nucleophile-promoted phosphonate-phosphate rearrangement to provide the corresponding acyl anion equivalents as reactive intermediates (**Figure 1.19**).³⁴

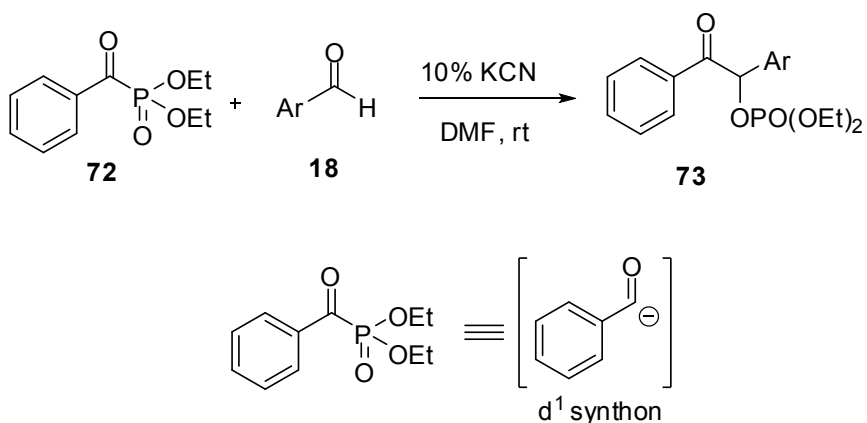


Figure 1.19 Generation of acyl anion equivalents from acylphosphonates via Phosphonate-phosphate rearrangement

The proposed mechanism, shown in **Figure 1.20**, resembles benzoin reaction mechanism and its congeners. Cyanide ion promoted rearrangement affords the critical acyl anion equivalent **73**, which reacts with aldehyde **74** to give the intermediate adduct **75**. This adduct undergoes a [1,4]-O,O-phosphate migration leading to retrocyanates as usual to give the desired benzoin product **77**.

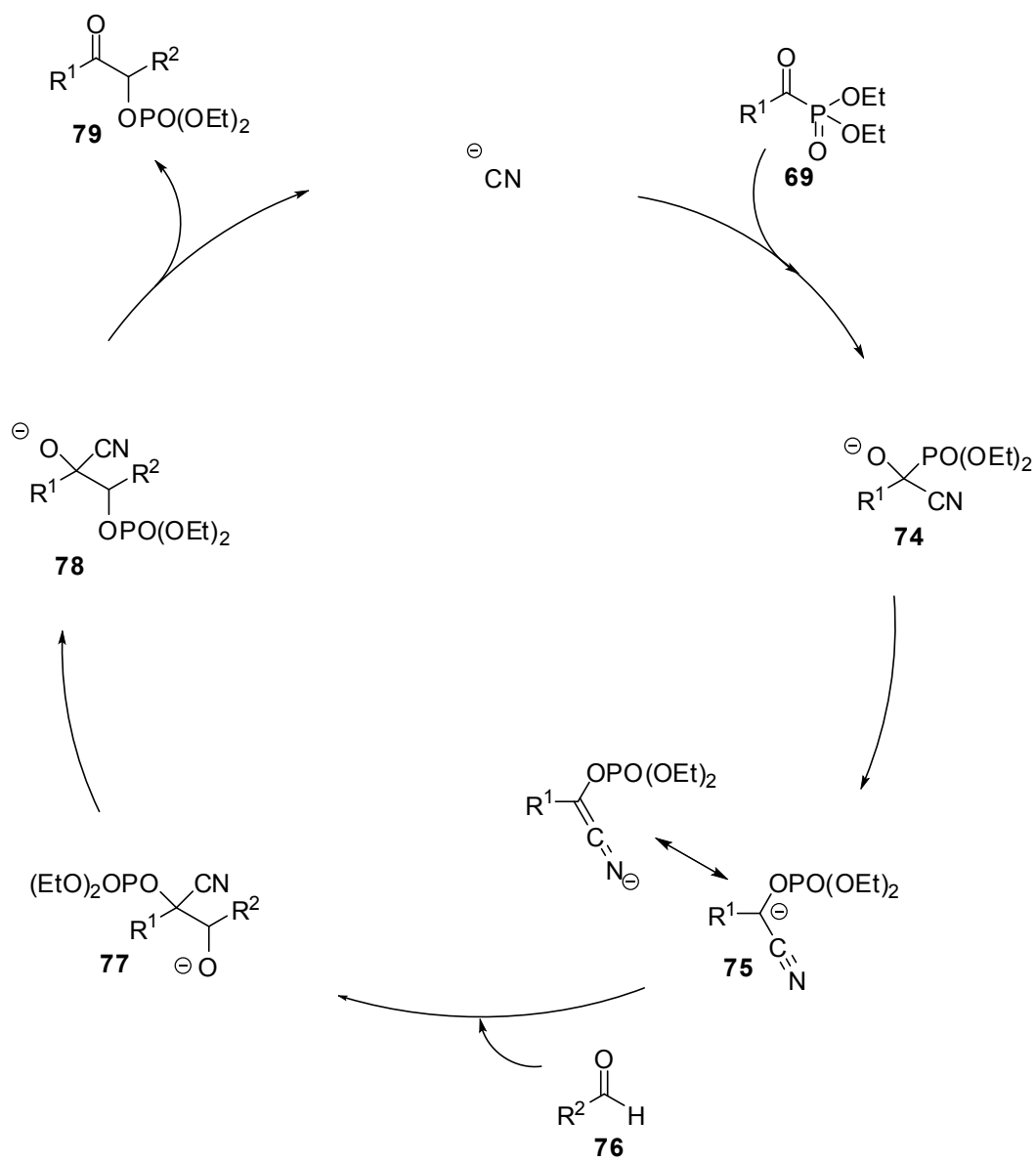


Figure 1.20 Mechanism of cross-benzoin reaction via cyanide ion promoted generation of acyl anions from acylphosphonates

This method provides a highly practical and flexible access to all isomers of cross benzoin s except for R¹ = alkyl and R² = alkyl combination. Beside this exception, the introduced method had no drawbacks for the synthesis of cross-unsymmetrical benzoin s. In any case, a meaningful chemical synthesis for alkyl-alkyl cross-unsymmetrical benzoin has not been introduced yet.

One of the most pronounced advantages of acylphosphonates over acyl silanes is that acylphosphonates are easily synthesized. Furthermore, acylphosphonates are readily available on a multigram scale from acyl chlorides and trialkyl phosphites via Arbuzov reaction without using any special condition or apparatus (**Figure 1.21**).³⁵ Acylphosphonates have superior stability under laboratory conditions over acylsilanes.

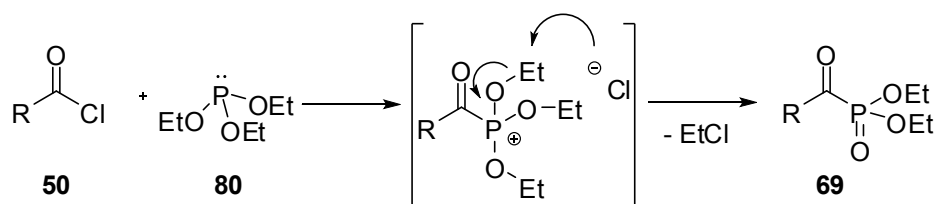


Figure 1.21 Synthesis of acylphosphonate via arbuzov reaction

One of the challenges in this area (organic synthesis) is aldehyde-ketone acyloin reaction due to the low electrophilic and enolizable nature of ketones. Although the nucleophilic carbene catalyzed intramolecular coupling reactions of aldehydes and ketones have been studied,³⁶ corresponding intermolecular catalytic couplings remained unsolved until recent examples from our research group. In this study, the first catalytic intermolecular aldehyde-ketone coupling via acylphosphonate was developed (**Figure 1.22**).³⁷ It was examined the reaction of

benzoylphosphonate **72** with potent electrophile 2,2,2-trifluoroacetophenone (**79**), which furnished the expected coupling product **80** in 87% yields. The proposed mechanism proceeds through similar steps with the cross-benzoin reactions that are mediated with acylsilanes and acylphosphonates.

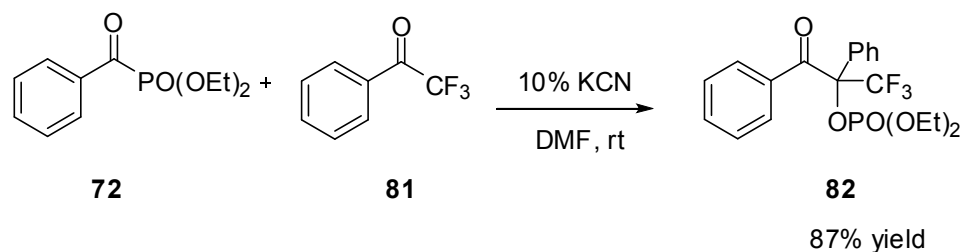


Figure 1.22 Catalytic intermolecular aldehyde–ketone coupling via acylphosphonates

Recent reports showed that protonation of acyl anion equivalents from acylphosphonates furnished cyanohydrin O-phosphates in high yields (**Figure 1.23**).³⁸ The acylphosphonate **72** reacts with the cyanide ion in DMF, resulting acyl anion intermediate **83**. Protonation of **83** leads to cyanohydrin O-phosphates **84**, which is equivalent to an aldehyde under the appropriate hydrolysis conditions. This study, in turn, the direct reduction of carboxylic acids to aldehydes under aqueous conditions.

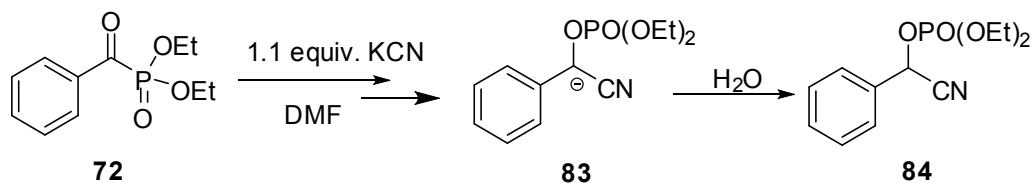


Figure 1.23 Protonation of acyl anion equivalents generated from acylphosphonates

Synthesis of cyanohydrins, versatile synthetic building block for a variety of pharmaceutically desirable compounds, has gained great attention.³⁹ Due to several functional groups on one carbon atom in cyanohydrins; the functional transformations provide easy access to many compounds. Therefore, a plethora of methods has been devoted to the synthesis of these targets.

Historically, the method for the synthesis of cyanohydrins is the addition of a cyanide ion to the corresponding carbonyl compounds as shown in **Figure 1.24, route A**.⁴⁰ Although route A has been widely used, other alternative methods have been developed to protect resulting hydroxyl group in situ. (**Figure 1.24, route B**). In route B, two sequential C-C bond formations take place via cyanide ion promoted carbanion generation and its subsequent reaction with the electrophilic carbon center.

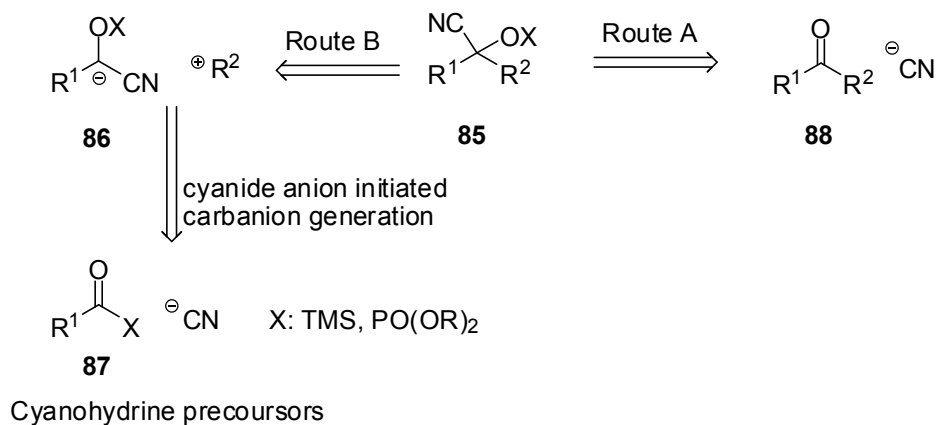


Figure 1.24 Methods for the synthesis of cyanohydrins

A one-pot reaction, shown in **Figure 1.25**, has been developed to get polyfunctionalized tertiary carbinols by Demir. In this reaction, two new C-C

bonds from acylphosphonate **87** and ethylcyanoformate (**88**) was made under mild conditions in good to excellent yields.⁴¹



Figure 1.25 Cyanide ion promoted addition of acyl phosphonates to ethyl cyanoformate

The proposed catalytic cycle for this transformation is outlined in **Figure 1.26**. The addition of cyanide anion to acylphosphonate **89** generates the intermediate alkoxide **92**, which rearranges to the carbanion **93** that reacts with the ethyl cyanoformate (**90**) to give the product **91**. While ethyl cyanoformate provides ethyl carboxylate to the acyl anion, it also keeps a catalytic amount of cyanide ion present in the reaction medium.

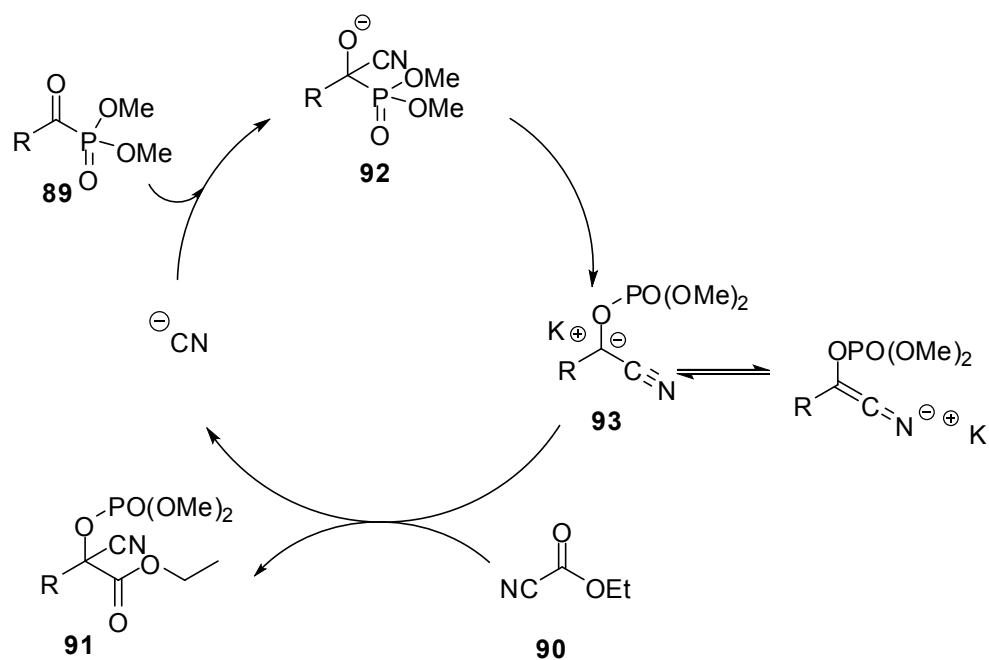


Figure 1.26 Proposed catalytic cycle for synthesis of tertiary carbinols via tandem carbon-carbon bond formations

The classical route to O-trimethylsilyl-protected cyanohydrins is the addition of TMSCN to the aldehydes (or ketones), which only takes place in the presence of Lewis acid catalysis (i.e. ZnI₂).⁴² When considering the value of O-trimethylsilyl-protected cyanohydrins, we can see in the literature that catalysis has been reported hundreds of times.⁴³ Demir *et al.* investigated the scope of the addition of TMSCN to acylphosphonate for the synthesis of interesting precursors, α -trimethylsilyloxynitrile **94**. It is found that TMSCN adds to acylphosphonate in high yield without a catalyst (**Figure 1.27**).⁴⁴ The enhanced reactivity of acylphosphonates was attributed to the presence of phosphonate moiety, which interacts with TMSCN. The interaction, in between silicon (Lewis acid) and the lone pair on oxygen in P=O moiety, activates both partners in the reaction.

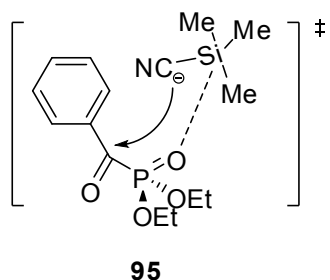
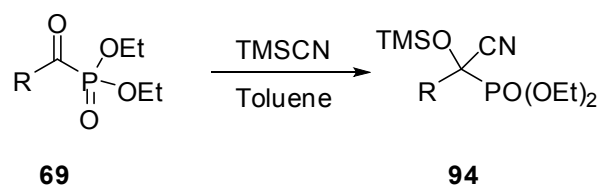


Figure 1.27 Uncatalyzed addition of TMSCN to acylphosphonates

To conclude this part of the introduction, acylphosphonates are found as effective acyl anion equivalents with respect to yields, purity of product, and reaction times in cross benzoin reactions. These reagents are superior over acylsilanes in terms of easy availability. Moreover, one can synthesize any benzoin derivative in a few hours starting from acylchlorides without using any special apparatus or taking any special precautions. It is for seen that acylphosphonates will be highly useful and original, addition to the known methods of bond forming reactions via acyl anion equivalents based on the steps this research has taken so far.

1.2 Organocatalytic Asymmetric C-C Bond Formation Reactions

Enantiopure compounds have attracted widespread interest from both the academic and, the commercial communities due to the fact that enantiomers of the same compound can display different biological activities. The well known examples of the different biological activity of enantiomeric compounds are the Timolol and Propoxyphene (**Figure 1.28**).⁴⁵ In the case of Timolol, *S*-enantiomer was found to be an adrenergic blocker, while the other enantiomer is ineffective. Alternatively, the *S*-isomer of Propoxyphene is an analgesic while the other shows an antitussive property.

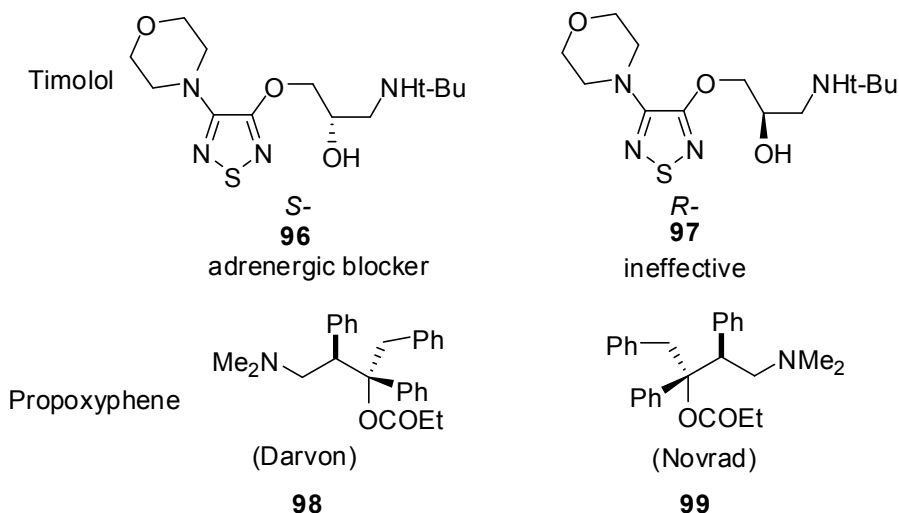


Figure 1.28 Examples of enantiomers

About 70 % of the new small-molecule drugs that the United States Food & Drug Administration (FDA) approved in 2007 contain at least one stereogenic center.⁴⁶ Therefore, it is highly desirable to construct enantiopure compounds. Scientific

communities, in turn, continuously explore new methods to produce their unique handedness. An increasing demand for chiral compounds has encouraged intensive research to improve methods for synthesizing such compounds. An array of synthetic methods that result in the desired transformation and control the absolute stereochemistry of stereogenic centers created as a result of the synthetic operations is called asymmetric synthesis.

Historically, enantiomerically enriched compounds (in any chemical asymmetric synthesis for a compound it is extremely difficult to get 100% one-enantiomer of the compound. Therefore, the term “enantiomerically enriched” is used) were synthesized by two main methods: (1) chemical transformation of enantiomerically enriched precursors deriving directly or indirectly from nature's chiral pool, (2) resolving a racemic mixture of the two enantiomers (kinetic resolution). Both of these methods have actually severe drawbacks, the former method demands stoichiometric amounts of a suitable precursor, and the latter method, naturally, yields only up to 50% of the desired enantiomer (except for meso compounds).

Asymmetric catalysis, in which chiral catalyst transfers chirality information through a well-described transition state to an achiral substrate, is a third approach for asymmetric induction. For this purpose, transition metal complexes (containing at least one stereogenic center) and enzymatic systems have been employed in asymmetric catalysis in the last five-decades.⁴⁷ Transition metal complexes with chiral ligands that the metal center can coordinate to the substrate one wants to do a chiral transformation. Either electronic or steric effects transfer the chirality from the ligand to the substrate. The 2001 Nobel Prize for chemistry was awarded to Knowles, Noyori and Sharpless for their seminal work in this field.⁴⁸

Even though transition metal catalysts have been employed in various applications, their potential drawbacks, *i.e.*, high toxicity, high price, and less stability have

pushed the chemists towards an inspection of nature's way of asymmetric induction, namely biocatalysis. Biocatalysis (enzymatic catalysis) is the use of natural catalysts, which are biomolecules evolved in nature to achieve the speed and coordination of a multitude of chemical reactions necessary to develop and maintain life, and to carry out chemical transformations on organic compounds. The development of enzymatic catalysis has grown tremendously in industrial production of chiral chemicals in recent years.⁴⁹ However, due to the molecular complexity and instability of enzymes, applications of biocatalysis are generally limited.

For the past 10 years, the concept of organocatalysis (concatenation of the terms organic + catalysis) has appeared as a distinct strategy for addressing challenges in asymmetric organic synthesis.⁵⁰ The term organocatalysis refers to a form of catalysis, whereby the rate of a chemical reaction is increased by an organic catalyst that does not contain a metal atom. Compared to the other asymmetric catalysis (enzymes or transition metal catalysts), organocatalysis definitely introduces some important advantages to the organic synthesis. Firstly, they are inexpensive and most of them (amino acids, alkaloids, and carbohydrates) are naturally available as single enantiomers. Secondly, since they do not contain toxic metals, they are environmentally friendly. Moreover, they are generally stable to air and moisture. Therefore, the field of organocatalysis has flourished.

The history of organocatalysis began with the discovery of oxamide synthesis from dicyan and water in the presence of acetaldehyde by German chemist Justus von Liebig in 1859.⁵¹ Nearly sixty years later, the term "organic catalyst" was coined by Langenbeck and he published a series of papers using small organic molecules as catalysts.⁵² Although these seminal works had initiated two main categories in organocatalysis, "covalent catalysis" and "non-covalent catalysis", they were not used to produce chiral compounds (asymmetric catalysis).

The first example of asymmetric organocatalytic reactions was introduced by Bredig and Fiske in 1912.⁵³ They investigated that cinchona alkaloids accelerates the rate of addition of HCN to benzaldehyde. However, their enantiomeric excess (*ee*) values were below 10%. In the early 1960's, Pracejus reported quinine catalyzed asymmetric ketene methanolysis reaction.⁵⁴ As shown in **Figure 1.29**, 1 mol% of compound **102** catalyzed the methanolysis of ketene **100** to produce the methyl ester **101** in 40% *ee*.

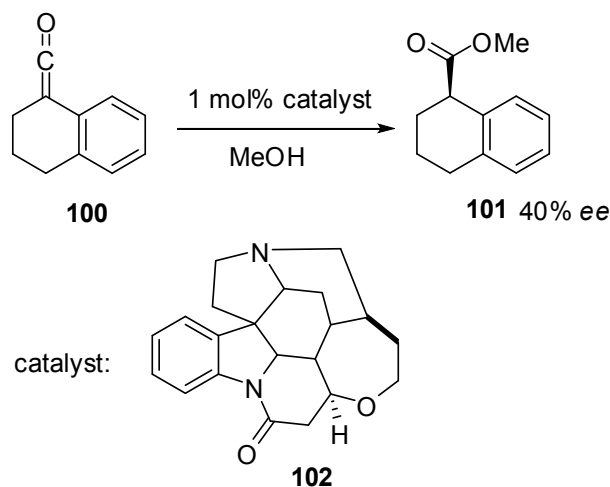


Figure 1.29 Compound **102** catalyzed the methanolysis of ketene **100**

A breakthrough in organocatalysis came in 1971, when two industrial groups led by Hajos at Roche[®] and Wiechert at Schering[®] discovered *L*-Proline **107** catalyzed intramolecular aldol reaction to afford bicyclic compound **104** with a high levels of enantioselectivity (**Figure 1.30**).⁵⁵ This reaction, recognized later as the Hajos-Parrish-Eder-Sauer-Wiechert reaction, is regarded as a milestone for the field of

asymmetric organocatalysis. However, there was no attention given to the importance of this reaction in terms of organocatalysis until early of this millennium. Giving the encouraging breakthrough reported in 1970's, synthetic chemists seem not to pay attention to the concept of organocatalysis.

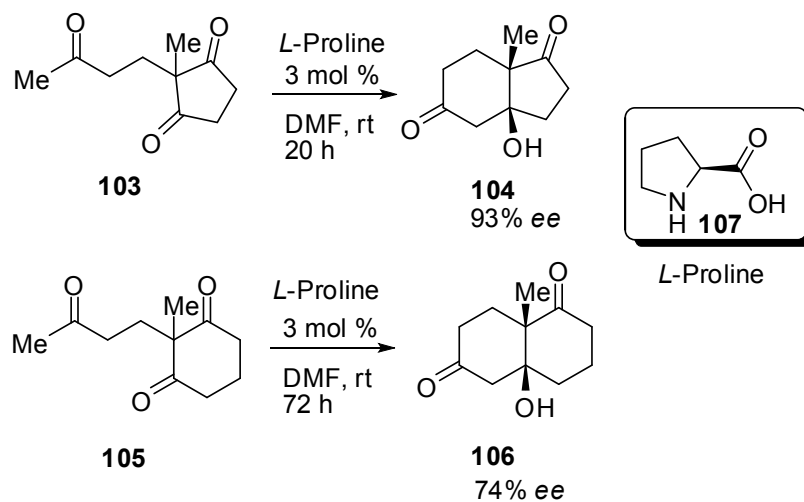


Figure 1.30 Hajos-Parrish-Eder-Sauer-Wiechert reaction

1.2.1 Classification of Organocatalysis

Over the past decade, increasing efforts have been devoted to develop and synthesize new organocatalysts for asymmetric C-C bond formation reactions. Organocatalysts, containing C, O, N, sometimes P and/or S atoms, accelerate organic reactions by activating electrophiles or nucleophiles. It should be noted that perfect classification of organocatalysis with only one methodology is not easy due to the diversity of mechanisms of the organocatalytic reactions.

Recently, most but not all organocatalysts have classified by List as Lewis bases, Lewis acids and Brønsted bases, Brønsted acids according their functions in reactions (**Figure 1.31**).⁵⁶ Lewis base catalysts **B**: start the catalytic cycle via nucleophilic attack to the substrate **S** to form complex **B-S**, which undergoes a reaction to afford another complex **B-P**. After releasing the product **P**, the catalyst recycles for further turnover. Similarly, Lewis acid catalysts **A** activate nucleophilic substrates **S**: to achieve chemical transformation and gives product **P**. Brønsted base and acid catalysts accelerate reactions via (partial) deprotonation or protonation processes.

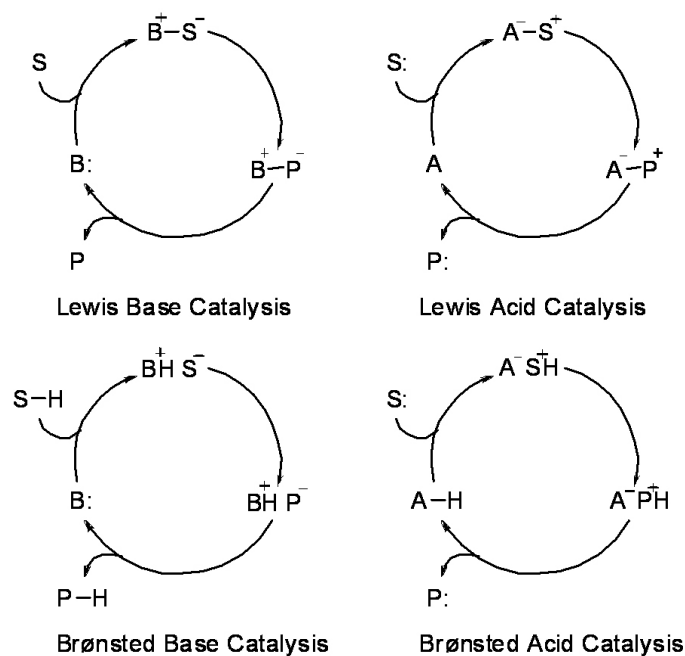


Figure 1.31 Classification of simplified organocatalytic cycles by List

Macmillan later focused on the importance of organization of the organocatalysis regarding generic mode of activation of catalytic systems as shown in **Figure 1.32**.⁵⁷ A generic mode of activation is related to a reactive species that can affiliate with many reaction types with consistently high levels of enantioselectivity. Such reactive species can be generated from the interaction of a chiral catalyst with simple functional groups of substrates (*i.e.* aldehyde, ketone, olefin or imine) in a highly organized and predictable manner. The significance of generic activation modes arise from the fact that once established, extrapolation of the new concept for the design of new enantioselective transformations becomes straightforward.

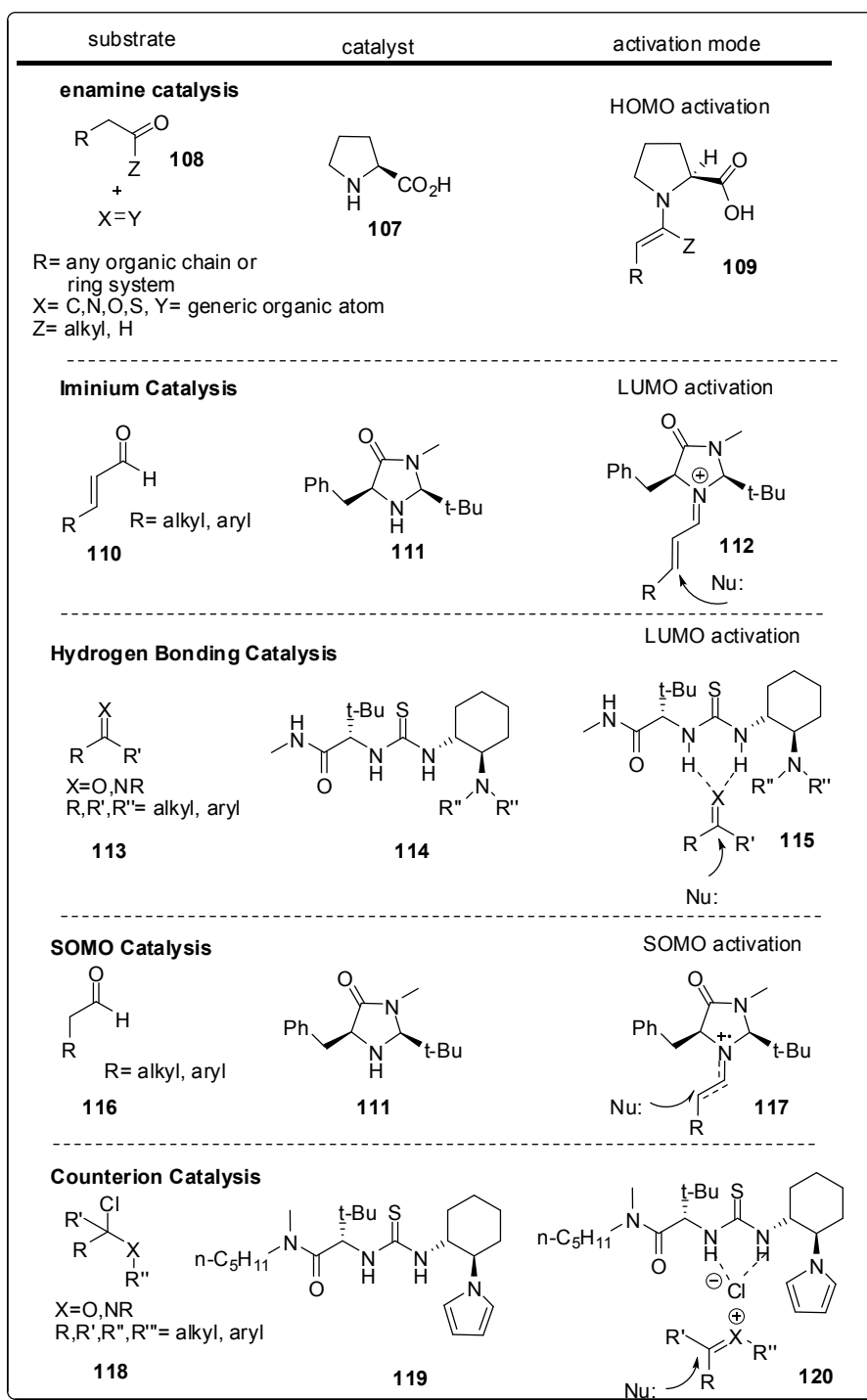


Figure 1.32 Organization of the organocatalysis regarding generic mode of activation of catalytic systems

The “enamine” and “iminium” catalysis are the most frequently encountered generic modes of activation in asymmetric organocatalysis. The enamine catalysis concept is based on the capacity of a chiral amine **123** to react reversibly with an aldehyde or ketone **121** to form a nucleophilic enamine **124**, leading to an overall increase in energy of the Highest Occupied Molecular Orbital (HOMO), thus mimicking the HOMO-raising ability of Lewis acids (**Figure 1.33**). The transiently formed enamine species can then facilitate enantioselective α -carbonyl functionalization with various electrophiles.

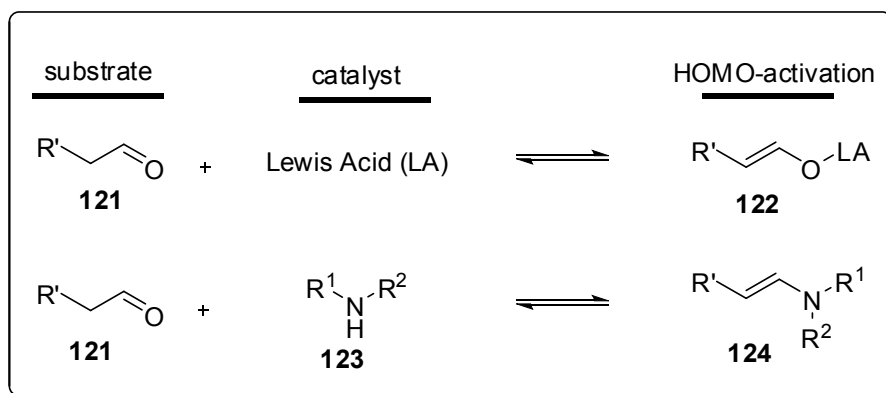


Figure 1.33 Enamine catalysis concepts

The iminium catalysis concept is based on the notion that upon condensation of α , β -unsaturated aldehyde **125** with a chiral amine **123**, an iminium ion **127** is produced as reactive intermediate (**Figure 1.34**). This transformation leads to an overall energy decrease of the substrate’s Lowest Unoccupied Molecular Orbital (LUMO), which promotes a variety of enantioselective organocatalytic transformations, and is in contrast to the enamine activation (HOMO activation).

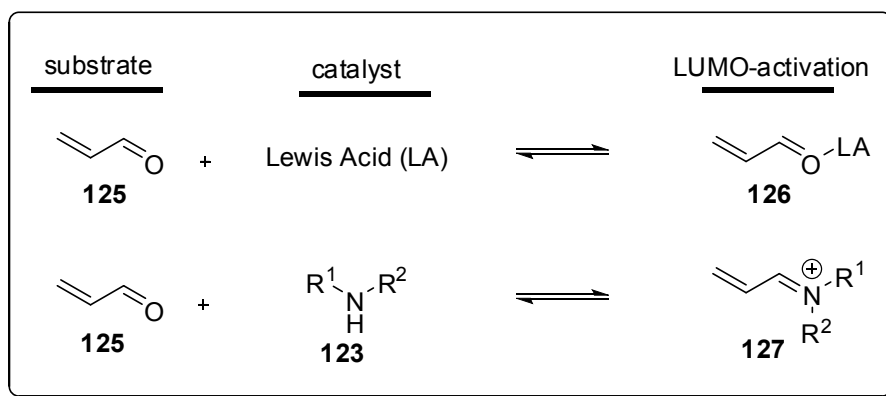


Figure 1.34 Iminium catalysis concepts

In other classification by Berkessel, organocatalysts are categorized as covalent catalysts and non-covalent catalysts according to bond formation between catalysts and substrates within the catalytic cycle.⁵⁸ Covalent catalysts activate organic reactions through covalent bond formation with substrates. Enamine and iminium catalysis are two important examples of covalent catalysis. Non-covalent catalysts activate substrates through non-covalent interactions, such as protonation or hydrogen bonding.

The rest of introduction part is mostly dedicated to the further explanation of the enamine catalysis, since it is closely related to our work.

1.2.2 Enamine Catalysis

The catalysis of carbonyl transformations via formation of enamine intermediates by using primary or secondary amines as catalysts is called “enamine catalysis”.⁵⁹ Enamine catalysis, originally reported by Stork, can be regarded as a catalytic version of the classical enamine chemistry.⁶⁰

As shown in **Figure 1.35**, in such catalytic cycle, carbonyl compound **128** reacts with an amine **123** to provide the enamine **130** under dehydration conditions. The catalytically generated enamine **130** is able to give addition reactions with different electrophiles ($X=Y$) to afford corresponding iminium ion **132**. Hydrolysis of the iminium ion **132** with in-situ-generated water yields the α -substituted carbonyl products **133**. In enamine catalysis, enolizable aldehydes or ketones are converted to more activated nucleophiles by HOMO raising activation mechanism. The HOMO of the resultant enamine **130** is higher than its aldehyde (or ketone) **128** and thus activated toward combination with the LUMO of an electrophile.

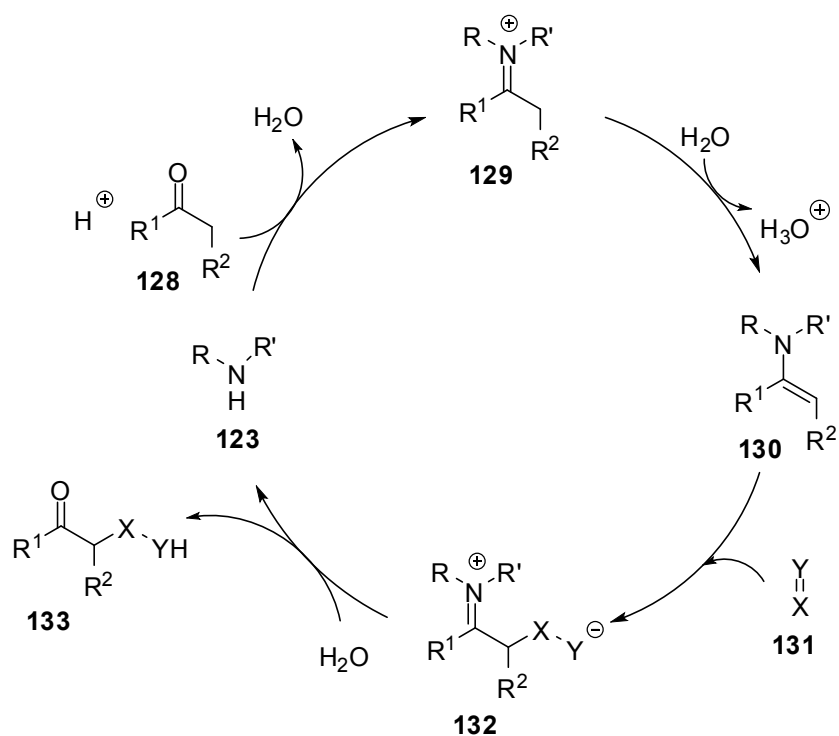


Figure 1.35 General mechanism of the enamine catalysis

The catalytic potential of enamine catalysis for intermolecular enantioselective direct aldol reactions between ketones and aldehydes was introduced by List.⁶¹ Since then, there have been extensive efforts to develop new asymmetric enamine catalysts. Although a wide variety of organocatalysts and organocatalytic reactions have been reported in this field, only general organocatalytic methodologies that use enamine formation for enantioselective “Aldol” and “Michael addition” reactions will be discussed in detail in the following chapters due to the relevance to the work of the author of this dissertation.

1.2.2.1 Enantioselective Organocatalytic Aldol Reactions by Enamine Catalysis

The aldol reaction is one of the most commonly applied methods for C-C bond constructions in both nature and synthetic organic chemistry.⁶² The strategy of this reaction combines two relatively simple molecules into a structurally complex one by creating β -hydroxy carbonyl structural unit found in many natural and non-natural pharmaceutically important compounds. Therefore, the investigations of efficient strategies for asymmetric catalysis involving small organic molecules for aldol reactions have been an extensively growing field of asymmetric synthesis.

The Hajos-Parrish-Eder-Sauer-Wiechert reaction is the first example of enamine catalyzed asymmetric aldol reaction. As seen in **Figure 1.36**, formation of the enamine intermediate **135** between ketone **103** and *L*-proline leads to acceleration of reaction rate and also helps to control stereochemistry of the aldol product.

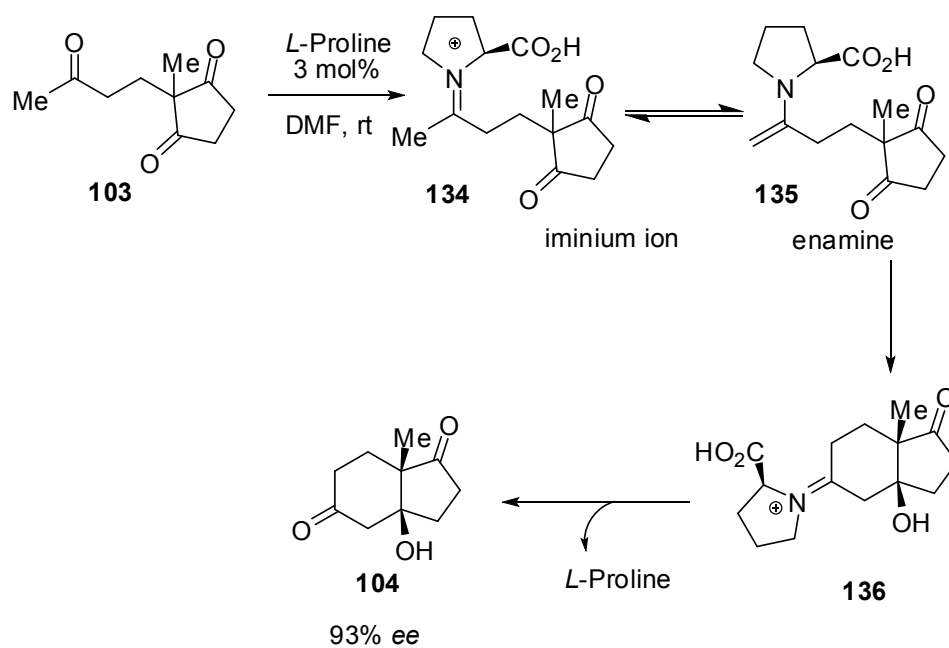


Figure 1.36 Mechanism of the Hajos-Parrish-Eder-Sauer-Wiechert reaction

On the other hand, since the mechanism of this cyclization was not fully understood, the potential of this method was not realized at the time of discovery. The mechanistic aspects (transition state) of this intramolecular aldol reaction remain a matter of debate. However, there are varieties of proposed transition states recognized by people in this field (**Figure 1.37**).

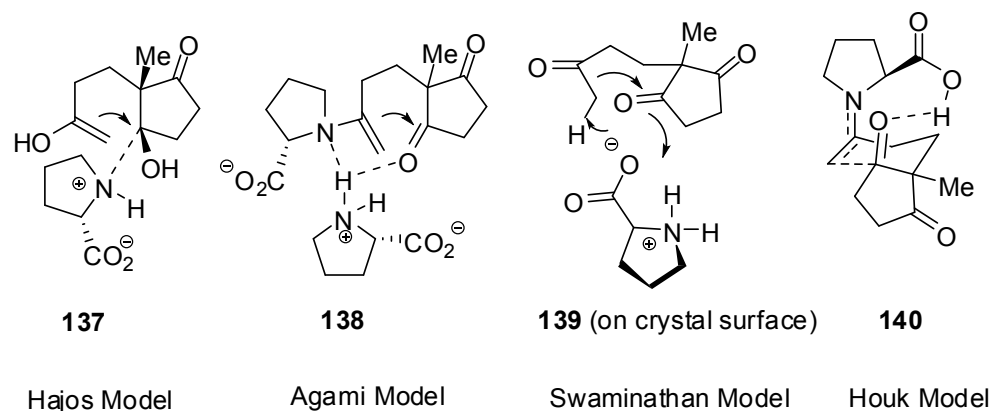


Figure 1.37 Proposed transition states for the Hajos-Parrish-Eder-Sauer-Wiechert reaction

As seen in Figure **1.37**, Hajos's proposed transition state (TS) **137** involves an enol attacking a carbonyl activated by proline.^{55b} Hajos model did not involve an enamine that was proposed to be intermediate. With the connection of the nonlinearity studies, Agami and co-workers proposed a side-chain enamine mechanism.⁶³ Agami's model **138** involves two proline molecules; one is engaged in enamine formation whereas the other one acts as a proton-transfer mediator. In another mechanistic proposal, Swaminathan's model **139**, that favors a heterogenous aldol mechanism on the crystal surface of the proline.⁶⁴ However, most of proline-catalyzed aldol reactions work in completely homogenous media. Therefore, Houk proposed one-proline enamine mechanism **140**, in which the transition state is highly stabilized by hydrogen bond donation from the carboxylic acid moiety to the ring acceptor carbonyl group, with concurrent development of partial iminium and carboxylate ions on the proline.⁶⁵

List and co-workers introduced the possibility of using *L*-proline, simple organic molecule, as a catalyst for the direct asymmetric intermolecular aldol reaction between acetone and a variety of aldehydes (**Figure 1.38**). Although they tested a variety of different amino acid derivatives as catalyst, *L*-proline was found to be the most efficient catalyst to get maximum enantioselectivity. Primary amino acids, such as *L*-Histidine and *L*-Valine, and acyclic secondary amino acids did not give desired product in appreciable yields. Therefore, they proposed that both the pyrrolidine ring and the carboxylate moiety are necessary for effective catalysis to occur.

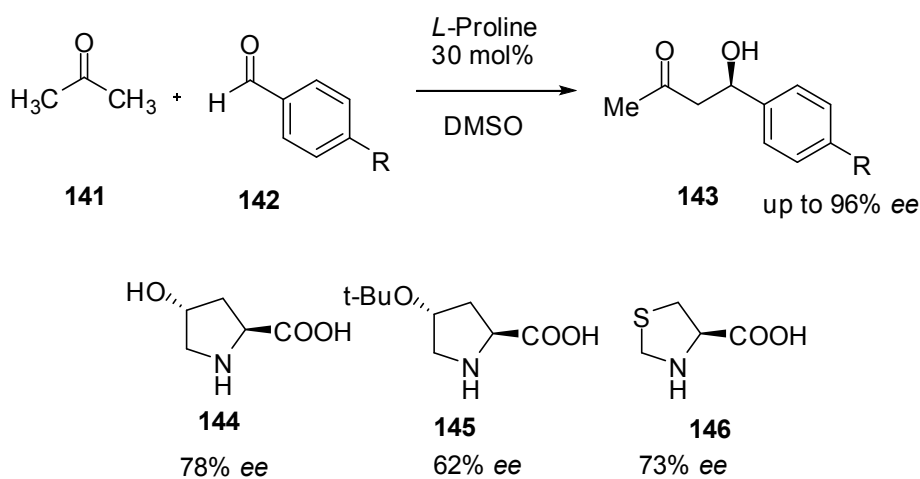


Figure 1.38 Direct asymmetric intermolecular aldol reactions

As seen in **Figure 1.39**, although phenylalanine was good catalyst for the intramolecular aldolization, simple amino acids are not effective catalysts for the intermolecular aldol reaction. Further screening of cyclic amino acids with different ring sizes demonstrated that proline is the best catalyst whereas six-membered pipercolic acid (**154**) is ineffective catalyst. *N*-methylproline (**155**) was found to be

inactive for the intermolecular aldolization. This further supports the mechanism going through an enamine intermediate. The essential role of carboxylate moiety was revealed from the result obtained with prolinamide (**156**). Even though this catalyst did not yield the desired product after 2h, the aldol product was obtained with low enantioselectivity after several days.

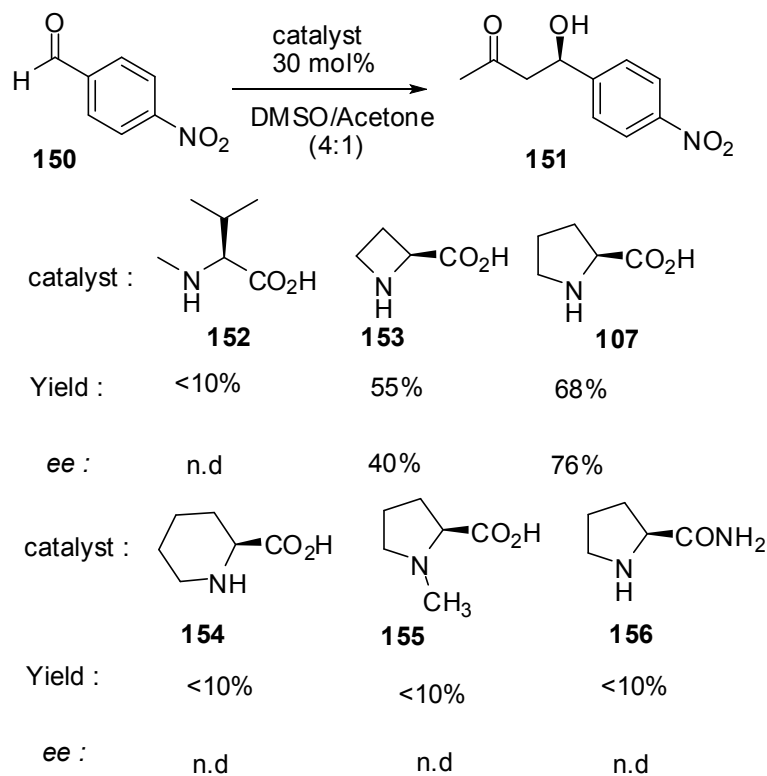


Figure 1.39 Screening of catalysts for direct asymmetric intermolecular aldol reactions

There are several reasons that contribute to effective proline's role in organocatalysis. First, it is inexpensive and available in both enantiomeric forms (*D* and *L*). Second, similar to general acid-base enzymatic catalysis, it acts as bifunctional catalysts. Modes of action in proline-catalysis are shown in **Figure 1.40**.

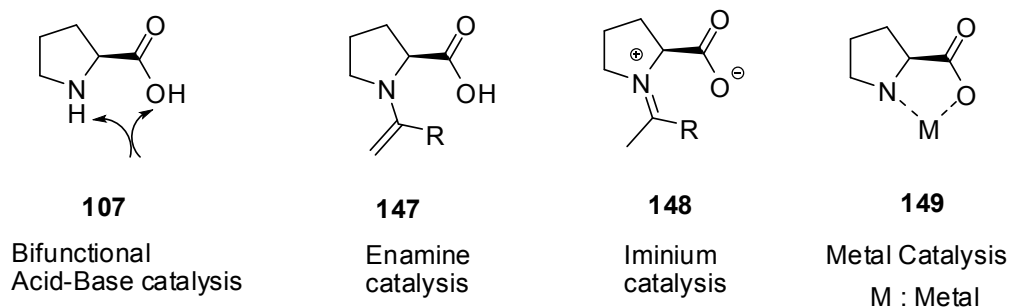


Figure 1.40 Modes of action in proline-catalysis

Interestingly, List and co-workers have also reported that there were no non-linear effects in proline catalyzed aldol reactions in contrast to earlier proposals. Addition to this observation, isotopic labelling studies also provide an experimental support for single proline enamine mechanism and Houk's similar DFT-model of the transition state of the intramolecular aldol reaction.⁶⁵

With these studies in hand, List *et al.* proposed enamine catalysis mechanism as shown in **Figure 1.41**. The mechanism involves carbinolamine, iminium ion, and enamine intermediates. The most important intermediates of this cycle are the iminium ion **159** and the enamine **160**. Iminium ion formation effectively leads to lowering of LUMO energy of the system. Thus, generation of enamine via α -deprotonation becomes more facile. Therefore, enamine intermediate **160** reacts with the aldehyde to give enantiomerically enriched aldol product **163** via transition state TS **109**. In transition state **109**, acceptor carbonyl group, which is protonated by carboxylic acid part of proline, is anti with respect to the (*E*)-enamine double bond. Shortly afterwards, a similar transition state for the intramolecular aldolization proposed by Houk and co-workers.⁶⁵

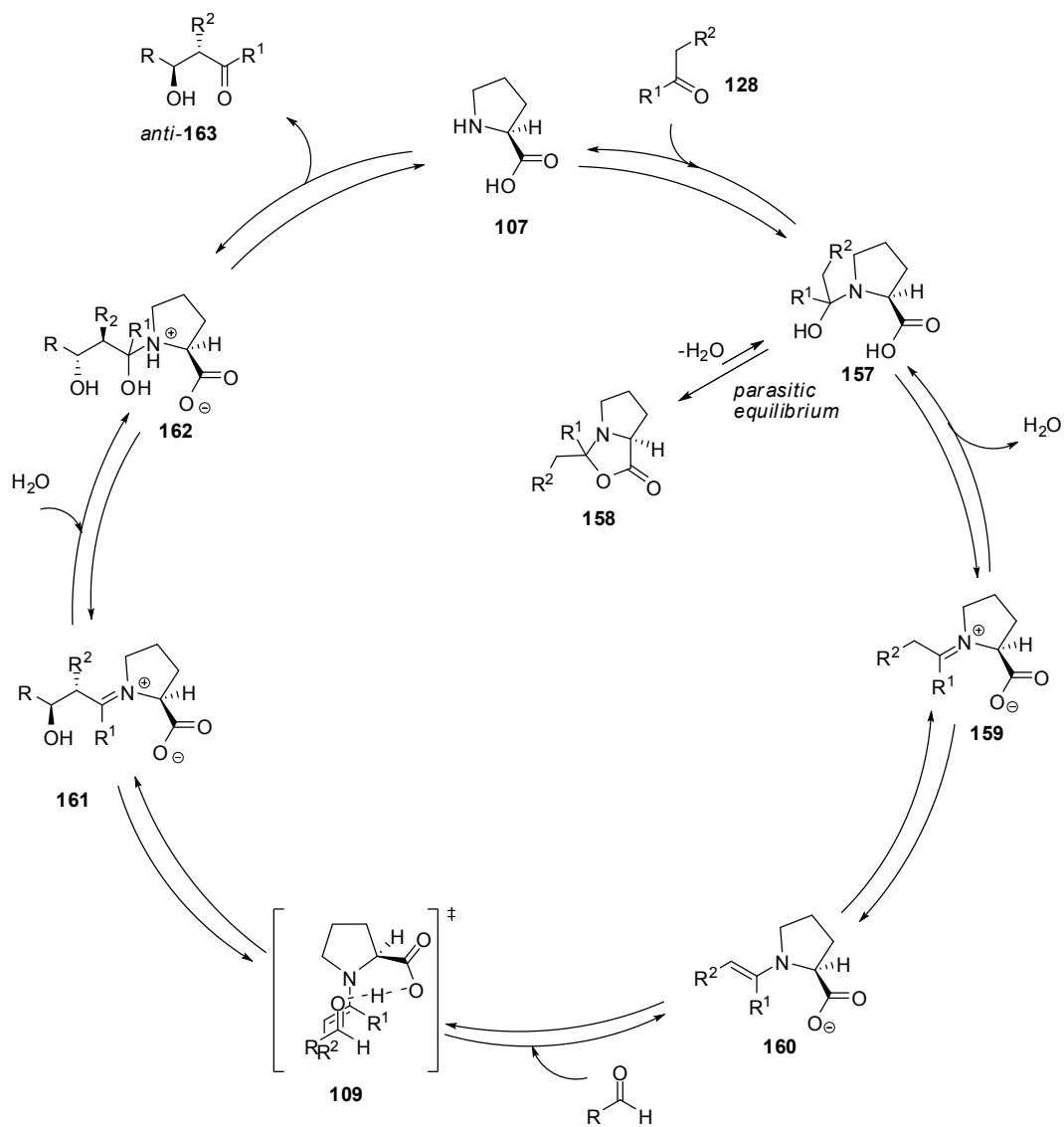


Figure 1.41 Proposed mechanism of the proline-catalyzed intermolecular aldol reaction

One of the main difficulties of proline catalyzed intermolecular aldol reaction is formation of oxazolidinone **158** from aldehyde or ketone substrates and proline (**Figure 1.42**). Rather than the enamine, thermodynamically favored the oxazolidinone constitutional isomer of the enamine, in which one C-O and one C-H- σ -bond is gained at the expense of one C-C- π bond and one O-H- σ bond, is formed. Oxazolidinone has been described to be a parasitic dead end as it was proposed to decrease the concentration of the active catalytic species.⁶⁶ This potential parasitic side reaction makes using high catalyst loadings necessary to afford acceptable yields.

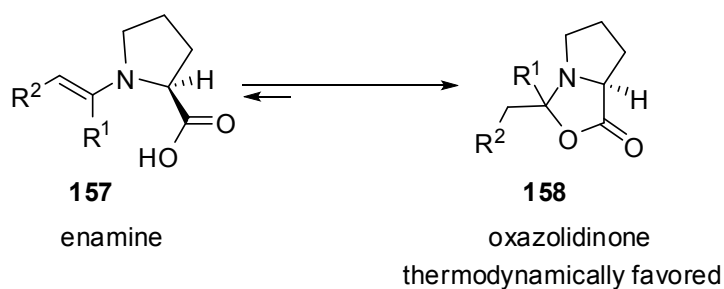


Figure 1.42 Parasitic off-cycle equilibrium

The *L*-proline-catalyzed direct aldol reaction has been extended to ketones other than acetone. Selected examples of the substituted ketone donors are shown in **Figure 1.43**.⁶⁷ Generally, the donor ketone was needed in very high concentrations. Therefore, the direct aldol reaction was limited to only simple ketones, such as cyclohexanone (**167**) and cyclopentanone (**168**), for practical synthesis. In most cases, the anti aldol products **166** were more favored compared to the syn products. The *E* enamine is the only possibility for cyclic ketones. The

suitable orientation of the aldehyde when approaching enamine **154**, therefore, leads to the diastereoselectivity.

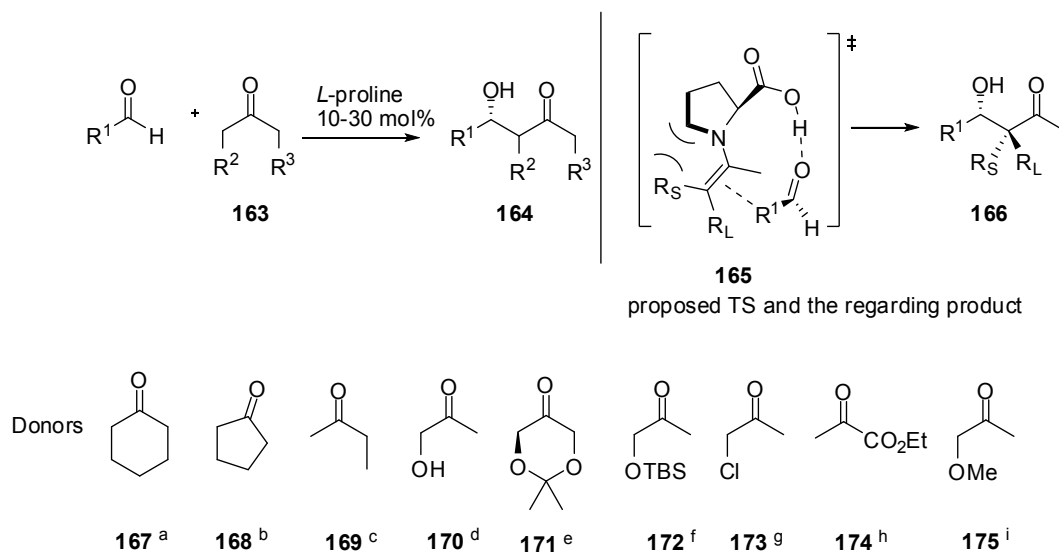


Figure 1.43 Typical Substituted ketone donors in asymmetric enamine catalysis

The field of proline catalyzed enantioselective aldol reactions between a variety of donor and acceptor molecules have witnessed a new era of asymmetric organocatalysis with an impressive pace. Design and development of numerous new catalysts based on *L*-proline skeleton have also attracted considerable interest for last decades.

Some important examples of proline based organocatalysts used in enamine catalyzed direct aldol reactions are shown in **Figure 1.44**.⁶⁸ Considering its low price and commercial availability, it is clear that *L*-proline would be a first-choice catalyst for enantioselective aldol reactions. In addition to this, great efforts are

devoted to the design and synthesis of novel catalysts that are catalyzing reactions more selectively than proline. Despite the excellent results obtained in some of these catalysts shown in **Figure 1.44**, the time consuming nature of this modification processes may significantly reduce their applicability.

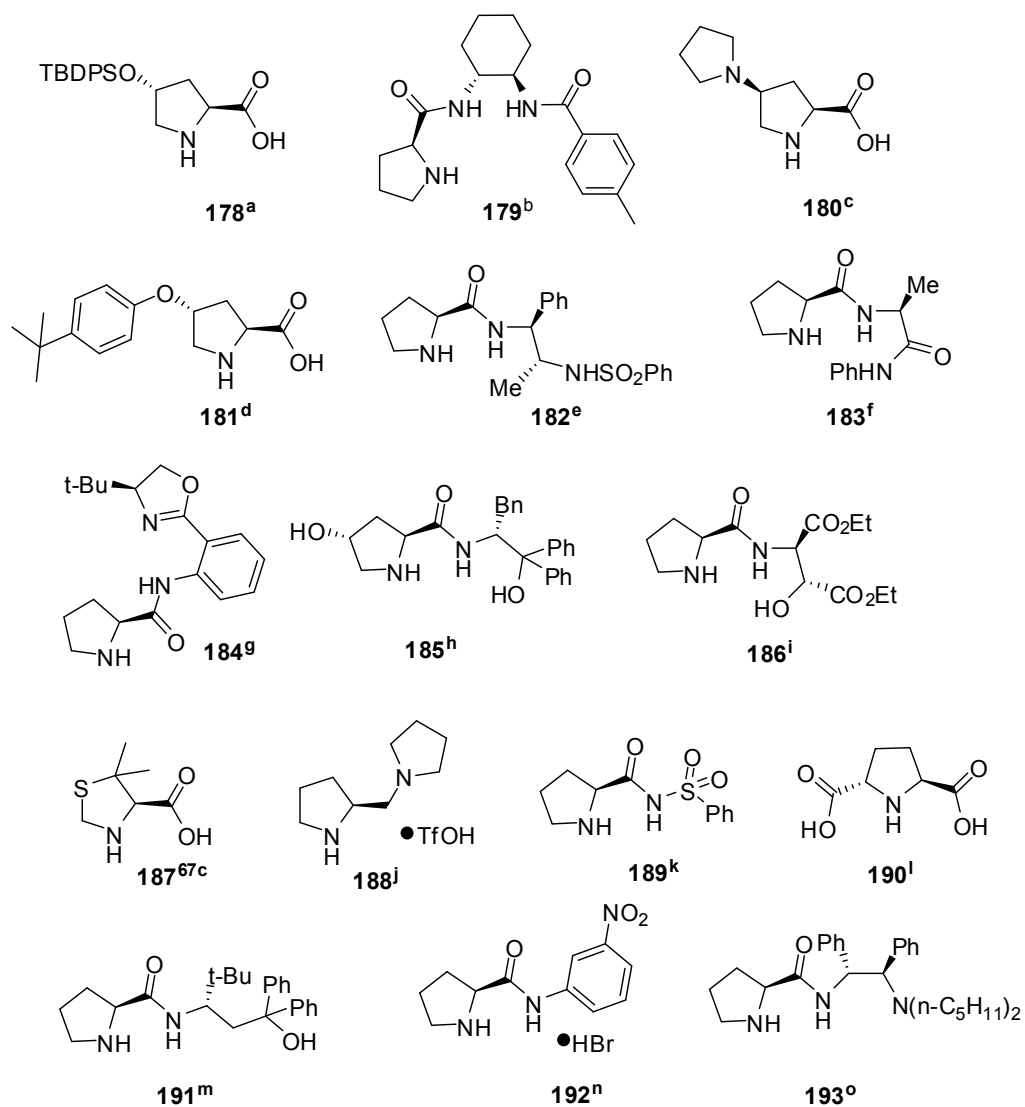


Figure 1.44 A literature selection of proline based organocatalysts used in enamine catalyzed direct aldol reactions

1.2.2.2 Enantioselective Organocatalytic Michael Reactions by Enamine Catalysis

Besides aldol reactions, Michael reactions and variants have also been carried out in the presence of organocatalysts with superior selectivities. The importance of Michael reactions comes from the fact that the resulting molecules will have two or more functionalities and stereogenic centers. The Michael reaction of carbon-centered nucleophiles with nitroalkenes, for example, is one such reaction that is catalyzed by organocatalysts as shown in **Figure 1.45**.⁶⁹

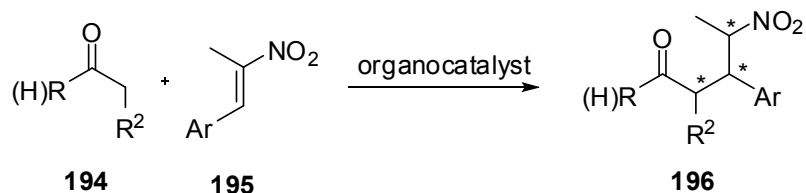


Figure 1.45 The Michael reaction of carbon-centered nucleophiles with nitroalkenes

Wynberg discovered the first catalytic enantioselective Michael addition reaction in 1975.⁷⁰ Since then, the Michael reaction has been regarded as one of the most powerful methods for C-C bond formation. Among the variety of different approaches to yield Michael adducts, the organocatalytic approach has become very popular in recent years since it enables us to construct three stereocenters in only one step.

Organocatalytic Michael addition reactions generally go through electrophile or nucleophile activation. The possible activation modes for Michael addition reactions are shown in **Figure 1.46**. The majority of organocatalysis of the

Michael reactions are enamine catalysis, which involves generated enamine intermediates that react with a wide variety of electrophiles.

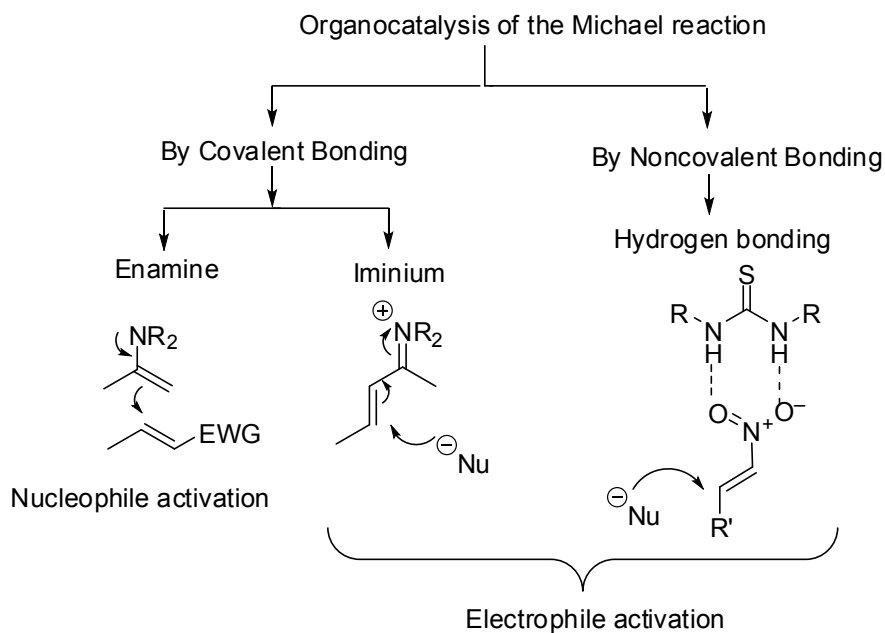


Figure 1.46 Organocatalysis of the Michael reactions

A wide variety of Michael acceptors have been successfully used in the organocatalytic enantioselective Michael addition reaction, such as β -nitrostyrenes, α,β -unsaturated carbonyl compounds and alkylidene malonates. Among these reactions, Michael addition of aldehydes to β -nitrostyrenes is particularly attractive since it generates valuable synthetic intermediates. In 2001, the first organocatalytic asymmetric Michael addition of unmodified aldehydes to nitroolefins was launched by Betancort and Barbas (**Figure 1.47**).⁷¹ They used (*S*)-2-(morpholinomethyl)-pyrrolidine (**200**) as a catalyst. This reaction yields a variety of γ -formyl nitro products like **199** from different starting materials in high yields

with moderate enantioselectivity. The products all had *syn*-diastereoselectivity. To explain *syn* selectivity, they proposed a transition state based on an acyclic synclinal model **201**. In this model, there are favorable electrostatic interactions between the partially positive nitrogen of the anti-enamine and the partially negative nitro group in the TS **201**.

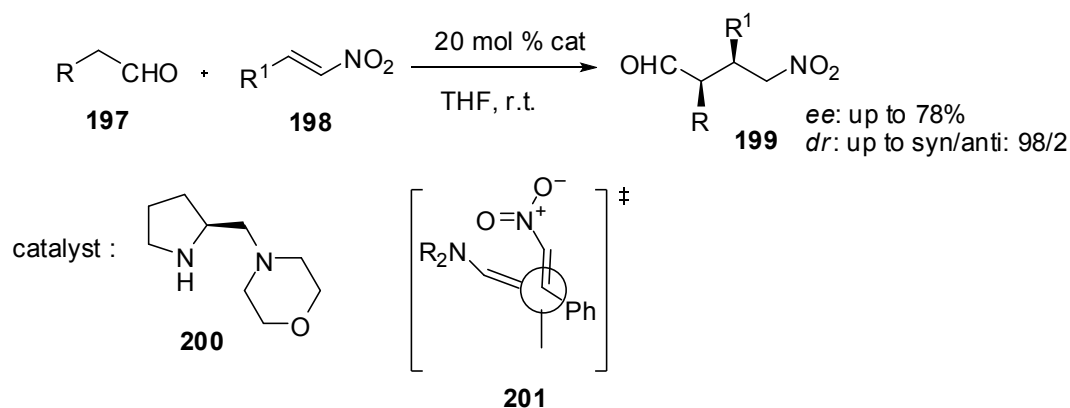


Figure 1.47 The first organocatalytic asymmetric Michael addition of unmodified aldehydes to nitroolefins

Further, (*S*)-pyrrolidine sulfonamide **204** has been introduced by Wang to serve as an efficient catalyst for Michael addition reaction of aldehydes and ketones to *trans*- β -nitrostyrenes as shown in **Figure 1.48-A**.⁷² Later, Hayashi has shown that diphenylprolinol trimethylsilyl ether (**207**), which is easily synthesized from commercially available diphenylprolinol in a single step, is highly effective catalyst in the addition of aldehydes to nitroalkenes (**Figure 1.48-B**).⁷³ Notably, both alkyl- and aryl-substituted nitroalkenes are appropriate Michael acceptors in this system. The Michael adducts were obtained in nearly optically pure form in almost all cases. Wennemers and co-workers have developed a highly

enantioselective Michael reaction of aldehydes and nitroolefins by using tripeptide catalyst **209** as shown in Figure 1.48-C.⁷⁴

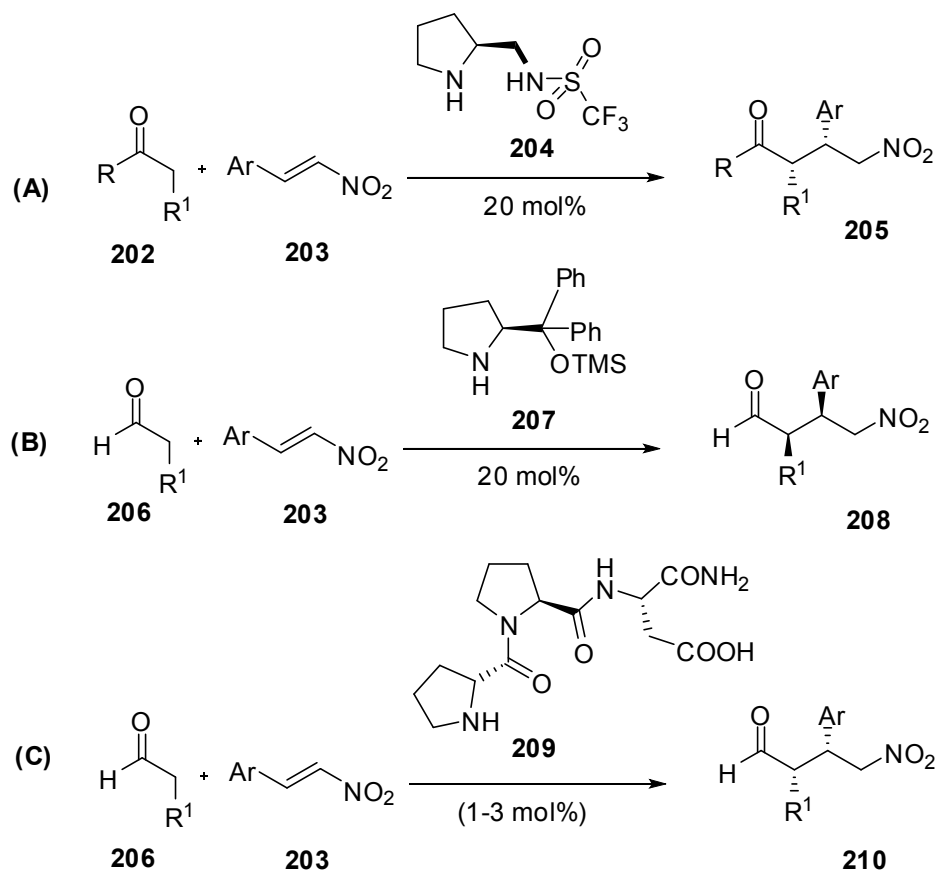


Figure 1.48 A literature selection of organocatalytic Michael addition reactions

Inspired by these precedents, the development of new organocatalysts for this excellent reaction has received great attention. Selected examples of proline-based organocatalysts, which are used in asymmetric conjugate additions of aldehydes and ketones to nitroalkenes, are shown in **Figure 1.49**.⁷⁵

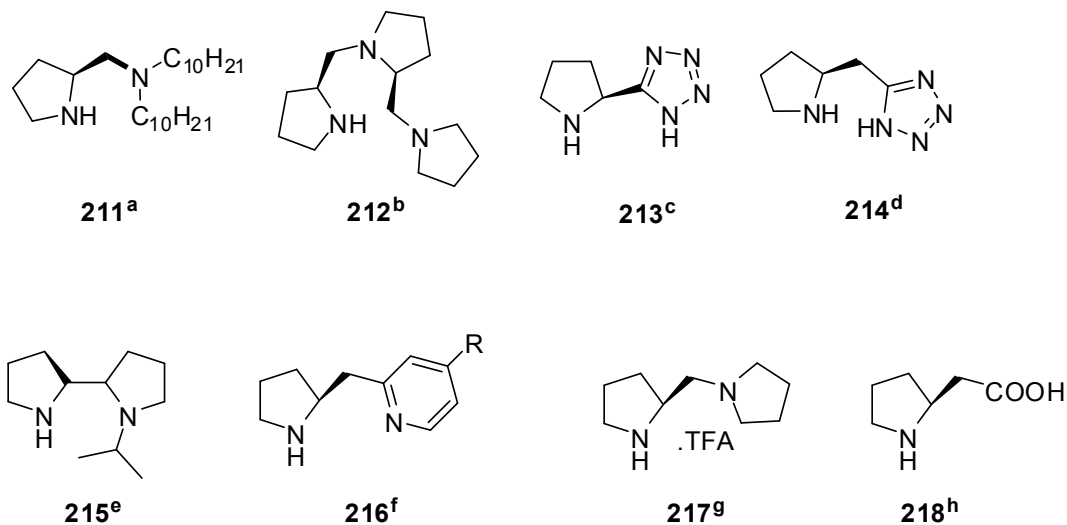


Figure 1.49 A literature selection of proline based organocatalysts used in enamine catalyzed asymmetric Michael addition reactions

In spite of the considerable efforts that have been devoted to improve the selectivity and catalyst activity by the synthesis of a wide variety of proline derivatives, it should also be noted that the design and synthesis of several of these proline based catalyts is quite complicated. Therefore, the identification and development of structurally simple catalytic systems is an ongoing challenge.

1.2.3 Asymmetric amplifications in Enantioselective Catalysis

Chirality displayed by organic molecules that are present in living organisms constitutes a distinct and scientifically challenging set of observations. This geometric preferences favoring one enantiomer over its mirror image are obvious in the observed structures of amino acids, sugars, and the biopolymers that they form. Understanding how the origins of biomolecular homochirality took place has

fascinated both scientists and laymen since Pasteur showed that salts of tartaric acid exist as mirror image crystals.⁷⁶

Although Wynberg and Feringa⁷⁷ recognized the implications of performing asymmetric reactions in the presence of non-enantiopure mixtures, the non-linear effect (NLE) of asymmetric reactions was first quantified by Kagan and co-workers.⁷⁸ Kagan reported the first example of a reaction showing a non-linear effect between the enantiopurity of the chiral catalyst and the product. Since then, many examples of this nonlinear behavior have been demonstrated,⁷⁹ and the use of non-enantiopure catalyst mixtures is rapidly becoming a common mechanistic tool based on Kagan's work.

Linear behavior in asymmetric catalysis is expected to be that the product enantiopurity is linearly proportional to the catalyst enantiopurity. On the other hand, nonlinear behavior in asymmetric catalysis is typically reported as product enantioselectivity (ee_{prod}) vs catalyst enantiomeric excess (ee_{cat}) as seen in **Figure 1.50**. In many asymmetrical stereoselective syntheses, ee_{prod} is not always proportional to ee_{cat} employed in the reaction. If ee_{prod} is higher than ee_{cat} , (+)-NLE (Asymmetric Amplification) is obtained with amplified enantioselectivity. Conversely, if ee_{prod} is lower than ee_{cat} , (-)-NLE (Asymmetric Depletion) is obtained with depleted enantioselectivity.

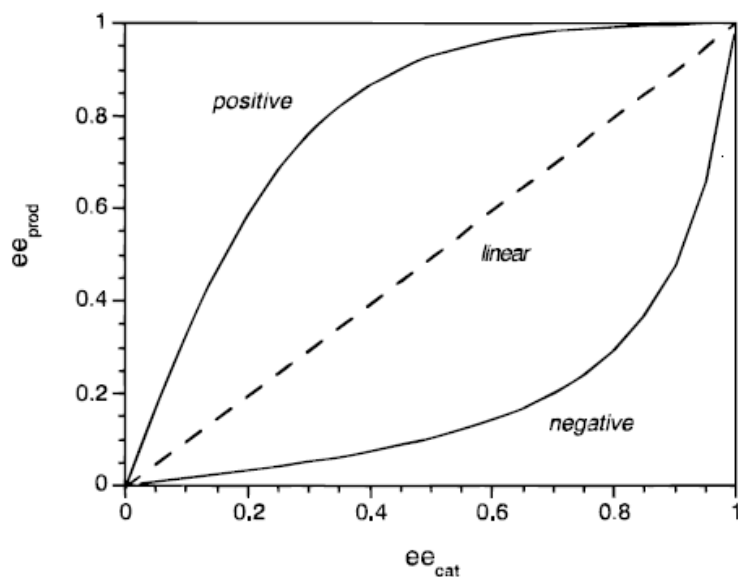


Figure 1.50 Relationships between enantioselectivity of the reaction product and enantiomeric excess of the chiral catalyst

In 1986, Kagan *et al.*⁷⁸ investigated the non-linear relationship in the Sharpless asymmetric epoxidation with titanium (IV) isopropoxide and scalemic (nonracemic) diethyl tartarate (**220**) (DET) (**Figure 1.51-A**). In the oxidation of geraniol (**219**) a (+)-NLE was observed between the enantiopurity of (*R,R*)-DET and the product epoxide **221**. The *ee* values of the epoxide were greater than those calculated for a linear correlation based on the *ee* values of the scalemic (*R,R*)-DET. In the same report, the asymmetric oxidation of sulfide **222** by a “water modified Sharpless reagent in the presence of scalemic (*R,R*)-DET on the other hand revealed the presence of a negative non-linear effect when (*R,R*)-DET of up to 70% *ee* was used (**Figure 1.51-B**). In this case, the *ee* values of the products were found to be lower than calculated for a linear correlation with ee_{DET} .

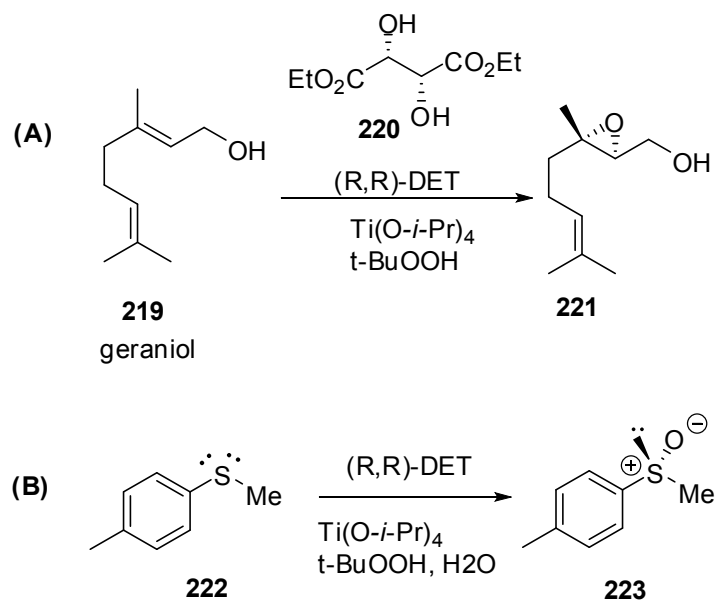


Figure 1.51 (a) Sharpless asymmetric epoxidation (b) oxidation of sulfide **222**

Kagan and co-workers interpreted the positive and negative detected NLE by proposing a diastereomeric association of chiral ligands outside and/or inside the catalytic cycles. The empirical models for NLEs focused on diastereomeric interactions between chiral ligands (L) and metal (M). With this, the monomeric chiral ligand - metal interaction would display a linear autoinduction. On the other hand, if two chiral enantiomeric ligands are associated on a metallic center, three different catalytic species form, which would not guarantee a linear autoinduction. Four basic models were proposed by Kagan: (1) ML_2 including bimetallic dimerization of (M-L), (2) reservoir effect model which is the most generalized model, (3) ML_3 , and (4) ML_4 model. To understand, only ML_2 and the reservoir effect model will be covered in this introductory part.

In ML_2 system, shown in **Figure 1.52**, fast ligand exchange among two enantiomers occur on a metallic center, giving rise to three different complexes; X, Y, and Z in their steady states. Each steady state complex undergoes an irreversible rate-determining step to generate a product in which the enantiomeric complexes, X and Y, produce their enantiomeric products, and the meso complex, Z, produces racemic products.

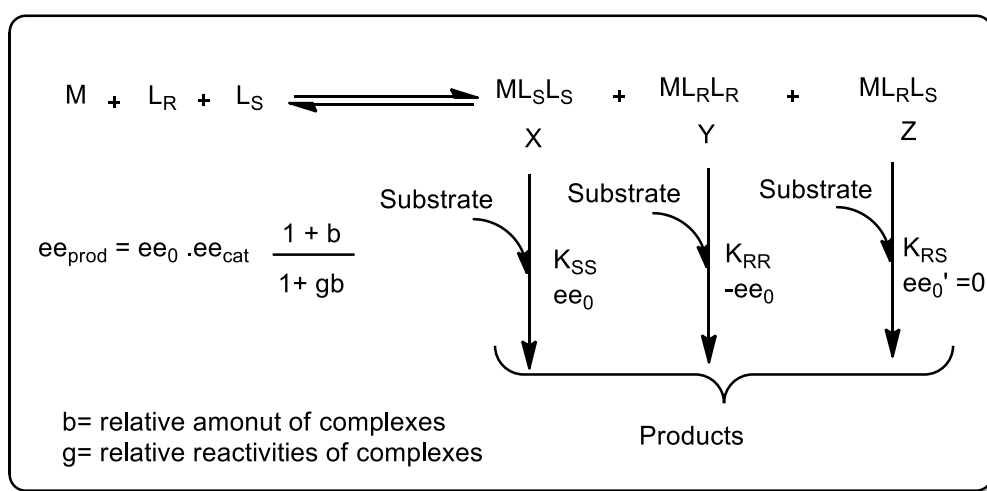


Figure 1.52 Schematic representation of ML_2 system

For example, in the Sharpless epoxidation, it was proposed that the heterochiral dimer (ML_RL_S) was more stable and less active than the homochiral species (ML_SL_S and ML_RL_R). So, the heterochiral dimer removes some racemic DET from the catalytic cycle, thereby leaving enantioenriched (R,R)-(+)-DET in the medium to take part in the catalytic cycle, hence leading to a (+)-NLE. Similarly, in the sulfide oxidation mentioned above, it was suggested that the heterochiral dimer more reactive than the homochiral species to explain the (-)-NLE.

As shown in **Figure 1.53**, Kagan's reservoir effect model, the most generalized model, is based on formation of two different catalytic species when two enantiomers are mixed in solution: (i) inactive reservoir catalysts and (ii) active catalysts. The inactive reservoir catalyst with ee of reservoir (ee_{res}), consists of aggregated ligand-metal complexes in which heterochiral complexes are predominantly present due to their thermodynamic stabilities. Meanwhile, the active catalyst with ee_{eff} consisting of a monomeric metal – ligand complex, undergoes its catalytic cycles. Assuming that two catalytic species are in equilibrium each other, ee_{eff} would be amplified due to the disposition of monomeric catalyst to form heterochiral complexes.

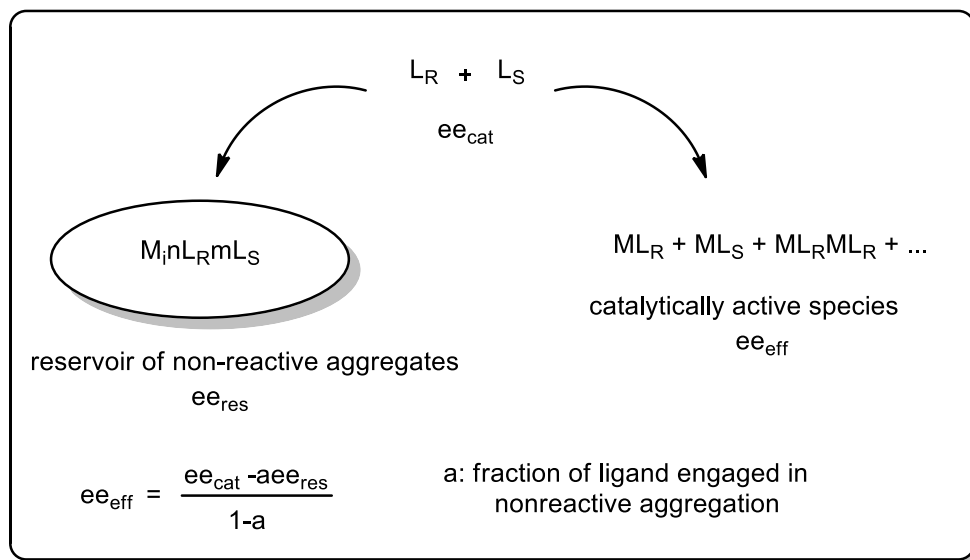


Figure 1.53 Schematic representation of reservoir effect model system

In 1953, Frank⁸⁰ described a reaction mechanism in which the chiral product acted as a catalyst in its own self-production (autocatalysis). The proposed mechanism did not contain any laboratory demonstration, but he explained the idea behind this mechanism as the chiral product can catalyze the production of the same enantiomeric product and inhibits the production of the other enantiomer. The first experimental proof of concept of autocatalysis was established by Soai and co-workers.⁸¹ As seen in **Figure 1.54**, they reported that isopropylation of pyridine-3-carboxyaldehyde (**232**) in the presence of catalytic amount of the reaction product **230**, amino alcohol, with 5% *ee* resulted in 42% yield with 55% *ee*, which is greater than that of the initial catalyst. The increased rate of reaction was resulted from the participation of the product in the reaction.

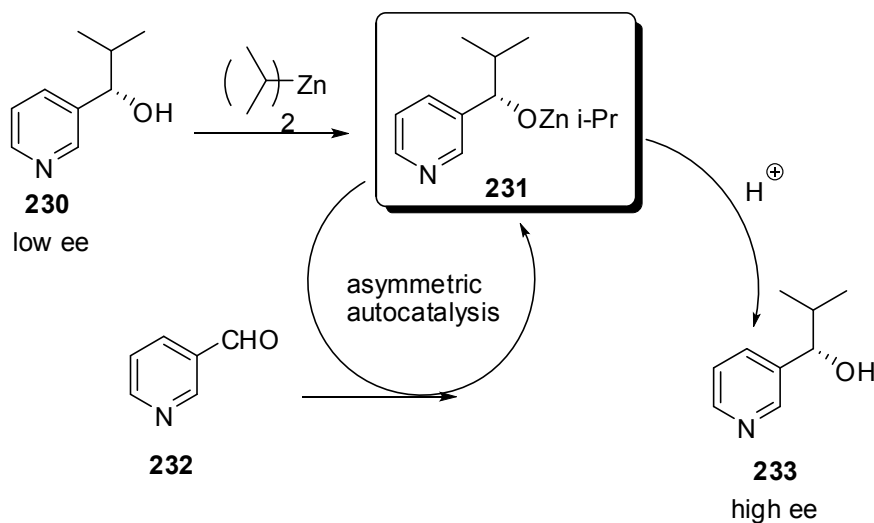


Figure 1.54 Isopropylation of pyridine-3-carboxyaldehyde (**232**) in the presence of catalytic amount of the reaction product **230**

Later, Blackmond successfully reported mechanistic details of the Soai reaction.⁸² Blackmond and co-workers modified Kagan's ML_2 system to explain the asymmetric amplification as arising from an increased reactivity of the homochiral dimers versus the heterochiral dimer. As shown in **Figure 1.55**, it was proposed that all the dimeric species are equally stable and nonlinear effects can only arise when there is an excess of one enantiomer in the catalyst.

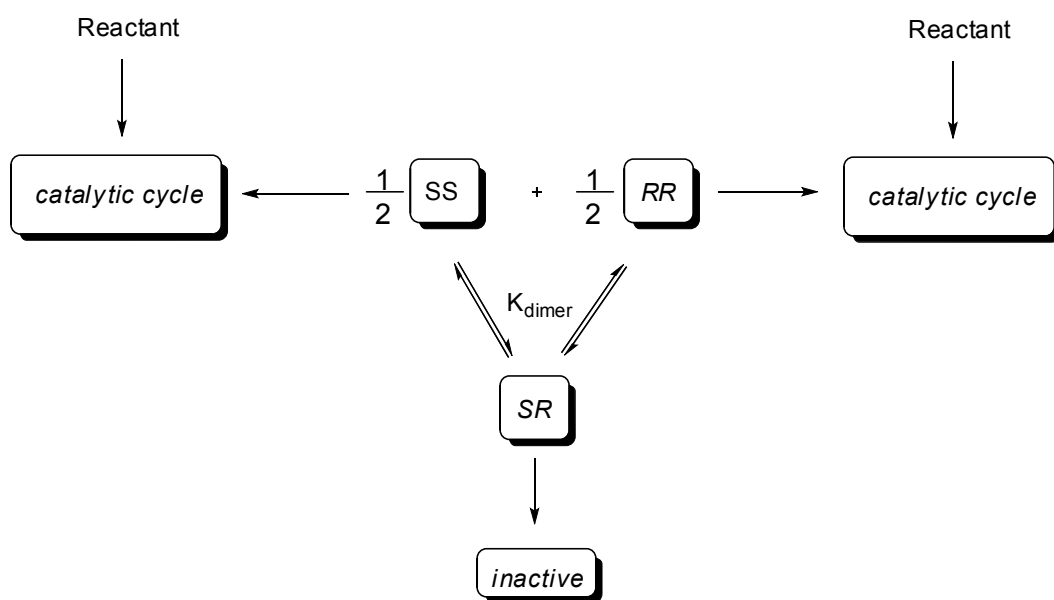


Figure 1.55 Blackmond's mechanistic model for the Soai reaction

Mechanistic model studies of Soai reaction help us to understand the evolution of homochirality. However, dialkyl zinc chemistry precludes the Soai reaction from being of prebiotic significance, because experimental conditions of Soai reaction are unlikely to have appeared in a prebiotic environment. Therefore, the

cogitations on the types of transformations, which are responsible for the origin of the optical activity in living organisms, remain prevalent among scientists.

It has been known for a decade that extraterrestrial amino acids have been detected on some meteorites with enantiomeric excesses of up to 9 %.⁸³ Since then, the field of amino acid chemistry has assumed a plausible area for the evolution of biological homochirality. As mentioned before, NLEs could possibly be responsible for the origin of the homochirality in the earth. Blackmond introduced the first example of nonlinear effects in amino acid catalysis and co-workers in 2004.⁸⁴ It was observed amplification of enantiomeric excess in a proline catalyzed α -aminooxylation of propionaldehyde in CHCl_3 under heterogeneous conditions. It should be emphasized that performing the same α -aminooxylation reaction in DMSO under homogeneous conditions does not show any nonlinear effect. These early observations of nonlinear effects in amino acid catalysis were analyzed by Blackmond⁸⁵ and Hayashi⁸⁶, to be due to “the equilibrium phase behavior model” of amino acids.

The solid-solution phase behavior of non-enantiopure mixtures of amino acids have been studied extensively by Blackmond.⁸⁷ According to these works, when equilibrium is established between solid and solution in a non-enantiopure mixture of most amino acids and solvent under isothermal conditions, this ternary system will consist of dissolved amino acid in the solution phase and two different solid phases: a racemate of *D* and *L* enantiomers (1:1 cocrystals), and a second solid phase of the pure enantiomer that is in excess. At a constant pressure and temperature, the composition of the solution phase at equilibrium, known as its eutectic, is fixed by the phase rule and can have an *ee* value anywhere between 0–100% *ee*. In other words, the *ee* of the amino acid in solution was determined to be independent of the overall amino acid *ee* under thermodynamic conditions, which is at equilibrium. For instance, 50% *ee* is reported as the eutectic value for

scalemic proline in DMSO at 25 °C. As a result, under solid-solution equilibrium, this eutectic value thus dictates the solution *ee* for all values of scalemic proline *ee* employed, which in turn dictates the product *ee* that may be achieved in solution phase reactions catalyzed by proline.

Ternary phase diagram for proline (**Figure 1.56**) shows that the eutectic *ee* value is directly related to the relative solubility of the racemate compared to the enantiopure compound in DMSO. High eutectic *ee* is obtained in cases where the racemate is much less soluble than the enantiopure compound. This solubility ratio between racemate and enantiopure compound has been denoted as a parameter termed α . The **equation-1** successfully developed for the prediction of eutectic *ee* value of chiral compound. The **Equation 1** can readily be applied to simple solubility measurements on racemate and pure enantiomers. The eutectic point can easily be estimated without the time-consuming construction of a ternary phase diagram.

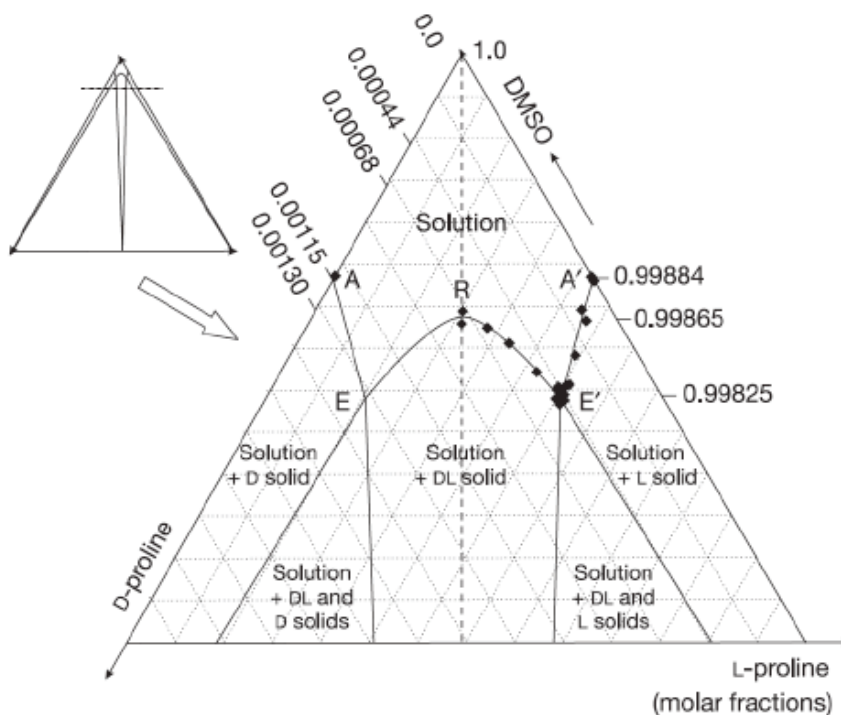


Figure 1.56 Ternary phase diagram for Proline in DMSO (taken from ref. 85)

$$ee(\text{eut}) = \frac{1 - \left(\frac{\alpha^2}{4}\right)}{1 + \left(\frac{\alpha^2}{4}\right)} \times 100\% \quad \alpha = \frac{\text{solubility of racemate}}{\text{solubility of pure enantiomer}}$$

Equation 1 (taken from ref. 84b)

Hayashi and co-workers showed that eutectic ee in CHCl_3 is indeed 99% and not 50% ee as reported in DMSO. Additionally, for proline in EtOH and MeOH, the eutectic ee values are 58%, and 54%, respectively. This significant enhancement of the eutectic ee in CHCl_3 is directly related to the relative solubilities of the enantiopure and racemic solid in a given solvent. Moreover, the exact role of the solvent in altering the eutectic value of proline is also explained by Blackmond.

During the crystallization of racemic proline from $\text{CHCl}_3/\text{EtOH}$, they were able to isolate a solvated proline that has one CHCl_3 molecule with each racemate pair of proline molecules (**Figure 1.57**). The solubility of this racemate, which is effectively reduced by extensive hydrogen bonding, is less than enantiopure proline, which crystallizes from CHCl_3 without incorporation of solvent. The authors also emphasized the exciting prospect of engineering the eutectic position by judicious choice of a small achiral molecule that can influence solubility behavior, for example, by means of hydrogen-bonding interactions.

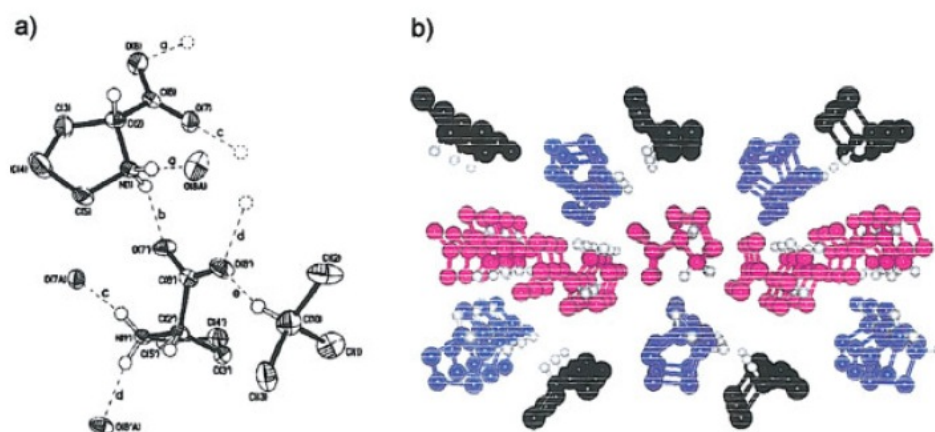


Figure 1.57 (a) The asymmetric unit of *DL*-Proline/chloroform (b) Structure of racemic proline crystallized from a $\text{CHCl}_3/\text{CH}_3\text{OH}$ mixture, with one CHCl_3 molecule (black) incorporated per pair of proline molecules (taken from ref. 86).

Recently, Blackmond and co-workers demonstrated that the eutectic composition of mixtures of *L* and *D* amino acids may be tuned by the addition of achiral additives, such as dicarboxylic acids, that are able to cocrystallize with chiral amino acids.⁸⁷ They find that these systems yield new eutectic compositions of 98% *ee* or higher. This work shows that as long as solid-liquid equilibrium is

maintained, a mixture of amino acid enantiomers will continue to exhibit its eutectic solution composition even in the face of slow racemization. Thus, these systems could afford highly enantioenriched aqueous solutions over an extended period of time.

1.3 The aim of the work

1.3.1 Addition of Trifluoromethyltrimethylsilane to Acyl Phosphonates

In last few years, many reports have been published concerning the new advances in the field of acyl anion chemistry. This suggests a reemerging interest in developing new catalyzed methods involving d^1 nucleophiles. Efforts to produce new acyl anion precursors and new transformations involving unpoled nucleophiles will undoubtedly be an active area of research.

Fluorinated and perfluoroalkylated organic compounds constitute important targets in many research fields. One of the most challenging synthetic problems is the introduction of a trifluoromethyl group in a mild manner. Therefore, the development of new methods for the introduction of trifluoromethyl groups onto organic molecules has received intensive attention.

In this context, the aim of this part is the investigation of the the reaction of the trifluoromethyltrimethylsilane (CF_3TMS) with acyl phosphonates. It was planned to gain a direct and uncatalyzed access to α -hydroxytrifluoromethylphosphonates.

1.3.2 Development of new supramolecular organocatalytic strategies for the enantioselective asymmetric C-C bond forming reactions

The significant progresses made in enantioselective catalytic C-C bond forming reactions mostly depend on the careful and time-consuming optimization of the structure of the chiral catalyst to get the maximum enantioselectivity and catalytic activity. Suitable chemical modifications in the catalyst structure can often make unpredictable differences to the activity of the catalyst, expressly in terms of the enantioselectivity. Given the important advances made in high-throughput screening and analysis techniques, the slow step in the screening of chiral catalysts is the chemical synthesis of the catalyst. Therefore, great interest in new methodology that allows the synthesis of libraries of structurally diverse catalysts.

The aim of this part is to develop new supramolecular organocatalytic systems (host-guest complex) for:

- (i) enantioselective direct aldol reactions of various aromatic aldehydes and cyclohexanone.
- (ii) enantioselective nitro-Michael addition of aldehydes to nitroalkenes.

1.3.3 Nonlinear effects in proline-thiourea host-guest complex catalyzed aldol reactions in nonpolar solvents

The presence of nonlinear effects in amino acid catalysis and its importance for the origins of homochirality in living organisms have long intrigued scientist. Early examples of nonlinear effects in amino acid catalysis were independently clarified by Blackmond⁸⁵ and Hayashi⁸⁶, to be due to the solid-liquid equilibrium of the amino acid catalyst. Since then, several nonlinearity studies have sought to explain and asymmetric amplifications in amino acid catalysis. Interest remains intense

with regards to how and why amino acids and structurally related systems function.

The aim of this part is to study the asymmetric amplifications in proline–thiourea host–guest complex catalyzed aldol reactions in nonpolar solvents.

CHAPTER 2

RESULTS AND DISCUSSION

2.1 Addition of Trifluoromethyltrimethylsilane to Acyl Phosphonates

Partially fluorinated as well as perfluorinated organic compounds exhibit interesting properties⁸⁸ that make them suitable for wide range of diverse applications.⁸⁹ This justifies the steadily growing number of new organofluorine products which appear every year.⁹⁰ In recent years, there have been several drugs where presence of fluorine is necessary for their activity as antiviral and anticancer agents. Therefore, organofluorine compounds are becoming increasingly useful for pharmaceuticals, agrochemicals and functional materials.

During the past few years, extensive research has been carried out to incorporate a fluorinated moiety into organic molecules by making carbon-fluorine (C-F) and carbon-trifluoromethyl (C-CF₃) bonds.⁹¹ The most highly used method for the direct incorporation of trifluoromethyl moiety into organic molecules involves nucleophilic addition of trifluoromethyl anion to carbonyl compounds.

For a long time, the development of nucleophilic trifluoromethylation has been hindered by instability of the naked trifluoromethyl anion because of a large Coulombic repulsion between the fluorine lone pairs and the anion on the carbon

atom. Due to this, a fluorine atom leaves the anion to form a stabilized singlet difluorocarbene (**Figure 2.1**).

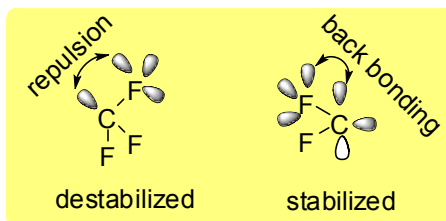


Figure 2.1 Instability of the naked trifluoromethyl anion

One of the most common strategies to stabilize the trifluoromethyl anion is to form a bond between CF_3 and silicon, which produces a labile C-Si bond due to high polarization of the bond. On the heels of extensive research in this field, the use of CF_3TMS (Ruppert-Prakash reagent) has emerged as an effective approach to get these desired transformations.⁹² It has also been reported that fluoride initiators, such as cesium fluoride (CsF) or tetra-*n*-butylammonium fluoride (TBAF), efficiently enhance trifluoromethyl anion formation via corresponding silicon activation.^{92b,93} It should be noted that, these reactions are not catalytic with respect to the moisture sensitive fluoride initiators used.

Prakash *et al.* carried out extensive studies to develop varieties of easily accessible nucleophilic catalysts to promote such reactions.⁹² It was reported that oxygen-containing nucleophiles (Lewis base catalysts), such as trimethylamine N-oxide **236** and potassium carbonate (K_2CO_3) (**237**), are suitable initiators (or catalysts) in CF_3TMS chemistry. As shown in **Figure 2.2**, with these methods, CF_3TMS was added to numerous ketones and aldehydes to get TMS-protected trifluoromethylated alcohols.^{93b}

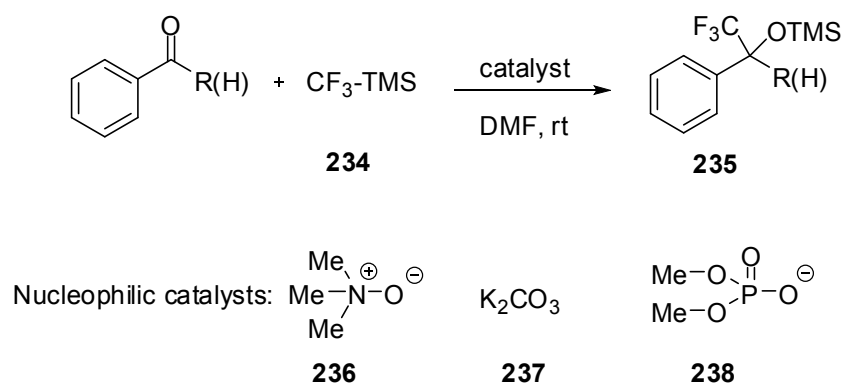


Figure 2.2 Facile syntheses of TMS-protected trifluoromethylated alcohols

Portella and co-workers developed a highly efficient method for the synthesis of α,α -difluoro- β -hydroxy ketones like **241** starting from an acylsilane **239**, CF_3TMS and an aldehyde (**Figure 2.3**).⁹⁴ The key intermediate of this synthesis is a difluoroenoxy silane **240** generated from CF_3TMS and acylsilanes via the Brook rearrangement of the alcohol adduct. Several approaches to difluoroenol silyl ethers have also appeared in the literature.⁹⁵

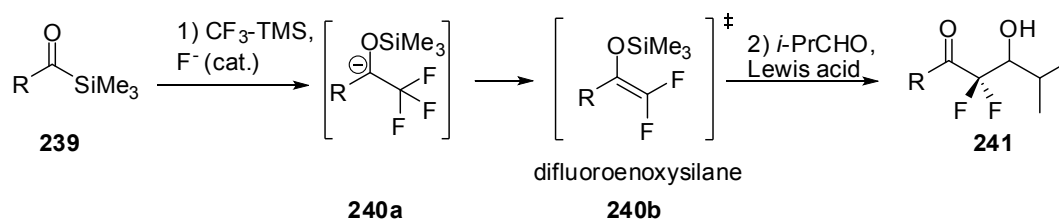


Figure 2.3 Formation of difluoroenol silyl ethers from acylsilanes

As explained in the introductory part of this dissertation, we have shown that acyl phosphonates are potent acyl anion precursors and undergo cyanide (nucleophile) promoted phosphonate-phosphate rearrangement to generate the corresponding acyl anion equivalents as reactive intermediates. As an extension of earlier work from our group, we proposed to investigate the reaction of the CF₃TMS (trifluoromethylation agent) with acyl phosphonates. With this, the plan was to gain a direct and uncatalyzed access to α -hydroxytrifluoromethylphosphonates. Moreover, we hoped that the CF₃ group could supply considerable carbanion stabilization to provide **242**, which can lead to a wide range of fluorinated carbinols upon reaction with electrophiles (**Figure 2.4**). The addition of TMSCN to acyl phosphonates encouraged us to apply the same strategy to the addition of CF₃TMS to the acyl phosphonates.

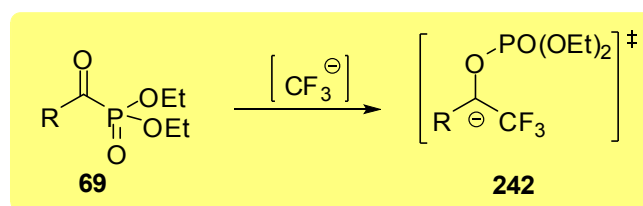


Figure 2.4 CF₃ additions to acylphosphonates

As seen in **Figure 2.5**, diethyl isobutyryl phosphonate **243** was chosen as model substrate to test the feasibility of the method for the addition of trifluoromethyl anion to acyl phosphonates. Compound **243** was treated with CF₃SiMe₃ at room temperature in DMF, but no product formation was observed. Increasing the reaction temperature also failed to give the desired addition product. Next, nucleophilic trifluoromethylation was employed to incorporate a trifluoromethyl moiety into acylphosphonates. For generation of nucleophilic CF₃ anion, to the reaction mixture of isobutyryl phosphonate (**243**) and CF₃TMS was added a

catalytic amount (20% mol) of K_2CO_3 and the reaction was monitored by thin layer chromatography (TLC) for 2h. A product formation was observed. After work-up procedure, the crude product was purified by flash column chromatography and identified with NMR spectroscopy (**Figure 2.6** and **2.7**).

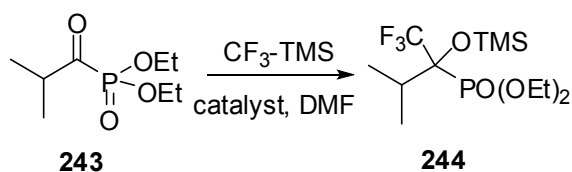


Figure 2.5 CF_3TMS addition to isobutyryl phosphonate **243**

The characteristic peaks in NMR spectra evidenced the formation of the product **244**. The first identifier is CF_3 - peak at ^{13}C -NMR. The CF_3 carbon showed peaks at 123 ppm as a doublet of quartets. This splitting pattern arises from fluorine atoms and also from the phosphorus atom. The typical one-bond coupling constant $^1J_{CF}$ is in the range of 165 - 370 Hz and two-bond coupling constant $^2J_{CP}$ is in the range of 4-10 Hz. In our case, we observed that $^1J_{CF}$ as 287 Hz and J_{CP} as 10.1 Hz. The carbon next to CF_3 - group gives specifically a doublet of quartets at around 80 ppm. This carbon was split with phosphorus atom first and additionally; there was also a clear splitting of the doublet into a doublet of quartets with the fluorine atoms. The typical two-bond coupling constant $^2J_{CF}$ is in the range of 18 - 45 Hz. In this case, we observed $^2J_{CF}$ as 27.5 Hz. In 1H -NMR, the singlet at around 0.1 ppm is obviously for methyl groups in the OTMS. The compound also exhibits a characteristic peak in the ^{31}P -NMR spectrum at 15.2 ppm.

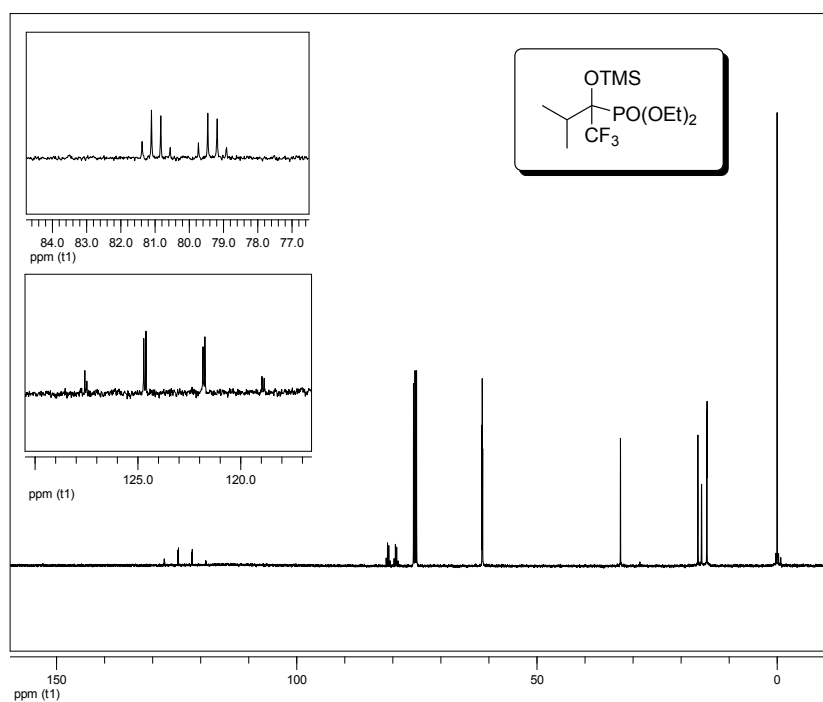


Figure 2.6 ¹³C NMR spectra of 244

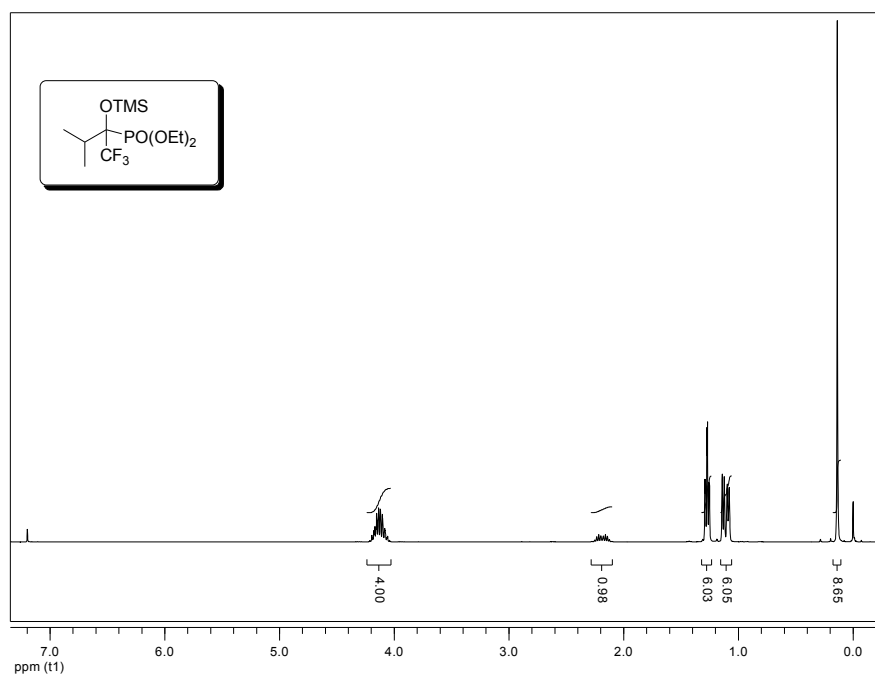


Figure 2.7 ¹H NMR spectra of 244

The reaction was repeated by using 15-50% of K_2CO_3 , sodium acetate (NaOAc), sodium bicarbonate ($NaHCO_3$), and sodium carbonate (Na_2CO_3). K_2CO_3 , NaOAc, and $NaHCO_3$ afforded comparable yields. When Na_2CO_3 was used, no product was obtained. In all cases DMF, CH_3CN , toluene, and THF were screened as solvents at various temperatures. The best yield obtained under the conditions of 1 equivalent of acylphosphonate, 1.5-2 equivalent of CF_3TMS , and 20% K_2CO_3 in DMF (100% conversion in 5 min) at room temperature. With these conditions in hand, we extended this reaction to a number of aliphatic phosphonates. As shown in **Figure 2.8**, desired products were obtained in 70-90% yields.

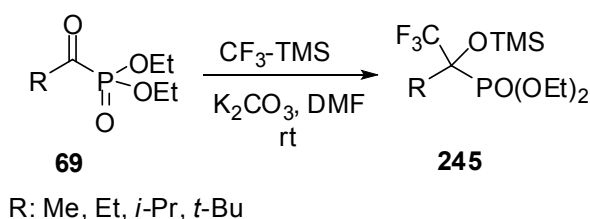
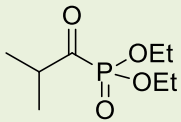
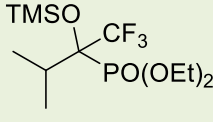
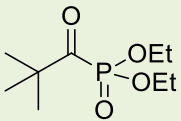
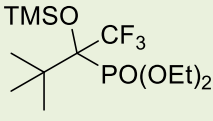
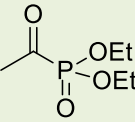
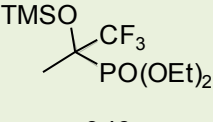
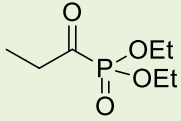
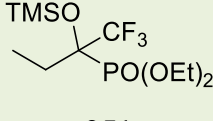


Figure 2.8 General reaction scheme of CF_3TMS addition reaction to alkylphosphonates

As seen in **Table 1**, four different alkyl phosphonates were selected as starting materials for the mentioned reactions. The order we choose these compounds are that for example, in entry 1, compound **243** is neither that bulky nor that naked. With the compound **243** producing **244**, we immediately tried the compound with the bulkiest side chain **246**. With this also giving the desired product, we tried the compound with relatively naked side chain **248**. The results are excellent for our purpose.

Table 1. The results of the addition of CF₃TMS to different alkyl phosphonates

Entry	Acyl phosphonate	Products	Yield (%)
1	 243	 244	90
2	 246	 247	88
3	 248	 249	70
4	 250	 251	89

Encouraged by the results obtained from aliphatic phosphonates, CF₃TMS addition reactions to aryl phosphonates were studied. As shown in **Figure 2.9**, the reaction of aryl phosphonate **252** under the standard reaction procedure described above for aliphatic phosphonates furnished not the expected addition product **253** but rather 1-phenyl-2,2-difluoroethenyl phosphate (**254**) in 96% yield.

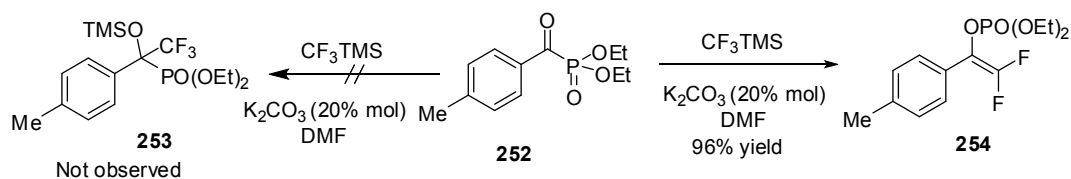


Figure 2.9 General reaction scheme of CF_3TMS addition reaction to aryl phosphonates

The characteristic peaks in NMR spectra showed the formation of the product **254**. The 1H NMR and ^{13}C NMR spectra are shown in **Figure 2.10** and **Figure 2.11**, respectively. Having no peaks in the 0.5-0.0 ppm range proved an absence of TMS group in the structure. The carbon attached to the fluorine atoms showed peaks at 154 ppm as a doublet of doublet of doublets. This splitting pattern arises from fluorine atoms and also from phosphorus atom. Observing such a peak at such a high value ppm supports idea of presence of a double bond. The carbon next to $OPO(OEt)_2$ group gives again a doublet of doublet of doublets at around 113 ppm. The compound also exhibits a characteristic peak in the ^{31}P -NMR spectrum at -4.6 ppm. This (-) value supports idea of presence of an $O-P=O$ bond.

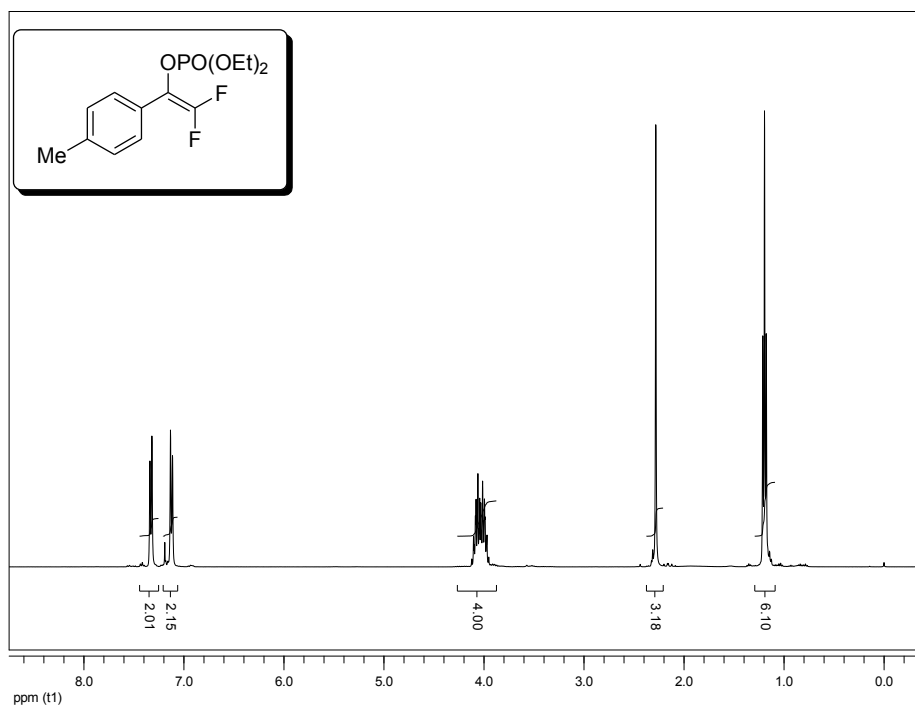


Figure 2.10 ^1H NMR spectra of 254

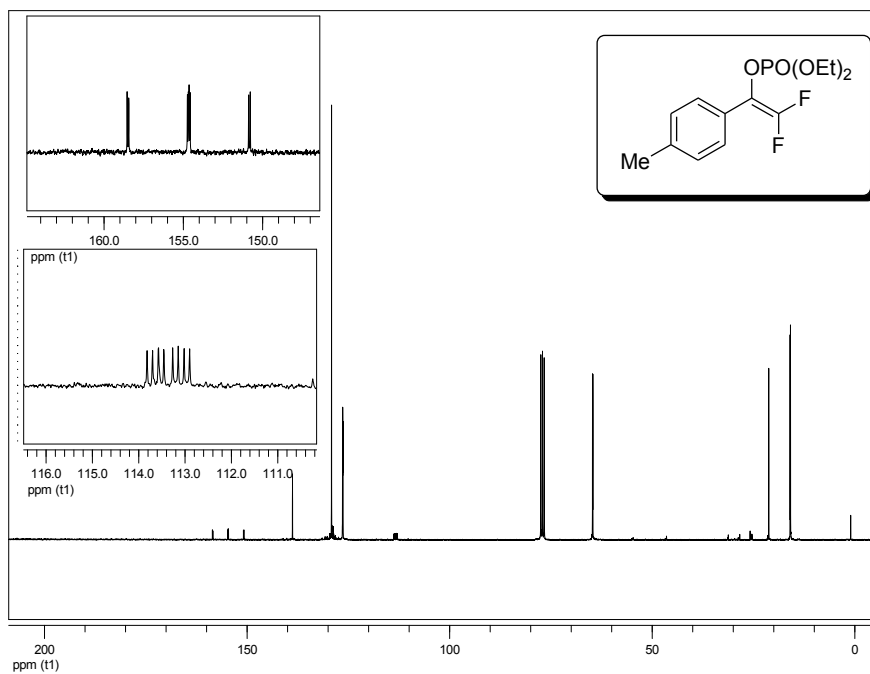


Figure 2.11 ^{13}C NMR spectra of 254

After characterizing compound **254**, we wanted to optimize reaction conditions. It was started with catalyst screening; this reaction was repeated at room temperature in DMF by using various additives. Shown in **Table 2**, it was found that 0.2 equivalent K_2CO_3 is necessary to obtain the desired product. NaOAc and $NaHCO_3$ also afforded high conversions compared to tertiary amines (triethylamine and cinchonidinium chloride). As it was observed in alkyl phosphonate cases, no product formation was observed when Na_2CO_3 is used.

Table 2. The results of addition of CF_3TMS to aryl phosphonate **252** using different catalysts

Entry	Catalyst (20%)	Time	Conversion (%)
1	K_2CO_3	15 min	100
2	CH_3COONa	30 min	100
3	$NaHCO_3$	24 h	90
4	Cinchonidinium chloride	24 h	35
5	Et_3N	24 h	25
6	Na_2CO_3	24 h	0

Having optimized K_2CO_3 as the optimum catalyst for the reaction, the effect of solvents on the reactivity of the reaction was screened (**Table 3**). The best conversion was obtained with DMF in only 15 min. In the case of CH_3CN , THF, or toluene, the conversion rate decreased. By using toluene and THF, the reaction was carried out at -20 and -40 °C and was monitored by TLC; even at -40 °C slow formation of the product was observed. In summary, despite many attempts to

obtain the addition product **253**, compound **254** was always isolated as sole product.

In all cases, from crude $^1\text{H-NMR}$ spectra, the trace amount of addition product **253** was observed, but it was failed to isolate it. To identify whether the formation of the elimination product occurred during the reaction, at the workup step, or during the purification step; we carried out several control experiments and found that the elimination reaction takes place during the reaction (the reaction was monitored by TLC and $^1\text{H-NMR}$).

Table 3. CF_3TMS Addition to benzoyl phosphonate **252** in different solvents

Entry	Solvent	Time (h)	Temp. ($^\circ\text{C}$)	Conv. (%)
1	DMF	15 min.	rt	100
2	CH_3CN	16	rt	70
3	THF	24	rt	65
4	THF	24	-20	10
5	THF	24	-40	10
6	Toluene	24	rt	40
7	Toluene	24	-20	15

In order to obtain further insight into the scope of the reaction, a series of electronically diverse aryl phosphonates were treated with CF_3TMS in DMF as shown in the **Table 4**. The reaction gave excellent results for electronically diverse range of aromatic acyl phosphonates. Substituents at the ortho-position do not give

any steric problems. Not only electron-withdrawing substituents but also electron-donating substituents gave excellent yields. Various substitutions at all positions we tried were tolerated.

Table 4. The results of the addition of CF₃TMS to different aryl phosphonates

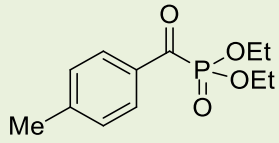
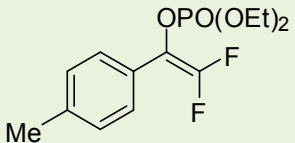
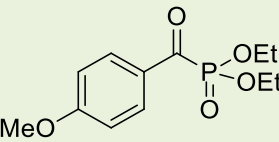
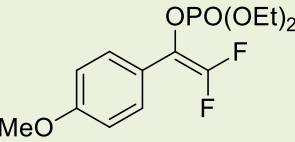
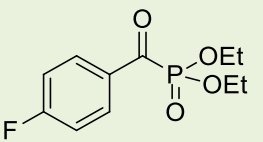
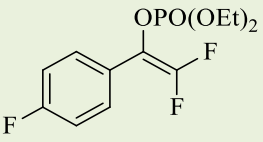
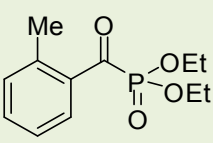
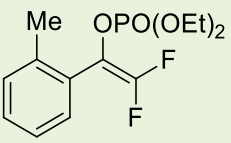
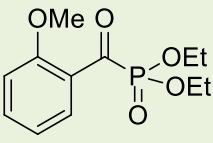
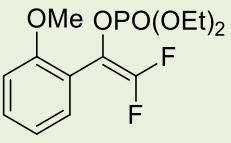
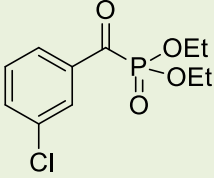
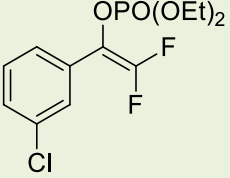
Entry	Acyl phosphonate	Products	Yield (%)
1	 252	 254	92
2	 255	 256	95
3	 257	 258	92
4	 259	 260	97
5	 261	 262	87

Table 7 (Continued)			
Entry	Acyl phosphonate	Products	Yield (%)
6	 263	 264	91

It should be stated that, under the standard procedures mentioned above, by using furoyl phosphonate **265**, both elimination product **266** and CF₃ addition product **267** were obtained in equivalent amounts with almost 100% conversion based on crude ¹H-NMR spectrum (**Figure 2.12**). Careful repetition of this reaction under various conditions (variation of temperature, amount of additives and solvents) resulted in no remarkable change on the product ratio.

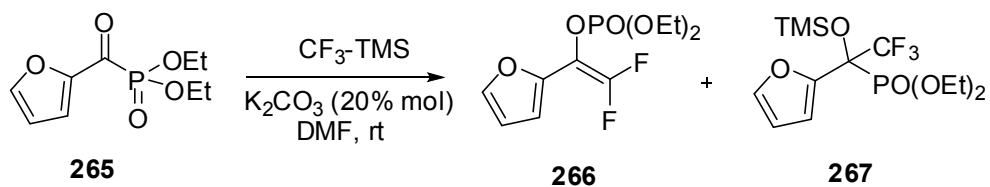


Figure 2.12 Addition of CF₃TMS to furoyl phosphonate **265**

We have already discussed the mechanism of addition of CF_3TMS to acyl phosphonates. Prakash and co-workers reported the formation of intermediates **268-270** from TMSCF_3 and potassium carbonate.^{93a} As shown in **Figure 2.13**, it was proposed path “a”, wherein only a single anionic center of K_2CO_3 is involved in the attack of TMSCF_3 to produce the trigonal bipyramidal intermediate **269** that can further forms the hexavalent intermediate **270** via expanding the valency of silicon, which has an empty d orbital. Alternatively, both anionic centers of K_2CO_3 can be involved in the attack of two molecules of TMSCF_3 to form a double trigonal bipyramidal intermediate **268**, wherein the carbonate can occupy the axial positions of both the trigonal bipyramids (path b).

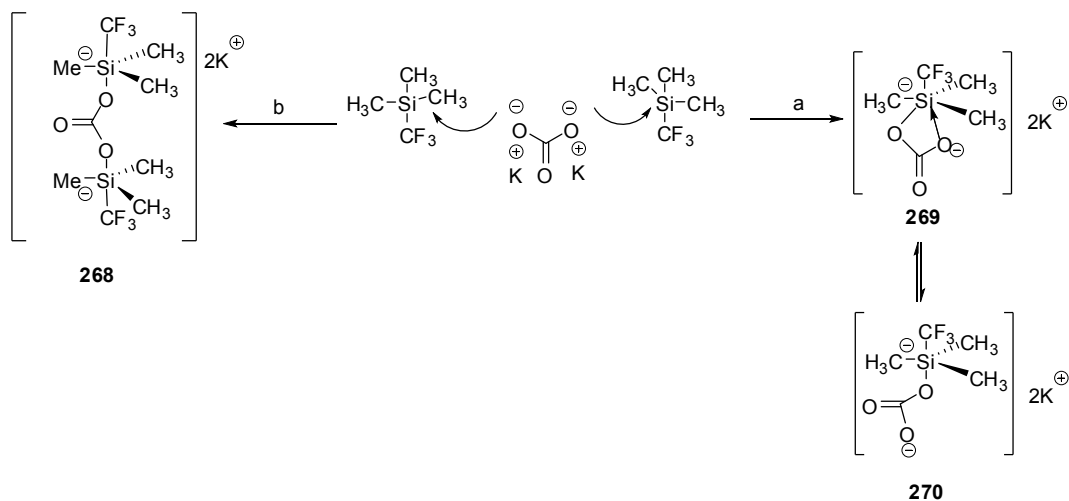


Figure 2.13 A possible mechanism for the formation of intermediates **268-270** from TMSCF_3 and potassium carbonate

Based on Prakash's proposal, a possible mechanism for our reaction is shown in **Figure 2.14**. Subsequently, intermediate **268**, **269**, or **270** can attack to the acyl phosphonate to produce the corresponding intermediate **273** (in **Figure 2.13**, **269** is taken as an example), which can then decompose to form the product **274** and regenerate the catalyst. In the case of benzoyl phosphonate (**Figure 2.14-b**), after the addition of CF_3 , a phosphonate-phosphate rearrangement occurs to generate 1-phosphonoxy-2,2,2-trifluoroethyl carbanion (**272**), which was stabilized by the aryl ring. Then, the elimination of F^- anion is preferred to form the stable conjugate product **273** as described. By the computational studies on enantioselective thiazolium-catalyzed benzoin reaction, Goldfuss⁹⁶ reported that alkyl substitution disfavors but π -conjugation favors formation of the carbanionic d^1 -intermediate. The mixed product formation with furoyl phosphonate **265**, which destabilized the carbanion, supported this suggestion.

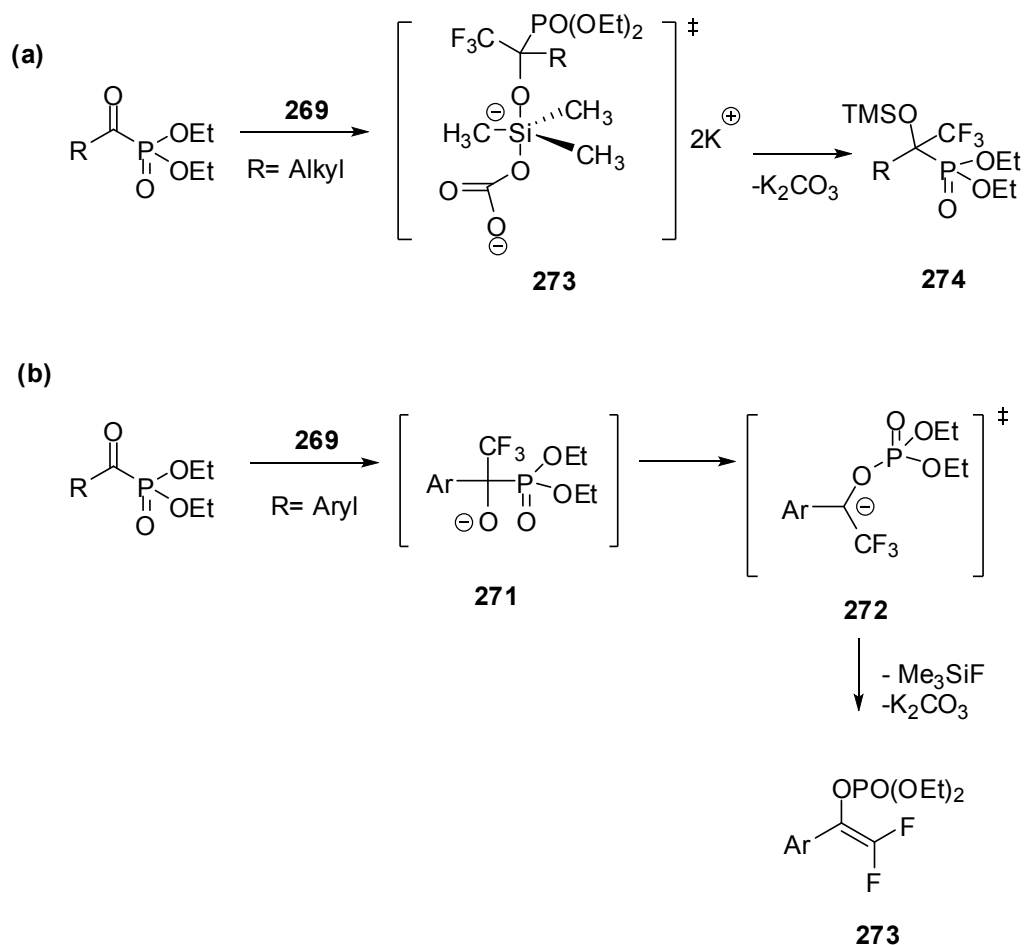


Figure 2.14 A possible mechanism for the addition of TMSCF_3 to acyl phosphonates

The present approach enables us to synthesize these important difluorinated compounds. Ishihara *et al.*⁹⁷ have been introduced the synthesis of these types of difluorovinylphosphates. It was reported the preparation of 1-substituted 2,2-difluoroethyl phosphates or 1-hydroxyalkanephosphonates through the reaction of chlorodifluoromethyl ketones with dialkyl or diaryl phosphites. 1-Hydroxyalkane phosphonates are converted to enolphosphates by the treatment with triethylamine

or sodium methoxide in refluxing tetrahydrofuran. The applicability of these procedures is limited because of the complexity and difficult availability of the reagents.

In conclusion, in this part of this dissertation, we have developed a convenient, one-pot procedure for preparing various 1-alkyl-2,2,2-trifluoro-1-trimethylsilyloxyethyl phosphonates and 1-aryldifluoroethenyl phosphates starting from readily available acyl phosphonates and trifluoromethyltrimethylsilane under mild conditions. K_2CO_3 has been used as an effective catalyst in the nucleophilic trifluoromethylation reactions successfully, and its catalytic property has been improved further by using DMF as a solvent. Addition of the nucleophilic CF_3 to acyl phosphonate furnished products in 70-90% yields. By using benzoyl phosphonates for the addition, phosphonate-phosphate rearrangement followed by fluorine elimination afforded products in 87- 97% yields.

2.2 Development of new supramolecular organocatalytic strategies for the enantioselective asymmetric C-C bond forming reactions

One of the cornerstones in chemistry nowadays is the synthesis and development of new and better catalysts that allow us to construct new molecules. This approach has been fulfilled by a carefully and time consuming optimization of many catalysts. The most common approach has been to design modular ligands and/or the modification of previous catalysts.

Since the rediscovery of proline as organocatalyst by List, Barbas and Lerner, the use of proline and amino acid derivatives as organocatalysts have grown exponentially. These initial reports not only provided a simple solution to one of the most important problems in catalytic asymmetric synthesis, but also attracted a

great deal of attention to the use of small organic molecules as catalysts in organic chemistry.

Although proline is a rather good catalyst, it is not without some potential drawbacks, such as low solubility in typical organic solvents, potential side reactions and established parasitic equilibria with substrates that make using high catalyst loadings necessary to achieve acceptable conversions,⁶⁶ low selectivities with planar aromatic aldehydes in direct aldol reactions, and low reactivity and enantioselectivities when is used as enamine catalyst with aldehydes. Therefore, considerable effort has been devoted to the development of proline analogs in order to improve their reactivity, selectivity and scope.

Considering the practical synthetic issues, the carboxylic acid moiety of proline has been targeted as a site for modification. Its reactivity and selectivity is enhanced in custom-made catalysts, even though the identification of a good catalyst requires the synthesis of various analogs of a proposed design in order to identify the optimum one. Moreover, the improved catalysts are usually obtained through the modification of proline with chiral molecules with additional functionality, and are much more precious than the proline itself.⁵⁸

In the way “*to make a good asymmetric catalyst perfect*”, the role of suitable additives, or co-catalysts, can be crucial in enhancing the reactivity and stereoselectivity of the catalytic system. In 2006, Shan and co-workers have shown that using chiral diols as additives can improve the enantioselectivity of proline catalyzed aldol reactions, probably through their involvement in the transition state, via formation of a hydrogen bonding network (**Figure 2.15-a**).⁹⁸ Later, Miller showed the cooperative effect of a co-catalyst in a proline-catalyzed Baylis–Hillmann reaction where the proline and co-catalyst were proposed to interact in a transition state assembly, forming a catalytic system that was “greater than the

sum of its parts”⁹⁹. Recently, Clarke elegantly developed an improvement in the reactivity and selectivity of a proline-derived amide decorated with a hydrogen bond acceptor site, which could then self-assemble with hydrogen bond donor additives, thereby improving a poor catalyst into a very good one in a Michael-type addition of ketones to nitro olefins (**Figure 2.15-b**).¹⁰⁰

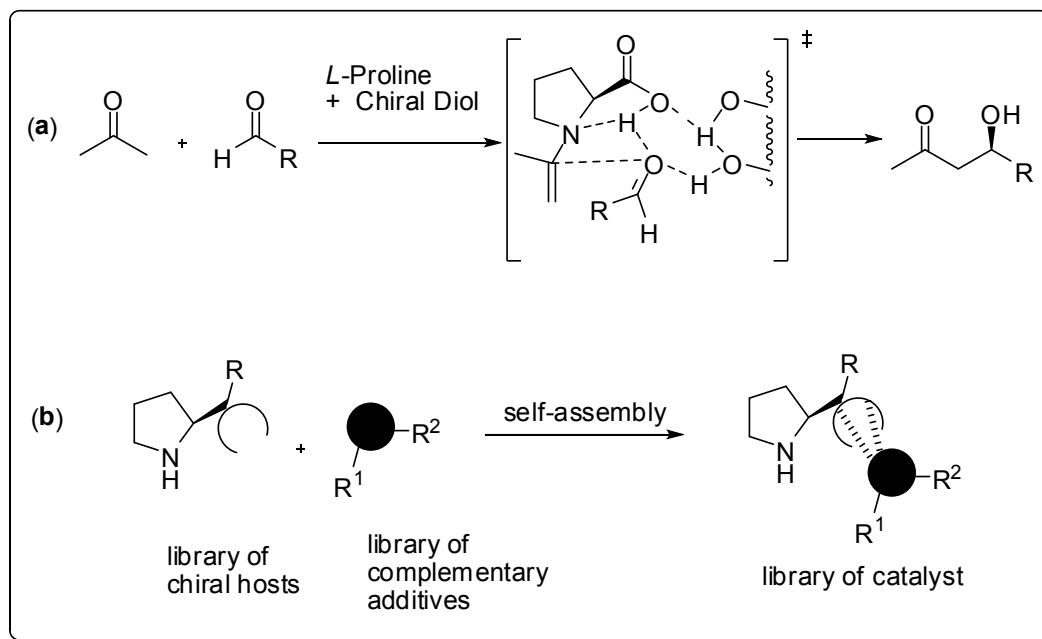


Figure 2.15 A literature example of self-assembly of organocatalysts

Supramolecular chemistry has witnessed an emergent power in chemistry since the pioneering works of Lehn.¹⁰¹ Supramolecular self assembly units have been used as a catalyst in organocatalytic reactions.⁹⁸⁻¹⁰⁰ In the field of organometallic chemistry, Breit and co-workers have showed that the use of supramolecular interactions as hydrogen bond can be used to improve an existent catalyst, obtaining amazing results in the enantioselective hydrogenation.¹⁰² With those

ideas in mind, we envisioned an easy method to generate new catalysts by auto assembling different units by supramolecular interactions.

2.2.1 Direct enantioselective aldol reactions catalyzed by a proline–thiourea host–guest complex

Proline catalyzed direct aldol reactions have been shown experimentally and theoretically to proceed through enamine intermediates, in which the transition state is highly stabilized by hydrogen bond donation from the carboxylic acid moiety to the electrophile, with concurrent formation of partial iminium and carboxylate ions on the proline as shown in **Figure 2.16**. Moreover, proline is known to exist as a zwitterion, which forms a highly insoluble network of hydrogen-bonded units. We anticipated that a chemical entity that selectively and strongly binds to the acetate functionality will; (1) interact with proline in solution, thus altering its solution properties and reactivity, (2) also bind to the transition state which lowers its energy, thereby improving the selectivity of the reaction. Based on this initial proposal, we decided to investigate the use of a diarylthiourea moiety, because of its well known ability of strong and well-defined binding to carboxylates through hydrogen bonding.¹⁰³

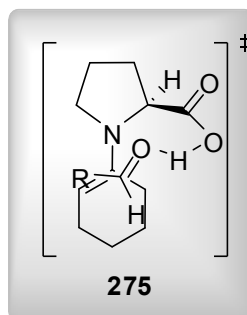


Figure 2.16 Houk model for the proline catalyzed intermolecular aldol reaction

In order to prove this concept, we made use of Schreiner thiourea **279** as a good self-assembly unit with carboxylate part of proline. As shown in **Figure 2.17**, it was thought that proline-carboxylate could interact with thiourea in order to form supramolecular units that can enhance the catalytic properties of proline itself.

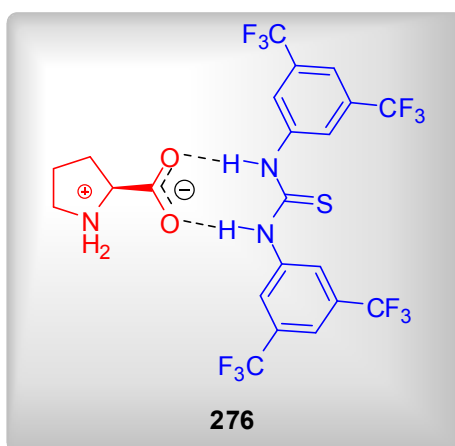


Figure 2.17 Supramolecular self-assembly organocatalysts

Therefore, we studied this catalytic system in direct aldol reactions between cyclic ketones and aldehydes (**Figure 2.18**). We began the investigations with cyclohexanone (**277**) as the donor ketone and 4-nitrobenzaldehyde (**150**) as the acceptor aldehyde, since these starting materials are common components for such a system.

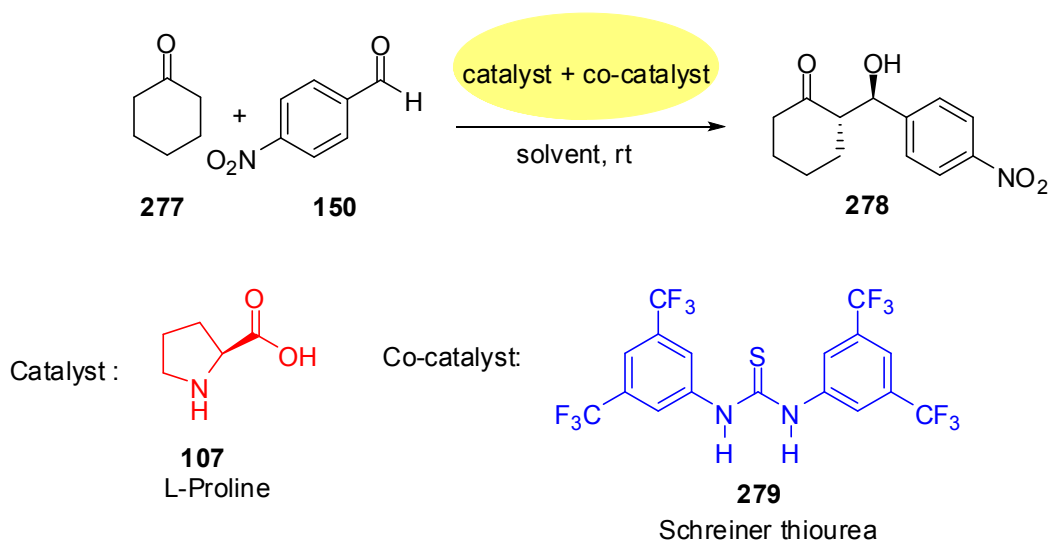


Figure 2.18 General reaction schemes for the direct enantioselective aldol reactions catalyzed by a proline–thiourea host–guest complex

In the course of the initial solvent screening, it was shown that the use of polar solvents did not improve the results compared to proline catalysis by itself. The reaction in DMSO, which is a typical solvent for this type of reaction, resulted in the same level of selectivity and product purity with or without the urea additive. As shown in **Table 5**, when MeCN was employed, the reaction was still sluggish and the selectivity was low. This was, of course, expected considering the inefficiency of hydrogen bonding interactions in polar mediums.

Table 5. Initial Screening of Conditions for the Formation of Aldol **278**

Entry	Solvent	L-proline:thiourea		Conv (%)	<i>anti:syn</i>	<i>ee</i> (%)
		279 (%)	Time (h)			
1	MeCN	20:20	16	28	71:29	92
2	CHCl ₃	20:20	16	80	80:20	96
3	Toluene	20:20	16	96	92:8	>99
4	Hexane	20:20	12	99	90:10	99
5	Hexane	20:5	12	99	91:9	99
6	Hexane	20:0	36	24	68:32	83
7^a	Hexane	20:20	12	37	81:19	93
8^b	Hexane	20:20	12	97	86:14	98
9	Hexane	10:10	16	96	90:10	99
10	Hexane	5:5	16	30	90:10	99
11	Toluene	5:5	16	44	90:10	99
12	neat	5:5	16	85	93:7	97

a. *S*-tryptophan is used as the catalyst, b. *S*-tert-leucin is used as the catalyst

When we switched to apolar solvents, both the efficiency and the selectivity were remarkably enhanced. Among the non-polar solvents used, toluene showed a slightly better selectivity, while the reaction proceeded faster and more clearly in

hexane. This observation is remarkable considering the solubility of proline in hexane.

We also found that the relative amount of additive could be reduced without a loss in reactivity and selectivity (**Table 5, entry 5**); on the other hand, it was found that the amount of proline is important for the rate of the reaction without compromising the selectivity (**Table 5, entry 10**). The aldol reaction performed without solvent also furnished the product in high diastereoselectivity and enantioselectivity (**Table 5, entry 12**). When the reaction was carried out without the thiourea additive, the reaction was slow, with low stereoselectivity (**Table 5, entry 6**). We also found that primary amino acids like *S*-tryptophan and *S*-tert-leucin were very good catalysts for this transformation (**Table 5, entries 7 and 8**), although proline gave superior results. These results clearly demonstrate the enormous effect of the thiourea on the reactivity and selectivity, even when an unconventional non-polar reaction medium was used without lowering temperature. It is also noteworthy that the sense of diastereoselection is the same as that when proline is the sole catalyst (*anti* selectivity).

Next, representative selections of aldehydes were investigated to determine the scope of this improved aldol protocol, as shown in **Table 6**. Hexane was chosen as the solvent, due to the faster reaction times and higher isolated yields compared to those of toluene, with similar levels of selectivity (**Table 6, entries 1 and 3**). A 16-fold excess of the ketones used proved to be sufficient for reaction. The reactions with aldehydes bearing highly electron-withdrawing groups proceeded smoothly, with a good level of diastereoselectivity.

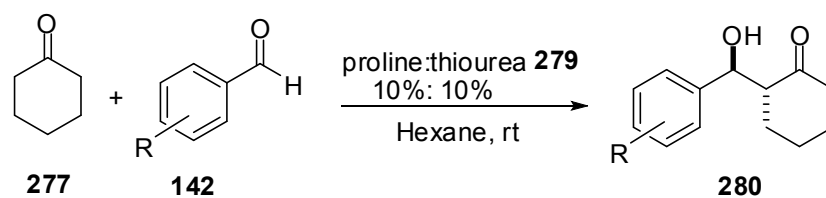


Figure 2.19 The direct enantioselective aldol reactions

Table 6. Enantioselective direct aldol reaction of aldehydes and cyclohexanone

Entry	Aldehyde (R)	Product	Time (h)	Yield (%)	<i>anti:syn</i> ^a	<i>ee</i> (%) ^b
1 ^c	4-NO ₂ Ph 150	281	24	75	92:8	>99
2	4-NO ₂ Ph	281	16	96	90:10	99
3 ^c	3-NO ₂ Ph 282	283	24	79	93:7	>99
4	3-NO ₂ Ph 284	285	16	94	92:8	>99
5	4-CNPh 286	287	16	98	93:7	99
6	4-CF ₃ Ph 288	289	24	93	94:6	99
7	4-ClPh 290	291	36	91	88:12	99
8	4-BrPh 292	293	36	87	90:10	99
9	2-ClPh 294	295	36	83	94:6	99
10	Ph	296	48	79	88:12	98
11 ^d	4-NO ₂ Ar 297	298	16	93	60:40	97

a. determined from crude ¹H-NMR spectra, b. Determined by HPLC with appropriate chiral column, c. Toluene is used d. Cyclopentanone is used.

Furthermore, the nature of the proline–thiourea complex was studied by ^1H -NMR experiments, with spectra being recorded in CDCl_3 as solvent. The observed results of these experiments showed that the solubility of the proline–thiourea mixture in chloroform was much better than each compound alone. As shown in **Figure 2.20**, it was seen that following the addition of proline, the N–H protons of the thiourea **279** underwent a downfield shift due to the dominant interactions that may present in the complex via the formation of a hydrogen bonding network.

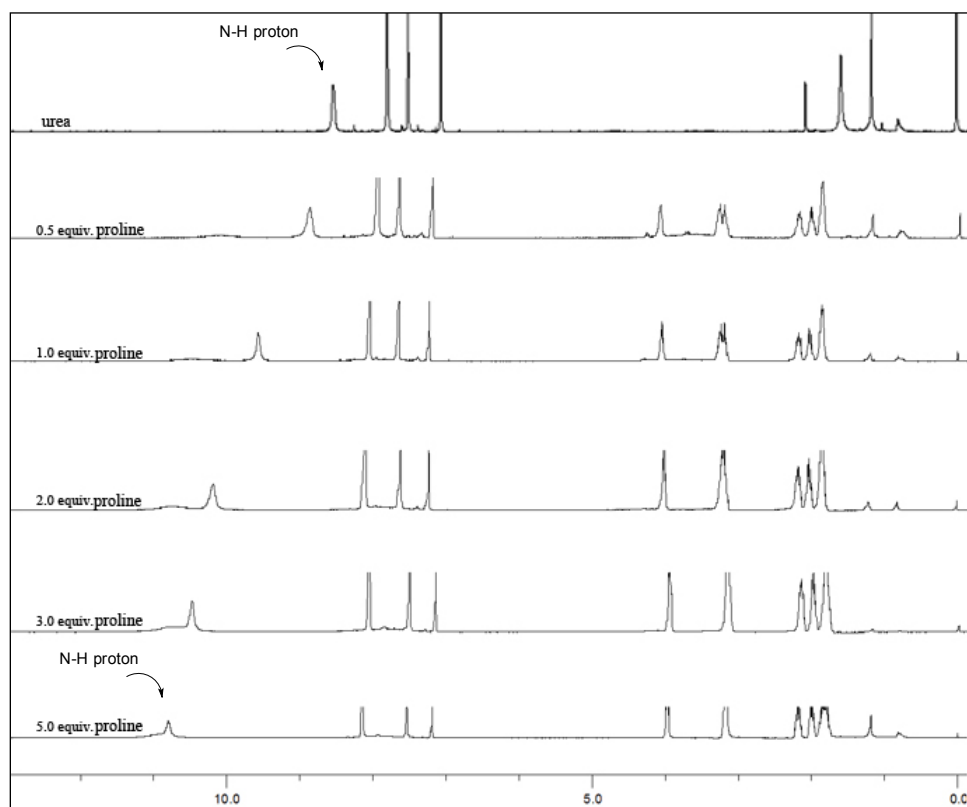


Figure 2.20 The ^1H NMR spectra of proline-thiourea complex

The data collected so far indicate that a specific proline–thiourea interaction may operate to afford an enantioselective reaction. The general stereochemical outcome of the reaction can be explained by the mechanism shown in **Figure 2.21**. It was proposed that the reaction would proceed according to a modified Houk–List model, in which the carboxylate moiety of the proline forms an assembly with the thiourea, in turn enhancing the reactivity and selectivity of the catalyst. This interaction between thiourea and proline increases the acidity of the carboxylic hydrogen of proline and at the same time stabilize the “chair” transition state **300**. This is in agreement with the stereoselectivity observed in the reaction. Furthermore, the thiourea is treated as a non-polar counterpart to proline, amplifying its solubility limits in non-polar solvents, such as hexane or toluene. The thiourea interacts with proline through two hydrogen bonds to form complex **276**. After a dehydration reaction with the ketone, iminium intermediate **298** or oxazolidinone intermediate **299** is generated. Deprotonation of **298** produces the enamine intermediate, which is more nucleophilic than the cyclohexanone because of its higher HOMO energy level. A new C-C bond is formed via transition state **300**. Finally, the product **278** with anti selectivity is released via hydration of iminium **301**, and complex **276** is regenerated.

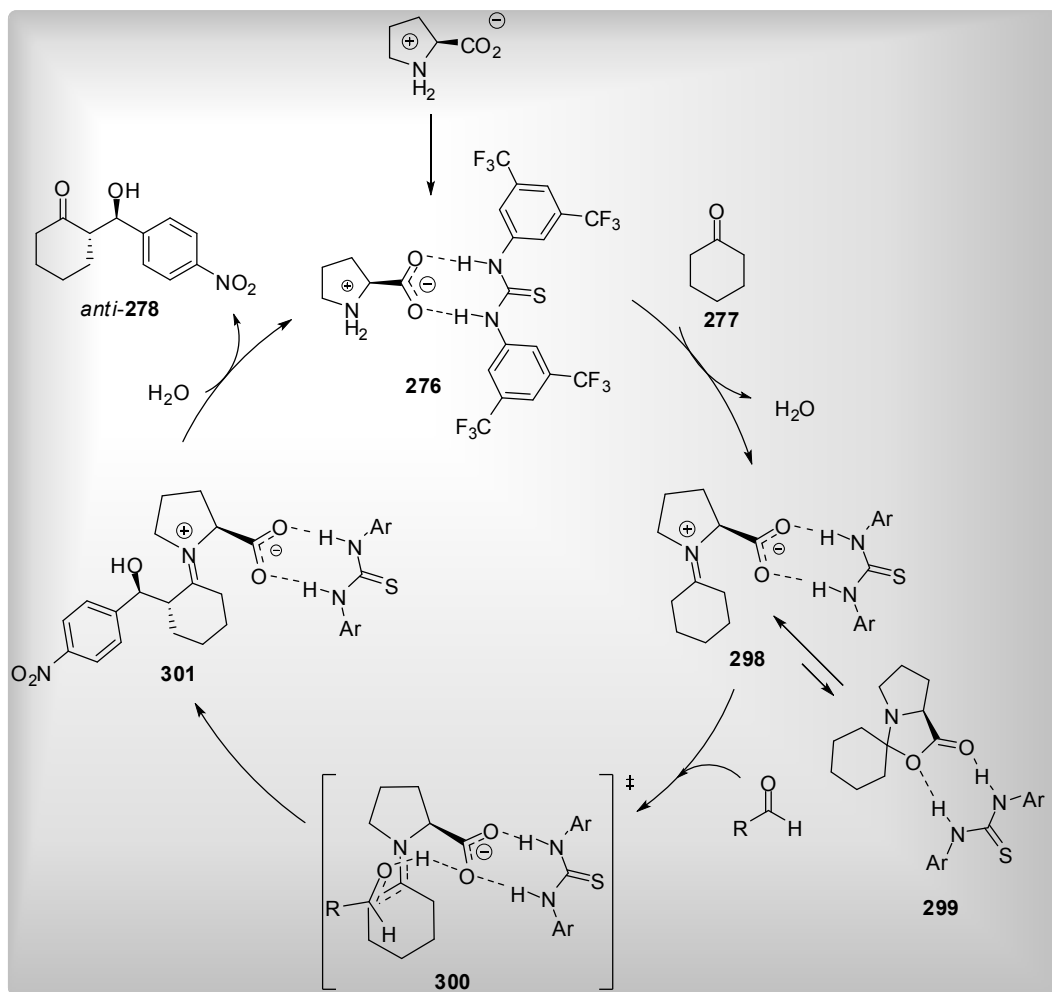


Figure 2.21 Proposed catalytic reaction mechanism for the direct enantioselective aldol reactions catalyzed by a proline–thiourea host–guest complex

In summary for this part, in this part of this dissertation, it was found that a proline–thiourea host–guest complex could catalyze direct enantioselective aldol reactions in non-polar solvents with high diastereoselectivity and enantioselectivity (up to 94:6 *dr* and 99% *ee*) better than proline. These results clearly demonstrate the enormous effect of the thiourea on the reactivity and

selectivity, even in an unconventional non-polar reaction medium, without a need for use of low temperatures.

2.2.2 Self-assembly of organocatalysts for the enantioselective Michael addition of aldehydes to nitroalkenes

The Michael addition reaction of carbon-centered nucleophiles to nitroalkenes is one such reaction that is catalyzed by organocatalysts. After the first organocatalytic asymmetric Michael addition of aldehydes to nitroalkenes was reported by Betancort and Barbas,¹⁰⁴ extraordinary progress has been devoted to find more selective and efficient catalytic systems for these Michael reactions due to the fact that nitroalkanes are crucial intermediates in organic synthesis due to their ability to transform the nitro group into other useful functionalities.

Even though *L*-proline has been described as a catalyst for direct asymmetric Michael reactions with aldehydes as the donor, poor enantioselectivity is typically observed. For example, as shown in **Figure 2.22**, Barbas noted that *L*-proline catalyzed direct Michael addition reactions of isovaleraldehyde (**282**) to trans- β -nitrostyrene (**283**) provided only trace amounts of the Michael adduct **284** with low enantioselectivity.

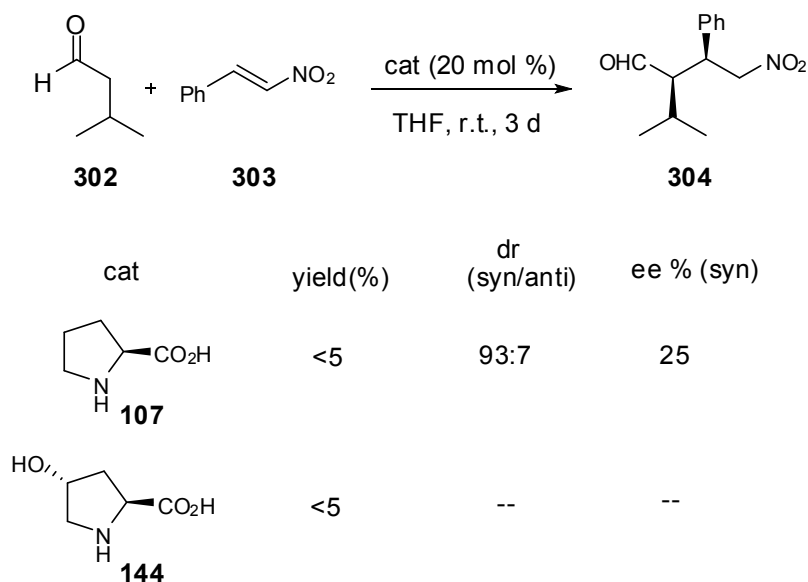


Figure 2.22 Michael addition reactions of isovaleraldehyde (**282**) to trans- β -nitrostyrene (**283**)

In 2007, Clarke and Funes introduced the first example of the self-assembly of organocatalysts for the direct Michael addition of ketones to nitroalkenes, wherein the addition of chiral additives to a chiral organocatalyst host can transform an unselective catalyst into a highly effective one through hydrogen-bonding interactions.¹⁰⁰ Later, Zhao and Mandal reported that organocatalysts that were formed through the self-assembly of simple α -amino acids and alkaloid thiourea derivatives could be used as efficient catalysts for the nitro-Michael addition of ketones and nitroalkenes.¹⁰⁵ This approach is not only beneficial in avoiding chemical synthesis, but it is also useful for constructing libraries of structurally diverse catalysts. To the best of our knowledge, there has been no report on the application of self-assembly of organocatalysts with an achiral additive in a Michael addition wherein aldehydes are utilized as donors. Therefore, we decided to investigate the use of proline–thiourea host–guest complex as a catalyst in direct asymmetric Michael reaction. As seen in **Figure 2.23**, the reaction between

isovaleraldehyde (**282**) and trans- β -nitrostyrene (**283**) was used as a model reaction system to screen different reaction conditions.

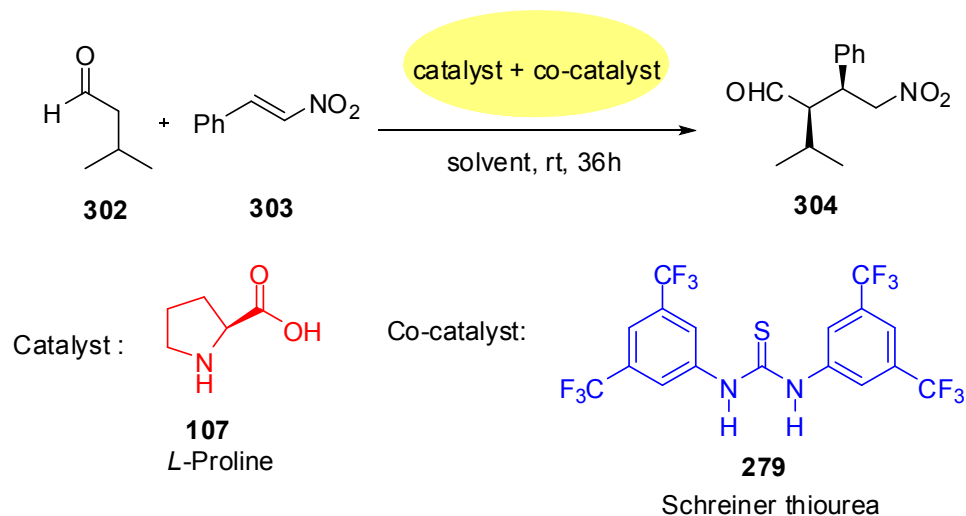


Figure 2.23 General reaction schemes for the direct asymmetric Michael reaction catalyzed by a proline–thiourea host–guest complex

The reaction was allowed to perform at room temperature for 36 h in the presence of *L*-proline and Schreiner thiourea **279**. As a prelude of our work, we examined our model reaction in different solvents. The screening results are summarized in **Table 10**. All reactions proceeded smoothly. As seen in **Table 7**, the first attempt in hexane achieved a good conversion but low enantioselectivity (**entry 1**). Under the same reaction conditions, a similar trend was observed for the other solvents, such as dioxane and chloroform. Screening of the solvents clearly showed that benzene as solvent gave the the best enantioselectivity (**entries 9** and **11**). Aiming at improving further our catalytic system, it was next surveyed the effect of an equivalent of the donor, and catalyst loading. From a practical point of view, the

Michael addition of aldehydes to β -nitrostyrene usually requires a large (10-fold) excess of the donor, due to competing aldol pathways. However, in our study, 3-fold excess of donor aldehyde proved to be sufficient. Further studies indicated that by using only 5% mol thiourea, the reaction produced a good conversion without any decrease in enantioselectivity. When the reaction was carried out without the thiourea additive, the reaction was very slow, with a low stereoselectivity as expected (**entry 12**). These results demonstrated the influential effect of the thiourea on both the reactivity and selectivity.

Table 7. The enantioselective Michael reaction of **302** and **303** under various conditions

entry	L-proline : 279 (%)	solvent	equiv.of aldehyde	Conv (%)	<i>syn:anti</i>	<i>ee</i> (%)
1	20:20	Hexane	10	94	97:3	25
2	20:20	Toluene	10	83	98:2	29
3	20:20	Chloroform	10	87	98:2	35
4	20:20	Chloroform	3	86	98:2	32
5	20:10	Chloroform	3	85	98:2	32
6	20:20	Dioxane	3	95	97:3	35
7	20:20	cyclohexane	3	94	97:3	53
8	20:20	benzene	3	99	97:3	76
9	20:10	benzene	3	99	98:2	72
10	20:5	benzene	3	98	97:3	76

Table 7. (continued)

entry	L-proline : 279 (%)	solvent	equiv. of aldehyde	Conv (%)	<i>syn:anti</i>	<i>ee</i> (%)
11	5:5	benzene	3	90	98:2	72
12	20:0	benzene	3	≤ 6	95:6	nd

With the optimized conditions in hand (**Table 7, entry 10**), a series of nitroalkenes and aldehydes were examined in order to establish the generality of the reaction and the results are summarized in **Table 8**. Unbranched aldehydes, such as propionaldehyde (**308**), butanal (**315**), and pentanal (**318**), gave the Michael addition in good yields and moderate to good enantioselectivities with excellent diastereoselectivities. We then continued to evaluate the scope of the reaction by testing the Michael addition of isovaleraldehyde (**302**) to various nitroalkenes, in which a good yield and moderate to good enantioselectivities were obtained. The reactions with nitroalkenes bearing not only phenyl, but also electron-rich and electron-deficient aryl groups on the nitroalkene proceeded efficiently, with a high diastereoselectivity. In all the cases, 5% mol thiourea was enough to obtain the best *ee* values.

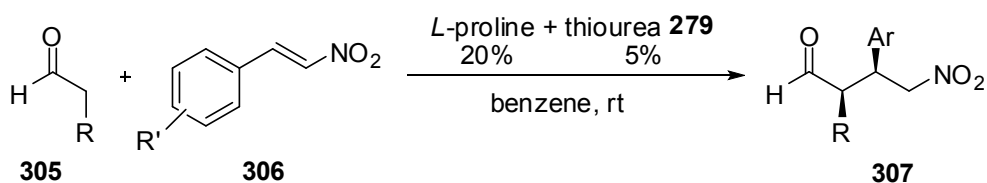
**Figure 2.24** The direct asymmetric Michael reaction

Table 8. The enantioselective Michael Addition of aldehydes to nitroalkenes

Entry	Aldehyde	R'	Yield (%)	<i>syn:anti</i>	<i>ee</i> (%)
1	R= -CH ₃ 308	H 309	85	93:7	76 (310)
2	R= -CH ₃	4-OMe 311	79	92:8	60 (312)
3	R= -CH ₃	4-Br 313	80	91:9	60 (314)
4	R= -CH ₂ CH ₃ 315	H	77	95:5	67 (316)
5	R= -CH ₂ CH ₃	4-Br	79	94:6	69 (317)
6	R= -CH ₂ CH ₂ CH ₃ 318	H	86	94:6	76 (319)
7	R= -CH ₂ CH ₂ CH ₃	4-OMe	50	93:7	44 (320)
8	R= -CH ₂ CH ₂ CH ₃	4-Br	65	94:6	50 (321)
9	R= -CH(CH ₃) ₂ 302	H	88	97:3	75 (304)
10	R= -CH(CH ₃) ₂	4-Br	80	97:3	60 (322)
11 ^a	R= -CH ₃ , -CH ₃ 323	H	66	-	72 (324)

a. 20:20% *L*-Proline–thiourea **279** was used.

Interestingly, α -branched aldehydes, isobutyraldehyde (**323**), led to a good isolated yield and good enantioselectivity (**Table 8, entry 11**). Self-assembly of catalyst as a strategy for organocatalytic direct Michael addition reactions with β -nitrostyrene is known.⁹⁸⁻¹⁰⁰ However, to our best knowledge, our catalyst assembly based approach is the first example for the catalytic enantioselective formation of an important class of Michael products bearing quaternary carbons.

As shown in **Table 8**, our supramolecular self-assembly organocatalyst always gives higher diastereoselectivity with respect to proline. To explain the stereochemical outcome of the reaction, a transition state **307** based on Seebach's model¹⁰⁶ was proposed as seen in **Figure 2.25**. In this model, the preferential formation of the anti-enamine with the double bond was oriented away from the bulky substituent at the 2-position of the pyrrolidine ring. Subsequently, the enamine reacts with the nitro olefin via an acyclic synclinal transition state. A bulky substituent at the 2-position of the pyrrolidine ring plays two important roles: it favors the selective formation of the anti-enamine and also shields its Re-face.

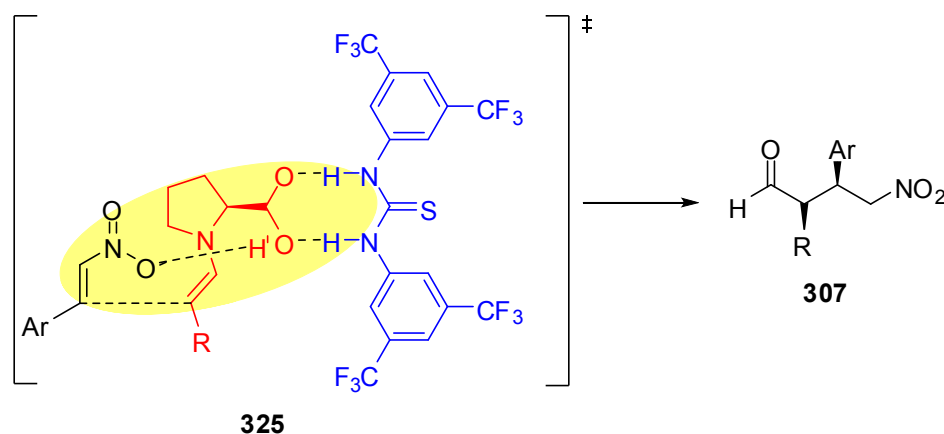


Figure 2.25 Stereochemical outcome of the the direct asymmetric Michael reaction catalyzed by a proline–thiourea host–guest complex

Based on the experimental results and our previously reported studies, it was proposed that the reaction proceeds through an enamine mechanism as shown in **Figure 2.26**.

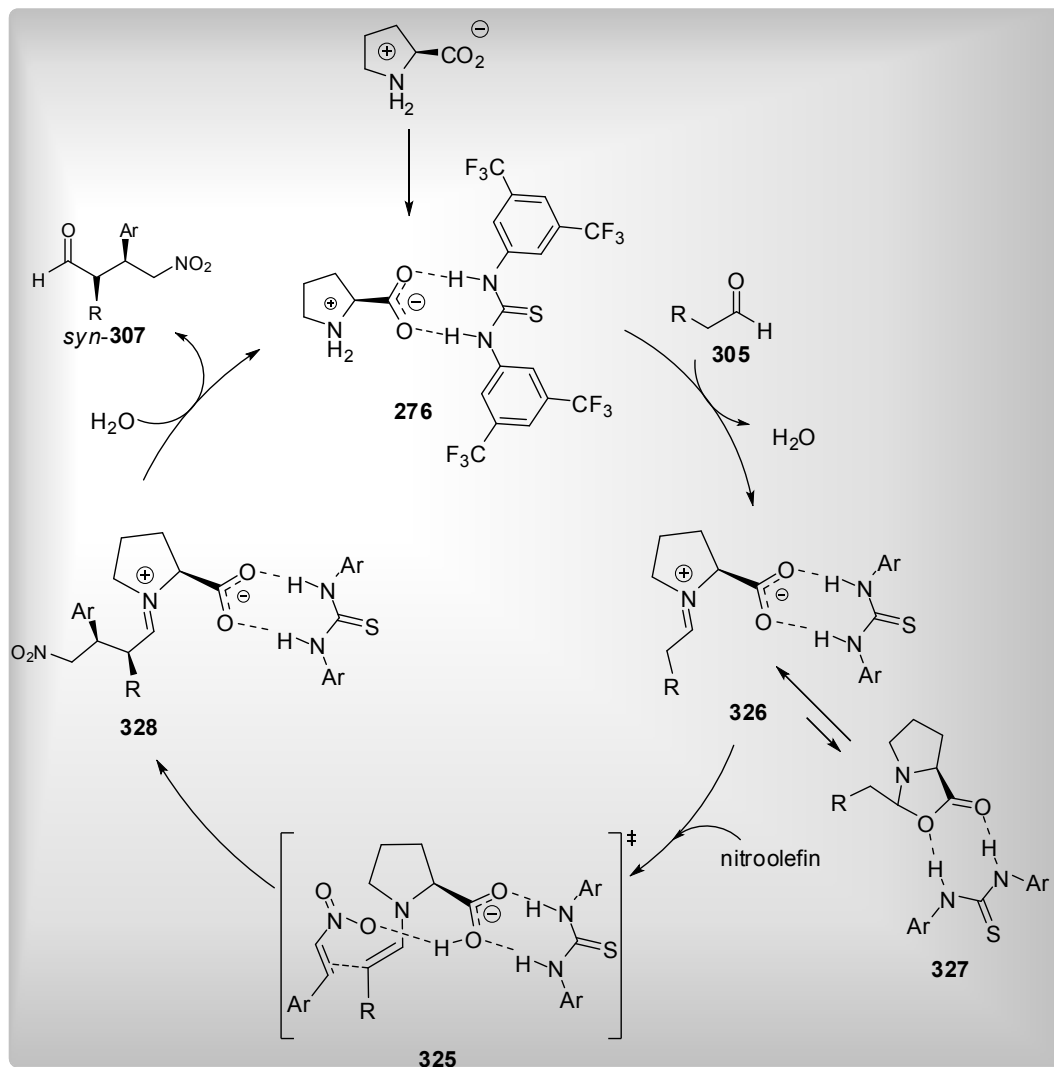


Figure 2.26 Proposed catalytic reaction mechanism for the direct asymmetric Michael reaction catalyzed by a proline–thiourea host–guest complex

To sum up, in this part, it was investigated that *L*-Proline-thiourea host guest complex is a good catalyst for the enantioselective direct nitro-Michael addition of aldehydes to nitroalkenes. Good selectivities were obtained even in an unconventional non-polar reaction medium at room temperature. The reaction is efficient with just 5% mol thiourea **279**, in which moderate to good enantioselectivity and high syn-selectivity was obtained in both branched and unbranched aliphatic aldehydes. This is the first example of self-assembly of organocatalysts with an achiral additive in a Michael addition wherein aldehydes are utilized as donors.

2.2.3 Nonlinear effects in proline–thiourea host–guest complex catalyzed aldol reactions in nonpolar solvents

Asymmetric amplifications in heterogenous amino-acid catalysis are crucial in the evolution of homochirality in biological systems. Therefore, it has become an object of concentration. This phenomenon is interpreted as ternary phase behaviour of the non-enantiopure mixtures of amino acids in solvents by Blackmond⁸⁵ and Hayashi⁸⁶. Of the twenty-proteinogenic amino acids, only threonine and asparagine crystallize as “conglomerates” or separate enantiomeric solid phases. All of the others, including proline, cocrystallize in a 1:1 ratio of the enantiomers, known as a “racemic compound”. A solid phase, a solid phase of excess enantiomer, and a solution phase, which has a constant eutectic point in the composition, are three phases that are formed by scalemic proline under solid-solution reaction conditions (in DMSO and CHCl₃-EtOH.) The ee of the proline in solution is observed, thus, greatly independent of the overall proline ee under thermodynamic conditions that is at equilibrium.

In recent times, the ternary phase behaviour of proline is studied under non-equilibrium conditions by Blackmond.^{84,85} According to this study, transition between a transient ‘kinetic conglomerate’ phase and the racemic compound formed by proline at equilibrium is detected provided that the two separate enantiomers are mixed physically. This state shows that for catalysis under the indicated conditions, the proline *ee* of the solution is determined by a linear combination of the two-separate enantiomers with a 0% of eutectic *ee*, which is similar to amino acids crystallizing as conglomerates. As the solid proline enantiomers start to dissolve, the proline *ee* of the solution is induced to rise by the solid-solution composition until the eutectic values of 50% *ee* is attained, which provides the equilibrium. This model provides Blackmond the first account of the origin of the negative nonlinear effects that were observed by Kagan and Blackmond in intra- and intermolecular aldol reactions, successively.

First-order kinetics is observed by the amino acid-catalyzed asymmetric aldol reaction between aldehydes and ketones regarding the amino acid. Therefore, the transition state of this reaction involves a single amino acid molecule. While the asymmetric amplifications in proline-catalyzed solution-phase reactions have attracted significant attention, proline–thiourea host–guest complex catalyzed aldol reactions in nonpolar solvents are still virgin regarding the investigation of how this system behaves under a solid-solution phase system. Inspired by the importance of nonlinear effects in asymmetric catalysis and its relevance to the origins of homochirality, we anticipated that proline–thiourea host–guest complex could show nonlinear effect in nonpolar solvents.

For investigating the dependence of the product enantioselectivity on the enantiopurity of the proline catalyst in nonpolar solvents, the reaction of cyclohexanone and *p*-nitrobenzaldehyde in the presence of a proline (20% *ee*)–thiourea complex [20:20(%)] was chosen as a model system (**Figure 2.27**). In

order to ensure experimental consistency, we used freshly purified starting materials in all experiments. In a first set of experiments, various solvents were tested for the direct aldol reaction (**Table 9**). By screening solvents, it was found that hexane gave the highest ee (**entries 1–7**). Additional optimizations were performed by changing the activities of starting materials. Our aim was to decrease the polarity of the reaction medium, which should change the *ee* and amount of proline in the solid–solution system. Two different methods were selected for decreasing the polarity; (1) decreasing the equivalents of ketone, which in turn would result in an increase in the *ee* but a decrease in the conversion (**Table 9, entries 8–11**), (2) the equivalents of ketone were kept at 16 fold, but the amount of hexane increased. As shown in **entries 12–14**, the *ee* increased while the conversion decreased. This result was first observed for the existence of a nonlinear effect between the *ee* of the proline and the *ee* of the product under solid–solution reaction conditions.

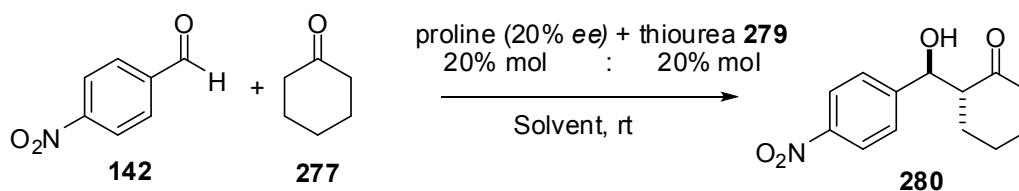


Figure 2.27 General reaction schemes for the direct enantioselective aldol reactions catalyzed by a proline–thiourea host–guest complex

Table 9. Screening of the solvent for an proline (20% *ee*)-thiourea **279** complex-(20:20%)-catalyzed enantioselective direct aldol reaction of aldehydes **2** and cyclohexanone

Entry	Solvent	Solvent (mL)	Equiv. of ketone	Time (h)	Conv (%)	<i>anti:syn</i>	<i>ee</i> (%)
1	MeCN	1.6	16	24	50	70:30	16
2	CHCl ₃	1.6	16	24	98	90:10	25
3	Toluene	1.6	16	24	99	93:7	24
4	Cyclohexane	1.6	16	24	99	94:06	29
5	Dioxane	1.6	16	24	95	75:25	17
6	CH ₂ Cl ₂	1.6	16	24	73	90:10	23
7	Hexane	1.6	16	24	99	93:7	32
8	Hexane	1.6	16	16	99	94:6	32
9	Hexane	1.6	8	16	69	90:10	45
10	Hexane	1.6	4	16	12	96:4	55
11	Hexane	1.6	2	16	≤ 5	nd	56
12	Hexane	3.2	16	16	62	92:7	46
13	Hexane	6.4	16	16	29	95:5	48
14	Hexane	9.6	16	16	13	97:3	51
15	Hexane	1.6	16	16	≤ 10	nd	≥ 19

As shown in **Table-10**, the aldol reaction was repeated with *L*-proline with *ee* values ranging from 5% to 100% wherein the product was obtained with an increased *ee* value from 40% to 99% *ee*. These results proved again that the *ee* values of the product versus the *ee* values of proline show a very good positive nonlinear effect (**Fig. 2.28**). In all cases, the diastereomeric excess of the product

was very high. This solid-solution system behaves similar, which was reported by Blackmond and Hayashi with a ternary phase behavior of a non-enantiopure (scalemic) mixture of amino acids in solvents.

Table 10. Relationship between the enantioselectivity of the reaction* and the enantiomeric excess of proline

Entry	<i>ee</i> of proline	Conversion (%)	<i>anti:syn</i>	<i>ee</i> (%)
1	5	22	97:3	40
2	10	27	97:3	48
3	20	29	96:4	53
4	40	33	96:4	75
5	60	32	97:3	91
6	80	43	97:3	97
7	100	75	95:5	≥99

* Proline – thiourea **279** complex-(20:20%)-catalyzed enantioselective direct aldol reaction of p-nitrobenzaldehyde and cyclohexanone

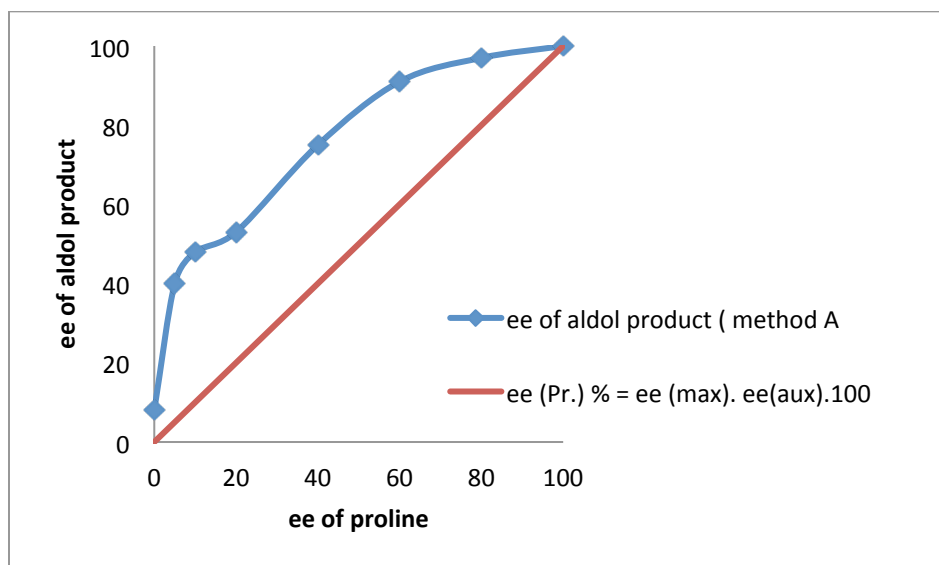


Figure 2.28 Relationship between the enantioselectivity of the reaction product and the enantiomeric excess of proline.

It is rather interesting to know the enantiometric excess of the soluble proline during the reaction change. Hayashi *et al.* investigated the ee value of proline from the solid part of the solid-solution system. For obtaining information about this change the following experiments were carried out under the standard conditions shown in **Table 11**.

The first experiment was started with L-proline (20 % ee) /thiourea (20/20 %), in hexane stirred for 16 h. According to previous work and the NMR spectra, structure **A** (**Figure 2.29**) was formed. Moreover, proline is known to exist as a zwitter-ion forming a highly insoluble network of hydrogen bonded prolines. We anticipated that a chemical entity, which selectively and strongly binds to acetate functionality, would (a) interact with proline in a solution, by altering its solution properties and reactivity and (b) also bind to the transition state in a stronger

fashion improving thereby the selectivity. The formation of structure **A** in a solid-solution system was established by the mixing of *L*-proline (20% *ee*) with thiourea **279** in hexane. After the filtration of the mixture followed by work up, the *ee* value of the isolated proline was found as 40% (**entry 1**). Then, as shown in entry 2, the proline-thiourea mixture was stirred for 30 minutes, and then cyclohexanone was added. After 16 h filtration and the work up procedure, the isolated proline showed 77% *ee* (**entry 2**). In entry 3, after the addition of cyclohexanone and an additional 30 minutes of stirring, *p*-nitro-benzaldehyde was added and stirring continued for 16h. Using a similar method as described above, the isolated proline showed 49% *ee*. This decrease in *ee* can be explained in some part as follows: the initial *ee* of the proline in solution is high, but as the reaction proceeds via the **TS B**, the *ee* of proline in solution begins to decrease because the generated product acts as a polarized solvent to bring both *D*- and *L*-proline from the solid into the organic phase. That is, while the *ee* of proline in the initial solution is high, this *ee* in solution decreases as the reaction progresses due to the increased solubility of both *D*- and *L*-proline in the solvent, and forming products. By using racemic proline, the *ee* of the product was found as 8%.

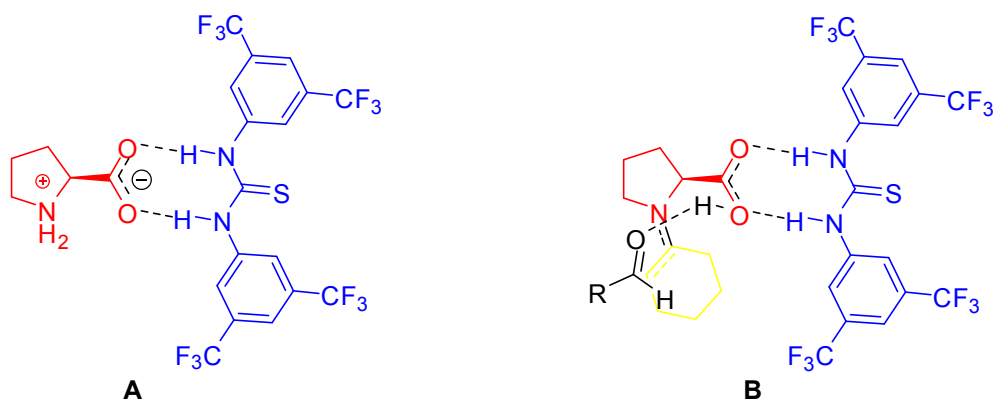


Figure 2.29 (A) and (B): The proposed interaction of the thiourea moiety with proline in solution and in the transition state, respectively.

Table 11. Determination of the soluble proline ee value during the experiment after 16h

Entry	ee of proline (initial)	ee of proline (after)	Proline : thiourea 279 (%)	conditions
1	20	40	20:20	in hexane
2	20	77	20:20	in hexane with cyclohexanone
3	20	49	20:20	in hexane with aldehyde and cyclohexanone
4	0 (racemic)	8 (ee of the product)	20:20	Same conditions as described in table 1

In order to decrease the solubility of the proline catalyst in the reaction mixture as the nonlinear effect expected to increase, the amount of urea is decreased (Condition B: 20:5; Cond. C; 20:10 proline (with various *ee*): urea %). Given the fact that under these reaction conditions a significant portion of the proline catalyst was not dissolved, the resulting dependence of the aldol product *ee* on the total proline *ee* is also shown in **Figure 2.30**. Furthermore, it is here that a constant aldol product *ee* over a wide range of total proline *ee* values in turn resulted in both cases.

Table 12. The *ee* value of the aldol reaction catalyzed by proline along with various *ee* values.

entry	Proline: 279 (%)	Solvent (mL)	Proline <i>ee</i> (%)	Product <i>ee</i> (%)
1	20:5	3.2	5	18
2	20:5	3.2	10	31
3	20:5	3.2	20	45
4	20:5	3.2	40	46
5	20:5	6.4	40	49
6	20:5	3.2	60	42
7	20:5	6.4	60	49
8	20:5	3.2	80	48
9	20:5	6.4	80	48
10	20:5	3.2	100	99
11	20:10	3.2	5	19
12	20:10	3.2	10	27
13	20:10	3.2	20	43
14	20:10	3.2	40	47
15	20:10	3.2	60	47
16	20:10	3.2	80	53
17	20:10	3.2	100	99
18	20:30	3.2	20	31

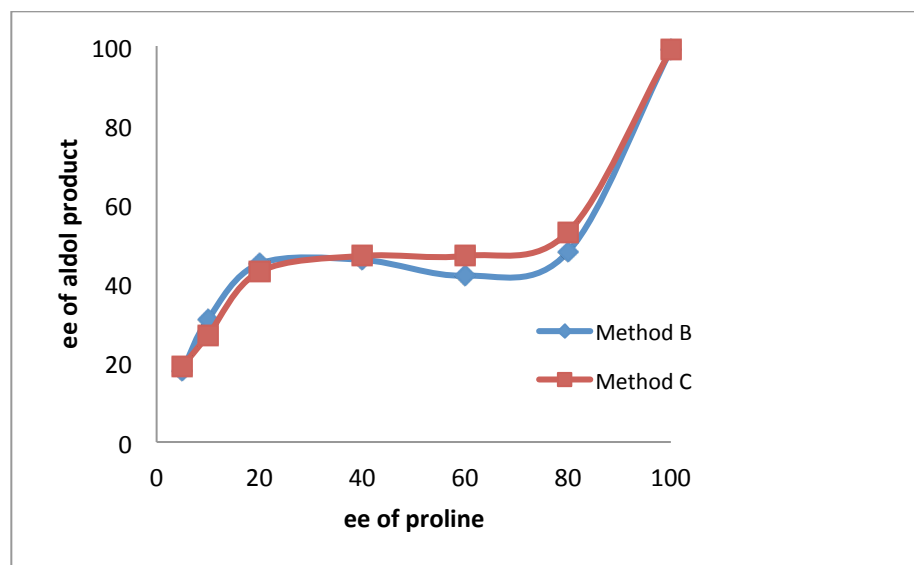


Figure 2.30 The *ee* value of the aldol reaction versus the *ee* of proline shows a constant *ee* value when increasing the *ee* value of proline

This observation could be explained with the models that are described by Blackmond (for reactions in solutions).⁸⁴ It was reported that due to the existence of an eutectic *ee* of proline (the eutectic value for proline in dimethyl sulfoxide (DMSO) at 25 °C is approximately 50%) under solid–solution equilibrium, this eutectic value dictates the enantiomeric excess of the solution for all the values of the scalemic proline *ee* employed, which in turn dictates the product *ee* that may be achieved in solution-phase reactions that are catalyzed by scalemic proline.

In summary, with an aldol reaction between cyclohexanone and p-nitrobenzaldehyde, we demonstrated that proline-thiourea complex catalyzed aldol reactions in non-polar solvent conditions exhibit ternary phase behavior. We showed a model based on simple solubility concepts that successfully rationalize the solution *ee* values for chiral compounds in solid–solution equilibrium.

CHAPTER 3

EXPERIMENTAL

NMR spectra were recorded on a Bruker DPX 400. ^1H -NMR spectra are reported in ppm using solvent as an internal standard (CHCl_3 at 7.26 ppm). Data are reported as (s = singlet, d = doublet, t = triplet, q = quartet, m = multiplet; coupling constant(s) in Hz; integration. Proton-decoupled ^{13}C -NMR spectra were recorded on a 400 (100 MHz) spectrometer and are reported in ppm using solvent as an internal standard (CDCl_3 at 77.0 ppm). Column chromatography was conducted on silica gel 60 (mesh size 40-63 μm). TLC was carried out on aluminum sheets precoated with silica gel 60F₂₅₄ (Merck).

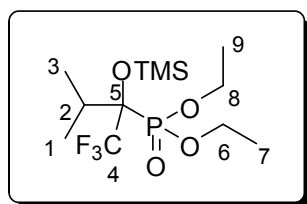
3.1 Synthesis of TMS Protected 1-Alkyl-1-trifluoromethyl-1-hydroxyphosphonates and 1-Aryl-difluoroethenyl Phosphates

All commercially available reagents were used without further purification. K_2CO_3 was stored at 80 °C. DMF was purified by distillation under vacuum and stored over 4A° Molecular Sieves. Visualization was accomplished with UV light and anisaldehyde or KMnO_4 followed by heating. Acyl phosphonates were prepared according to well-established procedures and purified by vacuum distillation. All acyl phosphonates were stored in flasks under nitrogen and they were stable at least for months.

3.1.1 General Procedure for the Addition of TMSCF₃ to Acyl Phosphonates:

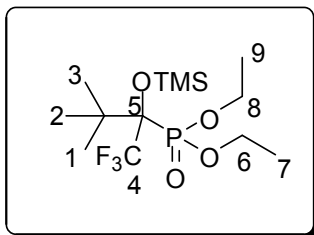
Acyl phosphonate (1 mmol) and TMSCF₃ (1.5 mmol) in dry DMF (5 mL) were placed in a 10 mL Schlenk flask. To this solution was added dry K₂CO₃ (20%), and the mixture was stirred vigorously at room temperature. Completion of the reaction was monitored by TLC. The reaction mixture was then poured into brine solution (15 mL) and extracted with diethyl ether (2 X 25 mL). The combined organic layers were finally washed with brine solution, dried over anhydrous Na₂SO₄, and then solvent was removed under reduced pressure. The crude product was further purified by column chromatography (silica eluted with 4:1 hexane/ethyl acetate) to afford pure TMS-protected 1-alkyl-1-trifluoromethyl-1-hydroxyphosphonate and 1-Aryl-difluoroethenyl phosphate.

3.1.1.1 Characterization of 244



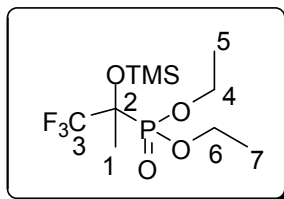
Diethyl 1,1,1-trifluoro-3-methyl-2-trimethylsilyloxy butane-2-ylphosphonate (244): Yield 145 mg (70%), colorless liquid; IR (neat) : $\nu = 2981, 2958, 1457, 1435, 1381, 1288, 1182, 1050, 1041, 980, 1020, 842, 762, 584, 503$ s cm^{-1} .; ¹H NMR (400 MHz, CDCl₃) δ 0.13 (s, 9H, Si(Me)₃), 1.08 (d, $J = 7.3$ Hz, 3H), 1.12 (d, $J = 7.3$ Hz, 3H), 1.31 (t, $J = 7.2$ Hz, 6H, H-7,9), 2.10-2.28 (m, 1H, H-2), 4.03-4.21 (m, 4H, H-6,8); ¹³C NMR (100 MHz, CDCl₃) δ 0.8, 15.4 (d, $J_{\text{CP}} = 6.2$ Hz), 16.5, 17.2, 33.3, 61.2, 61.3, 61.4, 80.1 (dq, $J_{\text{CP}} = 164$ Hz, $J_{\text{CF}} = 27.5$ Hz, C-5), 123.2 (dq, $J_{\text{CF}} = 287$ Hz, $J_{\text{CP}} = 10.1$ Hz, C-4); ³¹P NMR (161 MHz, CDCl₃) δ 15.2. Anal. Calcd. for C₁₂H₂₆F₃O₄PSi: C, 41.13; H, 7.48. Found: C, 41.10; H, 7.45.

3.1.1.2 Characterization of 247



Diethyl 1,1,1-trifluoro-3,3-dimethyl-2-trimethylsilyloxy butane-2-ylphosphonate (247): Yield 323 mg (89%), colorless liquid; IR (neat) : $\nu = 2992, 1445, 1388, 1254, 1171, 1061, 1039, 991, 853, 755, 581, 497 \text{ s cm}^{-1}$.; $^1\text{H NMR}$ (400 MHz, CDCl_3) δ 0.13 (s, 9H, $\text{Si}(\text{Me})_3$), 1.11 (s, 9H, $\text{C}(\text{CH}_3)_3$), 1.28 (q, $J = 14.6 \text{ Hz}$, 6H, H-7,9), 4.00-4.21 (m, 4H, H-6,8); $^{13}\text{C NMR}$ (100 MHz, CDCl_3) δ 0.0, 14.4, 14.6, 14.7, 14.8, 25.2, 37.5 (d, $J_{\text{CF}} = 4.4 \text{ Hz}$), 60.6 (d, $J_{\text{CP}} = 7.7 \text{ Hz}$), 61.1 (d, $J_{\text{CP}} = 7.6 \text{ Hz}$), 82.5 (dq, $J_{\text{CP}} = 160, J_{\text{CF}} = 26.2 \text{ Hz}$, C-5), 123.6 (dq, $J_{\text{CF}} = 292, J_{\text{CP}} = 10.1 \text{ Hz}$, C-4); $^{31}\text{P NMR}$ (161 MHz, CDCl_3) δ 17.0. Anal. Calcd. for $\text{C}_{13}\text{H}_{28}\text{F}_3\text{O}_4\text{PSi}$: C, 42.85; H, 7.74. Found: C, 42.88; H, 7.78.

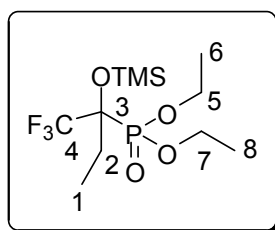
3.1.1.3 Characterization of 249



Diethyl 1,1,1-trifluoro-2-trimethylsilyloxy propane-2-ylphosphonate (249): Yield 289 mg (90%), yellowish liquid; IR (neat) : $\nu = 2986, 1455, 1394, 1293, 1171, 1051, 1026, 984, 847, 759, 579, 511 \text{ s cm}^{-1}$.; $^1\text{H NMR}$ (400 MHz, CDCl_3) δ : 0.15 (s, 9H, $\text{Si}(\text{Me})_3$), 1.27 (t, $J = 7.0 \text{ Hz}$, 6H, H-5,7), 1.60 (d, $^3J_{\text{PH}} = 15.2 \text{ Hz}$,

3H, H-1), 4.00-4.22 (m, 4H, H-4,6) ; ^{13}C NMR (100 MHz, CDCl_3) δ 1.1, 15.3 (d, $^3J_{\text{CP}} = 3.1$ Hz), 17.7, 62.0 (d, $^2J_{\text{CP}} = 7.4$ Hz), 62.9 (d, $J = 6.8$ Hz), 75.0*, 122.0* ; ^{31}P NMR (161 MHz, CDCl_3) δ 15.8. Anal. Calcd. for $\text{C}_{10}\text{H}_{22}\text{F}_3\text{O}_4\text{PSi}$: C, 37.26; H, 6.88. Found: C, 37.21; H, 6.90.

3.1.1.4 Characterization of 251

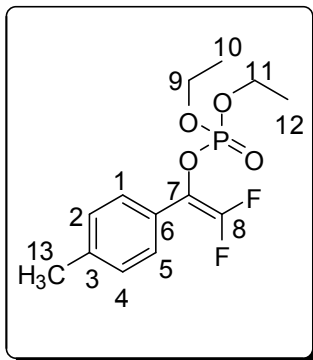


Diethyl 1,1,1-trifluoro-2-(trimethylsilyloxy)butane-2-ylphosphonate (251):

Yield 295 mg (88%), colorless liquid; IR (neat) : $\nu = 2989, 1628, 1459, 1398, 1293, 1258, 1165, 1030, 850, 560, 517$ s cm^{-1} .; ^1H NMR (400 MHz, CDCl_3) δ 0.15 (s, 9H, $\text{Si}(\text{Me})_3$), 1.03 (t, $J = 7.3$ Hz, 3H, H-1), 1.28 (t, $J = 7.3$ Hz, 6H, H-6,8), 1.91-2.02 (m, 2H, H-2), 4.03-4.20 (m, 4H, H-5,7); ^{13}C NMR (100 MHz, CDCl_3) δ 0.0, 6.1, 14.5 (d, $J_{\text{CP}} = 5.9$ Hz), 24.7, 61.3 (d, $J_{\text{CP}} = 7.6$ Hz), 61.6 (d, $J_{\text{CP}} = 6.9$ Hz), 77.0*, 123.0* ; ^{31}P NMR (161 MHz, CDCl_3) δ 15.9. Anal. Calcd. for $\text{C}_{11}\text{H}_{24}\text{F}_3\text{O}_4\text{PSi}$: C, 39.28; H, 7.19. Found: C, 39.22; H, 7.20.

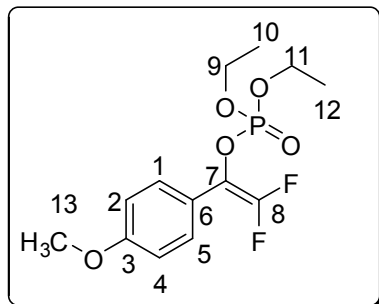
*The C-peaks of CF_3 and C-P can only be seen on ^{13}C -HMBC experiments.

3.1.1.5 Characterization of 253



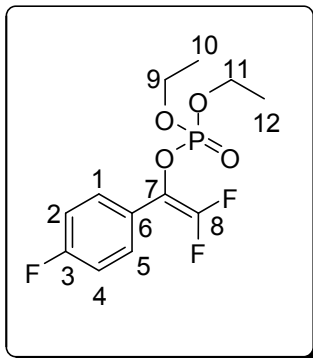
Diethyl 2,2-difluoro-1-(4-methylphenyl) ethenyl phosphate (253): Yield 281 mg (92%), colorless liquid; IR (neat) : $\nu = 2990, 2932, 1759, 1580, 1444, 1389, 1269, 1147, 1033, 983, 889$ s cm^{-1} ; ^1H NMR (400 MHz, CDCl_3) δ 1.21 (t, $J = 6.5$ Hz, 6H, H-10,12), 2.29 (s, 3H, H-13), 3.93-4.12 (m, 4H, H-9,11), 7.11 (d, $J = 8.5$ Hz, 2H, H-2,4), 7.32 (d, $J = 7.3$ Hz, 2H, H-1,5); ^{13}C NMR (100 MHz, CDCl_3) δ 14.9 (d, $^3J_{\text{CP}} = 7.3$ Hz), 20.2, 63.3 (d, $^2J_{\text{CP}} = 5.3$ Hz), 113.3 (ddd, $^2J_{\text{CF}} = 55.5, ^2J_{\text{CF}} = 24.0, ^2J_{\text{CP}} = 9.0$ Hz), 125.4, 125.5, 127.9, 128.0, 137.4, 154.7 (ddd, $^1J_{\text{CF}} = 390, ^1J_{\text{CF}} = 379, ^3J_{\text{CP}} = 7.6$ Hz); ^{31}P NMR (161 MHz, CDCl_3) δ -4.6. Anal. Calcd. for $\text{C}_{13}\text{H}_{17}\text{F}_2\text{O}_4\text{P}$: C, 50.99; H, 5.60. Found: C, 51.03; H, 5.66.

3.1.1.6 Characterization of 256



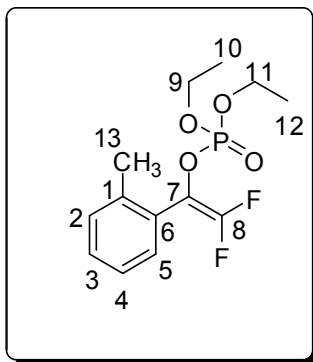
Diethyl 2,2-difluoro-1-(4-methoxyphenyl) ethenyl phosphate (256): Yield 305 mg (95%), colorless liquid; IR (neat) : $\nu = 2991, 2936, 1758, 1576, 1437, 1401, 1267, 1135, 1022, 992, 898 \text{ s cm}^{-1}$; $^1\text{H NMR}$ (400 MHz, CDCl_3) δ 1.28 (t, 6H, $J = 7.6 \text{ Hz}$, H-10,12), 3.82 (s, 3H, H-13), 4.01-4.19 (m, 4H, H-9,11), 6.90 (d, $J = 9.1 \text{ Hz}$, 2H, H-2,4), 7.43 (d, $J = 7.9 \text{ Hz}$, 2H, H-1,5); $^{13}\text{C NMR}$ (100 MHz, CDCl_3) δ 14.9 (d, $^3J_{\text{CP}} = 6.5 \text{ Hz}$), 54.3, 63.6 (d, $^2J_{\text{CP}} = 5.8 \text{ Hz}$), 112.2 (ddd, $^2J_{\text{CF}} = 48.4$, $^2J_{\text{CF}} = 17.4$, $^3J_{\text{CP}} = 8.3 \text{ Hz}$), 120.6 (d, $^3J_{\text{CF}} = 5.6 \text{ Hz}$) 127.1, 154.5 (ddd, $^1J_{\text{CF}} = 387$, $^1J_{\text{CF}} = 376.8$, $^3J_{\text{CP}} = 8.9 \text{ Hz}$), 158.8; $^{31}\text{P NMR}$ (161 MHz, CDCl_3) δ -4.6. Anal. Calcd. for $\text{C}_{13}\text{H}_{17}\text{F}_2\text{O}_5\text{P}$: C, 48.45; H, 5.32. Found: C, 48.43; H, 5.35.

3.1.1.7 Characterization of 258



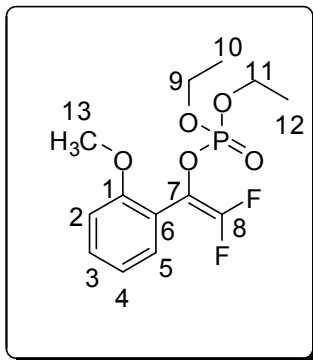
Diethyl 2,2-difluoro-1-(4-fluorophenyl) ethenyl phosphate (258): Yield 285 mg (92%), colorless liquid; IR (neat) : $\nu = 2971, 2920, 1748, 1584, 1447, 1382, 1360, 1276, 1141, 1017, 981 \text{ s cm}^{-1}$; $^1\text{H NMR}$ (400 MHz, CDCl_3) δ 1.17 (t, $J = 6.7 \text{ Hz}$, 6H, H-10,12), 3.87-4.09 (m, 4H, H-9,11), 7.07 (t, $J = 8.5 \text{ Hz}$, 2H, H-2,4), 7.39-7.59 (m, 2H, H-1,5); $^{13}\text{C NMR}$ (100 MHz, CDCl_3) δ 15.8 (d, $^3J_{\text{CP}} = 6.6 \text{ Hz}$), 64.8 (d, $^2J_{\text{CP}} = 5.9 \text{ Hz}$), 111.5, 111.6, 111.7, 114.6 (d, $^2J_{\text{CF}} = 21.8 \text{ Hz}$), 125.4, 127.6, 153.7 (ddd, $^1J_{\text{CF}} = 290, ^1J_{\text{CF}} = 284, ^3J_{\text{CP}} = 7.2 \text{ Hz}$), 161.5 (d, $^1J_{\text{CF}} = 249 \text{ Hz}$); $^{31}\text{P NMR}$ (161 MHz, CDCl_3) δ -4.5. Anal. Calcd. for $\text{C}_{12}\text{H}_{14}\text{F}_3\text{O}_4\text{P}$: C, 46.46; H, 4.55. Found: C, 46.41; H, 4.57.

3.1.1.8 Characterization of 260



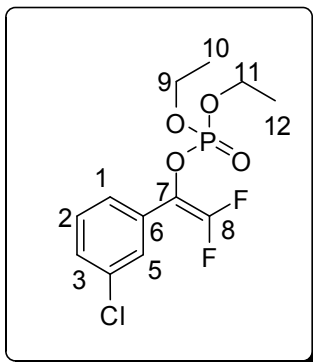
Diethyl 2,2-difluoro-1-(2-methylphenyl) ethenyl phosphate (260): Yield 296 mg (97%), colorless liquid; IR (neat) : $\nu = 2986, 2933, 1766, 1575, 1445, 1394, 1267, 1143, 1029, 983, 886$ s cm^{-1} ; ^1H NMR (400 MHz, CDCl_3) δ 1.12 (t, $J = 7.0$ Hz, 6H, H-10, 12), 2.32 (s, 3H, H-13), 3.78-4.00 (m, 4H, H-9,11), 7.11-7.36 (m, 4H, H-2,3,4,5); ^{13}C NMR (100 MHz, CDCl_3) δ 15.8 (d, $^3J_{\text{CP}} = 6.8$ Hz), 19.4, 64.2 (d, $^2J_{\text{CP}} = 5.8$ Hz), 111.8 (ddd, $^2J_{\text{CF}} = 48.6, ^2J_{\text{CF}} = 17.7, ^3J_{\text{CP}} = 8.3$ Hz), 125.6, 129.9, 130.3, 130.4, 137.2 138.1, 154.2 (ddd, $^1J_{\text{CF}} = 291, ^1J_{\text{CF}} = 277, ^3J_{\text{CP}} = 9.1$ Hz); ^{31}P NMR (161 MHz, CDCl_3) δ -4.5. Anal. Calcd. for $\text{C}_{13}\text{H}_{17}\text{F}_2\text{O}_4\text{P}$: C, 50.99; H, 5.60. Found: C, 50.96; H, 5.62.

3.1.1.9 Characterization of 262



Diethyl 2,2-difluoro-1-(2-methoxyphenyl)ethenyl phosphate (262): Yield 280 mg (87%), colorless liquid; IR (neat) : $\nu = 2982, 2930, 1768, 1577, 1445, 1393, 1261, 1145, 1025, 978, 887 \text{ s cm}^{-1}$; $^1\text{H NMR}$ (400 MHz, CDCl_3) δ 1.21, (t, $J = 7.3$ Hz, 6H, H-10,12), 3.86 (s, 3H, H-13), 3.92-4.10 (m, 4H, H-9,12), 6.92 (d, $J = 7.9$ Hz, 1H, H-2), 6.97 (t, $J = 7.6$ Hz, 1H, H-4), 7.33-7.43 (m, 2H, H-2,5); $^{13}\text{C NMR}$ (100 MHz, CDCl_3) δ 15.8 (d, $^3J_{\text{CP}} = 6.6$ Hz), 55.6, 64.2 (d, $^2J_{\text{CP}} = 5.6$ Hz), 109.5 (ddd, $^2J_{\text{CF}} = 48.6$, $^2J_{\text{CF}} = 19.9$, $^2J_{\text{CP}} = 9.0$ Hz), 111.0, 117.9 (d, $^3J_{\text{CP}} = 4.0$ Hz), 120.4, 131.4, 131.5, 154.4 (ddd, $^1J_{\text{CF}} = 289$, $^1J_{\text{CF}} = 280$, $^3J_{\text{CP}} = 9.0$ Hz), 157.6; $^{31}\text{P NMR}$ (161 MHz, CDCl_3) δ -4.8. Anal. Calcd. for $\text{C}_{13}\text{H}_{17}\text{F}_2\text{O}_5\text{P}$: C, 48.45; H, 5.32. Found: C, 48.46; H, 5.35.

3.1.1.10 Characterization of 264



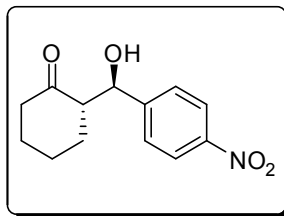
Diethyl 2,2-difluoro-1-(3-chlorophenyl) ethenyl phosphate (264): Yield 296 mg (91%), colorless liquid; IR (neat) : $\nu = 2986, 2932, 1765, 1575, 1445, 1388, 1266, 1148, 1026, 989, 897 \text{ s cm}^{-1}$; $^1\text{H NMR}$ (400 MHz, CDCl_3) δ 1.14, (t, $J = 6.1 \text{ Hz}$, 6H, H-10,12), 3.88-4.06 (m, 4H, H-9,11), 7.21-7.31 (m, 2H, H-2,5), 7.35-7.39 (m, 1H, H-3), 7.44-7.48 (m, 1H, H-1); $^{13}\text{C NMR}$ (100 MHz, CDCl_3) δ 15.7 (d, $^3J_{\text{CP}} = 7.4 \text{ Hz}$), 64.6 (d, $^2J_{\text{CP}} = 6.1 \text{ Hz}$), 110.2 (ddd, $^2J_{\text{CF}} = 48.2, ^2J_{\text{CF}} = 20.2, ^2J_{\text{CP}} = 9.3 \text{ Hz}$), 126.7, 128.0, 129.8, 131.2, 132.3, 134.7, 154.5 (ddd, $^1J_{\text{CF}} = 293, ^1J_{\text{CF}} = 281, ^3J_{\text{CP}} = 8.2 \text{ Hz}$); $^{31}\text{P NMR}$ (161 MHz, CDCl_3) δ -3.8. Anal. Calcd. for $\text{C}_{12}\text{H}_{14}\text{ClF}_2\text{O}_4\text{P}$: C, 44.12; H, 4.32. Found: C, 44.08; H, 4.30.

3.2 Direct Enantioselective Aldol Reactions catalyzed by a Proline-Thiourea Host-Guest Complex

3.2.1 General Procedure for the Enantioselective Direct Aldol Reaction

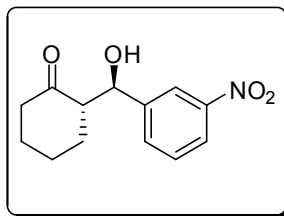
L-proline (0.025 mmol, 2.9 mg), thiourea **279** (0.025 mmol, 12.5 mg) and 1.8 mL hexane were placed in a screw capped vial, then cyclohexanone (4 mmol, 0.4 mL) was added, in which the resulting mixture was stirred for 15 min at ambient temperature followed by addition of aldehyde (0.25 mmol) wherein stirring was continued until no further conversion was observed by TLC. After completion of the reaction, the reaction mixture was treated with saturated aqueous ammonium chloride solution and the whole mixture was extracted with ethyl acetate. The organic layer was washed with brine, dried and concentrated to give a crude residue, which was purified with column chromatography over silica gel using hexane-ethyl acetate as an eluent to afford pure product. Diastereoselectivity and conversion were determined by ^1H NMR analysis of the crude aldol product. The enantiomeric excess of product was determined by chiral-phase HPLC analysis. The absolute configuration of aldol products were determined by comparing the values with those previously reported in the literature.

3.2.1.1 (S)-2-((R)-hydroxy(4-nitrophenyl)methyl)cyclohexan-1-one (281)



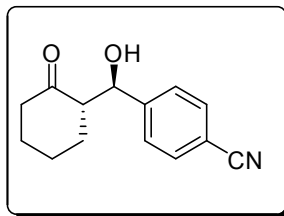
Yield 96%; *anti/syn* = 90/10, *anti*- diastereomer, ^1H NMR (400 MHz, CDCl_3) δ (ppm) 1.29-2.09 (m, 6H), 2.30-2.47 (m, 2H), 2.55-2.61 (m, 1H), 4.10 (s, 1H, -OH), 4.87 (d, $J = 8.4$ Hz, 1H), 7.48 (d, $J = 8.0$ Hz, 2H), 8.16 (d, $J = 8.4$ Hz, 2H); It was obtained in a maximum of >99% *ee*. The optical purity was determined by HPLC on chiralpak AD-H column [hexane/2-propanol 90.0:10.0]; flow rate 0.5 mL/min, *anti*: $t_{\text{minor}} = 48.3$ min and $t_{\text{major}} = 64.9$ min.

3.2.1.2 (S)-2-((R)-hydroxy(3-nitrophenyl)methyl)cyclohexan-1-one (283)



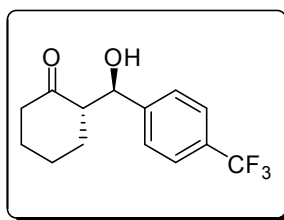
Yield 94%; *anti/syn* = 92/8, *anti*- diastereomer, ^1H NMR (400 MHz, CDCl_3) δ (ppm) 1.33-2.10 (m, 6H), 2.32-2.48 (m, 2H), 2.58-2.64 (m, 1H), 4.14 (s, 1H, -OH), 4.87 (d, $J = 8.4$ Hz, 1H), 7.50 (t, $J = 8.0$ Hz, 1H), 7.64 (d, $J = 7.6$ Hz, 1H), 8.12 (d, $J = 7.6$ Hz, 1H), 8.18 (s, 1H); it was obtained in a maximum of > 99% *ee*. The optical purity was determined by HPLC on chiralpak AD-H column [hexane/2-propanol 95.0:5.0]; flow rate 1.0mL/min, *anti*: $t_{\text{major}} = 37.0$ min and $t_{\text{minor}} = 47.9$ min.

3.2.1.3 (S)-2-((R)-hydroxy(4-cyanophenyl)methyl)cyclohexan-1-one (287)



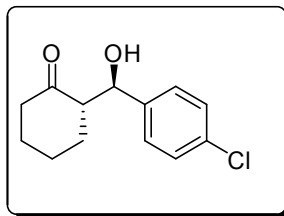
Yield 98%; *anti/syn* = 93/7, *anti*- diastereomer, ^1H NMR (400 MHz, CDCl_3) δ (ppm) 1.31-2.11 (m, 6H), 2.30-2.48 (m, 2H), 2.53-2.59 (m, 1H), 4.07 (s, 1H, -OH), 4.82 (d, J = 8.4 Hz, 1H), 7.43 (d, J = 8.4 Hz, 2H), 7.62 (d, J = 8.0 Hz, 2H); It was obtained in a maximum of 99% *ee*. The optical purity was determined by HPLC on chiralpak OD-H column [hexane/2-propanol 90.0:10.0]; flow rate 0.5 mL/min, *anti*: t_{minor} = 47.8 min and t_{major} = 60.3 min.

3.2.1.4 (S)-2-((R)-(4-(trifluoromethyl)phenyl)(hydroxy)methyl)cyclohexan-1-one (289)



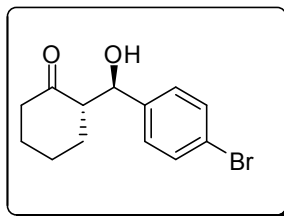
Yield 93 %; *anti/syn* = 94/6, *anti*- diastereomer, ^1H NMR (400 MHz, CDCl_3) δ (ppm) 1.23-2.37 (m, 6H), 2.45-2.55 (m, 1H), 2.69-2.81 (m, 1H), 4.03 (t, J = 3.0 Hz, 1H), 5.30 (d, J = 9.3 Hz, 1H), 7.40 (t, J = 7.2 Hz, 1H), 7.55-7.74 (m, 3H), It was obtained in a maximum of 99% *ee*. The optical purity was determined by HPLC on chiralpak OD-H column [hexane/2-propanol 95.0:5.0]; flow rate 1.0mL/min, *anti*: t_{major} = 12.4 min and t_{minor} = 17.0 min.

3.2.1.5 (S)-2-((R)-hydroxy(4-chlorophenyl)methyl)cyclohexan-1-one (291)



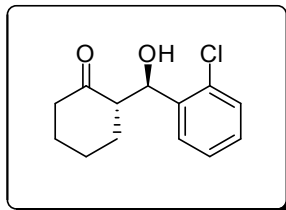
Yield 91% ; *anti/syn* = 88/12, *anti*- diastereomer, ^1H NMR (400 MHz, CDCl_3) δ (ppm) 1.26-2.11 (m, 6H), 2.31-2.49 (m, 2H), 2.52-2.59 (m, 1H), 3.61 (s, 1H, -OH), 4.76 (d, $J = 8.4$ Hz, 1H), 7.25 (d, $J = 8.4$ Hz, 2H), 7.31 (d, $J = 8.8$ Hz, 2H); It was obtained in a maximum of 99% *ee*. The optical purity was determined by HPLC on chiralpak AD-H column [hexane/2-propanol 90.0:10.0]; flow rate 0.5 mL/min, *anti*: $t_{\text{major}} = 26.5$ min and $t_{\text{minor}} = 30.6$ min.

3.2.1.6 (S)-2-((R)-hydroxy(4-bromophenyl)methyl)cyclohexan-1-one (293)



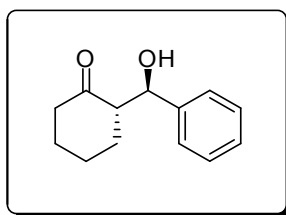
Yield 87%; *anti/syn* = 90/10, *anti*- diastereomer, ^1H NMR (400 MHz, CDCl_3) δ 1.24-2.08 (m, 6H), 2.28-2.37 (m, 2H), 2.43-2.57 (m, 1H), 3.40 (s, 1H, -OH), 4.73 (d, $J = 8.4$ Hz, 1H), 7.18 (d, $J = 8.0$ Hz, 2H), 7.45 (d, $J = 8.4$ Hz, 2H); It was obtained in a maximum of 99% *ee*. The optical purity was determined by HPLC on chiralpak AD-H column [hexane/2-propanol 90.0:10.0]; flow rate 0.5 mL/min, *anti*: $t_{\text{minor}} = 31.3$ min and $t_{\text{major}} = 36.4$ min.

3.2.1.7 (S)-2-((R)-hydroxy(2-chlorophenyl)methyl)cyclohexan-1-one (295)



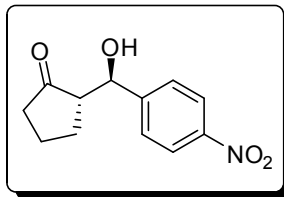
Yield 83%; *anti/syn* = 94/6, *anti*- diastereomer, ^1H NMR (400 MHz, CDCl_3) δ 1.51-2.09 (m, 6H), 2.28-2.46 (m, 2H), 2.63-2.70 (m, 1H), 3.92 (s, 1H, -OH), 5.34 (d, $J = 8.0$ Hz, 1H), 7.19 (t, $J = 7.6$ Hz, 1H), 7.28 (d, $J = 7.6$ Hz, 1H), 7.31 (t, $J = 8.0$ Hz, 1H), 7.53 (d, $J = 7.6$ Hz, 1H); It was obtained in a maximum of 99% *ee*. The optical purity was determined by HPLC on chiralpak OD-H column [hexane/2-propanol 95.0:5.0]; flow rate 0.5 mL/min, *anti*: $t_{\text{major}} = 19.7$ min and $t_{\text{minor}} = 25.2$ min.

3.2.1.8 (S)-2-((R)-hydroxy(phenyl)methyl)cyclohexan-1-one (296)



Yield 79%; *anti/syn* = 88/12, *anti*- diastereomer, ^1H NMR (400 MHz, CDCl_3) δ 1.25 –2.10 (m, 6H), 2.32-2.49 (m, 2H), 2.58-2.65 (m, 1H), 4.78 (d, $J = 6.0$ Hz, 1H), 7.29-7.36 (m, 5H); It was obtained in a maximum of 98% *ee*. The optical purity was determined by HPLC on chiralpak OD-H column [hexane/2-propanol 90.0:10.0]; flow rate 1.0 mL/min, *anti*: $t_{\text{major}} = 8.4$ min and $t_{\text{minor}} = 12.4$ min.

3.2.1.9 (S)-2-((R)-hydroxy(4-nitrophenyl)methyl)cyclopentan-1-one (298)



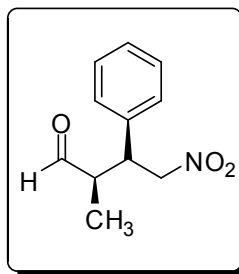
Yield 93%; *anti/syn*= 60/40, *anti*- diastereomer, ^1H NMR (400 MHz, CDCl_3) δ (ppm) 1.50-2.03 (m, 4H), 2.25-2.48 (m, 3H), 4.78 (s, 1H, -OH), 4.84 (d, J = 4.6 Hz, 1H), 7.54 (d, J = 4.3 Hz, 2H), 8.21 (d, J = 4.3 Hz, 2H); It was obtained in a maximum of 97% *ee*. The optical purity was determined by HPLC on chiralpak AD-H column [hexane/2-propanol 95.0:5.0]; flow rate 0.5 mL/min, *anti*: t_{minor} = 96.0 min and t_{major} = 99.4 min.

3.3 Self-assembly of organocatalysts for the enantioselective Michael addition of aldehydes to nitroalkenes

General procedure for the enantioselective Michael addition of aldehydes to nitroalkenes: *L*-proline (0.1 mmol, 11.5 mg), thiourea **279** (0.025 mmol, 12.5 mg), and 3.2 ml of benzene were placed in a screw-capped vial. Then aldehyde (1.5 mmol) was added, in which the resulting mixture was stirred for 30 min at ambient temperature followed by the addition of nitroalkene (0.50 mmol), wherein stirring was continued until the completion of the reaction (TLC monitoring). After completion of the reaction, the reaction mixture was treated with a saturated aqueous ammonium chloride solution and the whole mixture was extracted with ethyl acetate. The organic layer was washed with brine, dried and concentrated to give a crude residue, which was purified by column chromatography over silica gel using hexane–ethyl acetate as an eluent to afford a pure product. Diastereoselectivity and conversion were determined by ^1H NMR analysis of the

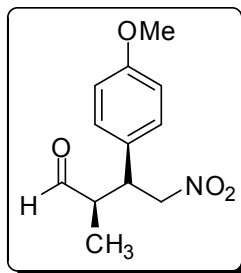
crude product. The enantiomeric excess of product was determined by chiral-phase HPLC analysis. The absolute configuration of the products was determined by comparing the values with those previously reported in the literature.

3.3.1 2-Methyl-4 nitro-3-phenylbutyraldehyde (310)



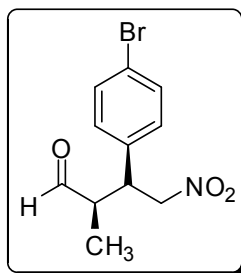
Yield 85 %; *syn/anti* = 12/1; *syn*- diastereomer, ^1H NMR (400 MHz, CDCl_3) δ 1.01 (d, $J = 7.3$ Hz, 3H), 2.78–2.70 (m, 1H), 3.76 (td, $J = 5.5$ Hz, $J = 9.2$ Hz, 1H), 4.65 (dd, $J = 9.3$ Hz, $J = 12.7$ Hz, 1H), 4.76 (dd, $J = 5.5$ Hz, $J = 12.7$ Hz, 1H), 7.14–7.10 (m, 2H), 7.33– 7.21 (m, 3H), 9.66 (d, $J = 1.7$ Hz, 1H); It was obtained in a maximum of 76% *ee*. The optical purity was determined by HPLC on chiralpak OD-H column , [hexane/2-propanol 80:20]; flow rate 0.8 ml/min, *syn*: $t_{\text{minor}} = 17.7$ min and $t_{\text{major}} = 22.6$ min.

3.3.2 3-(4-Methoxyphenyl)-2-methyl-4-nitrobutyraldehyde (312)



Yield 79 %; *syn/anti* = 11/1; *syn*- diastereomer, ^1H NMR (400 MHz, CDCl_3) δ 1.01 (d, $J = 7.3$ Hz, 3H), 2.81–2.64 (m, 1H), 3.76 (s, 3H), 3.80 (dt, 1H, $J = 5.6$ Hz, $J = 9.2$ Hz, 1H), 4.60 (dd, $J = 9.4$ Hz, $J = 12.5$ Hz, 1H), 4.80 (dd, $J = 5.6$, $J = 12.6$ Hz, 1H), 6.89 (d, $J = 8.7$ Hz, 2H), 7.12–7.03 (d, $J = 8.9$ Hz, 2H), 9.69 (d, $J = 1.7$ Hz, 1H); It was obtained in a maximum of 60% *ee*. The optical purity was determined by HPLC on chiralpak OD-H column, [hexane/2-propanol 85:15]; flow rate 1.0 ml/min, *syn*: $t_{\text{minor}} = 19.8$ min and $t_{\text{major}} = 22.2$ min.

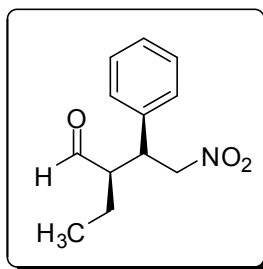
3.3.3 3-(4-Bromophenyl)-2-methyl-4-nitro-butylaldehyde (314)



Yield 80 %; *syn/anti* = 10/1; *syn*- diastereomer, ^1H NMR (400 MHz, CDCl_3) δ 1.01 (d, $J = 7.3$ Hz, 3H), 2.93–2.62 (m, 1H), 3.91–3.67 (m, 1H), 4.65 (dd, $J = 9.6$ Hz, $J = 12.8$, 1H), 4.80 (dd, $J = 5.2$ Hz, $J = 12.8$ Hz, 1H), 7.13–7.03 (m, 2H), 7.52–7.45 (m, 2H), 9.70 (d, $J = 1.5$ Hz, 1H); It was obtained in a maximum of 60% *ee*. The optical purity was determined by HPLC on chiralpak OD-H column,

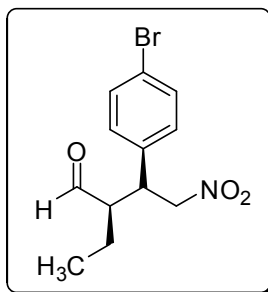
[hexane/2-propanol 80:20]; flow rate 0.8 ml/min, *syn*: $t_{\text{minor}} = 17.7$ min and $t_{\text{major}} = 22.6$ min.

3.3.4 2-Ethyl-4-nitro-3-phenyl butyraldehyde (316)



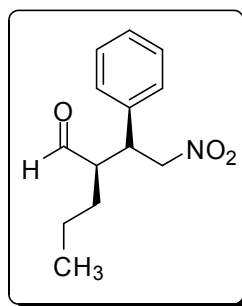
Yield 77 %; *syn/anti* = 20/1; *syn*- diastereomer, ^1H NMR (400 MHz, CDCl_3) δ 0.76 (dd, $J = 7.5$ Hz, $J = 7.5$ Hz, 3H), 1.48–1.38 (m, 2H), 2.66–2.58 (m, 1H), 3.72 (ddd, $J = 9.7$ Hz, $J = 9.7$ Hz, $J = 4.9$ Hz, 1H), 4.56 (dd, $J = 12.8$ Hz, $J = 9.7$ Hz, 1H), 4.65 (dd, $J = 12.8$ Hz, $J = 4.9$ Hz, 1H), 7.10–7.12 (m, 2H), 7.19–7.30 (m, 3H), 9.65 (d, $J = 2.6$ Hz, 1H); It was obtained in a maximum of 67% *ee*. The optical purity was determined by HPLC on chiralpak OD-H column, [hexane/2-propanol 80:20]; flow rate 0.8 ml/min, *syn*: $t_{\text{minor}} = 16.2$ min and $t_{\text{major}} = 17.4$ min.

3.3.5 3-(4-Bromophenyl)-2-ethyl-4-nitrobutanal (317)



Yield 79 %; *syn/anti* = 17/1; *syn*- diastereomer, ^1H NMR (400 MHz, CDCl_3) δ 0.77 (t, $J = 7.5$ Hz, 3H), 1.53–1.46 (m, 2H), 2.62 (m, 1H), 3.72 (dt, $J = 4.8$ Hz, $J = 9.9$ Hz, 1H), 4.56 (dd, $J = 9.9$ Hz, $J = 12.8$ Hz, 1H), 4.67 (dd, $J = 4.8$ Hz, $J = 12.8$ Hz, 1H), 7.02 (d, $J = 8.4$ Hz, 2H), 7.43 (d, $J = 8.4$ Hz, 2H), 9.65 (d, $J = 2.3$ Hz, 1H); It was obtained in a maximum of 69% *ee*. The optical purity was determined by HPLC on chiralpak AD-H column, [hexane/2-propanol 95.5:1.5]; flow rate 1.0 ml/min, *syn*: $t_{\text{major}} = 33.5$ min and $t_{\text{minor}} = 59.4$ min.

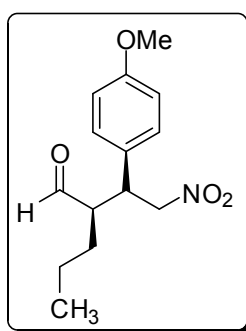
3.3.6 2-(2-Nitro-1-phenylethyl)pentanal (319)



Yield 86 %; *syn/anti* = 15/1; *syn*- diastereomer, ^1H NMR (400 MHz, CDCl_3) δ 0.77 (t, $J = 7.1$ Hz, 3H), 1.20–1.06 (m, 1H), 1.37–1.21 (m, 2H), 1.50–1.40 (m, 1H), 2.67 (tt, $J = 3.2$ Hz, $J = 9.5$ Hz, 1H), 3.73 (td, $J = 5.3$ Hz, $J = 9.5$, 1H), 4.70–

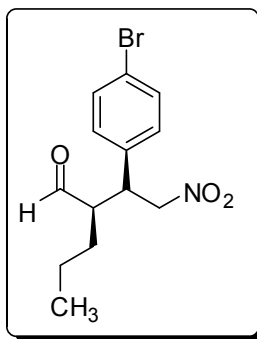
4.56 (m, 2H), 7.16–7.11 (m, 2H), 7.34–7.24 (m, 3H), 9.66 (d, $J = 2.8$ Hz, 1H); It was obtained in a maximum of 76% *ee*. The optical purity was determined by HPLC on chiralpak OD-H column, [hexane/2-propanol 90:10]; flow rate 1.0 ml/min, *syn*: $t_{\text{minor}} = 16.2$ min and $t_{\text{major}} = 18.7$ min.

3.3.7 2-(1-(4-Methoxyphenyl)-2-nitroethyl)pentanal (320)



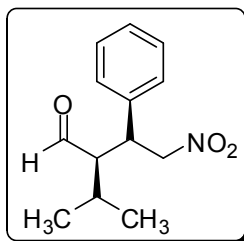
Yield 50 %; *syn/anti* = 14/1; *syn*- diastereomer, ^1H NMR (400 MHz, CDCl_3) δ 0.75 (t, $J = 6.9$ Hz, 3H), 1.49–1.10 (m, 4H), 2.64–2.67 (m, 1H), 3.63–3.75 (m, 1H), 3.79 (s, 3H), 4.52 (dd, $J = 9.3$ Hz, $J = 12.3$ Hz, 1H), 4.62 (dd, $J = 5.4$ Hz, $J = 12.6$ Hz, 1H), 6.81 (d, $J = 9.0$ Hz, 2H), 7.04 (d, $J = 8.7$ Hz, 2H), 9.63 (d, $J = 3.3$ Hz, 1H); It was obtained in a maximum of 44% *ee*. The optical purity was determined by HPLC on chiralpak OD-H column, [hexane/2-propanol 90:10]; flow rate 1.0 ml/min, *syn*: $t_{\text{minor}} = 20.4$ min and $t_{\text{major}} = 22.9$ min.

3.3.8 2-(1-(4-Bromophenyl)-2-nitroethyl)pentanal (321)



Yield 65 %; *syn/anti* = 15/1; *syn*- diastereomer, ^1H NMR (400 MHz, CDCl_3) δ 0.75 (t, $J = 7.2$ Hz, 3H), 1.46–1.05 (m, 4H), 2.66–2.71 (m, 1H), 3.68–3.78 (m, 1H), 4.54 (dd, $J = 9.9$ Hz, $J = 13.2$ Hz, 1H), 4.63 (dd, $J = 5.1$ Hz, $J = 12.9$ Hz, 1H), 7.00 (d, $J = 8.4$ Hz, 2H), 7.41 (d, $J = 8.1$ Hz, 2H), 9.63 (d, $J = 2.4$ Hz, 1H); It was obtained in a maximum of 50% *ee*. The optical purity was determined by HPLC on chiralpak OD-H column, [hexane/2-propanol 90:10]; flow rate 1.0 ml/min, *syn*: $t_{\text{minor}} = 20.5$ min and $t_{\text{major}} = 21.7$ min.

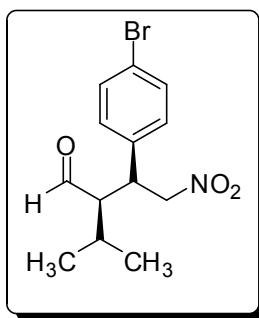
3.3.9 2-isopropyl-4-nitro-3-phenylbutanal (304)



Yield 88 %; *syn/anti* = 38/1; *syn*- diastereomer, ^1H NMR (400 MHz, CDCl_3) δ 0.79 (d, $J = 7.0$ Hz, 3H), 1.01 (d, $J = 7.2$ Hz, 3H), 1.70–1.57 (m, 1H), 2.71–2.79 (m, 1H), 3.81 (td, $J = 4.4$ Hz, $J = 10.4$ Hz, 1H), 4.48 (dd, $J = 10.0$ Hz, $J = 12.5$ Hz, 1H), 4.58 (dd, $J = 4.4$ Hz, $J = 12.5$ Hz, 1H), 7.12–7.07 (m, 2H), 7.28–7.17 (m,

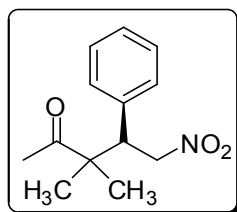
3H), 9.84 (d, $J = 2.4$ Hz, 1H); It was obtained in a maximum of 75% *ee*. The optical purity was determined by HPLC on chiralpak OD-H column, [hexane/2-propanol 97:03]; flow rate 0.7 ml/min, syn: $t_{\text{major}} = 28.1$ min and $t_{\text{minor}} = 30.4$ min.

3.3.10 3-(4-Bromophenyl)-2-isopropyl-4-nitrobutanal (322)



Yield 80 %; *syn/anti* = 35/1; *syn*- diastereomer, ^1H NMR (400 MHz, CDCl_3) δ 0.80 (d, $J = 7.2$ Hz, 3H), 1.04 (d, $J = 7.2$ Hz, 3H), 1.64-1.70 (m, 1H), 2.71-2.67 (m, 1H), 3.80-3.86 (m, 1H), 4.52-4.44 (m, 1H), 4.65-4.59 (m, 1H), 7.01 (dd, $J = 8.4$ Hz, $J = 1.5$ Hz, 2H), 7.42 (dd, $J = 8.4$ Hz, $J = 1.5$ Hz, 2H), 9.84 (d, $J = 2.4$ Hz, 1H); It was obtained in a maximum of 60% *ee*. The optical purity was determined by HPLC on chiralpak OD-H column, [hexane/2-propanol 90:10]; flow rate 1.0 ml/min, syn: $t_{\text{major}} = 15.7$ min and $t_{\text{minor}} = 17.2$ min.

3.3.11 3-(4-Bromophenyl)-2,2-dimethyl-4-nitrobutanal (324)



Yield 66 %; ^1H NMR (400 MHz, CDCl_3) δ 1.00 (s, 3H), 1.13 (s, 3H), 3.80 (d, $J = 11.7$ Hz, 1H), 4.70 (dd, $J = 4.1$ Hz, $J = 12.9$ Hz, 1H), 4.86 (dd, $J = 11.4$ Hz, $J = 12.9$ Hz, 1H), 7.30–7.19 (m, 5H), 9.53 (s, 1H); It was obtained in a maximum of 72% *ee*. The optical purity was determined by HPLC on chiralpak OD-H column, [hexane/2-propanol 80:20]; flow rate 1.0 ml/min, $t_{\text{major}} = 11.5$ min and $t_{\text{minor}} = 16.6$ min.

3.4 Nonlinear effects in proline–thiourea host–guest complex catalyzed aldol reactions in nonpolar solvents

3.4.1 General procedure for the enantioselective direct aldol reaction

Proline with a specific *ee* value (20% mol), thiourea **279** (20% mol) and 1.6 mL hexane were placed in a screw-capped vial. Cyclohexanone (4 mmol, 0.4 mL) was then added, and the resulting mixture was stirred for 15 min at ambient temperature followed by the addition of aldehyde (0.25 mmol) wherein stirring was continued until the completion of the reaction (TLC monitoring). After completion of the reaction, the reaction mixture was treated with saturated aqueous ammonium chloride solution and the whole mixture was extracted with ethyl acetate. The organic layer was washed with brine, dried, and concentrated to give a

crude residue, which was purified by column chromatography over silica gel using hexane–ethyl acetate as an eluent to afford the pure product. Diastereoselectivity and conversion were determined by ^1H NMR analysis of the crude aldol product. The enantiomeric excess (ee) of product was determined by chiral-phase HPLC analysis. The absolute configurations for aldol products were determined by comparing the values with those previously reported in the literature.

3.4.2 Determination of the enantiomeric excess of proline in solution

Non-enantiopure proline was prepared by mixing known amounts of *L*- and *D*-proline. Proline with a specific ee / thiourea (20:20), in hexane was stirred for 16 h. After filtration of the mixture followed by work-up, the ee value of the isolated proline was determined by HPLC. The HPLC-column used for analysis was a Macherey-Nagel Nucleosil Chiral 1 column, eluent was a mix of an aqueous solution of 0.25 mM CuSO_4 and 0.025 mM H_2SO_4 with 15% methanol, flow rate 1.5 mL/min, temperature 50 °C, UV–vis detector at 250 nm (retention times: *L*-proline, 6.5 min; *D*-proline, 18 min).

CHAPTER 4

CONCLUSIONS

4.1 Addition of Trifluoromethyltrimethylsilane to Acyl Phosphonates

In this part of this dissertation, a convenient, one-pot procedure for preparing various 1-alkyl-2,2,2-trifluoro-1-trimethylsilyloxyethyl phosphonates and 1-aryldifluoroethyl phosphates starting from readily available acyl phosphonates and trifluoromethyltrimethylsilane was developed.¹⁰⁷ Potassium carbonate (K_2CO_3) has been found to be an effective catalyst in the nucleophilic trifluoromethylation reactions. The catalytic activity of base has been improved further by using DMF as a solvent. Addition of the nucleophilic CF_3 to alkyl phosphonate furnished products in 70-90% yields. By using aryl phosphonates for the addition, phosphonate-phosphate rearrangement followed by fluorine elimination afforded products in 87- 97% yields. This area of research, after these initial explorations, remains to be studied further.

4.2 Development of new supramolecular organocatalytic strategies for the enantioselective asymmetric C-C bond forming reactions

It was found that a proline–thiourea host–guest complex can catalyze direct enantioselective aldol reactions in non-polar solvents (*e.g.* hexane) with high diastereoselectivity and enantioselectivity (up to 94:6 *dr* and 99% *ee*) better than proline.¹⁰⁸ These results clearly demonstrate the enormous effect of the thiourea on the reactivity and selectivity, even in an unconventional non-polar reaction medium, without a need for use of low temperatures.

It was also investigated that *L*-proline-thiourea host guest complex is a good catalyst for the enantioselective direct nitro-Michael addition of aldehydes to nitroalkenes.¹⁰⁹ Good selectivities were obtained even in an unconventional non-polar reaction medium at room temperature. The reaction is efficient with just 5 mol % thiourea, in which moderate to good enantioselectivity and high syn-selectivity was obtained in both branched and unbranched aliphatic aldehydes. With this study, it was demonstrated that the thiourea used as an achiral additive in Michael addition reactions in which aldehydes are utilized as donors for the first time in literature.

4.3 Nonlinear effects in proline–thiourea host–guest complex catalyzed aldol reactions in nonpolar solvents

To conclude this part, with an aldol reaction between cyclohexanone and *p*-nitrobenzaldehyde, it was investigated that proline-thiourea complex catalyzed aldol reactions in non-polar solvent conditions exhibit ternary phase behavior.¹¹⁰ We showed a model based on simple solubility concepts that successfully rationalize the solution ee values for chiral compounds in solid–solution equilibrium.

REFERENCES

1. Wöhler, F. *Ann. Phy. Chem.* **1828**, *12*, 253.
2. Corey, E. J.; Cheng, X. M. *The Logic of Chemical Synthesis*; John Wiley and Sons, Inc., New York, 1995.
3. Trost, B. M. *Angew. Chem. Int. Ed.* **1995**, *34*, 259.
4. Evans, D. A.; Andrews, G. C. *Acc. Chem. Res.* **1974**, *7*, 147.
5. Seebach, D. *Angew. Chem. Int. Ed.* **1979**, *18*, 239.
6. *IUPAC Comp. Chem. Term.* (2nd Edition) **1994**, *99*, 1174.
7. Seebach, D.; Corey E. J. *J. Org. Chem.* **1975**, *40*, 231.
8. (a) Yu, H.-Z.; Fu, Y.; Liu L.; Guo, Q.-X. *Chin. J. Org. Chem.* **2007**, *72*, 545.
(b) Enders, D.; Shil-Vock, J. P. *Chem. Soc. Rev.* **2000**, *29*, 359. (c) Enders, D.; Balensiefer, T. *Acc. Chem. Res.* **2004**, *37*, 534.
9. Wöhler, F.; Liebig, J. *Ann. Pharm.* **1832**, *3*, 249.
10. Lapworth, A. *J. Chem. Soc.* **1903**, *83*, 995.
11. Enders, D.; Breuer, K. *In Comprehensive Asymmetric Catalysis*; Jacobsen, E. N., Pfaltz, A., Yamamoto, H., Eds.; Springer: New York, 1999; Vol. 3, p. 1093.
12. (a) Seoane, G. *Curr. Org. Chem.* **2000**, *4*, 283. (b) Faber, K. *Biotransformations in Organic Chemistry*; Springer-Verlag, Berlin, 5th Edn. 2004.
13. Ukai, T.; Tanaka, R.; Dokawa, T. *J. Pharm. Soc. Jpn.* **1943**, *63*, 296.
14. Mizuhara, S.; Handler, P. *J. Am. Chem. Soc.* **1954**, *76*, 571.

15. Breslow, R. *J. Am. Chem. Soc.* **1958**, *80*, 3719.
16. (a) Enders, D.; Kalfass, U. *Angew. Chem. Int. Ed.* **2002**, *41*, 1743 and references therein. (b) Dunkelmann, P.; Kolter-Jung, D.; Nitsche, A.; Demir, A. S.; Siegert, P.; Lingen, B.; Baumann, M.; Pohl, M.; Muller, M. *J. Am. Chem. Soc.* **2002**, *124*, 12084. (c) Hachisu, Y.; Bode, J. W.; Suzuki, K. *Adv. Synth. Catal.* **2004**, *346*, 1097. (d) Enders, D.; Oliver, N. *Synlett* **2004**, 2111. (e) Kerr, M. S.; Rovis, T. *J. Am. Chem. Soc.* **2004**, *126*, 8876. (f) Read de Alaniz, J.; Rovis, T. *J. Am. Chem. Soc.* **2005**, *127*, 6284.
17. (a) Brook, A.G.; Bassindale, A.R. *Organic Chemistry, A Series of Monographs* **1980**, *42*, 149. (b) Kira, M.; Iwamoto, T. *Chem. Org. Silic. Comp.* **2001**, *3*, 853.
18. Speier, J. L. *J. Am. Chem. Soc.* **1952**, *74*, 1003.
19. (a) Brook, A.G. *J. Am. Chem. Soc.* **1958**, *80*, 1886. (b) Brook, A.G.; Warner, C. M.; McGricsin, M. E. *J. Am. Chem. Soc.* **1959**, *81*, 981. (c) Brook, A.G.; Schwartz, N. V. *J. Am. Chem. Soc.* **1960**, *82*, 2435. (d) Brook, A.G.; Iachia, B. *J. Am. Chem. Soc.* **1961**, *83*, 827.
20. Brook, A. G. *Acc. Chem. Res.* **1974**, *7*, 77.
21. For the latest review, see: (a) Patrocínio, A. F.; Moran, P. J. S. *J. Braz. Chem. Soc.* **2001**, *12*, 7. For recent representative studies on acylsilanes, see: (b) Li, F. Q.; Zhong, S.; Lu, G.; Chan, A. S. C. *Adv. Synth. Catal.* **2009**, *351*, 1955. (c)
22. (a) Ricci, A.; Degl'Innocenti, A. *Synthesis* **1989**, 647. (b) Clark, C. T.; Milgram, B. C.; Scheidt, K. A. *Org. Lett.* **2004**, *6*, 3977. (c) Tarr, J. C.; Johnson, J. S. *Org. Lett.* **2009**, *11*, 3870. (d) Lettan, R. B.; Galliford, C. V.; Woodward, C. C.; Scheidt, K. A. *J. Am. Chem. Soc.* **2009**, *131*, 8805. (e) Greszler, S. N.; Johnson, J. S. *Angew. Chem. Int. Ed.* **2009**, *48*, 3689.

23. (a) Brook, A. G.; Duff, J. M.; Jones, P. F.; Davis, N. R. *J. Am. Chem. Soc.* **1967**, *89*, 431. (b) Corey, E. J.; Seebach, D.; Freedman, R. *J. Am. Chem. Soc.* **1967**, *89*, 434.
24. Moser, W.H. *Tetrahedron* **2001**, *57*, 2065.
25. Mattson, A. E.; Bharadwaj, A. R.; Scheidt, K. A. *J. Am. Chem. Soc.* **2004**, *126*, 2314.
26. Ricci, A.; Degl'Innocenti, A.; Chimichi, S.; Fiorenza, M.; Rossini, G. *J. Org. Chem.* **1985**, *50*, 130.
27. (a) Linghu, X.; Johnson, J. S. *Angew. Chem. Int. Ed.* **2003**, *42*, 2534. (b) Linghu, X.; Potnick, J. R.; Johnson, J. S. *J. Am. Chem. Soc.* **2004**, *126*, 3070.
28. Linghu, X.; Bausch, C. C.; Johnson, J. S. *J. Am. Chem. Soc.* **2005**, *127*, 1833.
29. (a) Hammerschmidt, F.; Schneyder, E.; Zbiral, E. *Chem. Ber.* **1980**, *113*, 3891. (b) Fitch, S.; Moedritzer, K. *J. Am. Chem. Soc.* **1962**, *84*, 1876. (c) Ruel, R.; Bouvier, J.-P.; Young, R. N. *J. Org. Chem.* **1995**, *60*, 5209. Cyanide anion promoted phosphonate-phosphate rearrangement of acetylphosphonate in aqueous medium was reported; see: (d) Hall, L. A. R.; Stephens, C. W.; Drysdale, J. J. *J. Am. Chem. Soc.* **1957**, *79*, 1768.
30. Kurihara, T.; Santo, K.; Harusawa, S.; Yoneda, R. *Chem. Pharm. Bull.* **1987**, *12*, 35.
31. (a) Hammerschmidt, F.; Schmidt, S. *Eur. J. Org. Chem.* **2000**, 2239. (b) Hammerschmidt, F.; Hanbauer, M. *J. Org. Chem.* **2000**, *65*, 6121.
32. Page, P. C. B.; Clair, S. S.; Rosenthal, S. *Chem. Soc. Rev.* **1990**, *19*, 147.
33. Kurihara, T.; Santo, K.; Harusawa, S.; Yoneda, R.; *Chem. Pharm. Bull.* **1987**, *35*, 4777.

34. Demir, A. S.; Reis, Ö.; Iğdir, A. C.; Esiringü, İ.; Eymur, S. *J. Org. Chem.* **2005**, *70*, 10584.
35. Arbuzov, A. E. *J. Russ. Phys. Chem. Soc.* **1906**, *38*, 687.
36. Takikawa, H.; Hachisu, Y.; Bode, J. W.; Suzuki, K. *Angew. Chem. Int. Ed.* **2006**, *45*, 3492. (b) Enders, D.; Niemeier, O.; Balensiefer, T. *Angew. Chem. Int. Ed.* **2006**, *45*, 1463. (c) Hachisu, Y.; Bode, J. W.; Suzuki, K. *J. Am. Chem. Soc.* **2003**, *125*, 8432.
37. Demir, A. S.; Esiringü, İ, Göllü, M.; Reis, Ö. *J. Org. Chem.* **2009**, *74*, 2197.
38. Demir, A. S.; Reis, Ö.; Esiringü, İ.; Reis, B.; Barış, Ş. *Tetrahedron* **2007**, *63*, 160.
39. North, M. *Synlett* **1993**, 807.
40. (a) Evans, D. A.; Truesdale, L. K. *Tetrahedron Lett.* **1973**, *14*, 4929. (b) Okino, T.; Hoashi, Y.; Takemoto, Y. *Tetrahedron Lett.* **2003**, *44*, 2817.
41. Demir, A. S.; Reis, B.; Reis, Ö.; Eymur, S.; Göllü, M.; Tural, S.; Sağlam, G. *J. Org. Chem.* **2007**, *72*, 7439.
42. Evans, D. A.; Sarroll, G. L.; Truesdale, L. K. *J. Org. Chem.* **1974**, *39*, 914.
43. (a) Gregory, R. J. H. *Chem. Rev.* **1999**, *99*, 3649. (b) North, M. *Tetrahedron: Asymmetry* **2003**, *14*, 147. (c) Brunel, J.-M.; Holmes, I. P. *Angew. Chem. Int. Ed.* **2004**, *43*, 2752. (d) Kim, S. S.; Kwak, J. M. *Tetrahedron* **2006**, *62*, 49. (e) Liu, X.; Qin, B.; Zhou, X.; He, B.; Feng, X. *J. Am. Chem. Soc.* **2005**, *127*, 12224. For reviews on construction of quaternary stereocenters, see: (f) Fuji, K. *Chem. Rev.* **1993**, *93*, 2037. (g) Corey, E. J.; Guzmanperez, A. *Angew. Chem. Int. Ed.* **1998**, *37*, 388. (h) Christoffers, J.; Mann, A. *Angew. Chem. Int. Ed.* **2001**, *40*, 4591.

44. Demir, A. S.; Reis, Ö.; Kayalar, M.; Eymur, S.; Reis, B. *Synlett* **2006**, *19*, 3329.
45. Koskinen, A. *Chirality, Topology and Asymmetric Synthesis. In Asymmetric Synthesis of Natural Products*; Wiley: New York, 1993.
46. Thayer, A.M. *C&EN*, **2008**, August 4, 12.
47. (a) Noyori, R. *Asymmetric Catalysis in Organic Synthesis*; Wiley: New York, 1994. (b) Jacobsen, E. N.; Pfaltz, A.; Yamamoto, H., Eds. *Comprehensive Asymmetric Catalysis*; Springer: Berlin, 1999. (c) Ojima, I. *Catalytic Asymmetric Synthesis*; Wiley-VCH: New York, 2000. (d) Beller, M.; Bolm, C. *Transition Metals for Organic Synthesis*; Wiley-VCH: Weinheim, 2004.
48. For Nobel Lectures, see: (a) Knowles, W. S. *Angew. Chem. Int. Ed.* **2002**, *41*, 1998. (b) Noyori, R. *Angew. Chem. Int. Ed.* **2002**, *41*, 2008. (c) Sharpless, K. B. *Angew. Chem. Int. Ed.* **2002**, *41*, 2024.
49. (a) Roberts, S. M. *Biocatalysts for Fine Chemicals Synthesis*; Wiley-VCH: New York, 1999. (b) Drauz, K.; Waldmann, H. *Enzyme Catalysis in Organic Synthesis*; Wiley-VCH: Weinheim, 2002. (c) Bommarius, A. S.; Riebel, B. R. *Biocatalysis*; Wiley-VCH: Weinheim, 2004.
50. For authoritative reviews on the topic of asymmetric organocatalysis, see: (a) Dalko, P. I.; Moisan, L. *Angew. Chem. Int. Ed.* **2001**, *40*, 3726. (b) List, B. *Synlett* **2001**, 1675. (c) List, B. *Tetrahedron* **2002**, *58*, 2481. (d) Dalko, P. I.; Moisan, L. *Angew. Chem. Int. Ed.* **2004**, *43*, 5138. (e) Seayad, J.; List, B. *Org. Biomol. Chem.* **2005**, *3*, 719. (f) Lelais, G.; MacMillan, D. W. C. *Aldrichimica Acta* **2006**, *39*, 79. (g) Bressy, C.; Dalko, P. I. *Enantioselective Organocatalysis*; Wiley-VCH: Weinheim, 2007. (h) Guillena, G.; Nájera, C.; Ramón, D. J. *Tetrahedron: Asymmetry* **2007**, *18*, 2249. (i) Ting, A.; Schaus, S. E. *Eur. J. Org. Chem.* **2007**, 5797. (j)

Verkade, J. M. M.; Lieke, J. C.v.H.; Quadflieg, P. J. L. M.; Rutjes, F. P. J. T. *Chem. Soc. Rev.* **2008**, *37*, 29. (k) Dondoni, A.; Massi, A. *Angew. Chem. Int. Ed.* **2008**, *47*, 4638. (l) Melchiorre, P.; Marigo, M.; Carlone, A.; Bartoli, G. *Angew. Chem. Int. Ed.* **2008**, *47*, 6138. (m) Bertelsen, S.; Jørgensen, K. A. *Chem. Soc. Rev.* **2009**, *38*, 2178. (n) Bartoli, G.; Melchiorre, P. *Synlett* **2008**, 1759. (o) Connon, S. J. *Org. Biomol. Chem.* **2007**, *5*, 3407. (p) Yu, X.; Wang, W. *Chem. Asian J.* **2008**, *3*, 516. (q) Gruttadauria, M.; Giacalone, F.; Noto, R. *Adv. Synth. Catal.* **2009**, *351*, 33. (r) Peng, F.; Shao, Z. J. *Mol. Catal. A: Chem.* **2008**, *285*, 1. (s) Werner, T. *Adv. Synth. Catal.* **2009**, *351*, 1469. (t) Paradowska, J.; Stodulski, M.; Mlynarski, J. *Angew. Chem. Int. Ed.* **2009**, *48*, 4288. (u) Toma, S.; Meciárová, M.; Sebesta, R. *Eur. J. Org. Chem.* **2009**, 321. (v) Enders, D.; Wang, C.; Liebich, J. X. *Chem. Eur. J.* **2009**, *15*, 11058. (w) Liu, X.; Lin, L.; Feng, X. *Chem. Commun.* **2009**, 6145.

51. Liebig, J. *Ann. Chem. Pharm.* **1860**, *113*, 246.

52. Langenbeck, W. *Angew. Chem.* **1932**, *45*, 97.

53. Breiding, G.; Fiske, P. S. *Biochem. Z.* **1912**, *46*, 7.

54. Pracejus, H. *Justus Liebigs Ann. Chem.* **1960**, *634*, 9.

55. (a) Eder, U.; Sauer, G.; Wiechert, R. *Angew. Chem. Int. Ed.* **1971**, *10*, 496.

(b) Hajos, Z. G.; Parrish, D. R. *J. Org. Chem.* **1974**, *39*, 1615.

56. Seayad, J.; List, B. *Org. Biomol. Chem.* **2005**, *3*, 719.

57. MacMillan, D. W. C. *Nature* **2008**, *455*, 304.

58. Berkessel, A.; Gröger, H. *Asymmetric Organocatalysis*; Wiley-VCH: Weinheim, 2005.

59. Pihko, P. M.; Majander, I; Erkkil, A. *Top. Curr. Chem.* **2009**, *291*, 29.

60. Stork, G.; Brizzolara, A.; Landesman, H.; Smuszkovicz, J.; Terrel, R. *J. Am. Chem. Soc.* **1963**, *85*, 207.
61. List, B.; Lerner, A. R.; Barbas, C. F. *J. Am. Chem. Soc.* **2000**, *122*, 2395.
62. (a) Evans, D. A.; Nelson, J. V.; Taber, T. *In Topics in Stereochemistry*; John Wiley & Sons: New York, 1982; Vol. 13, p 1. (b) Heathcock, C. H. *Asymmetric Synthesis*; Morrison, J. D., Ed.; Academic Press: New York, 1984; Vol. 3, part B, p 111. (c) Kim, B. M.; Williams, S. F.; Masamune, S. *In Comprehensive Organic Synthesis*; Trost, B. M., Fleming, I., Eds.; Pergamon Press: Oxford, 1991; Vol. 2 (Heathcock, C. H., Ed.), Chapter 1.7, p. 239. (d) Mukaiyama, T. *The Directed Aldol Reaction. In Organic Reactions*; John Wiley & Sons: New York, 1982; Vol. 28, p 203.
63. (a) Agami, C.; Levisalle, J.; Puchot, C. *J. Chem. Soc., Chem. Comm.* **1985**, 441. (b) Agami, C.; Puchot, C. *J. Mol. Catal.* **1986**, *38*, 341.
64. Rajagopal, D.; Moni, M. S.; Subramanian, S.; Swaminathan, S. *Tetrahedron: Asymmetry* **1999**, *10*, 1631.
65. (a) Bahmanyar, S.; Houk, K. N. *J. Am. Chem. Soc.* **2001**, *123*, 9922. (b) Bahmanyar, S.; Houk, K. N. *J. Am. Chem. Soc.* **2001**, *123*, 11273. (c) Bahmanyar, S.; Houk, K. N.; Martin, H. J.; List, B. *J. Am. Chem. Soc.* **2003**, *125*, 2475.
66. Hoang, L.; Bahmanyar, S.; Houk, K. N.; List, B. *J. Am. Chem. Soc.* **2003**, *125*, 16.
67. (a) List, B. *Tetrahedron* **2002**, *58*, 5573. (b) Xie, Z. X.; Zhang, L. Z.; Ren, X. J.; Tang, S. Y.; Li, Y. *Chin. J. Chem.* **2008**, *26*, 1272. (c) Sakthivel, K.; Notz, W.; Bui, T.; Barbas, C. F. III, *J. Am. Chem. Soc.* **2001**, *123*, 5260. (d) Notz, W.; List, B. *J. Am. Chem. Soc.* **2000**, *122*, 7386. (e) Grondal, C.; Enders, D. *Adv. Synth. Catal.* **2007**, *349*, 694. (f) Liu, H. W.; Peng, L. Z.; Zhang, T.; Li, Y. L. *New J. Chem.* **2003**, *27*, 1159.

68. (a) Guillena, G.; Carmen Hita M. and Najera, C. *Tetrahedron: Asymmetry* **2006**, *17*, 1493. (b) Chen, J. R.; Li, X. Y.; Xing X. N.; Xiao, W. J. *J. Org. Chem.* **2006**, *71*, 8198. (c) Wang, Y.; Wei S.; Sun, J. *Synlett* **2006**, 3319. (d) Huang, J.; Zhang X.; Armstrong, D. W. *Angew. Chem. Int. Ed.* **2007**, *46*, 9073. (e) Gandhi S.; Singh, V. K. *J. Org. Chem.* **2008**, *73*, 9411. (f) Chen, F.; Huang, S.; Zhang, H.; Liu, F.; Peng, Y. *Tetrahedron* **2008**, *64*, 9585. (g) Doherty, S.; Knight, J. G.; McRae, A.; Harrington R. W.; Clegg, W. *Eur. J. Org. Chem.* **2008**, *10*, 1759. (h) Okuyama, Y.; Nakano, H.; Watanabe, Y.; Makabe, M.; Takeshita, M.; Uwai, K.; Kabuto, C.; Kwon, E. *Tetrahedron Lett.* **2009**, *50*, 193. (i) Zhao, J. F.; He, L.; Jiang, J.; Tang, Z.; Cun, L. F.; Gong, L. Z. *Tetrahedron Lett.* **2008**, *49*, 3372. (j) Nakadai, M.; Saito, S.; Yamamoto, H. *Tetrahedron* **2002**, *58*, 8167. (k) Cobb, A. J. A.; Shaw, D. M.; Longbottom, D. A.; Gold, J. B.; Ley, S. V. *Org. Biomol. Chem.* **2005**, *3*, 84. (l) Gu, Q.; Wang, X. F.; Wang, L.; Wu, X. Y.; Zhou, Q. L. *Tetrahedron: Asymmetry* **2006**, *17*, 1537. (m) Raj, M.; Vishnumaya, S. K. G.; Singh, V. K. *Org. Lett.* **2006**, *8*, 4097. (n) Chimni, S. S.; Singh, S.; Mahajan, D. *Tetrahedron: Asymmetry* **2008**, *19*, 2276. (o) Jia, Y.-N.; Wu, F.-C.; Ma, X.; Zhu, G.-J.; Da, C.-S. *Tetrahedron Lett.* **2009**, *50*, 3059.
69. For selected reviews and recent examples, see: (a) Tsogoeva, S. B. *Eur. J. Org. Chem.* **2007**, *11*, 1701. (b) Almasi, D.; Alonso, D. A.; Najera, C. *Tetrahedron: Asymmetry* **2007**, *18*, 299. (c) Perlmutter, P. *Conjugate Addition Reactions in Organic Synthesis*; Pergamon Press: Oxford, 1992. (c) Mase, N.; Watanabe, K.; Yoda, H.; Takabe, K.; Tanaka, F.; Barbas, C. F., III *J. Am. Chem. Soc.* **2006**, *128*, 4966. (d) Wang, J.; Ma, A.; Ma, D. *Org. Lett.* **2008**, *10*, 5425. (e) Zhu, Q.; Cheng, L.; Lu, Y. *Chem. Commun.* **2008**, *47*, 6315. (f) Enders, D.; Wang, C.; Bats, J. W. *Angew. Chem. Int. Ed.* **2008**, *47*, 7539. (g) Enders, D.; Huttl, C.; Grondal, M. R. B.; Raabe, G. *Nature* **2006**, *441*, 861.

70. Wynberg, H.; Helder, R. *Tetrahedron Lett.* **1975**, *46*, 4057.
71. Betancort, J. M.; Barbas, C. F., III *Org. Lett.* **2001**, *3*, 3737.
72. Wang, W.; Wang, J.; Li, H. *Angew. Chem. Int. Ed.* **2005**, *44*, 1369.
73. (a) Hayashi, Y.; Itoh, T.; Ohkubo, M.; Ishikawa, H. *Angew. Chem. Int. Ed.* **2008**, *47*, 4722. (b) Hayashi, Y.; Gotoh, H.; Hayashi, T.; Shoji, M. *Angew. Chem. Int. Ed.* **2005**, *44*, 4212.
74. Wiesner, M.; Revell, J. D.; Wennemers, H. *Angew. Chem. Int. Ed.* **2008**, *47*, 1871.
75. (a) Betancort, J. M.; Sakthivel, K.; Thayumanavan, R.; Tanaka, F.; Barbas, C. F., III *Synthesis*, **2004**, *9*, 1509. (b) Zhu, M-K.; Cun, L-F.; Mi, A-Q.; Jiang, Y-Z.; Gong, L-Z. *Tetrahedron: Asymmetry* **2006**, *17*, 491. (c) Cobb, A. J. A.; Longbottom, D. A.; Shaw, D. M.; Ley, S. V. *Chem. Commun.* **2004**, *16*, 1808. (d) Mitchell, C. E. T.; Cobb, A. J. A.; Ley, S. V. *Synlett* **2005**, *4*, 611. (e) Andrey, O.; Alexakis, A.; Bernardinelli, G. *Org. Lett.* **2003**, *5*, 2559. (g) Tania I.; Poe, S. L.; McQuade, D. T. *Org. Lett.* **2012**, *14*, 4394. (h) Terakado, D.; Takano, M.; Oriyama, T. *Chem. Lett.* **2005**, *34*, 962.
76. Pasteur, L. C. R. *Hebd. Séanc. Acad. Sci. Paris* **1848**, *26*, 535.
77. (a) Wynberg, H.; Feringa, B. *Tetrahedron* **1976**, *32*, 2831. (b) Wynberg, H. *Chimia* **1976**, *30*, 445.
78. (a) Puchot, C.; Samuel, O.; Dunach, E.; Zhao, S.; Agami, C.; Kagan, H. B. *J. Am. Chem. Soc.* **1986**, *108*, 2353.
79. For selected examples see: (a) Bonner, W. A. *Origins Life Evol. Biospheres* **1994**, *24*, 63. (b) Bada, J. L. *Origins Life Evol. Biospheres* **1996**, *26*, 518. (c) Lahav, N. *Biogenesis: Theories of Life's Origin*, Oxford University Press, New York: 1999, p. 257. (d) Siegel, J. S. *Chirality* **1998**,

- 10, 24. (e) Siegel, J. S. *Nature* **2002**, *419*, 346. (f) Miller, S. L. *The Origin of Homochirality in Life*, Santa Monica, 1995. (g) Ribo, J.M.; Crusats, J. M.; Sagues, F.; Claret, J.; Rubires, R. *Science* **2001**, *292*, 2063. (h) Mauksch, M.; Tsogoeva, S. B. *ChemPhysChem* **2008**, *9*, 2359. (i) Blackmond, D. G. *Proc. Natl. Acad. Sci. U. S. A.* **2004**, *101*, 5732. (j) Cronin, J.; Pizzarello, S. *Science* **1997**, *275*, 95. (k) Pizzarello, S. *Acc. Chem. Res.* **2006**, *39*, 231. (l) Breslow, R.; Cheng, Z. L. *Proc. Natl. Acad. Sci. U. S. A.* **2009**, *106*, 9144. (m) Viedma, C. *Phys. Rev. Lett.* **2005**, *94*, 065504.
80. Frank, F. C. *Biochim. Biophys. Acta* **1953**, *11*, 459.
81. Soai, K.; Niwa, S.; Hori, H. *Chem. Commun.* **1990**, 982.
82. (a) Blackmond, D. G. *J. Am. Chem. Soc.* **1998**, *120*, 13349. (b) Blackmond, D. G. *J. Am. Chem. Soc.* **1997**, *119*, 12934. For a review see (c) Blackmond, D. G. *Acc. Chem. Res.* **2000**, *33*, 402.
83. (a) Shock, E. L.; Shulte, M. D. *Geochim. Cosmochim. Acta* **1990**, *54*, 3159. (b) Cronin, J. R.; Pizarello, S.; Cruikshank, D. P. *In Meteorites and the Early Solar System*; Kerridge, J. F.; Matthews, M. S., Eds.; University Arizona Press: Tucson, 1988, p. 819.
84. (a) Mathew, S. P.; Iwamura, H.; Blackmond, D. G. *Angew. Chem. Int. Ed.* **2004**, *43*, 3317. (b) Klusmann, M.; Mathew, S. P.; Iwamura, H.; Wells, D. H. Jr.; Armstrong, A.; Blackmond, D. G. *Angew. Chem. Int. Ed.* **2006**, *45*, 7985.
85. Klusmann, M.; Iwamura, H.; Mathew, S. P.; Wells, Jr. D. H.; Pandya, U.; Armstrong, A.; Blackmond, D. G. *Nature* **2006**, *441*, 621.
86. Hayashi, Y.; Matsuzawa, M.; Yamaguchi, J.; Yonehara, S.; Matsumoto, Y.; Shoji, M.; Hashizume, D.; Koshino, H. *Angew. Chem. Int. Ed.* **2006**, *45*, 4593.

87. Klussmann, M.; Izumi, T.; White, A. J. P.; Armstrong, A.; Blackmond, D. *G. J. Am. Chem. Soc.* **2007**, *129*, 7657.
88. (a) Kirsch, P. *Modern Fluoroorganic Chemistry*; Wiley-VCH: Weinheim, Germany, 2004. (b) Chambers, R. D. *Fluorine in Organic Chemistry*; Blackwell: Oxford, 2004. (c) Liebman, J. F., Greenberg, A., Dolbier, W. R., Jr., Eds. *Fluorine Containing Molecules: Structure, Reactivity, Synthesis, and Applications*; VCH: New York, 1988. (d) Large-Radix, S.; Billard, T.; Langlois, B. R. *J. Fluorine Chem.* **2003**, *124*, 147. (e) Stahly, G. P.; Bell, D. R. *J. Org. Chem.* **1989**, *54*, 2873. (f) Thayer, A. M. *Chem. Eng. News* **2006**, *June 5*, 15. (g) Smart, B. E. *J. Fluorine Chem.* **2001**, *109*, 3. (g) Uneyama, K. *Organofluorine Chemistry*; Blackwell: Oxford, 2006.
89. (a) Filler, R.; Kobayashi, Y.; Yagulpolskii, L. M. *Organofluorine compounds in Medicinal Chemistry and Biomedical Applications*; Elsevier, Amsterdam, 1993. (b) Welch, J. T., Ewarakrishnan, S. E. *Fluorine in Bioorganic Chemistry*; Wiley: New York, 1991. (c) Kukhar, V. P.; Soloshonok, V. A. *Fluorine-containing amino acids: Synthesis and Properties*; Wiley: Chichester, 1995. (d) Becker, A. *In Ventry of Industrial Fluoro-Biochemicals*; Eyrolles: Paris, 1996. (e) Banks, R. E.; Smart, B. E.; Tatlow, J. C. *Organofluorine Chemistry: Principles and Commercial Applications*; Plenum Press: New York, 1994. (f) Hiyama, T. *Organofluorine Compounds: Chemistry and Properties*; Springer-Verlag: Berlin, 2000.
90. Schofield, H. *J. Fluorine Chem.* **1999**, *100*, 7.
91. (a) Kirk, K. L. *Org. Process Res. Dev.* **2008**, *12*, 305. (b) Furuya, T.; Kuttruff, C. A.; Ritter, T. *Curr. Opin. Drug Discov. Dev.* **2008**, *11*, 803. (c) Furuya, T.; Klein, J. E. M. N.; Ritter, T. *Synthesis* **2010**, 1804.

92. (a) Ruppert, I.; Schlich, K.; Volbach, W. *Tetrahedron Lett.* **1984**, *24*, 2195.
(b) Prakash, G. K. S.; Panja, C.; Vaghoo, H.; Surampudi, V.; Kultyshev, R.; Mandal, M.; Rasul, G.; Mathew, T.; Olah, G. A. *J. Org. Chem.* **2006**, *71*, 6806.
93. (a) Singh, R. P.; Shreeve, J. M. *Tetrahedron* **2000**, *56*, 7613. (b) Nelson, D. W.; Owens, J.; Hiraldo, D. *J. Org. Chem.* **2001**, *66*, 2572. (c) Petrov, V. A. *Tetrahedron Lett.* **2000**, *41*, 6959. (d) Li, N. S.; Tang, X. P.; Piccirilli, J. *Org. Lett.* **2001**, *3*, 1025. (e) Sevenard, D. V.; Kirsch, P.; Roschenthaler, G. V.; Movchun, V. N.; Kolomeitsev, A. A. *Synlett* **2001**, 379. (f) Benayood, F.; Abouabdellah, A.; Richard, C.; Bonnet-Delpon, D.; Bejgue, J. P.; Levasseur, D.; Boutaud, O.; Schuber, F. *Tetrahedron Lett.* **2000**, *41*, 6367. (g) Lin, P.; Jiang, J. *Tetrahedron* **2000**, *56*, 3635.
94. Lefebvre, O.; Brigaud, T.; Portella, C. *J. Org. Chem.* **2001**, *66*, 1941.
95. (a) Uneyama, K.; Tanaka, H.; Kobayashi, S.; Shioyama, M.; Amii, H. *Org. Lett.* **2004**, *6*, 2733. (b) Ishihara, T.; Yamana, M.; Ando, T. *Tetrahedron Lett.* **1983**, *24*, 5657. (c) Portella, C.; Brigaud, T.; Lefebvre, O.; Plantier-Royon, R. *J. Fluorine Chem.* **2000**, *101*, 193. (d) Garayt, M. R.; Percy, J. M. *Tetrahedron Lett.* **2001**, *42*, 6377.
96. Goldfuss, B.; Schumacher, M. *J. Mol. Model.* **2006**, *12*, 591.
97. (a) Ishihara, T.; Yamana, M.; Maekawa, T.; Kuroboshi, M.; Ando, T. *J. Fluorine Chem.* **1988**, *38*, 263. (b) Yamana, M.; Ishihara, T.; Ando, T. *Tetrahedron Lett.* **1983**, *24*, 507.
98. Zhou, Y.; Shan, Z. *J. Org. Chem.* **2006**, *71*, 9510.
99. Vasbinder, M. M.; Imbriglio, J. E.; Miller, S. J. *Tetrahedron* **2006**, *62*, 11450.
100. Clarke M. L.; Fuentes, J. A. *Angew. Chem. Int. Ed.* **2007**, *46*, 930.

101. (a) Lehn, J.-M. *Supramolecular Chemistry. Concepts and Perspectives*, VHC, Weinheim, 1995. (b) Lehn, J.-M. *Science* **2002**, *295*, 2400. (c) Lehn, J.-M. *Proc. Natl. Acad. Sci. U. S. A.* **2002**, *99*, 4763. (d) Lehn, J.-M.; Ball, P. *New Chemistry* **2000**, *9*, 300. (e) Lehn, J.-M. *Science* **1993**, *260*, 1762. (f) Lehn, J.-M. *Ang. Chem.* **1990**, *102*, 1347. (g) Lehn, J.-M. *Ang. Chem.* **1988**, *100*, 91.
102. (a) Birkholz, M.-N.; Dubrovina, N. V.; Jiao, H.; Michalik, D.; Holz, J.; Paciello, R.; Breit, B.; Börner, A. *Chem. Eur. J.* **2007**, *13*, 5896. For selected examples of self-assembly ligands: (b) Chevallier, F.; Breit, B. *Angew. Chem. Int. Ed.* **2006**, *45*, 1599. (c) Waloch, C.; Wieland, J.; Keller, M.; Breit, B. *Angew. Chem. Int. Ed.* **2007**, *46*, 3037. (d) Laungani, A. C.; Slattery, J. M.; Krossing, I.; Breit, B. *Chem. Eur. J.* **2008**, *14*, 4488. (e) Smejkal, T.; Breit. *Angew. Chem. Int. Ed.* **2008**, *47*, 3946.
103. Schreiner P. R.; Wittkopp, A. *Org. Lett.* **2002**, *4*, 217. (b) Wittkopp A.; Schreiner, P. R. *Chem. Eur. J.* **2003**, *9*, 407. (c) Casas, C. P.; Yatsimirsky, A. K. *J. Org. Chem.* **2008**, *73*, 2275. (d) Schreiner, P. R. *Chem. Soc. Rev.* **2003**, *32*, 289.
104. Betancort, J. M.; Barbas, C. F., III *Org. Lett.* **2001**, *3*, 3737.
105. Mandal, T.; Zhao, C.-G. *Angew. Chem. Int. Ed.* **2008**, *47*, 7714.
106. Seebach, D.; Golinski, J. *Helv. Chim. Acta* **1981**, *64*, 1413.
107. Demir, A. S.; Eymur, S. *J. Org. Chem.* **2007**, *72*, 8527.
108. Reis, Ö; Eymur, S.; Reis, B.; Demir, A. S. *Chem. Commun.* **2009**, *9*, 1088.
109. Demir, A. S.; Eymur, S. *Tetrahedron: Asymmetry* **2010**, *21*, 112.
110. Demir, A. S.; Eymur, S. *Tetrahedron: Asymmetry* **2010**, *21*, 405.

APPENDIX A

NMR

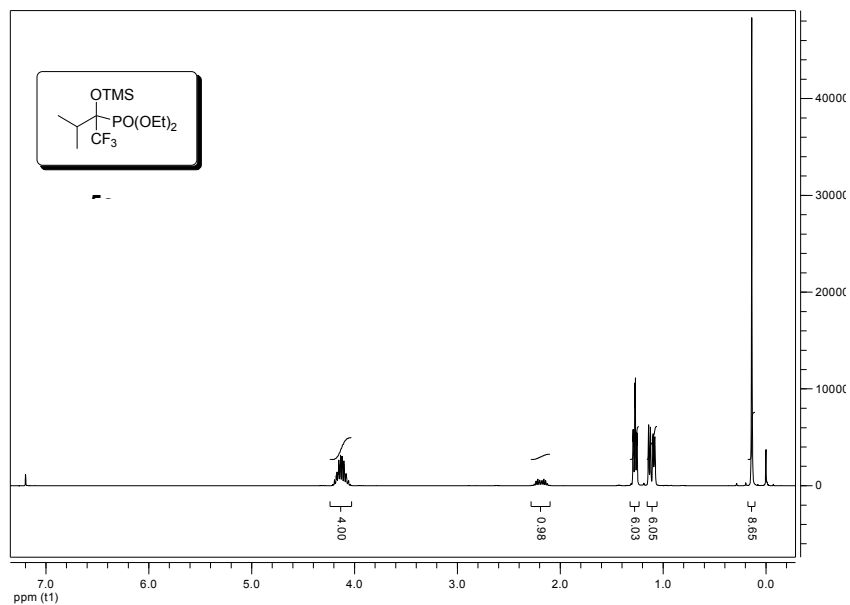


Figure A1. ^1H NMR spectrum of 244

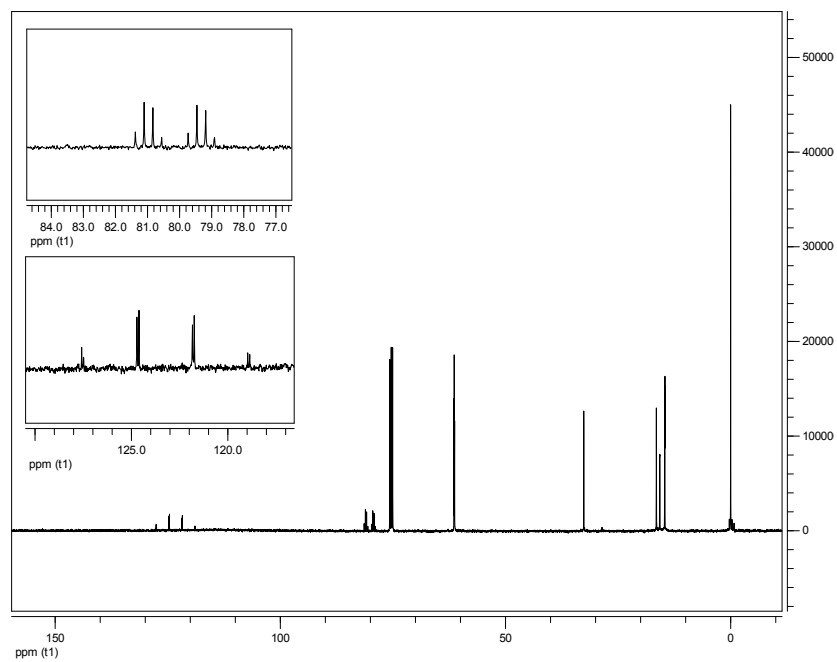


Figure A2. ^{13}C NMR spectrum of 244

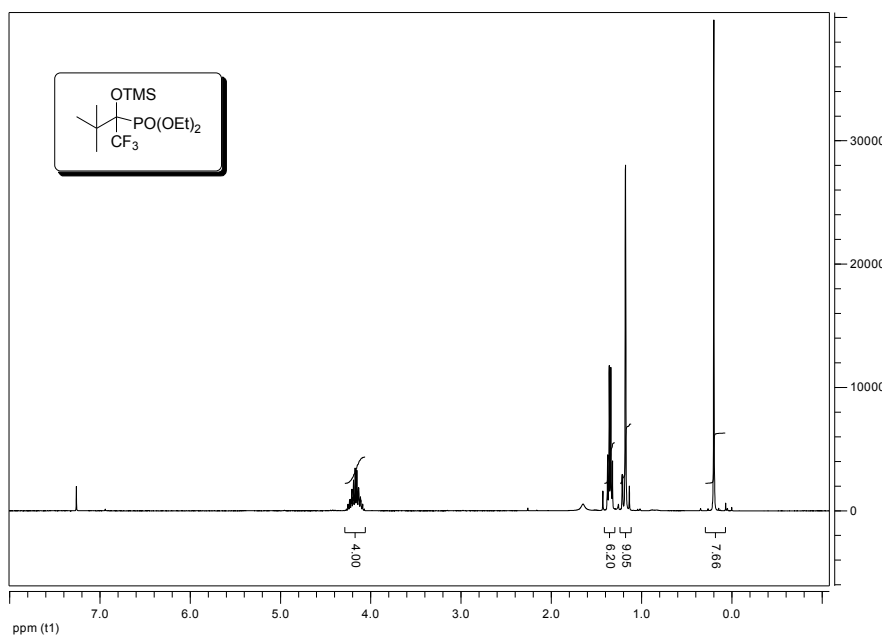


Figure A3. ^1H NMR spectrum of **247**

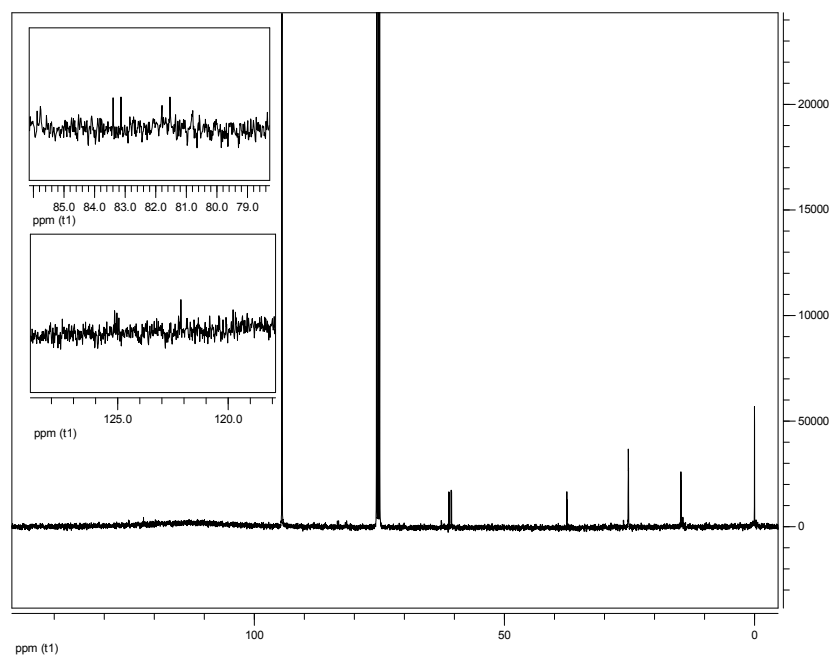


Figure A4. ^{13}C NMR spectrum of **247**

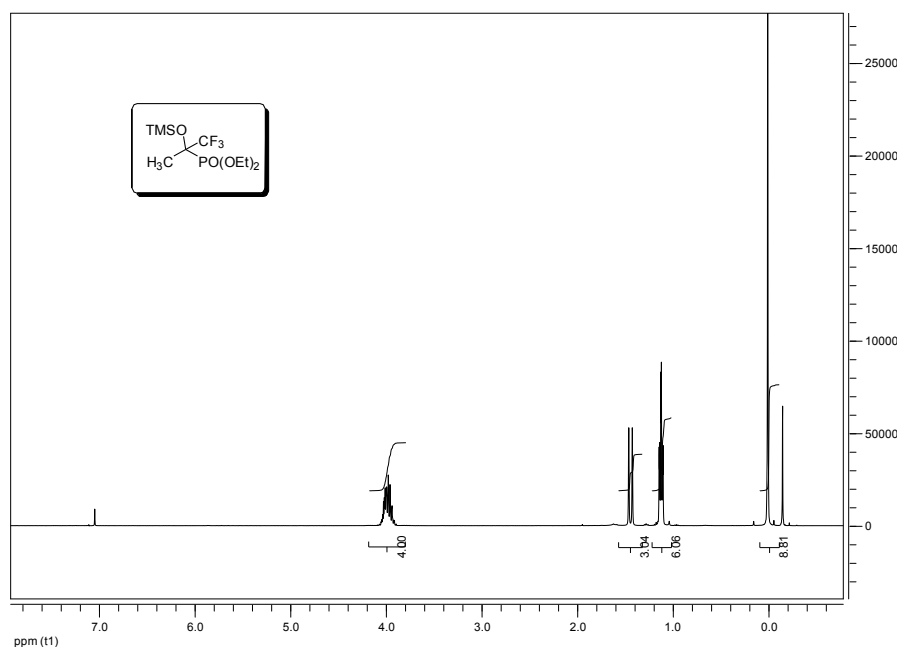


Figure A5. ^1H NMR spectrum of **249**

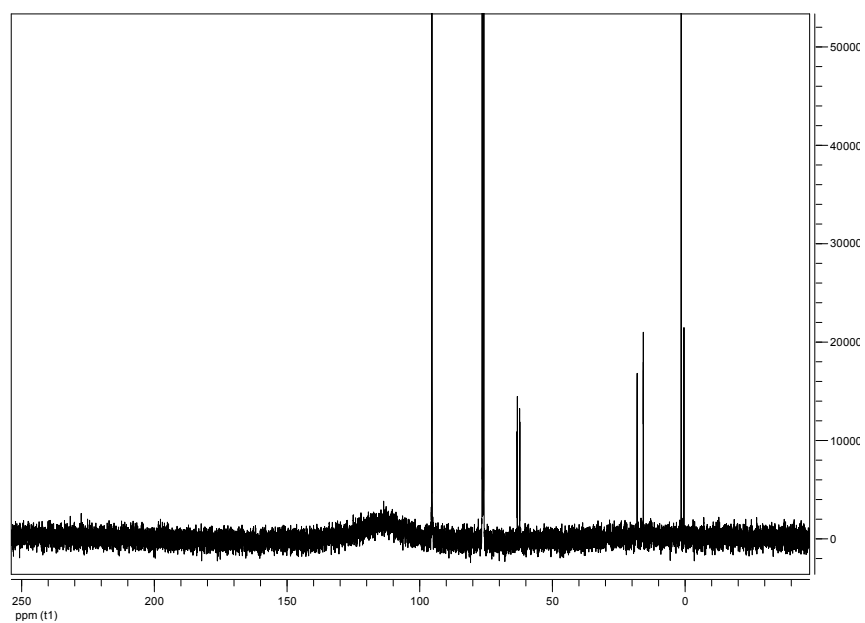


Figure A6. ^{13}C NMR spectrum of **249**

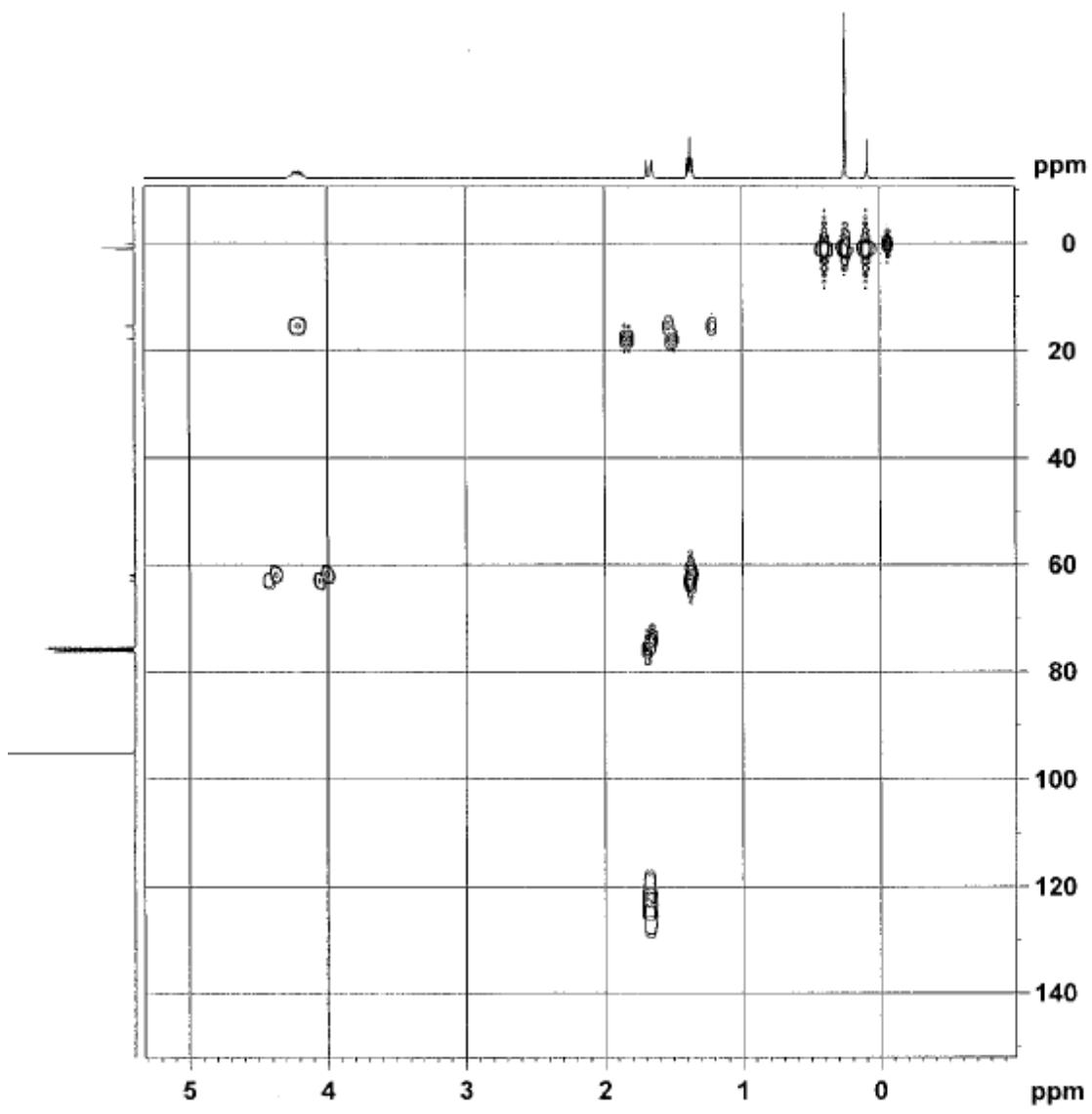


Figure A7. HBMC spectrum of 249

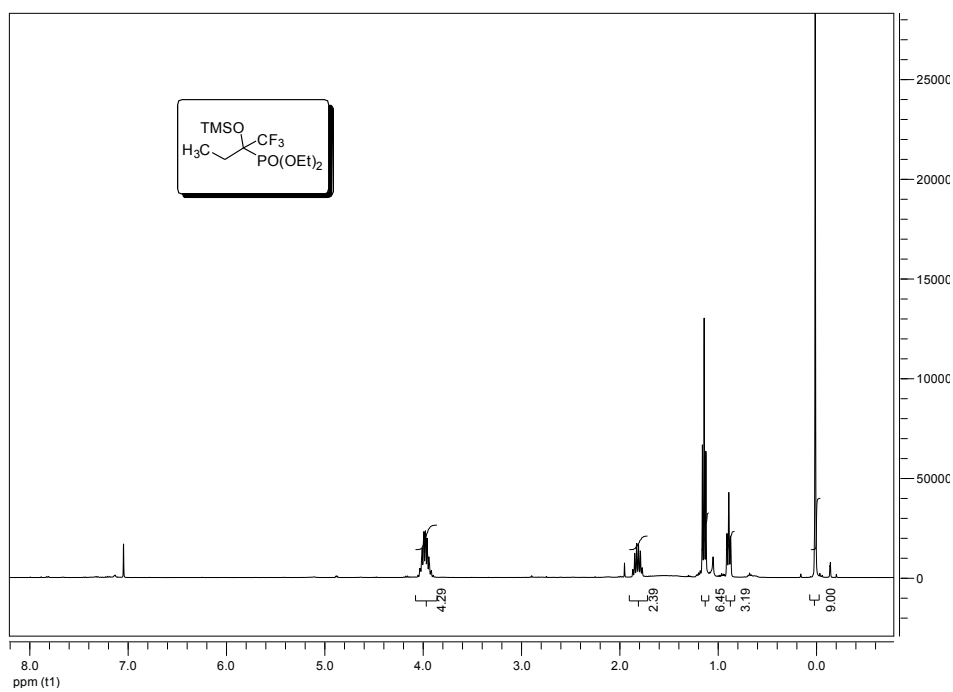


Figure A8. ^1H NMR spectrum of **251**

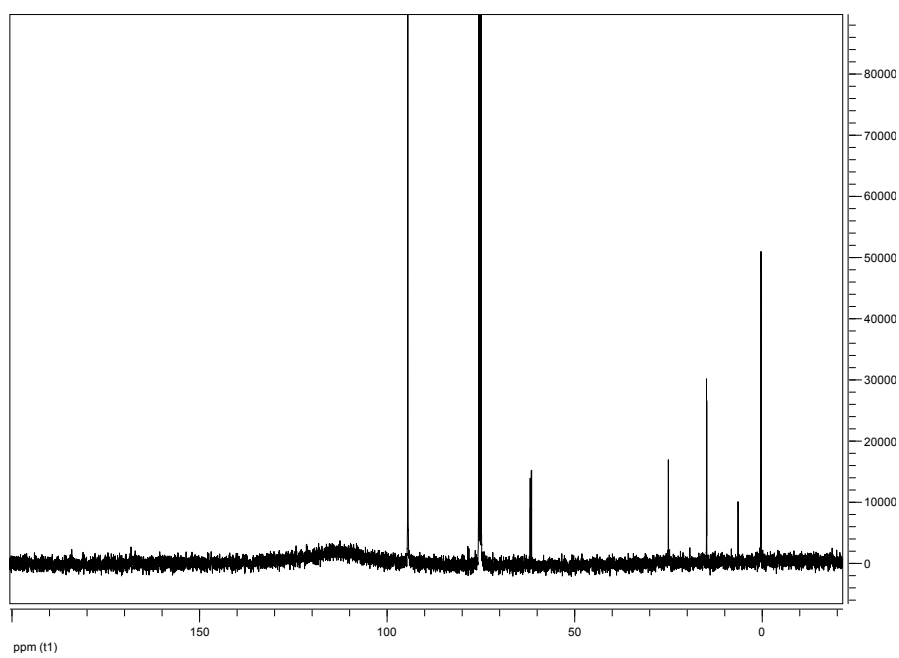


Figure A9. ^{13}C NMR spectrum of **251**

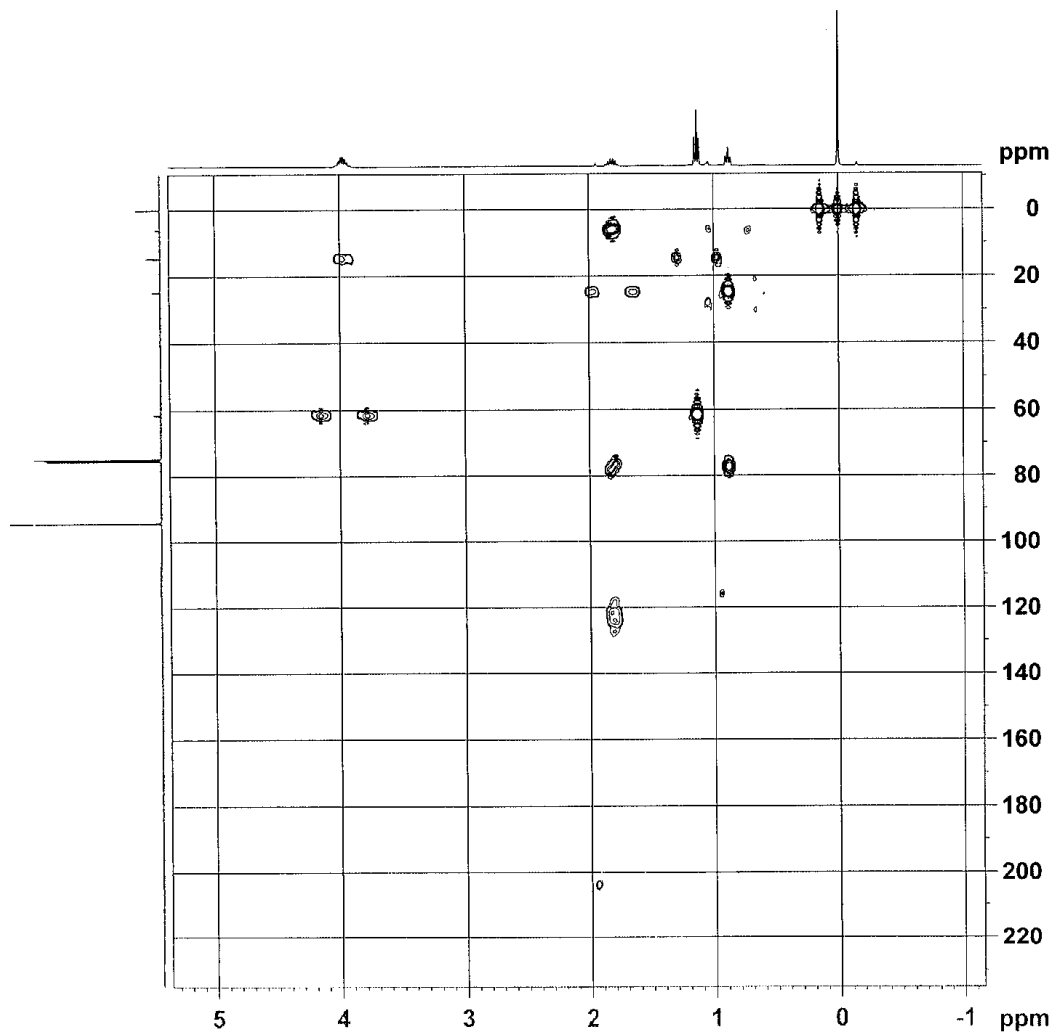


Figure A10. HBMC spectrum of **251**

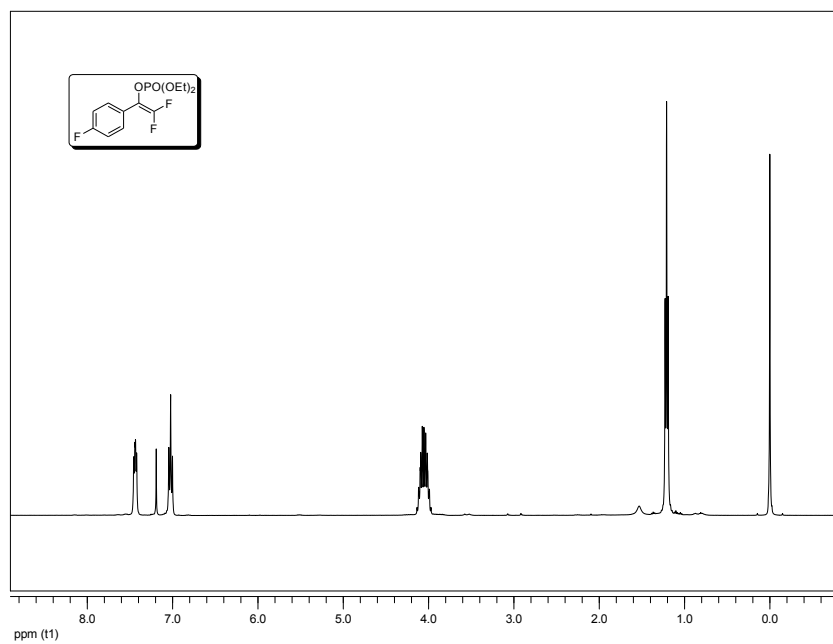


Figure A11. ¹H NMR spectrum of **258**

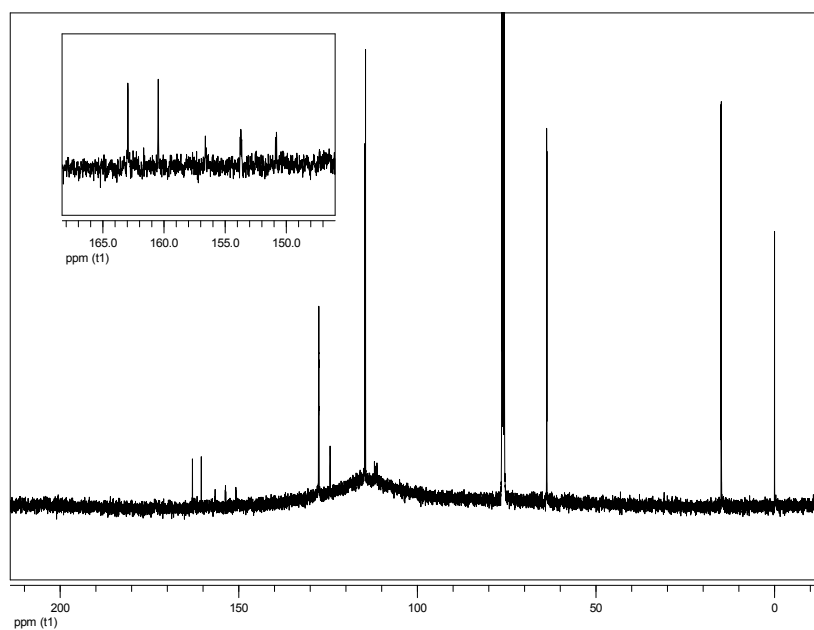


Figure A12. ¹³C NMR spectrum of **258**

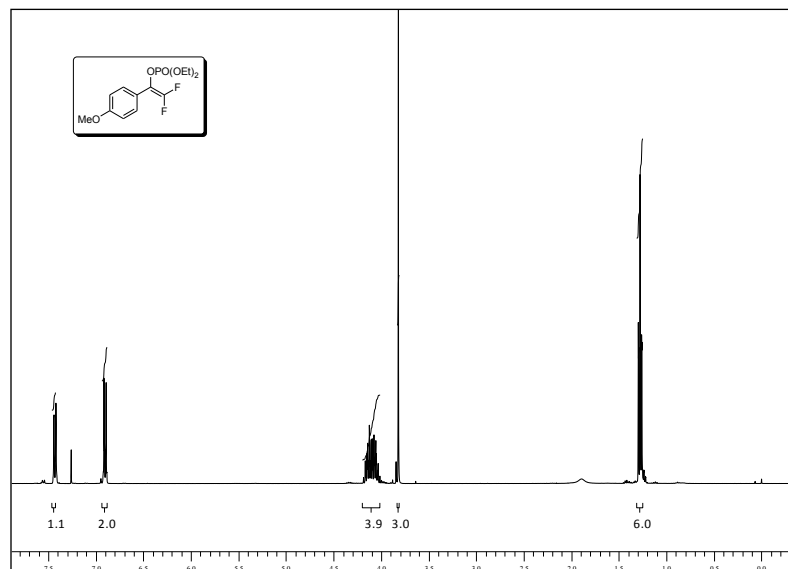


Figure A13. ^1H NMR spectrum of 256

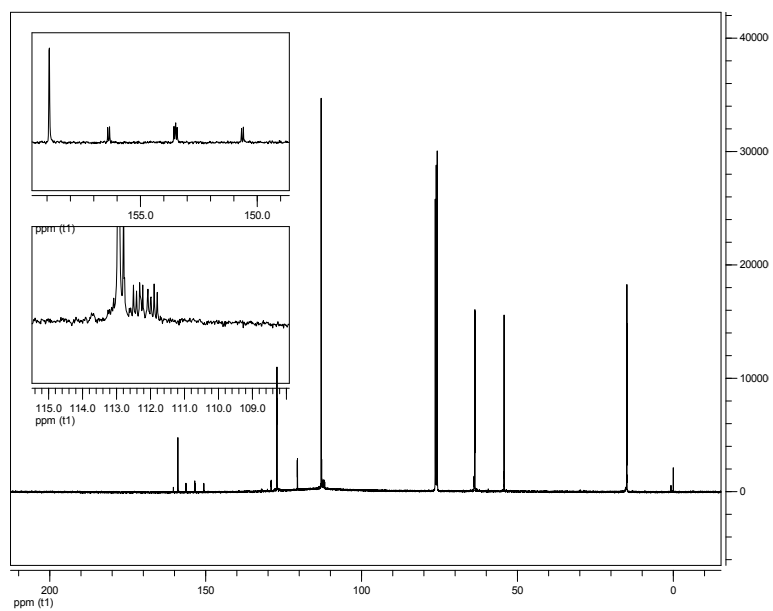


Figure A14. ^{13}C NMR spectrum of 256

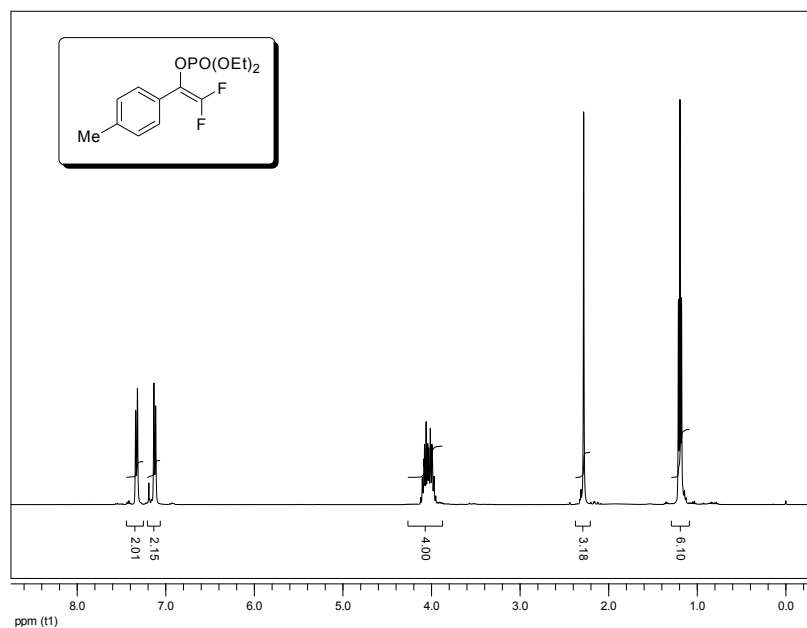


Figure A15. ^1H NMR spectrum of **253**

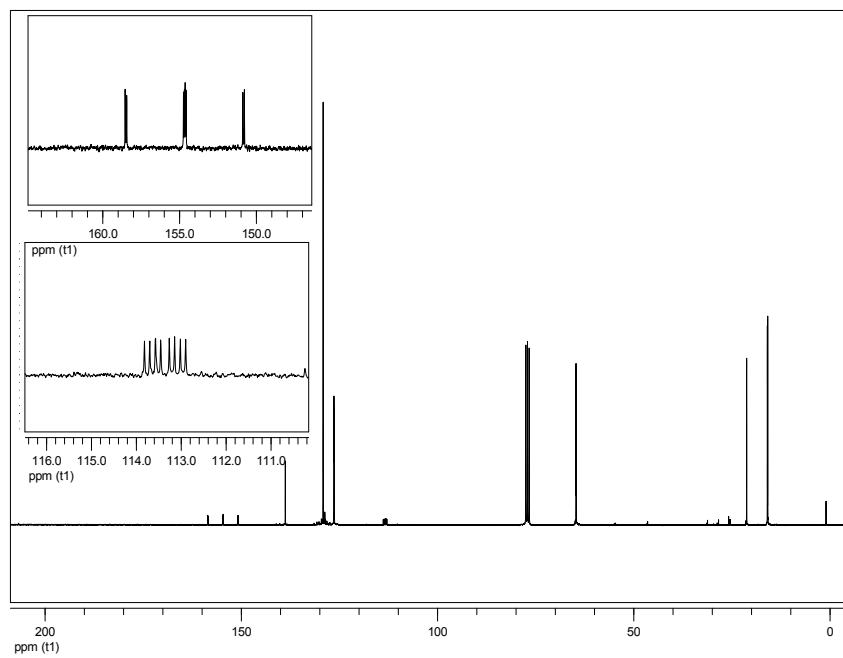


Figure A16. ^{13}C NMR spectrum of **253**

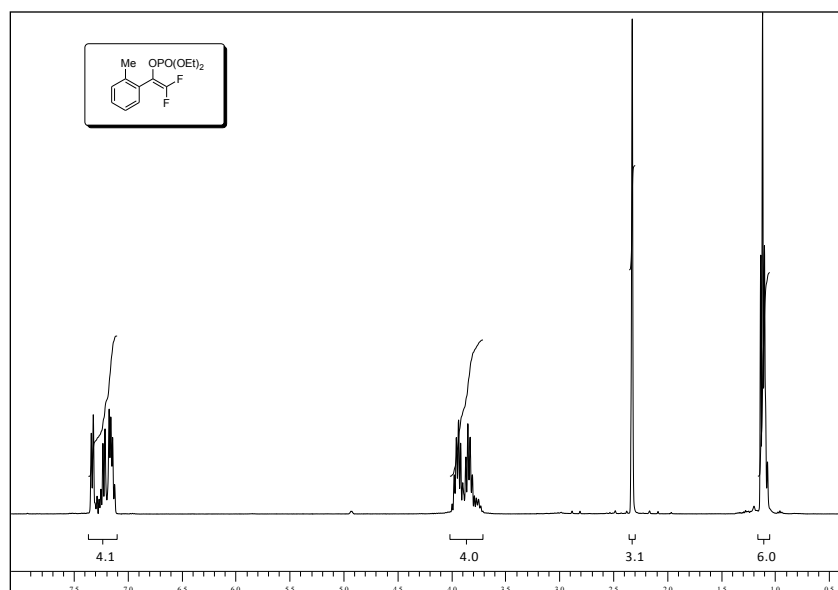


Figure A17. ¹H NMR spectrum of 260

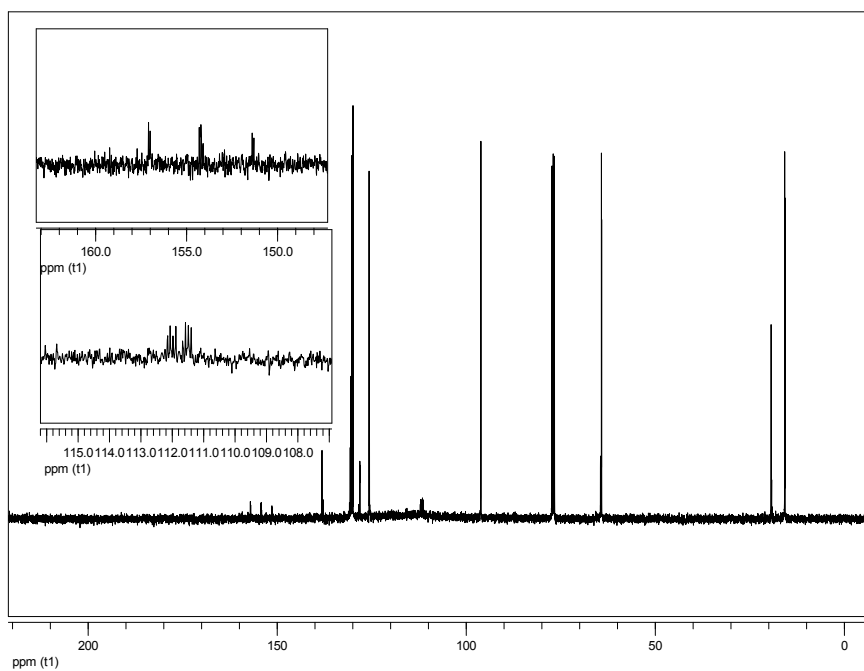


Figure A18. ¹³C NMR spectrum of 260

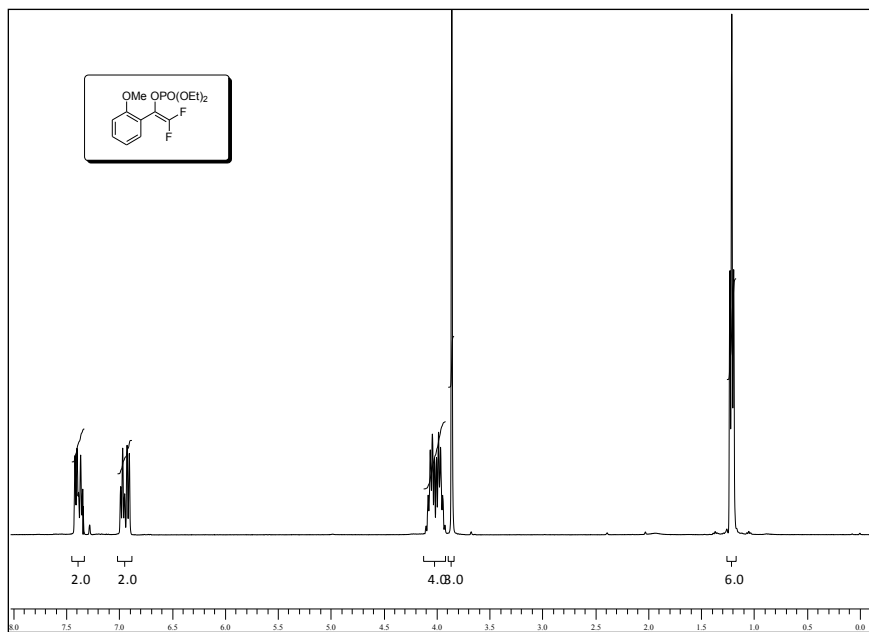


Figure A19. ^1H NMR spectrum of **262**

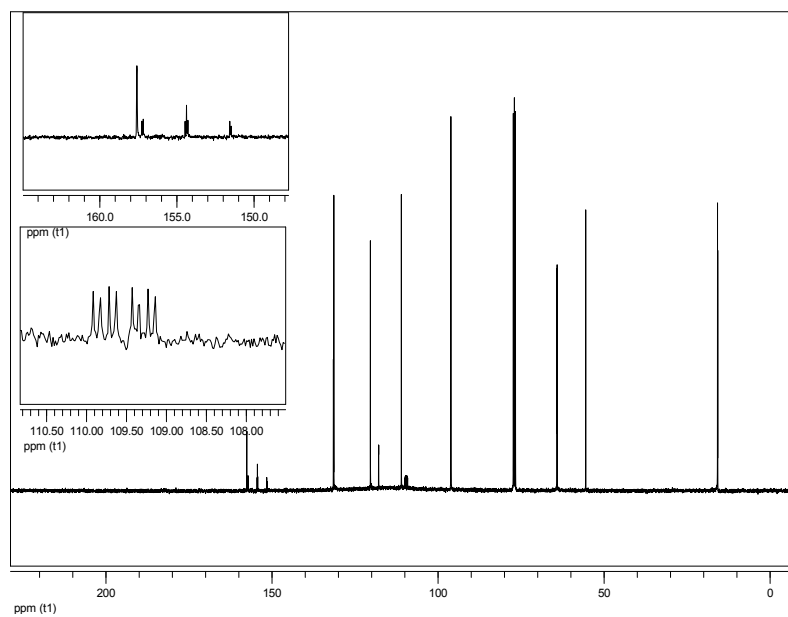
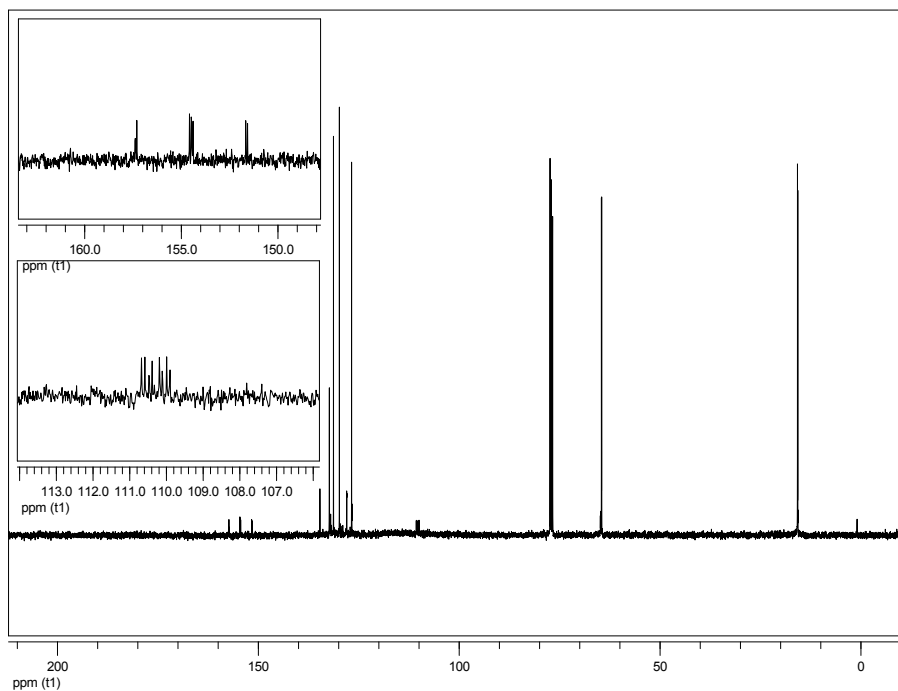
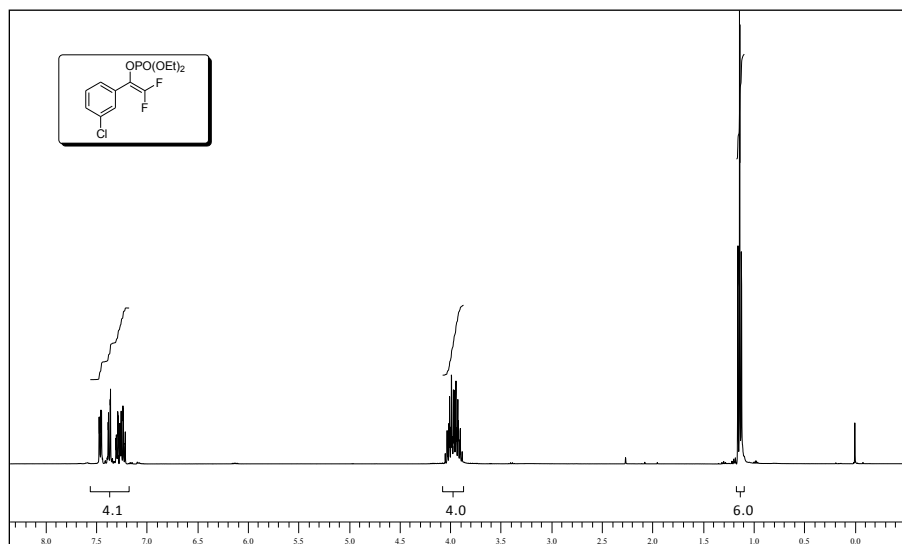


Figure A20. ^{13}C NMR spectrum of **262**



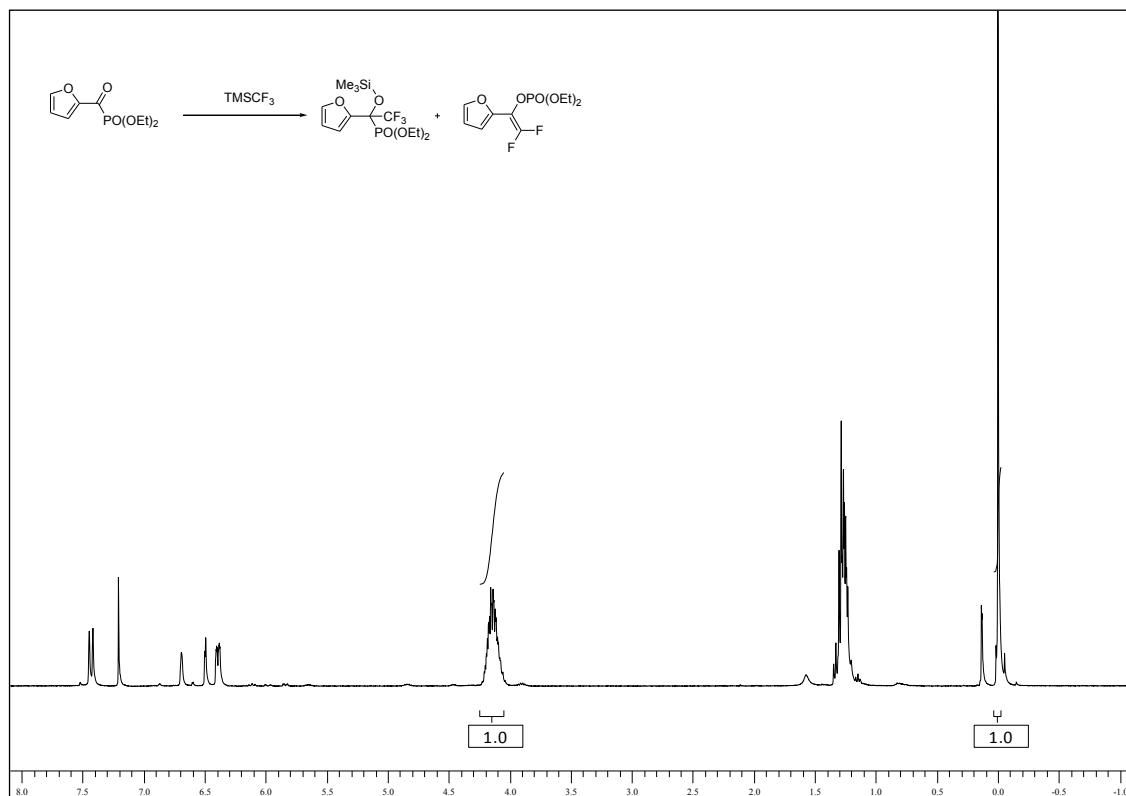


Figure A23. ¹H NMR spectrum of **267** and **268**

APPENDIX B

HPLC

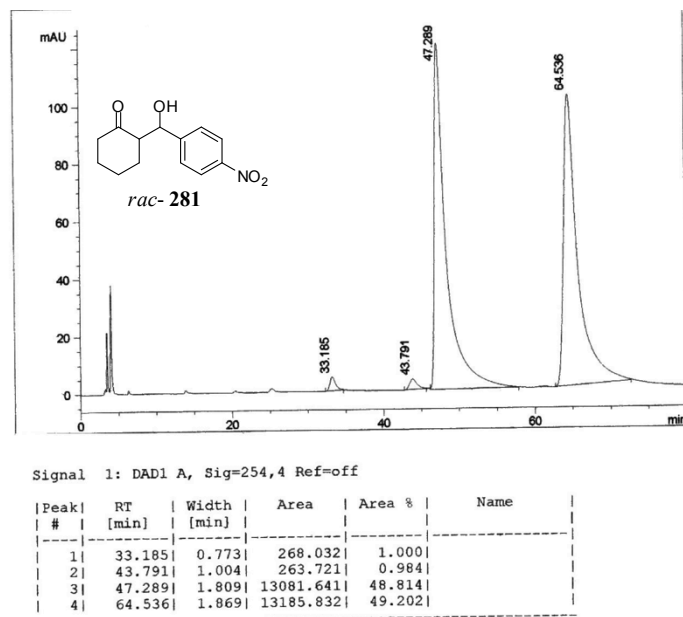


Figure B1. HPLC chromatogram of *rac*-281

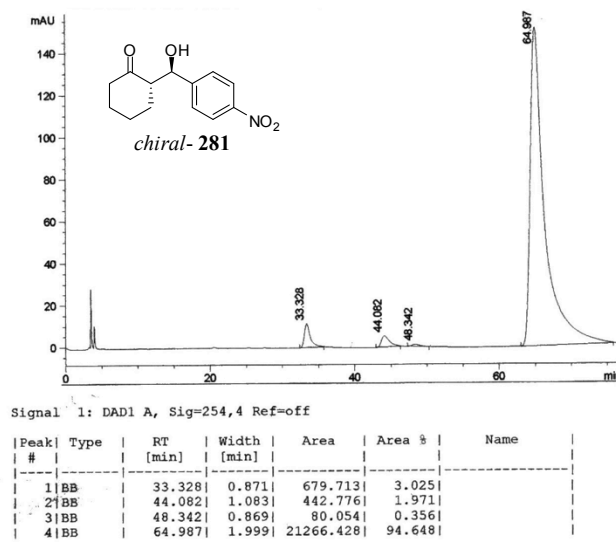
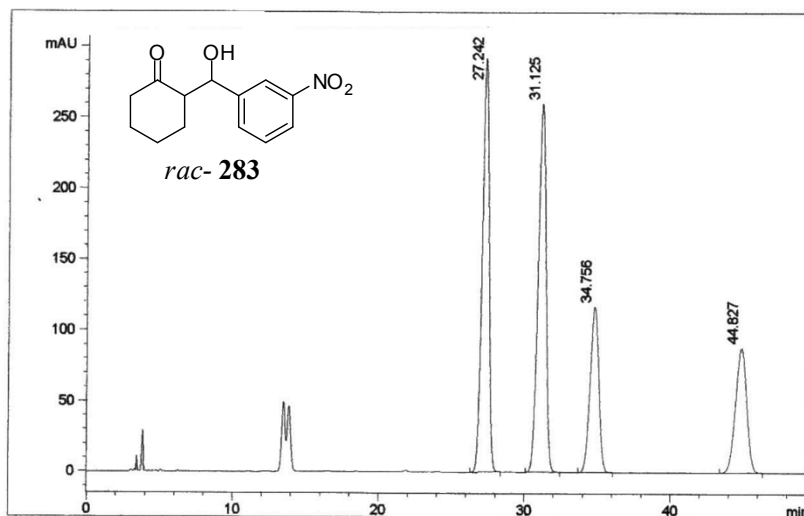


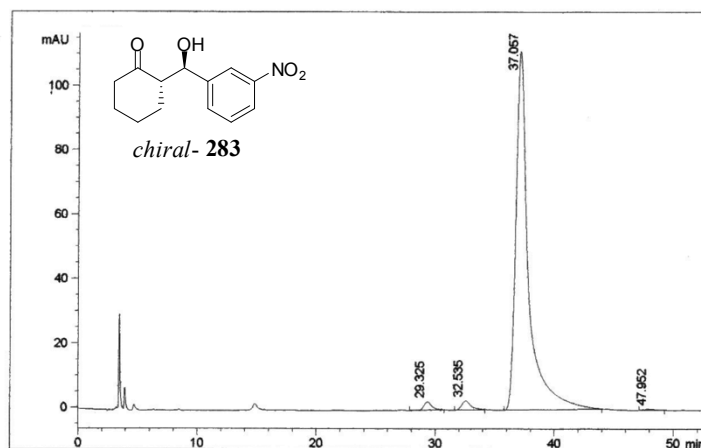
Figure B2. HPLC chromatogram of enantioenriched 281



Signal 1: DAD1 A, Sig=254,4 Ref=off

Peak #	RT [min]	Type	Width [min]	Area	Area %	Name
1	27.242	BB	0.505	9450.118	32.843	
2	31.125	BB	0.590	9777.838	33.982	
3	34.756	BB	0.646	4832.918	16.796	
4	44.827	BB	0.835	4712.805	16.379	

Figure B3. HPLC chromatogram of *rac*-283



Signal 1: DAD1 A, Sig=254,4 Ref=off

Peak #	Type	RT [min]	Width [min]	Area	Area %
1	VB	29.325	0.701	135.438	1.572
2	BB	32.535	0.769	160.480	1.862
3	BB	37.057	1.073	8297.462	96.284
4	BB	47.952	0.854	24.320	0.282

Figure B4. HPLC chromatogram of enantioenriched 283

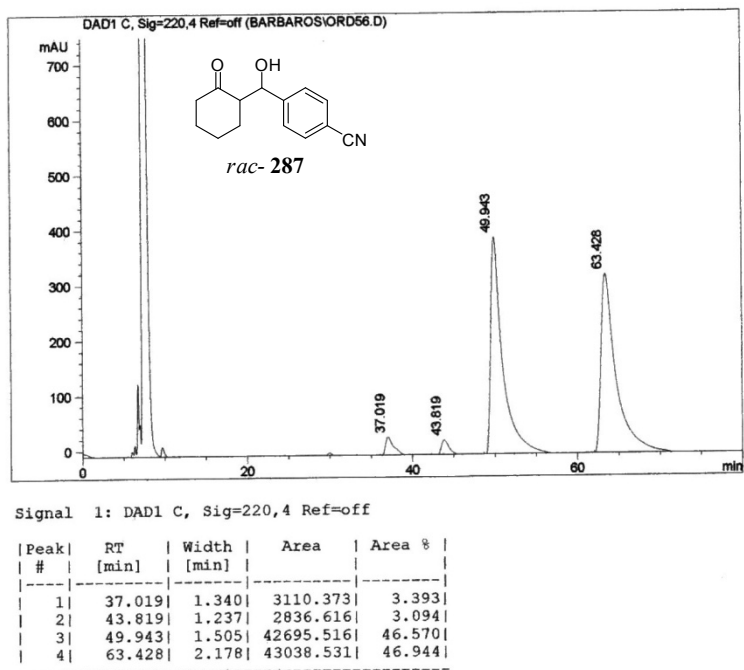


Figure B5. HPLC chromatogram of *rac-287*

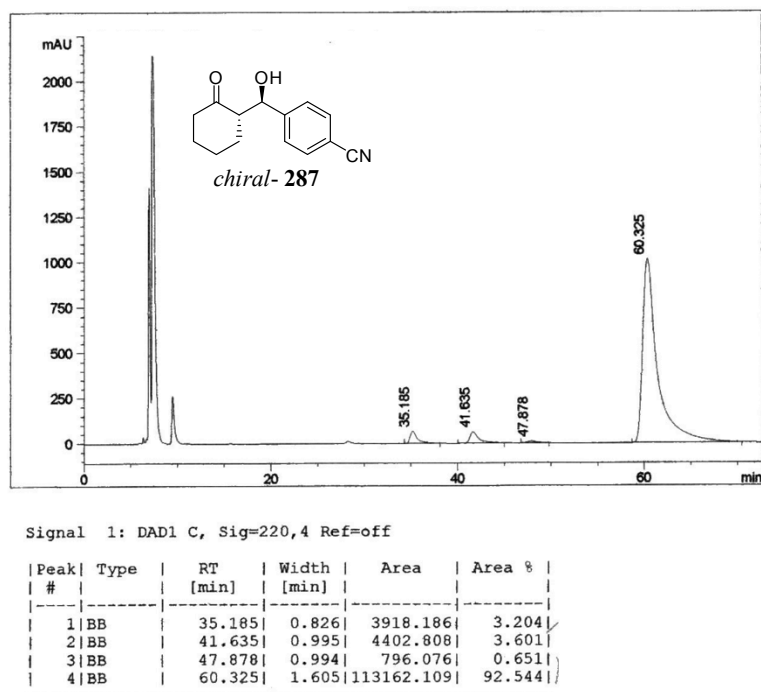
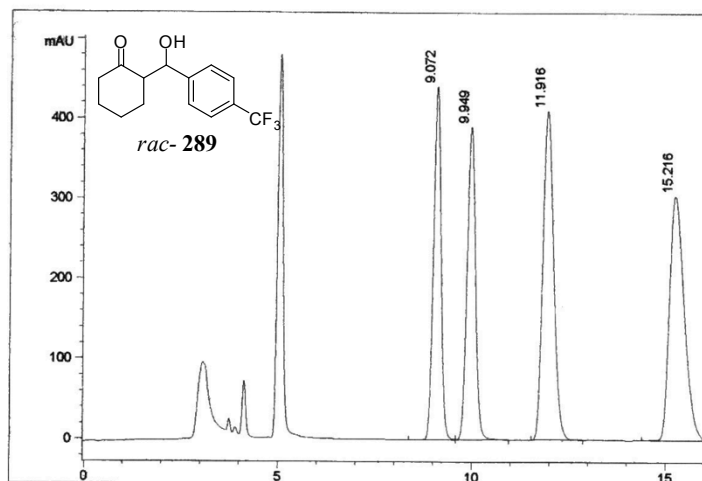


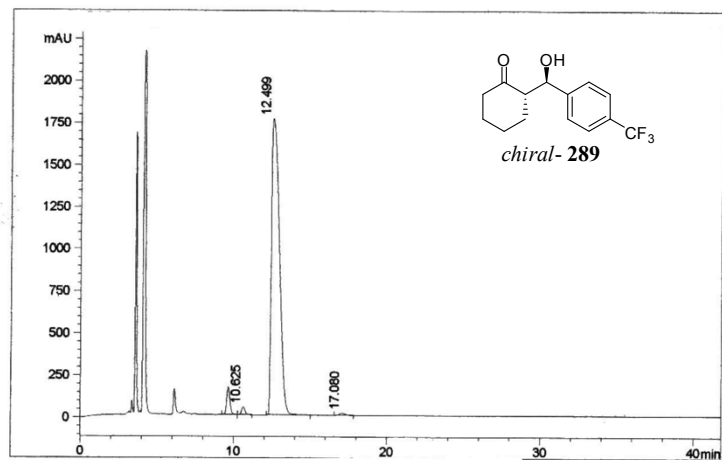
Figure B6. HPLC chromatogram of enantioenriched **287**



Signal 1: DAD1 C, Sig=220,4 Ref=off

Peak #	RT [min]	Type	Width [min]	Area	Area %
1	9.072	VV	0.209	5920.487	21.232
2	9.949	VB	0.236	5899.665	21.157
3	11.916	BB	0.302	7966.257	28.568
4	15.216	BB	0.410	8098.664	29.043

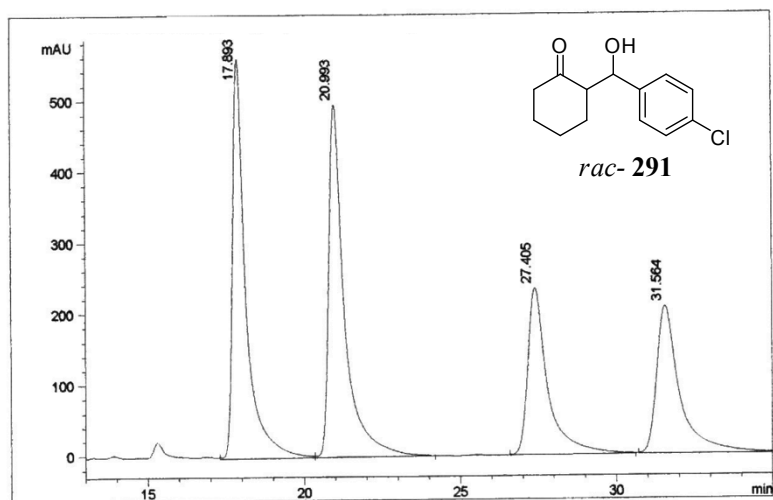
Figure B7. HPLC chromatogram of *rac*-289



Signal 1: DAD1 C, Sig=220,4 Ref=off

Peak #	RT [min]	Type	Width [min]	Area	Area %
1	9.642	BV	0.230	2490.367	3.732
2	10.625	VB	0.249	779.659	1.168
3	12.499	BB	0.574	63072.078	94.522
4	17.080	BB	0.425	385.224	0.577

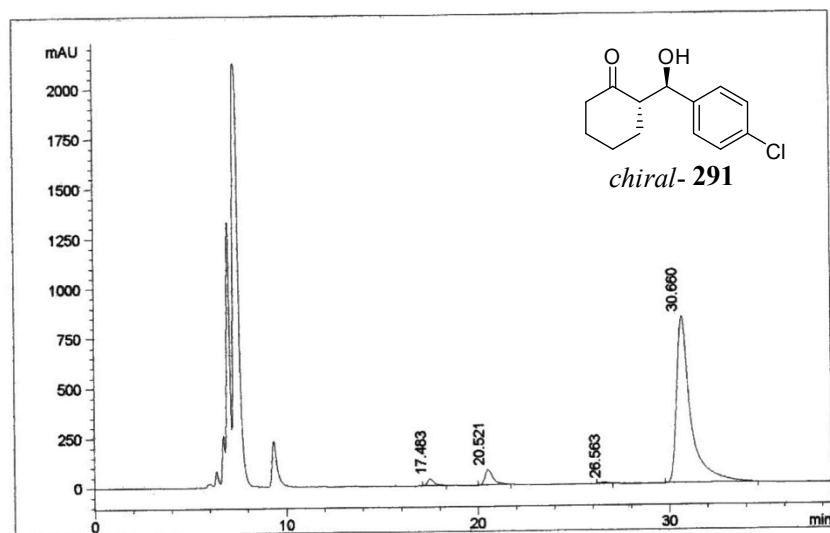
Figure B8. HPLC chromatogram of enantioenriched 289



Signal 1: DAD1 C, Sig=220,4 Ref=off

Peak #	Type	RT [min]	Width [min]	Area	Area %
1	VV	17.893	0.430	16669.184	30.059
2	VB	20.993	0.506	17446.316	31.461
3	BB	27.405	0.647	10535.146	18.998
4	BB	31.564	0.753	10804.015	19.483

Figure B9. HPLC chromatogram of *rac-291*



5	17.483	BB	0.369	862.576	1.869
6	20.521	BB	0.443	2328.896	5.045
7	26.563	MM	0.468	149.401	0.324
8	30.660	BB	0.740	42823.004	92.763

Figure B10. HPLC chromatogram of enantioenriched **291**

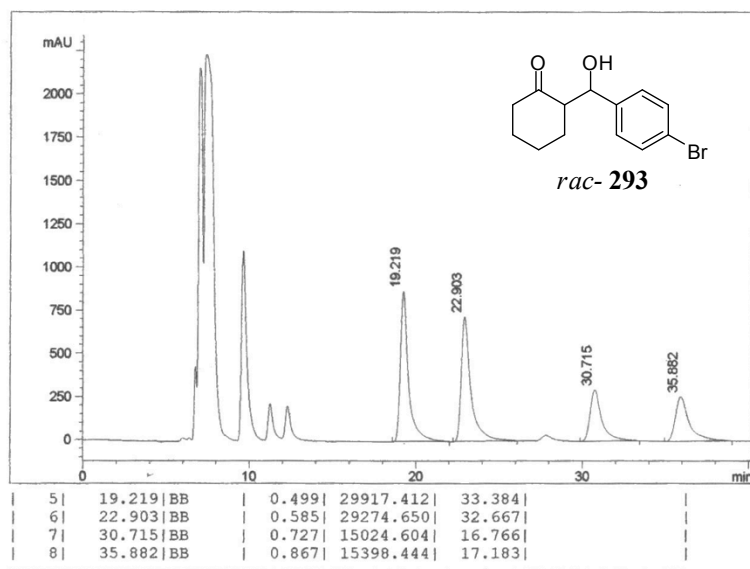


Figure B11. HPLC chromatogram of *rac-293*

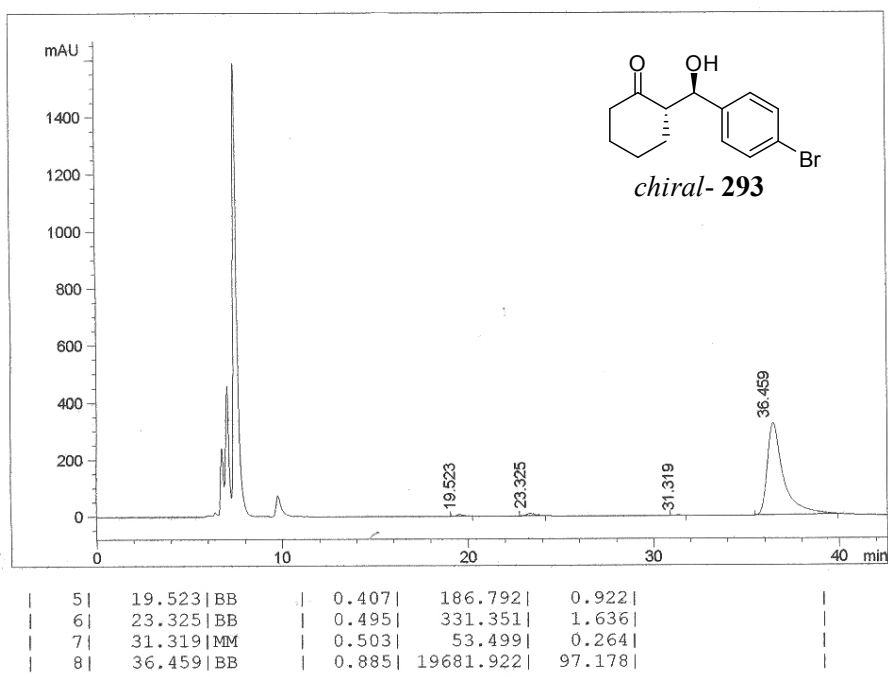
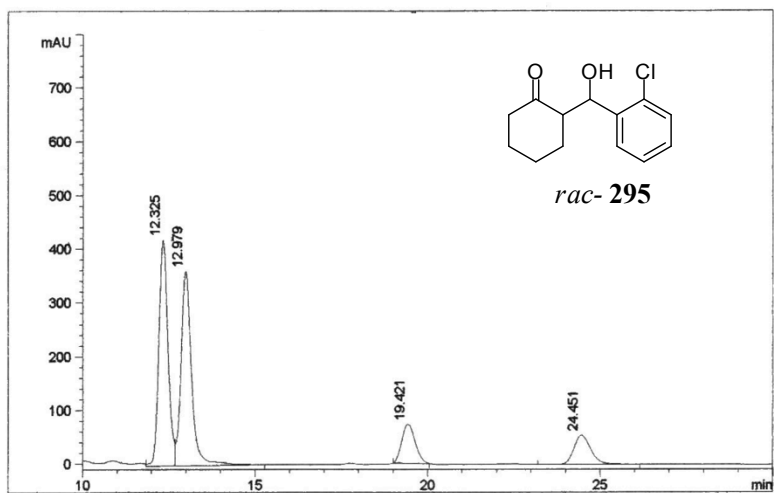


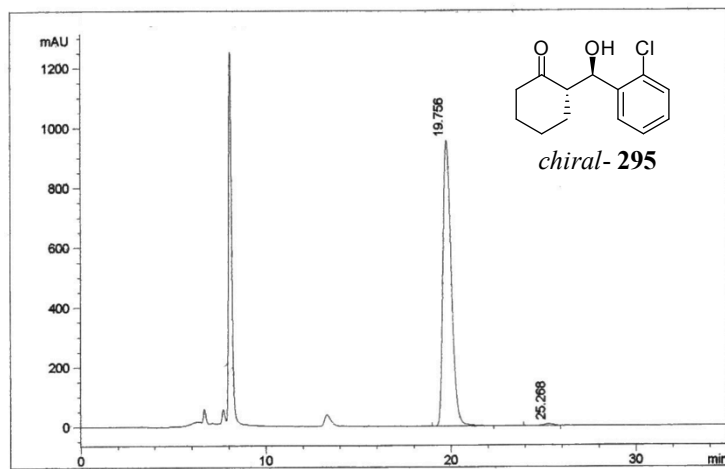
Figure B12. HPLC chromatogram of enantioenriched **293**



Signal 1: DAD1 C, Sig=220,4 Ref=off

Peak #	RT [min]	Width [min]	Area	Area %
1	12.325	0.283	7764.859	40.028
2	12.979	0.322	7756.875	39.987
3	19.421	0.456	2014.495	10.385
4	24.451	0.527	1862.190	9.600

Figure B13. HPLC chromatogram of *rac-295*



Peak #	RT [min]	Type	Width [min]	Area	Area %	Name
1	19.756	BB	0.495	30105.145	99.228	
2	25.268	BV	0.533	234.336	0.772	

Figure B14. HPLC chromatogram of enantioenriched 295

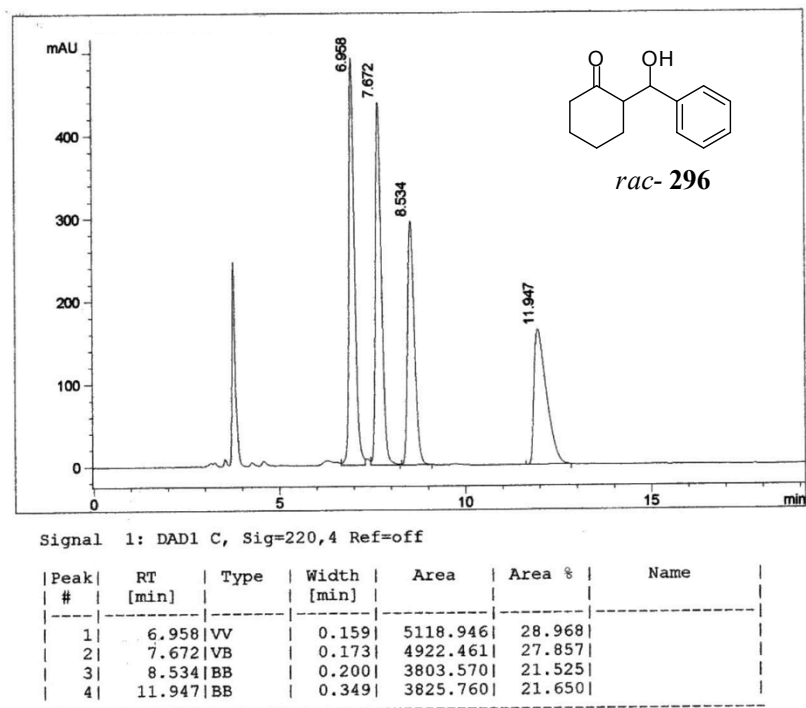


Figure B15. HPLC chromatogram of *rac*-190

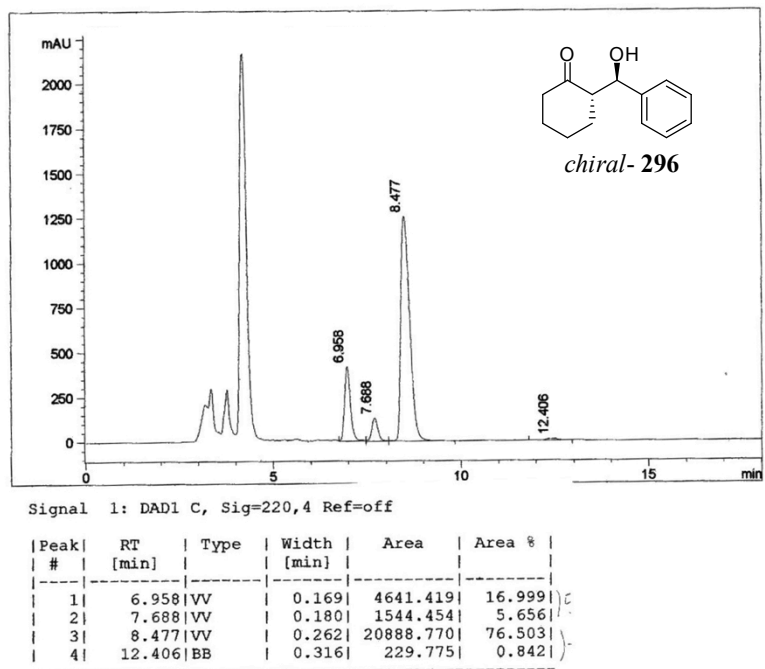


Figure B16. HPLC chromatogram of enantioenriched 190

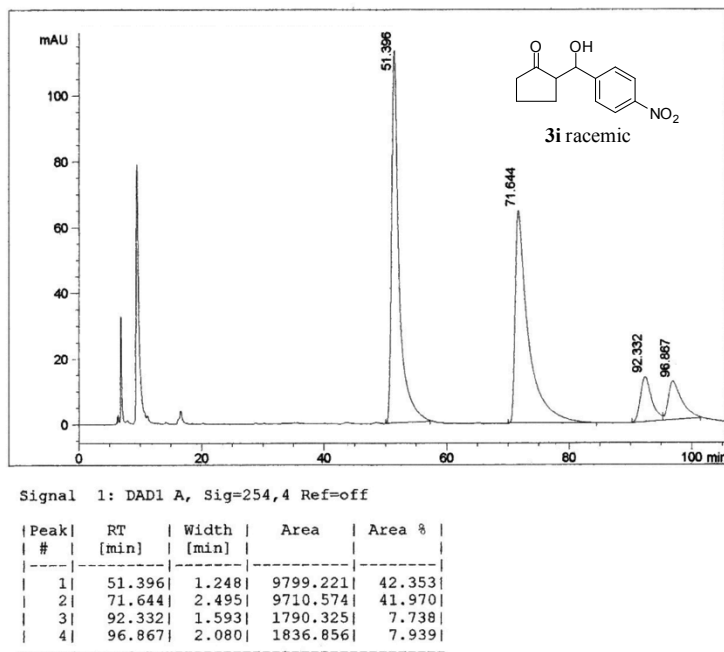


Figure B17. HPLC chromatogram of *rac*-298

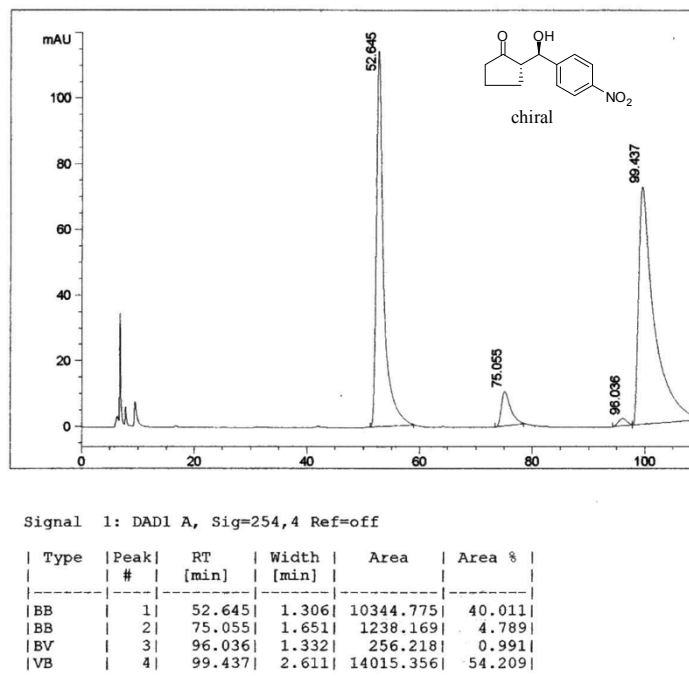
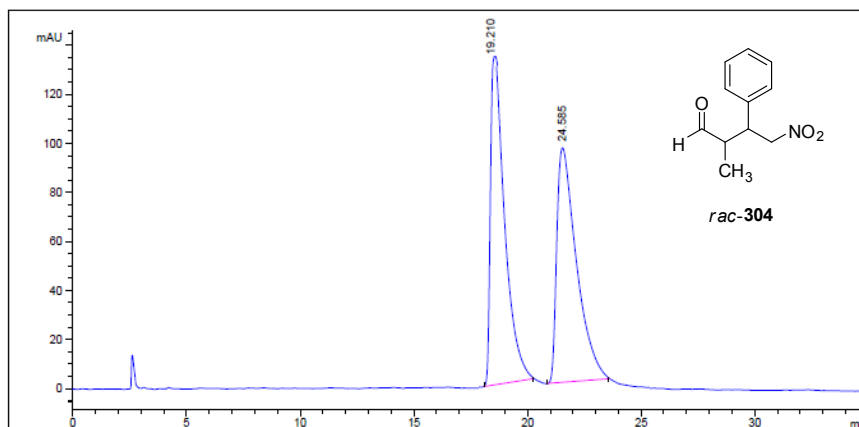


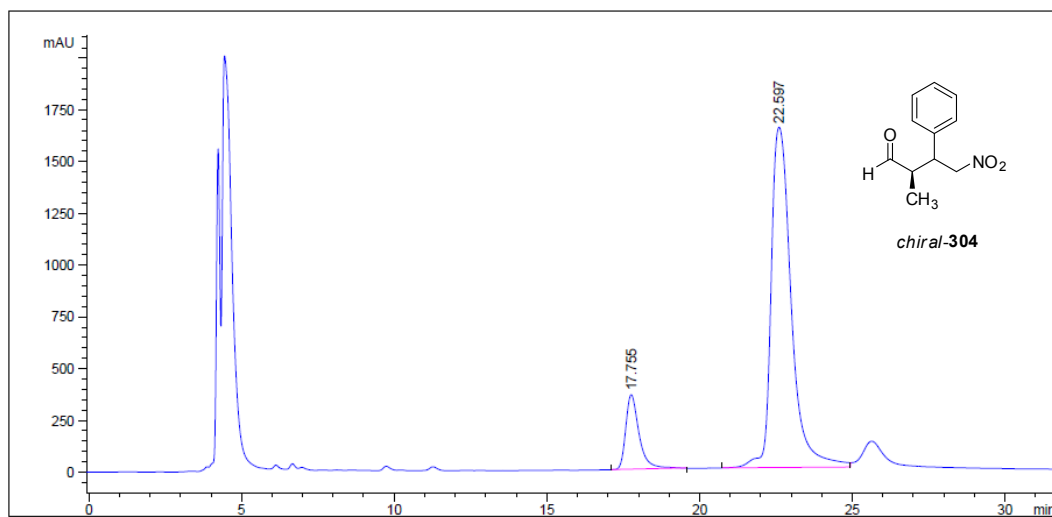
Figure B18. HPLC chromatogram of enantioenriched 298



Area Percent Report

Peak #	RetTime [min]	Type	Width [min]	Area [mAU*s]	Height [mAU]	Area %
1	19.210	MM	0.9591	9067.05078	137.90535	50.4251
2	24.585	MM	1.3328	8914.17090	95.69015	49.5749

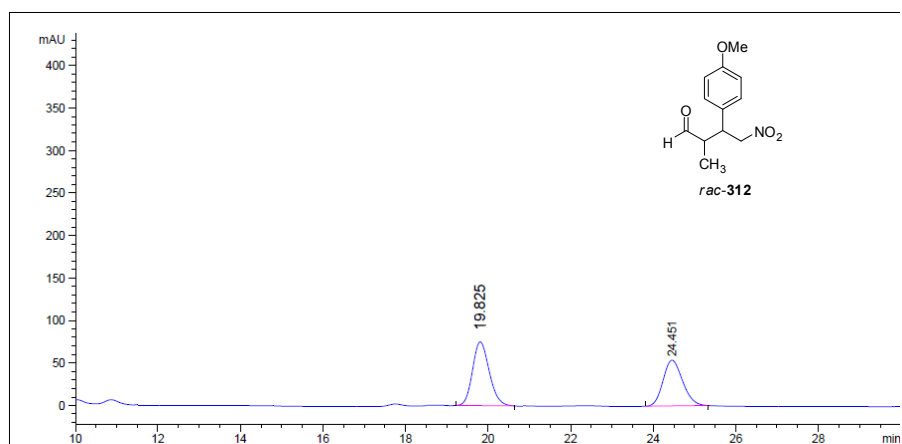
Figure B19. HPLC chromatogram of *rac-304*



Area Percent Report

Peak #	RetTime [min]	Type	Width [min]	Area [mAU*s]	Height [mAU]	Area %
1	17.755	BB	0.4606	1.10228e4	360.63525	12.6865
2	22.597	BV	0.7102	7.58634e4	1644.50574	87.3135

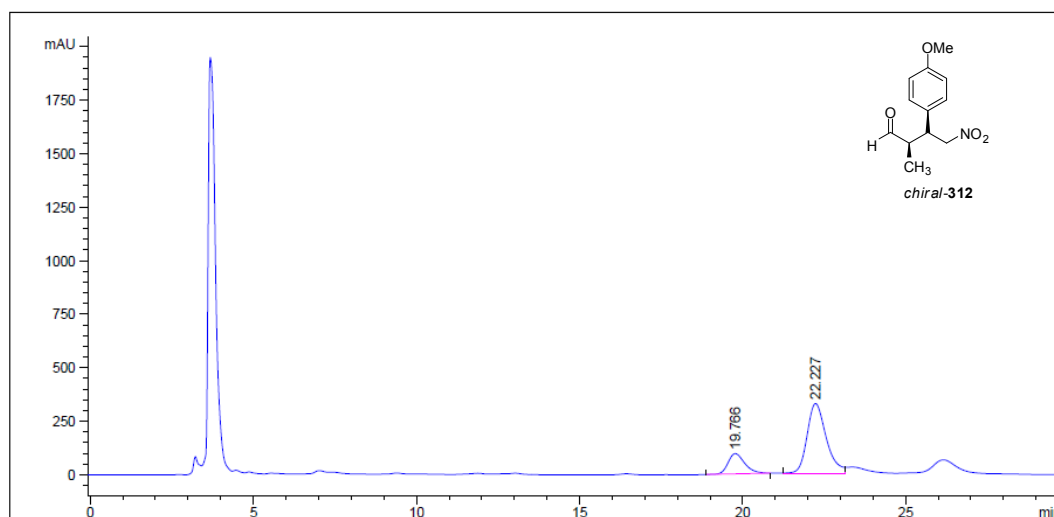
Figure B20. HPLC chromatogram of enantioenriched **304**



Area Percent Report

Peak #	RetTime [min]	Type	Width [min]	Area [mAU*s]	Height [mAU]	Area %
1	19.825	MM	0.4076	1648.12781	67.38767	47.9866
2	24.451	BB	0.5160	1786.43262	53.98713	52.0134

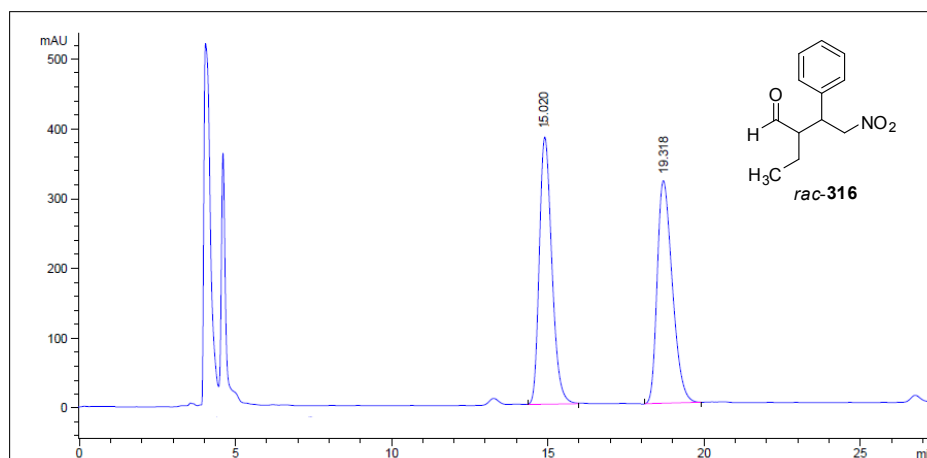
Figure B21. HPLC chromatogram of *rac-312*



Area Percent Report

Peak #	RetTime [min]	Type	Width [min]	Area [mAU*s]	Height [mAU]	Area %
1	19.766	BB	0.5455	3408.14063	95.24883	20.3884
2	22.227	BV	0.6201	1.33079e4	326.12839	79.6116

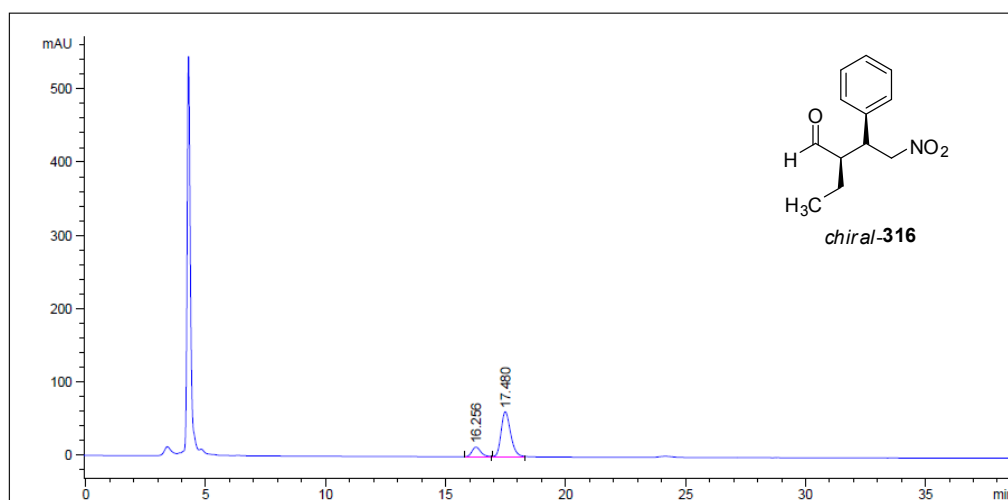
Figure B22. HPLC chromatogram of enantioenriched **312**



Area Percent Report

Peak #	RetTime [min]	Type	Width [min]	Area [mAU*s]	Height [mAU]	Area %
1	19.318	EB	0.4344	1.07164e4	383.02597	49.9271
2	24.334	EB	0.5208	1.07477e4	319.18723	50.0729

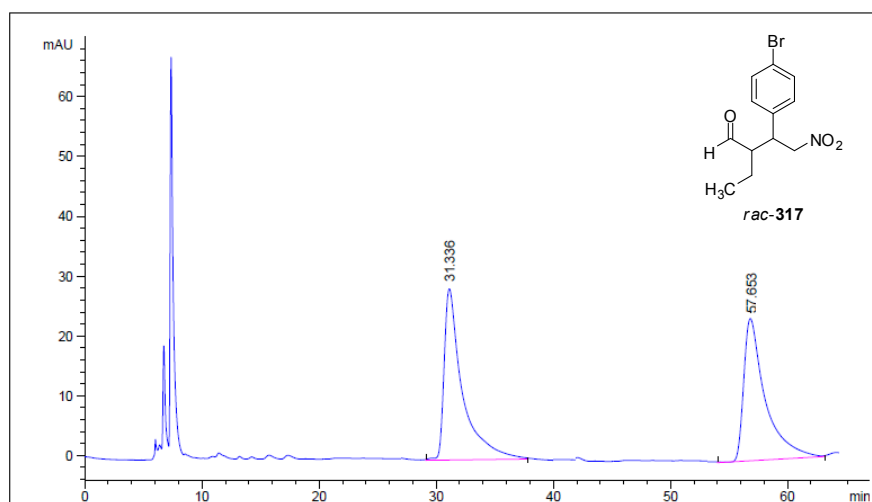
Figure B23. HPLC chromatogram of *rac*-316



Area Percent Report

Peak #	RetTime [min]	Type	Width [min]	Area [mAU*s]	Height [mAU]	Area %
1	16.256	EB	0.3921	333.17651	13.12824	16.5502
2	17.480	EB	0.4239	1679.94629	61.27369	83.4498

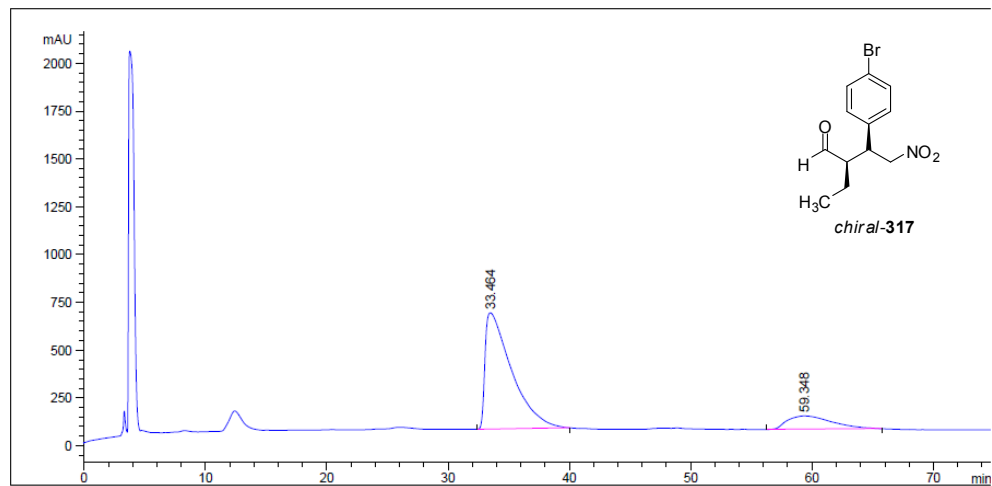
Figure B24. HPLC chromatogram of enantioenriched 316



Area Percent Report

Peak #	RetTime [min]	Type	Width [min]	Area [mAU*s]	Height [mAU]	Area %
1	31.418	BB	1.1201	2146.68164	26.75517	49.7523
2	57.653	BB	1.3310	2168.05884	22.09117	50.2477

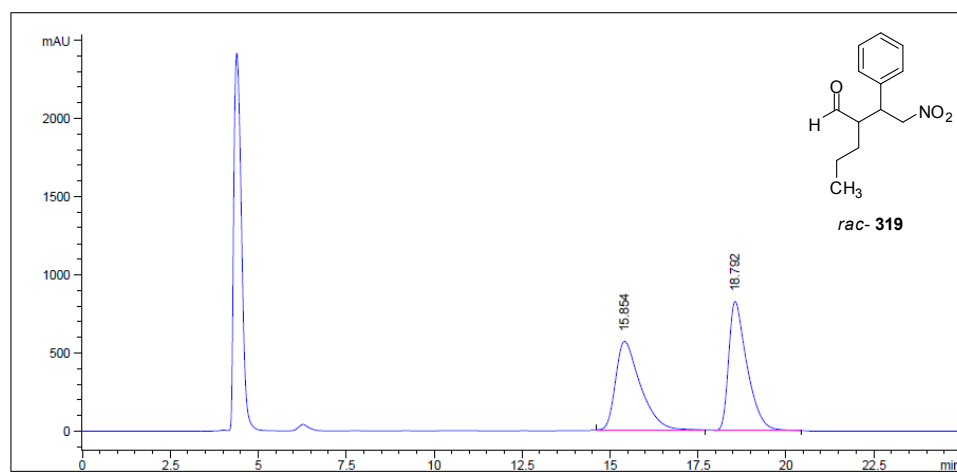
Figure B25. HPLC chromatogram of *rac*-317



Area Percent Report

Peak #	RetTime [min]	Type	Width [min]	Area [mAU*s]	Height [mAU]	Area %
1	33.463	BB	2.1386	3.11098e4	208.27887	84.5205
2	59.353	BB	2.8869	5697.58301	23.41444	15.4795

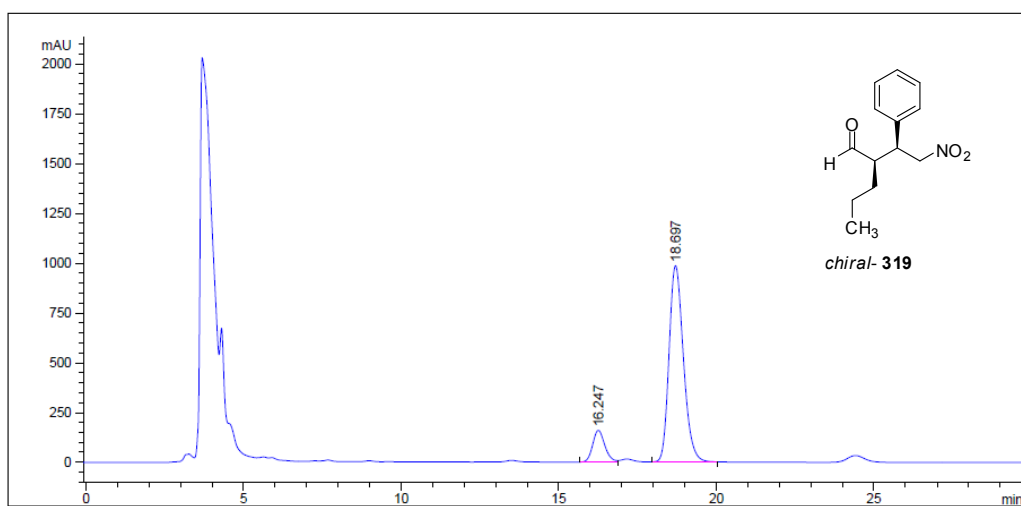
Figure B26. HPLC chromatogram of enantioenriched 317



Area Percent Report

Peak #	RetTime [min]	Type	Width [min]	Area [mAU*s]	Height [mAU]	Area %
1	15.854	BB	0.7216	2.76149e4	565.57379	47.8754
2	18.792	BB	0.5360	3.00659e4	827.31500	52.1246

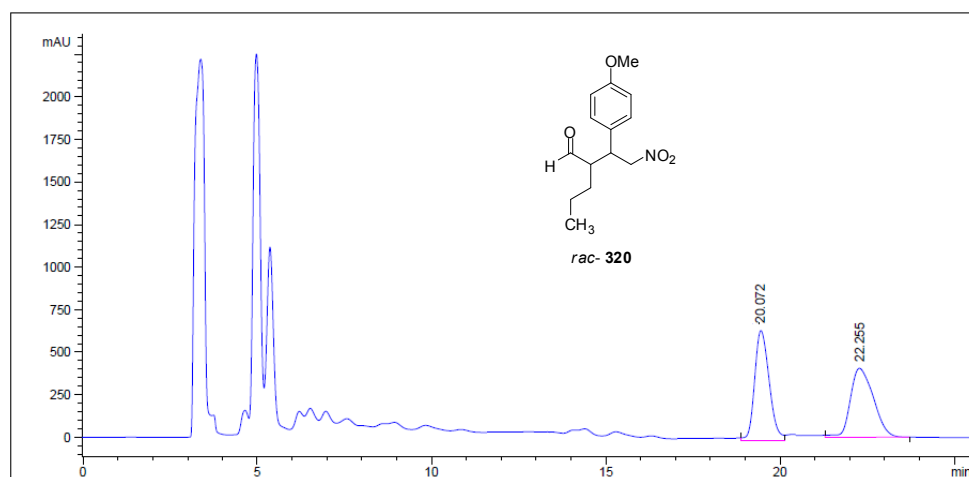
Figure B27. HPLC chromatogram of *rac*-319



Area Percent Report

Peak #	RetTime [min]	Type	Width [min]	Area [mAU*s]	Height [mAU]	Area %
1	16.247	BV	0.4088	4278.76807	159.61238	12.0514
2	18.697	BB	0.4898	3.12257e4	985.18726	87.9486

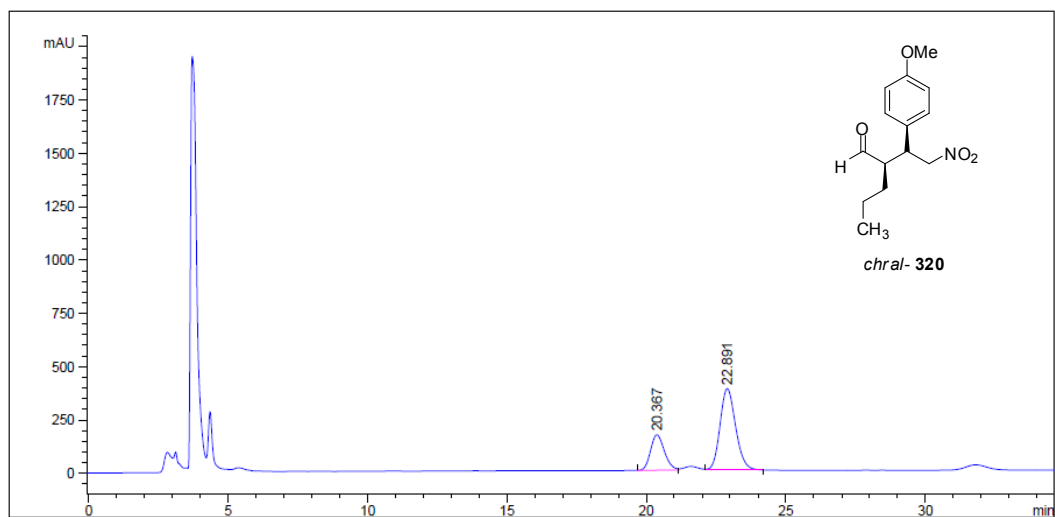
Figure B28. HPLC chromatogram of enantioenriched 319



=====
Area Percent Report
=====

Peak #	RetTime [min]	Type	Width [min]	Area [mAU*s]	Height [mAU]	Area %
1	20.072	BV	0.4599	1.90621e4	650.38611	50.3974
2	22.255	VB	0.7544	1.87615e4	406.53165	49.6026

Figure B29. HPLC chromatogram of *rac-320*



=====
Area Percent Report
=====

Peak #	RetTime [min]	Type	Width [min]	Area [mAU*s]	Height [mAU]	Area %
1	20.367	BV	0.5375	5801.54150	166.91057	27.9489
2	22.891	VB	0.6042	1.49561e4	382.44974	72.0511

Figure B30. HPLC chromatogram of enantioenriched **320**

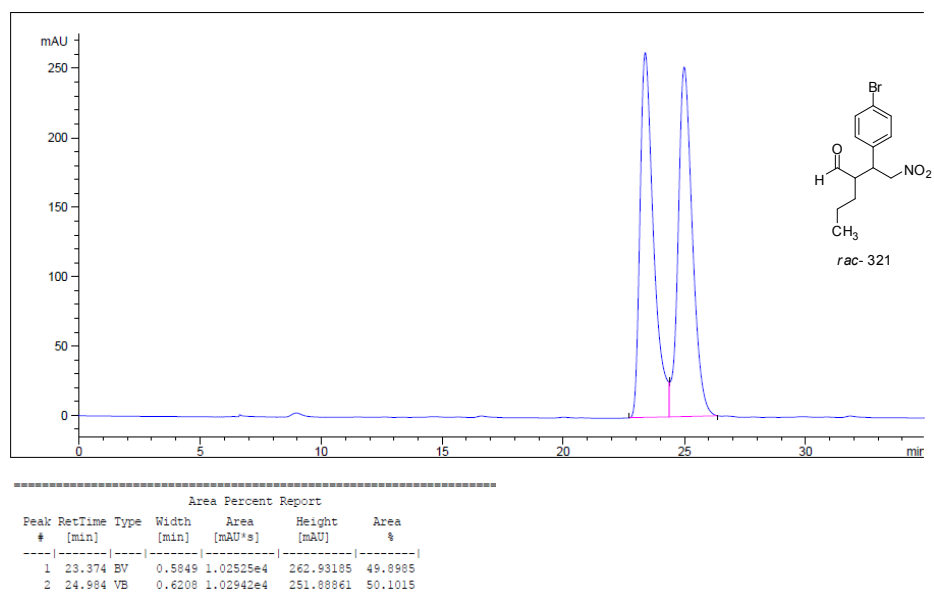


Figure B31. HPLC chromatogram of *rac*-321

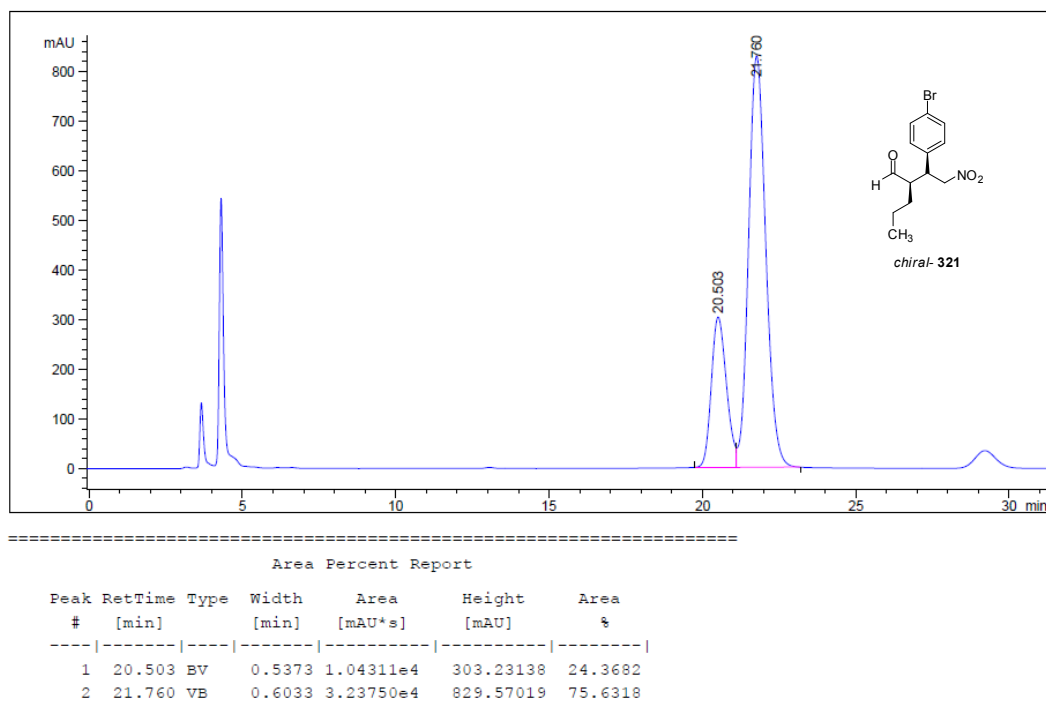
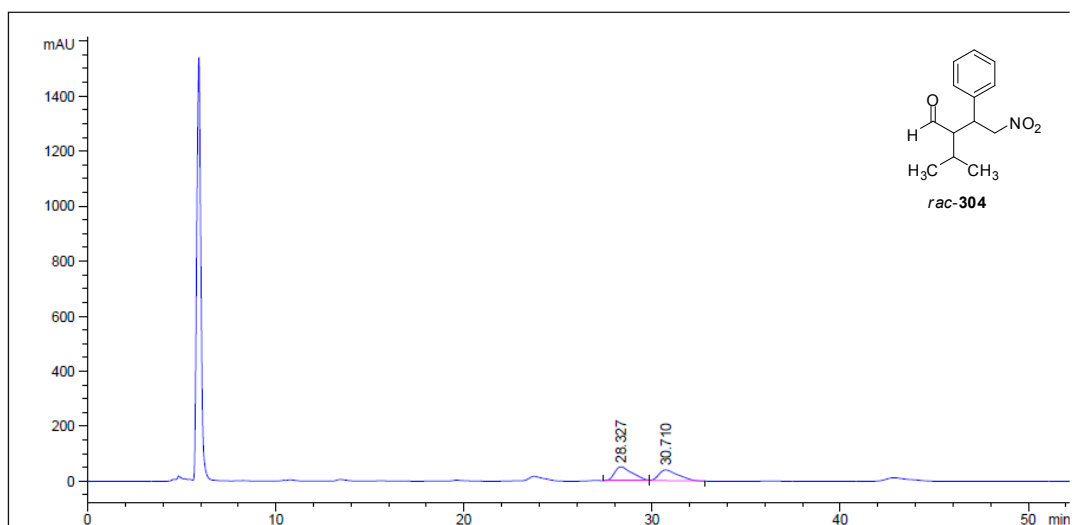


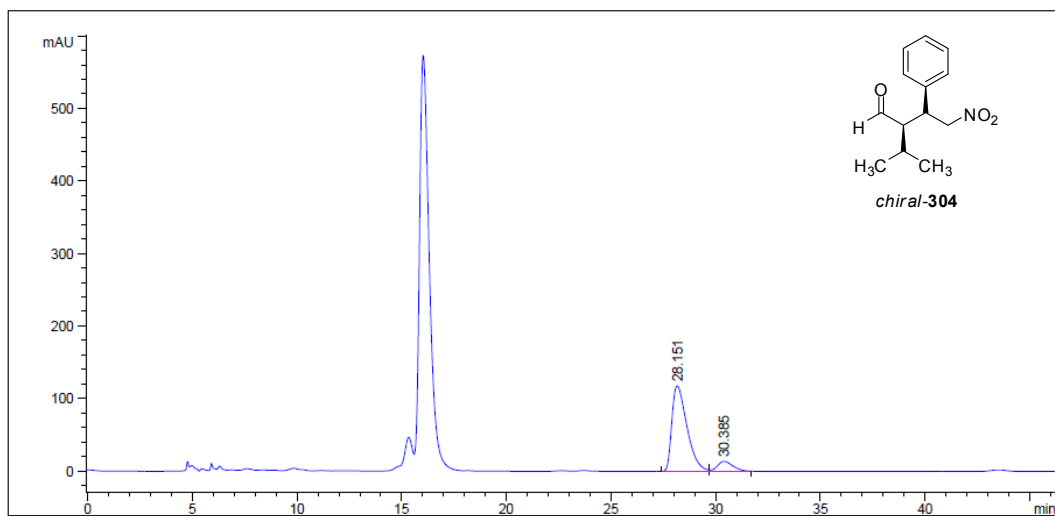
Figure B32. HPLC chromatogram of enantioenriched 321



=====
 Area Percent Report
 =====

Peak #	RetTime [min]	Type	Width [min]	Area [mAU*s]	Height [mAU]	Area %
1	28.327	BV	0.9323	2644.38989	40.05142	50.6118
2	30.710	VB	1.5046	2580.45947	20.27847	49.3882

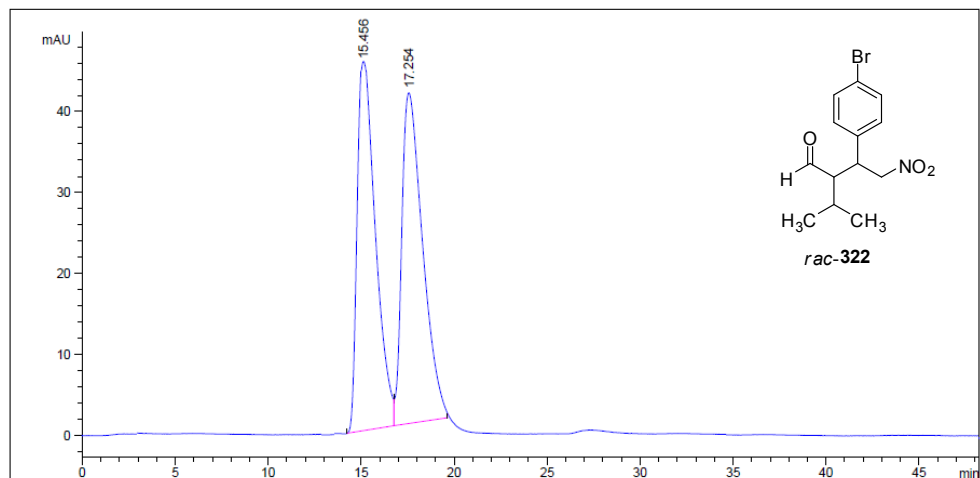
Figure B33. HPLC chromatogram of *rac*-304



=====
 Area Percent Report
 =====

Peak #	RetTime [min]	Type	Width [min]	Area [mAU*s]	Height [mAU]	Area %
1	28.151	BB	0.7679	5898.01465	117.85520	89.3202
2	30.385	BB	0.8005	705.20953	13.61025	10.6798

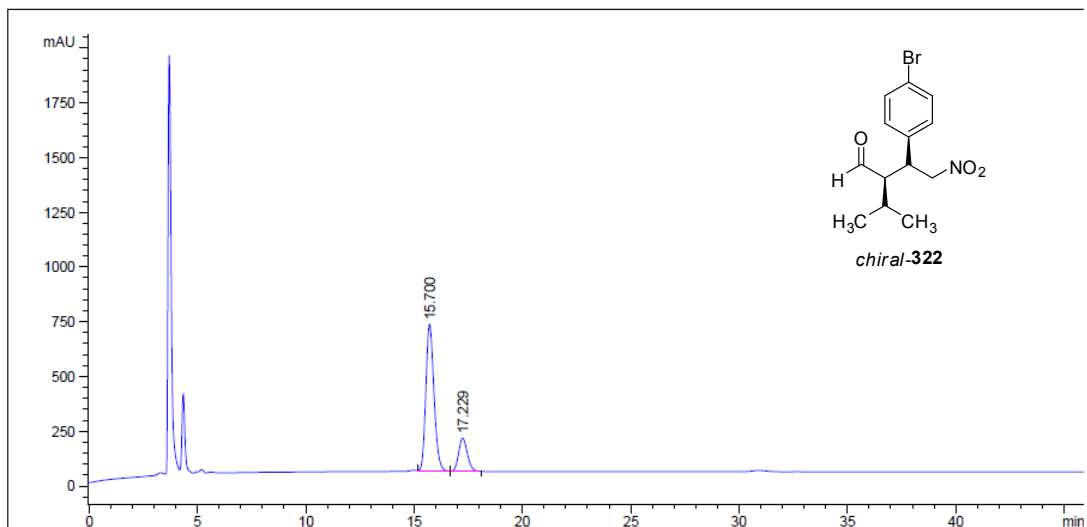
Figure B34. HPLC chromatogram of enantioenriched 304



=====
 Area Percent Report
 =====

Peak #	RetTime [min]	Type	Width [min]	Area [mAU*s]	Height [mAU]	Area %
1	15.456	BV	0.9859	3151.74780	47.14666	49.6911
2	17.254	VB	1.1242	3190.92969	40.89930	50.3089

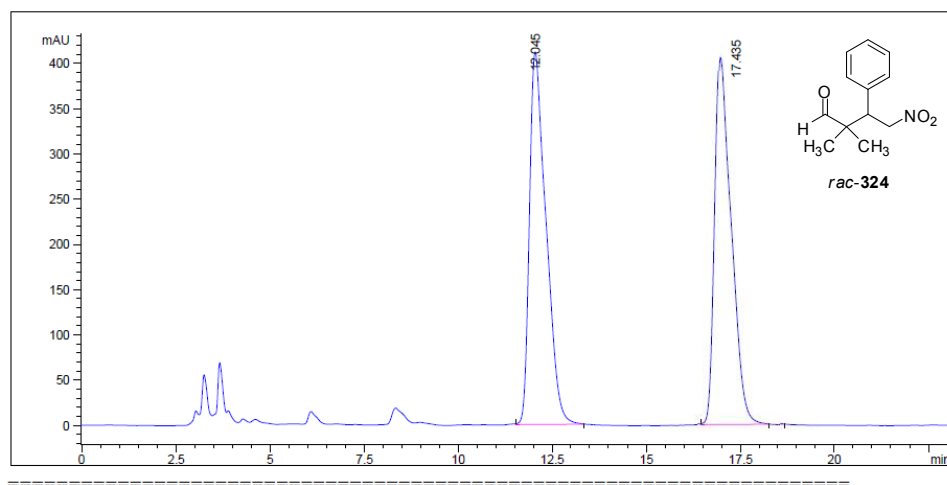
Figure B35. HPLC chromatogram of *rac*-322



=====
 Area Percent Report
 =====

Peak #	RetTime [min]	Type	Width [min]	Area [mAU*s]	Height [mAU]	Area %
1	15.700	VV	0.4064	1.76329e4	671.47272	80.3935
2	17.229	VB	0.4376	4300.33984	152.23325	19.6065

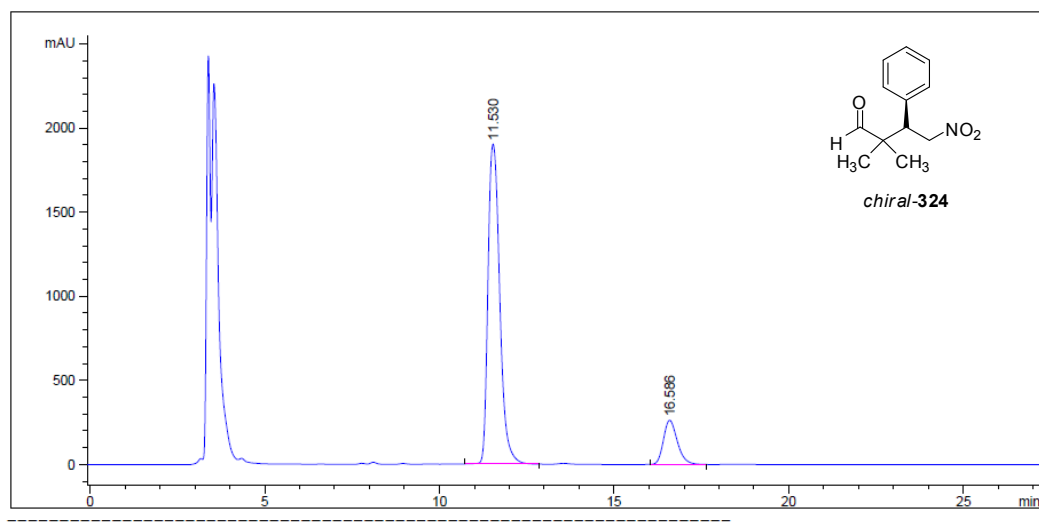
Figure B36. HPLC chromatogram of enantioenriched 322



Area Percent Report

Peak #	RetTime [min]	Type	Width [min]	Area [mAU*s]	Height [mAU]	Area %
1	12.045	MM	0.4653	1.10023e4	394.07233	50.9309
2	17.435	BB	0.6265	1.06001e4	243.17908	49.0691

Figure B37. HPLC chromatogram of *rac*-324



Area Percent Report

Peak #	RetTime [min]	Type	Width [min]	Area [mAU*s]	Height [mAU]	Area %
1	11.530	BB	0.3686	4.44544e4	1902.24963	85.9238
2	16.586	BB	0.4272	7282.60889	262.91437	14.0762

Figure B38. HPLC chromatogram of enantioenriched 324

CURRICULUM VITAE

PERSONAL INFORMATION

Surname, Name: Eymur, Serkan

Nationality: Turkish (T.C.)

Date and Place of Birth: 23 March 1980, Almus- Tokat

Marital Status: Married

Phone: +90 312 210 5340

Fax: +90 312 210 3200

E-mail: serkan_eymur@yahoo.com

EDUCATION

Degree	Institution	Year of Graduation
Ph.D	METU	2012
BS	Ankara Univ., Dept. of Chem.	2003
High school	Fethiye Lisesi, Muğla	1997

WORK EXPERIENCE

Year	Place	Enrollment
2003-2012	METU Dept. of Chem., Turkey	Research Assistant
2010, One Year	Univ. Of Mass. Amherst-USA	Visiting Scientist

FOREIGN LANGUAGES: English

ALL PUBLICATIONS OF THE WRITER

1. Demir*, A.S, Reis, Ö.; İğdir, Ç. A.; Esiringü, I. and **Eymur, S.**, Generation of Acyl Anion Equivalents from Acylphosphonates via Phosphonate–Phosphate Rearrangement: A Highly Practical Method for Cross-Benzoin Reaction, *Journal of Organic Chemistry*, **2005**, *70*, 10584–10587.
2. Demir*, A. S.; Reis Ö.; Kayalar, M.; **Eymur, S.**; Reis, B., Uncatalyzed Addition of TMSCN to Acylphosphonates, *Synlett*, **2006**, 3329-3331.
3. Demir*, A. S.; **Eymur, S.**, Addition of Trifluoromethyltrimethylsilane to Acyl Phosphonates: Synthesis of TMS-Protected 1-Alkyl-1-trifluoromethyl-1-hydroxyphosphonates and 1-aryldifluoroethenyl Phosphates, *Journal of Organic Chemistry*, **2007**, *72*, 8527-8530.
4. Demir*, A. S.; Reis, B.; Reis, Ö, **Eymur, S.**; Tural, S.; Göllü, M.; Sağlam, G., Cyanide Ion Promoted Addition of Acyl Phosphonates to Ethyl Cyanoformate: Synthesis of Tertiary Carbinols via Tandem Carbon-Carbon Bond Formations, *Journal of Organic Chemistry*, **2007**, *72*, 7439–7442.
5. Reis, Ö.; **Eymur, S.**; Reis, B.; Demir*, A. S., Direct enantioselective aldol reactions catalyzed by a proline-thiourea host-guest complex, *Chemical Communications*, **2009**, 1088–1090, (Highlighted in *Synfacts* **2009**, 325).
6. Demir*, A. S.; **Eymur, S.**, Self-assembly of organocatalysts for the enantioselective Michael addition of aldehydes to nitroalkenes, *Tetrahedron: Asymmetry*, **2010**, *21*, 112-115.
7. Demir*, A. S.; **Eymur, S.**, Nonlinear effects in proline–thiourea host–guest complex catalyzed aldol reactions in non-polar solvents, *Tetrahedron: Asymmetry*, **2010**, *21*, 405-409.
8. Subramani, C.; Yu, X.; Agasti, S.; Duncan, B.; **Eymur, S.**; Tonga, M.; Rotello*, V.M., Direct photopatterning of light-activated gold nanoparticles, *Journal of Materials Chemistry*, **2011**, *21*, 14156-14158.
9. Nandwana, V.; Subramani, C.; **Eymur, S.**; Yeh, Y-C.; Tonga, M.; Jeong, Y.; Yang, B.; Barnes, M.D.; Cooke, G.; Rotello*, V.M., Recognition-mediated assembly of quantum dot polymer conjugates with controlled

morphology, *International Journal of Molecular Sciences*, **2011**, *12*, 6357-6366.

10. Xi, Y.; **Eymur, S.**; Singh, V.; Yang, B.; Tonga, M.; Bheemaraju, A.; Cooke, G.; Venkataraman, D.; Stanley, R.J.; Rotello* V.M., Flavin as Photo-Active Acceptor for Efficient Energy and Charge Transfer in a Model Donor-Acceptor System, *Physical Chemistry Chemical Physics*, **2012**, *14*, 6749-6754.
11. Nandwana, V.; Fitzpatrick, B.; Liu Q.; Solntsev, K. M.; Yu, X.; Tonga, G.Y.; **Eymur, S.**; Tonga, M.; Cooke, G.; Rotello*, V.M., Fluorescence resonance energy transfer in recognition-mediated polymer-quantum dot assemblies, *Polymer Chemistry*, **2012**, *3*, 3072-3076.

CONFERENCE AND MEETINGS

- 233rd ACS National Meeting, Chicago, IL, United States, March 25-29, ORGN-596, Acylphosphonates as donor and acceptor in organocatalytic asymmetric reactions. Demir, Ayhan S.; Reis, Ömer; Esiringu, Ilker; **Eymur, Serkan**; Reis, Barbaros; Baris, Sehriban; Yalcinkaya, Hatice.
- XIX. National Chemistry Congress, Organocatalytic Enantioselective Synthesis of α -Hydroxy Phosphonates, 2007; **Serkan Eymur**, Ayhan S. Demir
- XX. National Chemistry Congress, Addition of Trifluoromethyltrimethylsilane to Acyl Phosphonates, 2008; **Serkan Eymur**, Ayhan S. Demir
- XXI. National Chemistry Congress, 2009; Proline–Thiourea Self-Assemblies in Aldol Reactions, **Serkan Eymur**- *Oral presentation*

- 237th National Meeting of American Chemical Society, Salt Lake City, Utah, USA; March 22-26, 2009; ORGN 457, Self-assembled proline-thiourea host-guest complex catalyzed direct enantioselective aldol reactions. A. S. Demir, Ö. Reis, **S. Eymur**, B. Reis.